# Pathophysiological and molecular characterization of a mouse model of ARCA2, a recessive cerebellar ataxia associated to Coenzyme Q10 deficiency

Floriana Licitra

# UNIVERSITÉ DE STRASBOURG

*Ecole doctorale des Sciences de la Vie et de la Santé*

*Institut de Génétique et de Biologie Moléculaire et Cellulaire*

# THÈSE présentée par :


## Floriana Licitra


soutenue le : **04 Septembre 2013**

pour obtenir le grade de : **Docteur de l'université de Strasbourg**

Discipline/ Spécialité : Aspects moléculaires et cellulaires de la biologie

## Pathophysiological and molecular characterization of a mouse model of ARCA2, a recessive cerebellar ataxia associated to Coenzyme $Q_{10}$ deficiency

| | |
|---|---|
| **Mme Le Docteur Hélène Puccio** | Directrice de thèse |
| **Mme Le Professeur Rita Horvath** | Rapporteur externe |
| **Mme Le Docteur Esther Becker** | Rapporteur externe |
| **Mr Le Docteur Luc Dupuis** | Examinateur |
| **Mr Le Docteur Fabien Pierrel** | Examinateur |

*Considerate la vostra semenza:*
*fatti non foste a viver come bruti,*
*ma per seguir virtute e canoscenza.*

*Consider well the seed that gave you birth:*
*you were not made to live as brutes,*
*but to follow virtue and knowledge.*

*Dante, Inferno, Canto XXVI*

**ACKNOWLEDGEMENTS**

Looking back over the past four years I realize that this journey would not have been possible without the support that I received from many people around me.

I would like to express my sincere gratitude to my mentor Hélène to have welcomed me in her team four years ago. She convinced me to join her lab with a single word: curiosity. I still believe that this is one of the most important lessons I learned from her. She patiently provided the encouragement and enthusiasm necessary for me to proceed through my PhD. She supported me in the hard moments of my thesis, believing in me more than I was doing. I am honored to have been in her lab during these years, heaving her as positive model of scientist and woman.

I would like to thank Leila for having shared with me the interest in the ARCA2 topic, with enthusiasm since the first day. Since she joined the lab, I felt less lonely discussing with her not only about Coenzyme Q and ADCK3, but also about our southern origins! Thank you for all your advices and your sincere friendship.

I would like to thank all the members of the Puccio's lab for the collaborative environment, the scientific discussions, the (short) coffee breaks and our Spanish retreat. I thank Aurore, my French teacher, for the patience she had with me; Brahim, for having unveiled all the secrets of a cryostat; Florent, for his joy and all the coffees drunk together; Nadège, for her kindness and availability; Alain, for his irony and wisdom.

I thank Laurence who, first, showed me how to work with mice. Thank you for taking care of my many and old mice, I know that it was sometimes hard. Thank you for your delicious *mousse au chocolat,* and for all the supply of rhubarb that you provided me!

I thank Lena for all the jokes and the laughs, because she helped me in keeping a positive mood even when there were negative results. Thank you for all the 'Ricola bonbons', the 'new' singers discovered in your car and the patience that you had trying hardly to teach me some German!

I thank Morgane, my neighbor, always kind and available. Thank you for the support you gave me in the hard moments, all the advices about my experiments and the encouragement in the common time of writing up.

Just a couple of more acknowledgements for my colleagues: to my dear 'runner colleagues', Lena and Morgane, thank you for all the kilometers run together. To my dear drivers, thank you for helping me and sorry for the early waking up.

I thank all the former members of the lab: Fred, Julia, Marie, Agnieszka and Charlotte. I truly appreciated the time that you spent thinking with me about the different aspects of my project. I owe special thanks to Stéphane who patently helped me with my first experiments and was always available to discuss my data.

I would like to thank all the people of the *Human Genetics*, for the interesting discussions and the collaborative environment. I address special thanks to Yvon who always showed curiosity about my work and helped me in the interpretation of some tricky results.

I thank all our collaborators who helped me in developing new aspects of my project. In particular, I thank Dr. Fabien Pierrel and Dr. Philippe Isope for their availability and the interesting discussions. I would like to thank also AnaÏs, who patiently explained me all I know about electrophysiology.

I would like to thank several people from the common services/platforms of the IGBMC that helped me during my work. In particular, I thank the people of the histology facility for their kindness and availability; Nadia and Jean-Luc, for their patience in analyzing my samples; Marc and Pascal for all their technical support.

Un ringraziamento speciale va a Ebe, Manuela e Maria Vittoria. Ebe, senza di te questi quattro anni non riuscirei proprio ad immaginarli. Abbiamo condiviso tutto, sostenendoci a vicenda dal primo giorno di colloqui fino alla fine di questo duro percorso. Grazie per le passeggiate notturne “fino a Gallia”, le soppressate, le confidenze e i viaggetti in giro per l’Europa. Manu, sempre un raggio di luce ogni volta che ti ho incontrata nei corridoi! Grazie per tutto il sostegno datomi in questi quattro anni, per le pause caffè e la sincera amicizia che ci lega. Maria Vittoria, grazie per tutte le birre bevute insieme e per la tua disponibiltà; con la tua saggezza sei stata un punto di riferimento importante nei momenti di scoraggiamento.

Ringrazio tutti gli amici Italiani, Rocco, Angelo, Goffredo, Claudia e Serena per le belle serate, i picnic, le scampagnate trascorse insieme. Un ringraziamento speciale va a Rocco, per la sua vitalità ed ottimismo. Grazie ad Angelo, sempre d’aiuto nei miei traslochi. Ringrazio Claudia per gli incoraggiamenti nei momenti difficili.

Vorrei ringraziare la Prof.ssa Fadini, lei che per prima ha seminato in me la passione per la genetica. Grazie per averla alimentata ed aver creduto in me.

Un ringraziamento speciale va a Laura, la mia amica di sempre. Seppure diverse, siamo riuscite a costruire una salda amicizia che non teme distanza.

Infine ringrazio la mia famiglia, senza la quale non sarebbe possibile per me immaginare di essere arrivata fin qui. Ringrazio i miei genitori per avermi sostenuto in tutte le scelte della

mia vita. Grazie per avermi insegnato a riflettere sulle cose e a non temere di pensarla diversamente dal gruppo. Grazie per avermi insegnato ad andare oltre, alla ricerca di una dimensione adatta alle mie inclinazioni, pur sapendo che questo avrebbe potuto significare lontano da voi. Ringrazio le mie sorelle, Nadia e Rossella, per il supporto e l'affetto che mi hanno sempre dato. Sebbene abbiamo scelto strade diverse, ci siamo ritrovate tutte alle prese con un dottorato, esperienza che ci ha unite ancora di più. Grazie perché nonostante la distanza siete sempre presenti; la certezza di poter condividere con voi preoccupazioni e pensieri, cosi' come le gioie della mia vita, mi ha sostenuto in questi anni di lontanza dalla famiglia.

## TABLE OF CONTENTS

## LIST OF FIGURES

## LIST OF TABLES



## LIST OF MANUSCRIPTS

**ABBREVIATIONS**

| | |
|---|---|
| 4-HB | 4-hydroxybenzoic acid |
| Aa | Amino acid |
| AOA1 | Ataxia oculomotor apraxia 1 |
| AOA2 | Ataxia oculomotor apraxia 2 |
| ARCA2 | Autosomal recessive cerebellar ataxia type 2 |
| ARSACS | Spastic ataxia of Charlevoix-Saguenay |
| A-T | Ataxia telangiectasia |
| AKs | Atypical kinases |
| AUC | Area under the curve |
| AVED | Ataxia with isolated vitamin E deficiency |
| CK | Creatine kinase |
| CNS | Central nervous system |
| CoQ | Coenzyme Q |
| CV2 | Coefficient of variation |
| DHE | Dihydroethidium |
| DRPLA | Dentatorubro-palldoluysian atrophy |
| EAs | Episodic ataxias |
| ER | Endoplasmic reticulum |
| FPP | Farnesyl pyrophosphate |
| FXTAS | Fragile X associated tremor ataxia syndrome |
| GABA | γ-aminobutyric acid |
| HAB | 3-hexaprenyl-4-aminobenzoic acid |
| HDL | High density lipoprotein |
| HHB | 3-hexaprenyl-4-hydroxybenzoic acid |
| HMGCR | 3-hydroxy-3-methylglutaryl-CoA reductase |
| IMM | Inner mitochondrial membrane |
| ISI | Interspike interval |
| KO | Knockout |
| $K_v$ | Koltage-gated $K^+$ channels |
| LDL | Low density lipoprotein |
| MADD | Multiple acyl-CoA dehydrogenase deficiency |
| MDA | Malonaldehyde or malonyldialdehyde |
| MIRAS | Mitochondrial recessive ataxia syndrome |
| MSS | Marinesco-Sjogren |

| | |
|---|---|
| mtDNA | Mitochondrial DNA |
| $Na_v$ | Voltage-gated sodium channel |
| NGS | Normal goat serum |
| NMD | Non sense mediated decay |
| NOX | NADH oxidase |
| OGGT | Oral glucose tolerance test |
| OXPHOS | Oxidative phosphorylation |
| pABA | Para-aminobenzoic acid |
| PC | Purkinje cell |
| PHARC | Polyneuropathy, hearing loss, ataxia, retinitis pigmentosa, and cataract |
| PTP | Permeability transition pore |
| PTZ | Pentylenetetrazol |
| qRT-PCR | Real Time quantitative Reverse Transcription PCR |
| ROS | Reactive oxygen species |
| SANDO | Sensory ataxic neuropathy dysarthria and ophthalmoparesis |
| SCAs | Spinocerebellar ataxias |
| shRNA | Short hairpin RNA |
| SOD | Superoxide dismutase |
| TBA | Thiobarbituric acid |
| TBARS | Thiobarbituric acid reactive substances |
| TPKs | Typical protein kinases |
| UCPs | Uncoupling proteins |
| VLDL | Very-low density lipoprotein |
| WT | Wild-type |
| XLSA/A | X-linked ataxia sideroblastic anemia |

# INTRODUCTION

# INTRODUCTION

During my PhD work, I have been working on a new form of recessive ataxia, ARCA2 (autosomal recessive cerebellar ataxia type 2). The genetic cause of this rare cerebellar ataxia has been found in 2008 in the laboratory of Prof. Michel Koenig, just before my arrival in the laboratory of Dr. Hélène Puccio in 2009.

My PhD project aimed to elucidate the pathophysiology of ARCA2 through the generation and characterization of a mouse model, in the hope to have a relevant model to recapitulate features of the human disease.

ARCA2 is associated to a Coenzyme $Q_{10}$ deficit in humans. Therefore, this disease belongs to two different groups of diseases, namely recessive ataxias and Coenzyme $Q_{10}$ deficiencies. For this reason, in my introduction, I will first introduce cerebellar ataxias with a particular emphasis on the recessive forms. A brief description of the structure of the cerebellum is also given since the cerebellum is primarily affected in ARCA2. Subsequently, I will present Coenzyme Q and the human conditions linked to a deficiency of Coenzyme $Q_{10}$. Lastly, I will describe the clinical features and the genetic causes of ARCA2.

# 1. Genetic ataxias and cerebellar organization

## *1.1. Cerebellar ataxias*

Ataxias are a heterogeneous group of neurological disorders characterized by loss of coordination and imbalance. The cerebellum is usually primarily affected, either by degeneration or abnormal development, although extra-cerebellar neurological lesions can also be present, involving mostly brain stem and spinal cord (Sailer and Houlden, 2012).

Cerebellar ataxias have a wide range of potential causes from alcohol abuse, to exposure to toxins and infections. Moreover, a large proportion of cerebellar ataxias are hereditary (genetic ataxias) (Manto and Marmolino, 2009).

Genetic ataxias have very diverse clinical manifestations, with different age of onset and progression of movement disorders. Furthermore, additional signs, such as neuropathy, cognitive impairment and retinopathy, can be present to varying degrees. Moreover, genetic ataxias are often associated to non-neurological signs, such as myopathy, cardiomyopathy or diabetes. This marked heterogeneity is due to the multitude of genes and the diversity of mutations that can be associated to hereditary ataxias.

Based on their mode of inheritance, genetic ataxias can be classified into autosomal dominant, X-linked and autosomal recessive. Epidemiological studies reveal that autosomal recessive ataxias are the most frequent, with a prevalence of 5 in 100,000, whereas the prevalence of dominant cerebellar ataxias is around 3 in 100,000 (Sailer and Houlden, 2012).

### *1.1.1. Autosomal dominant cerebellar ataxias*

Autosomal dominantly inherited ataxias include spinocerebellar ataxias (SCAs) and episodic ataxias (EAs). The general classification of SCAs is reported in table 1.

SCAs are often due to repeat expansions in either coding or non-coding parts of the affected gene. Polyglutamine expansions are the most common among these mutations and they are found in nearly 50% of patients with autosomal dominant ataxias. The prevalence of SCA is 1-3 in 100 000 in the European population (Durr, 2010). The correlation genotype–phenotype is well characterized in these disorders, as larger repeat numbers generally result in an

earlier age of onset and a more severe phenotype. In addition to polyglutamine expansions, untranslated expansions are also responsible for some forms of SCAs through a gain of function mechanism due to RNA (Todd and Paulson, 2010). However, a number of dominant ataxia syndromes is caused by conventional mutations (Hersheson et al., 2012).

EAs are characterized by discrete attacks of ataxia, which may be associated with a range of other neurological signs such as vertigo, seizures and often migraines. Seven forms have been described so far and, in four of these, the causal genes have been identified (Sailer and Houlden, 2012).

| Ataxia | Gene | Protein |
|---|---|---|
| ***Polyglutamine expansion SCA*** | | |
| SCA1 | *ATXN1* | Ataxin 1 |
| SCA2 | *ATXN2* | Ataxin 2 |
| SCA3 | *ATXN3* | Ataxin 3 |
| SCA6 | *CACNA1A* | Calcium channel, voltage dependent, P/Q type, $\alpha_{1A}$ subunit |
| SCA7 | *ATXN7* | Ataxin 7 |
| SCA17 | *TBP* | TATA box-binding protein |
| DRPLA | *ATN1* | Atrophin-1 |
| ***Non coding expansion SCA*** | | |
| SCA8 | *ATXN8OS* | Ataxin 8 opposite strand |
| SCA10 | *ATXN10* | Ataxin 10 |
| SCA12 | *PPP2R2B* | Protein phosphatase 2, regulatory subunit B, β |
| SCA31 | *BEAN* | Brain expressed associated with NEDD4 |
| SCA36 | *NOP56* | Nuclear protein 56 |
| ***Conventional mutation SCA*** | | |
| SCA5 | *SPTBN2* | β-3 spectrin |
| SCA11 | *TTBK2* | Tau tubulin kinase 2 |
| SCA13 | *KCNC3* | Potassium voltage-gated channel, member 3 |
| SCA14 | *PRKCG* | Protein kinase Cγ |
| SCA15/16 | *ITPR1* | Inositol 1,4,5-triphosphate receptor, type 1 |
| SCA20 | Duplication within the region 11q12 | |
| SCA23 | *PDYN* | Prodynorphin |
| SCA27 | *FGF14* | Fibroblast growth factor 14 |
| SCA28 | *AFG3L2* | AFG3 ATPase family member gene 3-like 2 |
| SCA35 | *TGM6* | Transglutaminase 6 |

**Table 1. Spinocerebellar ataxias.** Adapted from *Sailer at al., 2012*.

### *1.1.2. X-linked cerebellar ataxias*

This group includes Fragile X-associated tremor/ataxia syndrome (FXTAS) and X-linked ataxia sideroblastic anemia (XLSA/A). FXTAS is due to a CGG repeat expansion in the 5' untranslated region of *FMR1*, which codes for a protein involved in mRNA metabolism. Interestingly, mutations with more than 200 repeats cause Fragile X syndrome due to a loss of function mechanism (Santoro et al., 2012), whereas pre-mutations (55-200 repeats) with RNA toxic functions are associated with FXTAS (Hagerman, 2013).

XLSA/A is a very rare disorder that is characterized by infantile non progressive ataxia and anemia. It is caused by mutations in the *ABCB7* gene that codes for a mitochondrial ATP half-transporter, involved in Fe/S protein metabolism (Allikmets et al., 1999, Bekri et al., 2000).

Recently, a missense mutation in the *ATP2B3* gene, coding for a calcium transporting ATPase, was identified in a patient with congenital cerebellar atrophy and ataxia (Zanni et al., 2012).

### *1.1.3. Recessive cerebellar ataxias*

Different forms of ataxias belong to this group. Most recessive ataxias present a childhood onset of symptoms, although some adult forms are also reported as in Friedreich ataxia (Tranchant and Anheim, 2009).

Different classifications of recessive ataxias have been proposed based on the clinical manifestations and/or the pathophysiology of the disease. However, these classifications are sometimes controversial, since new findings constantly lead to the discovery of new recessive ataxia genes but also to a better understanding of the molecular mechanisms involved in the different diseases (Embirucu et al., 2009, Manto and Marmolino, 2009, Tranchant and Anheim, 2009). However, although many efforts have been made to find the genetic causes of genetic ataxias, a large proportion of recessive ataxias still lacks a genetic diagnosis probably because they are caused by private mutations.

A classification of recessive ataxias based on the function of the mutated protein is reported in table 2. According to this classification, four main groups of recessive ataxias exist.

The first group includes disorders linked to DNA repair defects. This is the case for ataxia-telangiectasia (A-T), which is due to mutations in the *ATM* gene that codes for a phosphoinositol-3-kinase involved in cell cycle checkpoint control and DNA repair (Shiloh, 2003). Ataxias with oculomotor apraxia type 1 and 2 (AOA1 and AOA2) are associated with mutations in aprataxin, a nuclear protein involved in single-strand DNA repair, and senataxin involved in RNA processing and DNA repair, respectively (Le Ber et al., 2006).

A large group of recessive ataxias is linked to metabolic defects due to lipid metabolism alteration. This group is quite heterogeneous, and includes progressive ataxias as well as conditions where ataxia is intermittent or a minor feature (Palau and Espinos, 2006). Refsum's disease and Niemann-Pick type C are examples of such disorders. The former is characterized by a defect in the alpha-oxidation of fatty acids leading to an accumulation of phytanic acid in the blood and other tissues (Palau and Espinos, 2006), and the latter is a neurodegenerative lysosomal storage disorder, characterized by the accumulation of cholesterol and other lipids in the viscera and the central nervous system. It is caused by mutations in NP-C1 and NP-C2, two proteins involved in intracellular cholesterol trafficking (Peake and Vance, 2010).

Another group of recessive ataxias are caused by mutations in proteins involved in membranes and/or cytoskeleton dynamics. This is the case, for instance, for Salih ataxia caused by mutations in Rubicon, a protein involved in the endosomal/lysosomal machinery (Assoum et al., 2013). PHARC (Polyneuropathy, Hearing loss, Ataxia, Retinitis pigmentosa and Cataract) is another example. It is caused by alterations in ABHD12, the most abundant lysophosphatidylserine lipase in the mammalian brain (Blankman et al., 2013).

Finally, several ataxias are associated with a defect in mitochondrial proteins (Tranchant and Anheim, 2009). This is the case for Friedreich ataxia (FRDA), the most frequent form of recessive ataxias, as well as Mitochondrial recessive ataxia syndrome (MIRAS). FA is caused by a reduced expression of the mitochondrial protein frataxin implicated in the biogenesis of Fe-S clusters, small inorganic cofactors involved in many essential cellular pathways, from mitochondrial respiration to DNA synthesis and repair (Martelli et al., 2012). MIRAS and SANDO (sensory ataxic neuropathy dysarthria and ophthalmoparesis), are caused by mutations in polymerase gamma (*POLG*), which is the replicative polymerase for mitochondrial DNA (Fogel and Perlman, 2007).

ARCA2 is a recently described form of pure cerebellar ataxia associated to a deficiency in Coenzyme $Q_{10}$, a lipophylic compound involved in electron transport in the mitochondrial

respiratory chain (Lagier-Tourenne et al., 2008, Mollet et al., 2008). A complete description of ARCA2 is given in section 3 of the Introduction.

Interestingly, apart from ARCA2, other types of $CoQ_{10}$ deficiencies have ataxia as the main or secondary symptom. Among these, mutations in the genes *COQ6*, *APTX*, *PDSS1*, *PDSS2* and *COQ2* have been reported to be associated with ataxia and Coenzyme Q deficit. Although $CoQ_{10}$ deficiencies are associated to a wide spectrum of phenotypes (see paragraph 2.3 in the Introduction), the ataxic form is the most frequent, probably because it is less severe (Montero et al., 2007). $CoQ_{10}$ deficiencies will be described in greater details in section 2.

The few examples reported here give us an idea of how different the molecular and cellular pathogenesis of recessive ataxias can be. Indeed, very distinct pathways are affected, from global metabolic changes involving mitochondria and lipid biochemistry, to fundamental cellular processes such as DNA repair, protein folding and RNA processing. Moreover, altered pathways can affect different cell organelles, from mitochondria to peroxisome and lysosomes.

Why different cellular alterations can cause ataxia and affect cerebellar function so specifically is not clear. However, it seems evident that often a specific class of cerebellar neurons is more sensitive than others to these cellular defects. Affected neurons lead ultimately to a global dysfunction of the cerebellum.

| Ataxia | Gene | Protein | Function |
|---|---|---|---|
| ***DNA repair and RNA metabolism*** | | | |
| Ataxia telangiectasia (AT) | *ATM* | ATM | DNA repair |
| AT-like disorder (ATLD) | *MRE11* | MRE11 | DNA repair |
| AOA1 | *APTX* | Aprataxin | DNA repair |
| AOA2 | *SETX* | Senataxin | DNA/RNA helicase |
| SCAN1 | *TDP1* | Tyrosyl-DNA phosphodiesterase 1 | DNA repair |
| ***Lipid metabolism*** | | | |
| AVED | *ATTP* | α-Tocopherol transfer protein | VLDL formation |
| Abetalipoproteinemia | *ABL* | Microsomal triglyceride transfer protein | Transport of triglyceride |
| Neimann-Pick type C | *NPC1, NPC2* | NPC1, NPC2 | Cholesterol trafficking |
| Refsum syndrome | *PEX7, PHYH* | Peroxin-7, phytanoyl CoA hydrolase | Peroxisomal oxidation of fatty acids |
| ***Membrane/Cytoskeleton function*** | | | |
| SCAR8 (or ARCA1) | *SYNE1* | SYNE1 | Cytoskeleton |
| Salih ataxia (SAA) | *KIAA0226* | Rubicon | Endocytic trafficking |
| ANO10 (or SCAR10) | *ANO10* | ANO10 | Calcium activated chloride channels |
| PHARC | *ABHD12* | ABHD12 | lysophosphatidylserine metabolism |
| ARSACS | *SACS* | Sacsin | Protein folding |
| SCAR11 | *SYT14* | Synaptotagmin XIV | Membrane trafficking |
| MSS | *SIL1* | SIL1 | Protein folding in ER |
| Cayman ataxia | *ATCAY* | Caytaxin | Phosphatidylinositol signaling and Ca homeostasis |
| ***Mitochondrial function*** | | | |
| FRDA | *FXN* | Frataxin | Fe-S cluster biogenesis |
| IOSCA | *C10ORF2* | C10orf2 | mtDNA helicase |
| MIRAS & SANDO | *POLG* | Polymerase gamma | mtDNA replication |
| ARCA2 | *ADCK3* | ADCK3 | CoQ biosynthesis |

**Table 2. Classification of recessive ataxias based on the function of the mutated protein**. AOA: ataxia with oculomotor apraxia. ARSACS: spastic ataxia of Charlevoix-Saguenay. AVED: ataxia with isolated vitamin E deficiency. FRDA: Friedreich ataxia. IOSCA: infantile-onset spinocerebellar ataxia. MIRAS: mitochondrial recessive ataxia syndrome. MSS: Marinesco-Sjogren syndrome. PHARC: polyneuropathy, hearing loss, ataxia, retinitis pigmentosa, and cataract. SCAN1: spinocerebellar ataxia with axonal neuropathy. SCAR: spinocerebellar ataxia recessive. SANDO: sensory ataxic neuropathy dysarthria and ophthalmoparesis. VLDL: very low density lipoprotein.

### *1.2. Organization and function of the cerebellum*

The cerebellum is the area of the central nervous system that controls movements, motor coordination, balance and muscle tone. The cerebellum constitutes only 10% of the total volume of the brain, but contains more than one-half of its neurons (Kandel, 2013). Although it plays an important role in motor control, a growing body of evidence indicates that it might also be involved in other functions, especially certain cognitive processes (Apps and Garwicz, 2005).

The surface of the cerebellum is highly convoluted, with many parallel folds called *folia*. Two fissures divide the cerebellum into three lobes. The primary fissure separates the anterior and the posterior lobes, whereas the posterolateral fissure separates the smaller flocculonodular lobe (Figure 1).

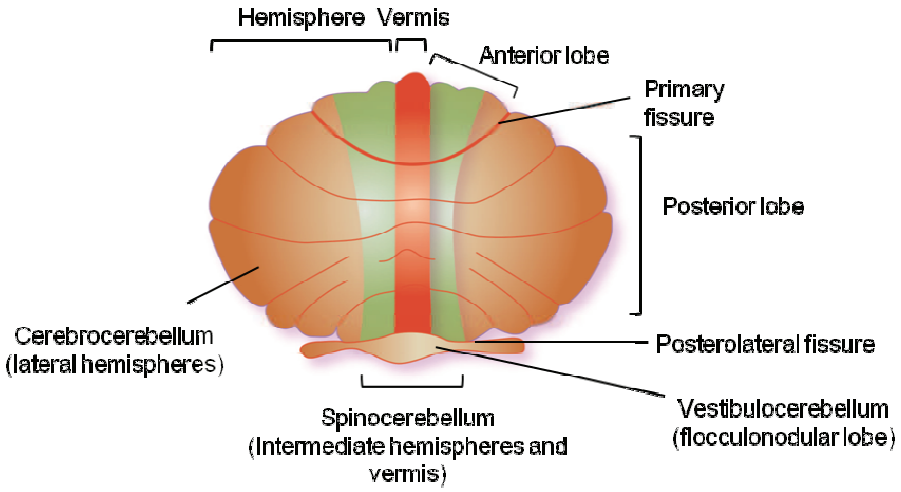


**Figure 1. Structure of the cerebellum.** A schematic representation of the gross morphology of the cerebellum. Functional regions (vetibulocerebellum, spinocerebellum and cerebrocerebellum) are also represented.

In the antero-posterior direction, two longitudinal furrows divide the cerebellum into three regions: the midline *vermis* (Latin, worm) and the *cerebellar hemispheres*. The small portion between vermis and hemisphere is often referred to as the *paravermis* (Figure 1 and 2). Both the vermis and the hemispheres are folded into lobules (and each lobule is subdivided into folia) that are well visible in midsagittal sections (Figure 2) (Kandel, 2013).

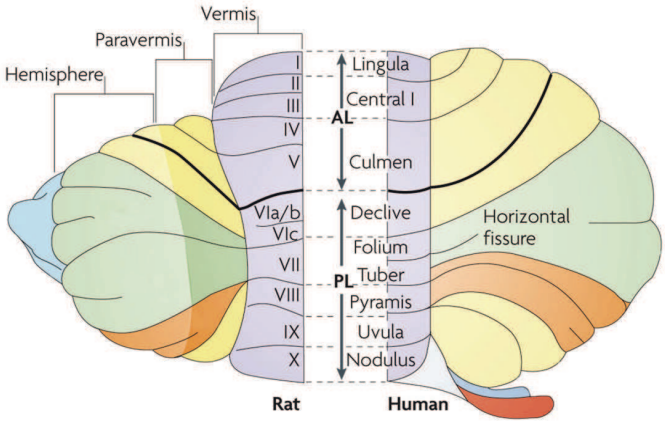


**Figure 2. Comparative morphology of rat and human cerebellum.** A dorsal view of the rat cerebellum (left) and the human cerebellum (right) to indicate the comparative nomenclature. Equivalent regions in the rat and human cerebellum are given the same color. On the left, the three longitudinal compartments are indicated (the vermis, the paravermis and the hemisphere). On the left, lobules (in violet) in the vermis are numbered according to Larsell's schema, whereas on the right, the corresponding nomenclature is provided as described by Bolk. *Adapted from Apps et al., 2009.*

Sagittal sections of the cerebellum illustrate clearly the general organization of the cerebellar cortex, which is divided into three layers and involves five main types of neurons (Figure 3). The deepest layer is the granular layer, which contains a vast number of granule cells that are small and densely packed neurons. This layer contains also a few larger Golgi interneurons. The middle layer is the Purkinje cell layer, which consists of a single sheet of Purkinje cells (PCs or Purkinje neurons). The superficial layer is the molecular layer, which contains two types of interneurons, the stellate and the basket cells. All of these cell types, with the exception of the granule cells, use the inhibitory neurotransmitter, GABA (γ-aminobutyric acid) (Kandel, 2013).

The granular cells are excitatory neurons that use glutamate as a neurotransmitter. They have small soma (5-10 μm in diameter) and send their axons into the molecular layer, where they bifurcate, in a typical "T" shape, to become parallel fibers (Figure 3). The parallel fibers run toward the cortical surface along the axis of the cerebellar folia, making excitatory synapses with the dendritic arbors of many Purkinje cells. Parallel fibers are also the main excitatory input to the Golgi, stellate and basket cells (Apps and Garwicz, 2005).

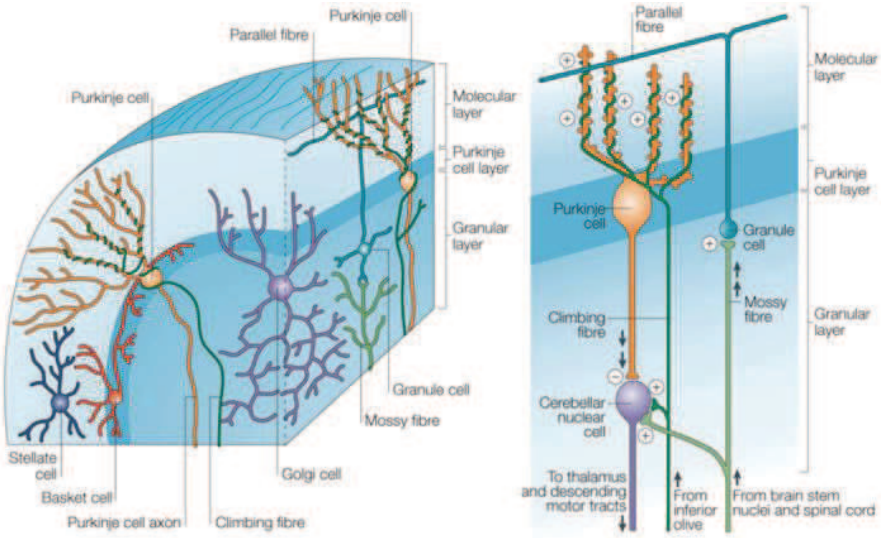


**Figure 3. Structure of the cerebellar cortex.** A sagittal section of the cerebellar cortex is showed on the right. Synapses of Purkinje neurons and granule cells are shown on the left. With the exception of granule cells, all cerebellar cortical neurons make inhibitory synaptic connections with their target neurons. *Adapted from Apps et al., 2005.*

Purkinje cells are big neurons (with cell bodies of 50-80 μm in diameter) that extend their planar dendritic trees into the molecular layer, where they synapse with parallel fibers. Purkinje cells are the sole output neurons of the cerebellar cortex, projecting their axons to the deep nuclei in the underlying white matter, or to the vestibular nuclei in the brain stem where GABA is released with inhibitory action (Kandel, 2013). The four paired deep cerebellar nuclei are imbedded in the white matter of the cerebellum (Ramnani, 2006) (Figure 4). From medial to lateral, these nuclei are the fasigial, the globose, the emboliform and the dentate (Figure 4) (Carpenter, 1996) .

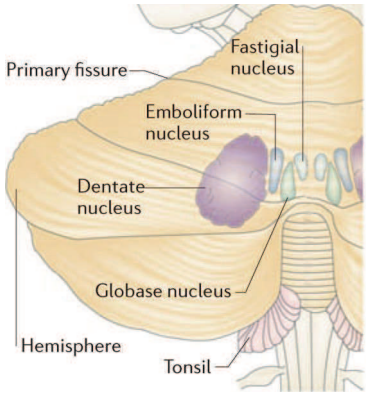


**Figure 4. Deep cerebellar nuclei.** A posterior view of the human cerebellum, showing the cerebellar nuclei imbedded below the cerebellar cortex. *Adapted from Ramnani, 2006*.

Basket cell somata are located in the lower portion of the molecular layer, close to the PCs. Each basket cell can be in contact with up to ten PCs. They can project their axons either into the molecular layer to be in contact with the proximal portions of PCs dendrites or to the base of the Purkinje cell somata (Watson, 2012).

The cerebellum is connected to the brain stem via three symmetrical pairs of peduncles: the *inferior cerebellar peduncle*, the *middle cerebellar peduncle* and the *superior cerebellar peduncle*. Most of the output axons of the cerebellum arise from the deep nuclei and project through the superior cerebellar peduncle. Afferents tracts enter the cerebellum mainly via the inferior and the middle cerebellar peduncles. Within the cerebellar cortex, these fibers lose their myelin sheath (Carpenter, 1996). There are only two types of afferent axons that enter the cerebellum, mossy fibers and climbing fibers. Both of these fiber types release excitatory neurotransmitters, glutamate in the case of the mossy fibers and aspartate in the case of climbing fibers (Figure 3).

Mossy fibers afferents originate from cell bodies in the spinal cord and brain stem. They target the dendrites of granule cells and, therefore, excite Purkinje cells indirectly. They are also in contact with various types of interneurons in the cerebellar cortex, both directly and indirectly through the parallel fibers (Apps and Garwicz, 2005).

The climbing fibers arise exclusively from the inferior olive, a well-defined complex of sub-nuclei in the ventral part of the caudal brain stem. In marked contrast to mossy fibers, the climbing fibers make direct synaptic contacts with Purkinje cells, enwrapping the cell body and the proximal dendrites of a PC. Each climbing fiber comes in contact with 1 to 10 Purkinje neurons, but each Purkinje neuron receives synaptic input from a single climbing fiber.

Based on the different inputs and outputs and the cerebellar connections, the cerebellum is divisible into three areas that have distinct roles in different kinds of movements: the vetibulocerebellum, the spinocerebellum and the cerebrocerebellum (Figure 1) (Kandel, 2013).

The vestibulocerebellum is the most primitive part of the cerebellum. It receives vestibular and visual inputs, and projects to the vestibular nuclei in the brain stem, hence participating in balance and eye movements (Swenson, 2006). The spinocerebellum comprises the vermis and the intermediates parts of the hemispheres and appeared later in phylogeny (Figure 1). It receives somatosensory and proprioceptive inputs from the spinal cord. The vermis receives visual, auditory and vestibular impulses as well as somatic sensory inputs

from the head and the proximal parts of the body (Carpenter, 1996). The vermis projects to the fastigial nucleus controlling the proximal muscles of the body and limbs. The intermediate parts of the hemispheres also receive somatosensory input from the limbs and project to the interposed nucleus, controlling more distal muscles of limbs and digits. Therefore, spinocerebellum controls muscle tone and coordination of the extremities. The cerebrocerebellum comprises the lateral parts of the hemispheres (Figure 1). The inputs to and the outputs from this region involve connections with the cerebral cortex. The output is transmitted through the dentate nucleus. The main function of the cerebrocerebellum is to participate in motor planning and execution of movements (Kandel, 2013).

Apart from the size of some cerebellar portions, the anatomy of mammalian cerebella is well conserved among different species. In Figure 2, equivalent regions of the rat and human cerebellum are marked with the same color. However, it is known that some differences exist. For example, mouse Purkinje cells are smaller and have less cytoplasm than human PCs (Treuting, 2012).

## 2. Coenzyme Q

### *2.1. Structure and distribution of Coenzyme Q*

Coenzyme Q (CoQ, UQ or Q) was isolated in 1955 (Festenstein et al., 1955), and in 1957, it was established by Crane and colleagues that CoQ functions as a member of the mitochondrial respiratory chain (Crane et al., 1957).

Coenzyme Q is a lipophilic molecule that is composed of a substituted benzoquinone and a long isoprenoid side chain. As the benzoquinone ring is redox active, CoQ exists in different redox forms: a form that is completely oxidized (ubiquinone), a form that is partially oxidized (ubisemiquinone), and a reduced form (ubiquinol).

The length of the lateral chain varies in different species and it contains six units in *S. cerevisiae* ($Q_6$), eight ($Q_8$) in *E. coli*, nine in mouse and rat ($Q_9$) and ten in humans ($Q_{10}$). However, in most species, one chain length of CoQ is dominating and in a minor extent a CoQ with a shorter or longer side chain is also found. For instance, about 10-20% of the total CoQ in most rat tissues is the $CoQ_{10}$ form (Aberg et al., 1992).

Coenzyme Q is present in all tissues and cells in variable amounts. In rat, as well as in humans, CoQ is more abundant in heart, kidney and liver (Table 3) (Aberg et al., 1992).

| | Rat | | Human | |
|---|---|---|---|---|
| | **$CoQ_9$** | **$CoQ_{10}$** | **$CoQ_9$** | **$CoQ_{10}$** |
| Heart | 202 | 17 | 3 | 114 |
| Kidney | 124 | 22 | 3 | 67 |
| Liver | 131 | 21 | 2 | 55 |
| Muscle | 43 | 3 | 1 | 40 |
| Brain | 37 | 19 | 1 | 13 |
| Pancreas | 37 | 3 | 2 | 33 |
| Spleen | 23 | 9 | 1 | 25 |
| Lung | 17 | 2 | 1 | 8 |

**Table 3**. **Coenzyme Q levels in rat and human tissues (µg/g tissue).** Adapted from *Turunen et al., 2003*.

In the cell, Coenzyme Q is located in all membranes, and it is particularly abundant in mitochondria, lysosomes and the Golgi apparatus (Table 4) (Kalen et al., 1987).

| Organelle | CoQ | Cholesterol |
|---|---|---|
| Nuclear envelope | 0.2 | 37.5 |
| Mitochondria | 1.4 | 2.3 |
| Microsomes | 0.2 | 28 |
| Lysosomes | 1.9 | 38 |
| Golgi vesicles | 2.6 | 71 |
| Peroxisomes | 0.3 | 6.4 |
| Plasma membrane | 0.7 | 128 |

**Table 4**. **Coenzyme Q and cholesterol concentration in subcellular organelles of rat liver (µg/mg proteins).** Adapted from *Turunen et al., 2004*.

Interestingly, the localization of lipids generated by the mevalonate pathway (see paragraph 2.2.1), such as Coenzyme Q and cholesterol, influences the properties of membranes. The long lateral chain of Coenzyme Q is localized between the two leaflets of a membrane pushing them away. This position destabilizes the membranes, increasing their fluidity and permeability. On the other hand, cholesterol is located between fatty acids on one side of the lipid leaflet, stabilizing it and decreasing the fluidity and permeability of the membrane (Figure 5) (Lenaz et al., 1992).

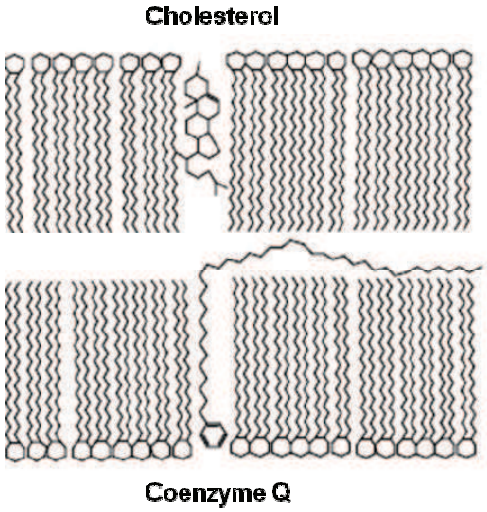


**Figure 5**. **Intramembraneous distribution of the lipids synthetized by the mevalonate pathway.** Adapted from *Turunen et al., 2004*.

### *2.1.1. Functions of Coenzyme Q*

Coenzyme Q is involved in a number of cellular functions due to its wide distribution in the cell. The most important and most extensively investigated role of Coenzyme Q is its involvement in cellular energy production, participating in oxidative phosphorylation (OXPHOS) by carrying electrons from mitochondrial complexes I and II to complex III (Figure 6). The crucial function of CoQ in the mitochondrial respiratory chain was first described by Crane and colleagues in 1957 (Crane et al., 1957). Subsequently, in 1975, Mitchell proposed the theory of the proton-motive ubiquinone cycle. According to this theory, CoQ undergoes a series of reduction and oxidation reactions, allowing the transfer of protons to the mitochondrial intermembrane space. The proton-motive force generated by this proton gradient is then used to produce ATP (Mitchell, 1975).

The capacity of Coenzyme Q to undergo cycles of reduction and oxidation is also important in lysosomes and plasma membranes. In lysosomes, CoQ is a constituent of the lysosomal electron transport chain. There, CoQ promotes proton translocation across the lysosomal membrane, and it is responsible for the acidification of lysosomes (Gille and Nohl, 2000). In plasma membranes, CoQ participates in the electron transfer necessary for the activation of the antiport $H^+/Na^+$, which in turn leads to cytoplasmic pH changes (Crane et al., 1991). Moreover, in plasma membranes, CoQ shuttles electrons to NOX (NADH oxidase), a protein located at the external surface of the plasma membrane. Consequently, CoQ is involved in the regulation of the cytosolic $NAD^+$/NADH ratio through its function in electron transfer (Larm et al., 1994).

Coenzyme Q is also an obligatory cofactor for the activation of mitochondrial uncoupling proteins (UCPs). These proteins, located in the inner mitochondrial membrane, are able to decouple the proton gradient generated by the respiratory chain from oxidative phosphorylation and generate heat rather than energy (Echtay et al., 2000).

Coenzyme Q is also known to prevent the opening of the mitochondria permeability transition pores (PTPs) (Fontaine et al., 1998). Upon $Ca^{2+}$ accumulation, PTP opens and macromolecules with a size of approximately 1500 Da can cross the membrane, causing a collapse of the mitochondrial function. Since the permeability transition is an early event in several models of apoptosis, Coenzyme Q was suggested to negatively regulate apoptosis (Papucci et al., 2003).

Another very important function of Coenzyme Q is to act, in its reduced form (ubiquinol), as an effective antioxidant. Oxidative stress is caused by an excessive production of reactive oxygen species (ROS), which include superoxide radicals ($O_2^{-\bullet}$), hydrogen peroxide ($H_2O_2$) and hydroxyl radicals ($HO^{\bullet}$). ROS are produced in multiple cell compartments and in a number of enzymatic processes from the metabolism of molecular oxygen. However, mitochondria are considered the major source of $O_2^{\bullet -}$ and $H_2O_2$ production in the cell. The production of mitochondrial superoxide radicals occurs primarily at complex I (NADH dehydrogenase) and complex III (ubiquionone-cytocrome c reductase) of the respiratory chain (Figure 6) (Finkel and Holbrook, 2000).

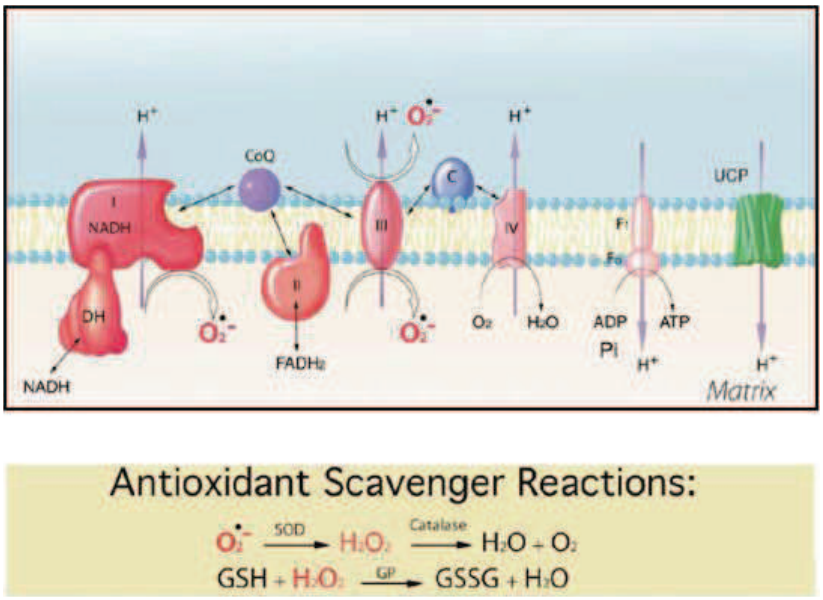


**Figure 6. A schematic model of ROS generation in mitochondria.** The mitochondrial respiratory chain is showed (upper part) with complexes I and III as major sources of ROS. The antioxidant reactions catalyzed by superoxide dismutase (SOD), catalase and gutathione peroxidase (GP) are described (bottom part). *Adapted from Balaban et al., 2005.*

ROS are known to affect the constituents of the cells: protein, DNA and lipids. To minimize the damaging effects of ROS, organisms have developed non-enzymatic and enzymatic antioxidant defenses. Non-enzymatic defenses include several compounds, such as vitamin C, vitamin E and Coenzyme Q. Enzymatic defenses include several enzymes that scavenge superoxide radicals and hydrogen peroxide converting them to less reactive species. Examples of such enzymes are: superoxide dismutase (SOD), catalase and glutathione

peroxidase. SOD eliminates the superoxide radical converting it to oxygen and $H_2O_2$. There are different forms of SOD: a Cu/Zn form predominantly localized in the cytosol (SOD1) and a Mn form in mitochondria (SOD2). Catalase and glutathione peroxidase reduce $H_2O_2$ to $2H_2O$ (Figure 6) (Scandalios, 2005).

Coenzyme Q executes its antioxidant role mainly by inhibiting lipid peroxidation, but also by interfering with protein and DNA oxidation (Bentinger et al., 2007). Several studies documented the potential therapeutic role of CoQ for the treatment of neurodegenerative diseases. For instance, it has been shown that $CoQ_{10}$ administration inhibits ROS formation in $H_2O_2$ pre-treated neuronal cell lines, therefore preventing mitochondrial dysfunction and apoptosis (Somayajulu et al., 2005).

#### *2.1.2. Coenzyme Q and metabolism*

Recent lines of evidence suggest that Coenzyme Q can play an important role in the regulation of mammalian metabolism.

Bour and colleagues showed that Coenzyme Q is an anti-adipogenic factor as it was found to be decreased in adipose tissues of obese mice. Moreover, inhibition of CoQ biosynthesis in a preadipocyte cell line leads to adipose differentiation (Bour et al., 2011).

Furthermore, it has been reported that short term, as well as long term, ubiquinol supplementation affects genes involved in liver lipid metabolism, cholesterol metabolism and PPAR signalling (Schmelzer et al., 2010) (Schmelzer et al., 2012).

Finally, Coenzyme Q distribution and biosynthesis itself seems to be regulated by diet in a tissue-specific manner. In particular, calorie restriction increased both ubiquinone forms, $Q_9$ and $Q_{10}$, in skeletal muscle whereas it decreased $Q_9$ in heart (Parrado-Fernandez et al., 2011).

### *2.2. Biosynthesis of Coenzyme Q*

Cells commonly rely on *de novo* synthesis for their supply of ubiquinone. The biosynthetic pathway of CoQ has been extensively studied in yeast and bacteria, whereas less is known about this process in mammals. In the budding yeast *S. cerevisiae,* 11 genes have been

characterized as essential for CoQ biosynthesis, so far (Tran and Clarke, 2007). These are *coq1* through *coq9*. Recently, Pierrel and colleagues identified ferredoxin (Yah1p) and ferredoxin reductase (Arh1p) as essential for CoQ biosynthesis in yeast (Tran and Clarke, 2007, Pierrel et al., 2010).

Figure 7 depicts the pathway of CoQ biosynthesis in *S. cerevisiae*. Coq1p, an isoprenyl diphosphate synthase, generates the isoprenoid chain that constitutes the final lateral chain of CoQ. Coq2p successively couples the isoprenoid chain to the quinone ring precursors, 4-hydroxybenzoic acid (4-HB) or para-aminobenzoic acid (pABA), to generate 3-hexaprenyl-4-hydroxybenzoic acid (HHB) and 3-hexaprenyl-4-aminobenzoic acid (HAB), respectively. The aromatic ring then undergoes a series of modifications to produce Coenzyme Q. At least 4 Coq proteins are involved in these modifications, although not all steps have been associated to a specific enzyme. First Coq6p catalyzes the hydroxylation at position C5 of the benzoquinone ring. Coq3p is responsible for two *O*-methylation steps. Coq5p carries out the C-methylation step, whereas Coq7p is required for the penultimate step introducing the last hydroxyl group (Tran and Clarke, 2007, Wang and Hekimi, 2013).

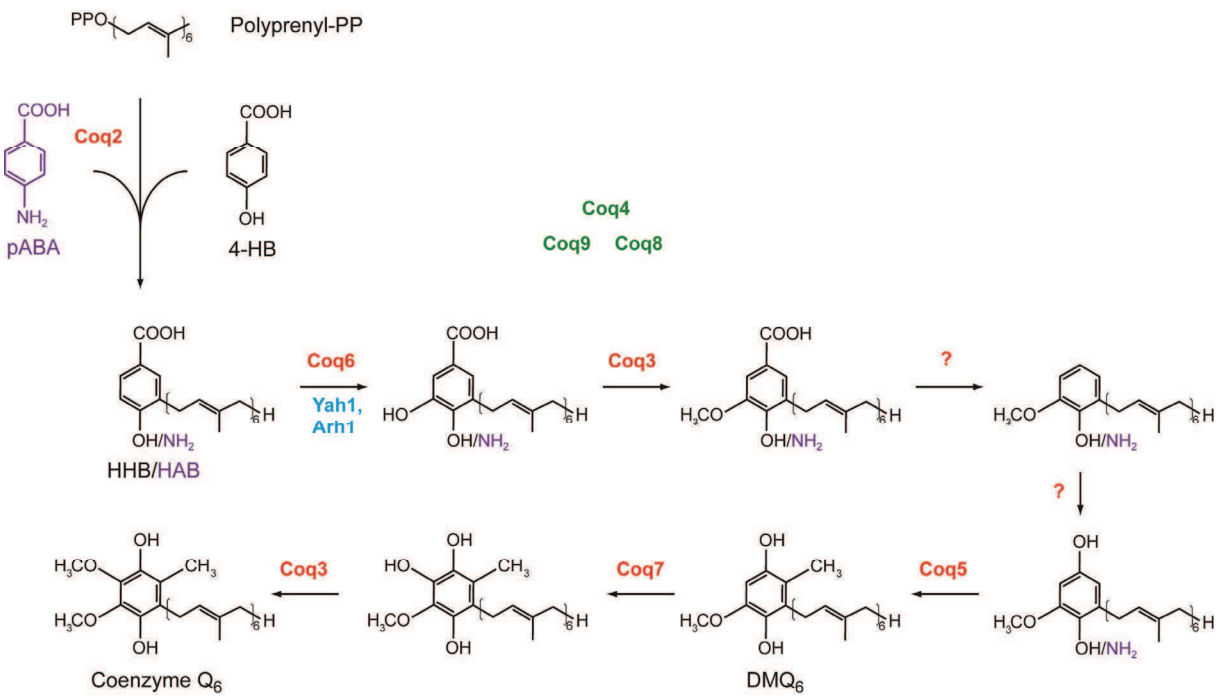


**Figure 7. Coenzyme Q biosynthesis in *Saccharomyces cerevisiae*.** The pathway starts with the assembly of the isoprenoid tail (polyprenyl-PP) catalyzed by Coq1p (not shown). $NH_2$ and the intermediate HAB derived from pABA are shown in purple. Enzymes required for modifications of benzoquinone ring are shown in red. Question mark (?) indicates that the

enzyme involved the reaction has not been identified yet. Coq proteins involved in the regulation of the pathway or with undefined function are shown in green. Abbreviations: pABA, para-aminobenzoic acid; HHB, 3-hexaprenyl-4-hydroxybenzoic acid; HAB, 3-hexaprenyl-4-aminobenzoic acid; DMQ, demethoxyubiquinone.

Coenzyme Q biosynthesis requires the formation of a high molecular mass complex involving most Coq proteins, which associates to the mitochondrial inner membrane on the matrix side (Figure 8) (Tran and Clarke, 2007). The initial hint for the existence of a complex was that yeast mutants carrying single deletions in *coq3-coq9* genes do not produce $Q_6$ and accumulate the intermediate HHB (Poon et al., 1997). Furthermore, the steady-state levels of Coq3p, Coq4p, Coq6p, Coq7p and Coq9p are strongly decreased in any of *coq1-coq9* null mutants suggesting that the stability of Coq proteins depends on each other (Hsieh et al., 2007). Moreover, gel filtration and blue native (BN)-PAGE experiments provided further insight into the composition of the Coq complex although the data available so far are controversial. Using (BN)-PAGE, Coq3p and Coq4p were shown to associate in a complex of > 1MDa (Marbois et al., 2005), together with Coq7p (Tran et al., 2006) or Coq9p (Hsieh et al., 2007). Gel filtration experiments revealed that Coq3p, Coq4p and Coq6p (Marbois et al., 2005) or Coq7p (Tran et al., 2006) coelute in a complex of > 700 kDa. On the other hand, Tauche and colleagues reported the existence of a complex of about 1.3 MDa, including Coq3p, Coq5p and Coq9p as main constituents, with Coq8p weakly or transiently associated to it (Tauche et al., 2008). The authors also found an additional complex of 500-760 kDa composed of Coq2p, Coq5p, Coq8p and Coq10p, representing an intermediate or an additional separate complex. Although the organization of the complex has not been resolved yet, it seems evident that Coq8p plays a crucial role in stabilizing it. First, overexpression of Coq8p restores steady-state levels of some Coq proteins (Coq3p, Coq4p, Coq 7p and Coq9p) in several *coq* null mutants, indicating that Coq polypeptides are stabilized in presence of more Coq8p (Zampol et al., 2010, Xie et al., 2012). Moreover, in several *coq* null mutants, the overexpression of Coq8p allowed the accumulation of the $Q_6$ biosynthetic intermediates whereas only early precursors are usually detectable under basal expression of Coq8p (Padilla et al., 2009, Xie et al., 2012). In addition, depletion of Coq8p leads to the disappearance of Coq3p from the 1.3 MDa complex (Tauche et al., 2008). Altogether, these findings suggest that Coq8p prevents the complex from dissociating, and that it has a regulatory role in Coenzyme Q biosynthesis.

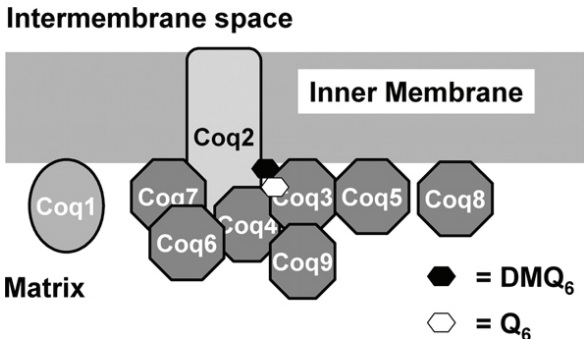


**Figure 8. Model of the mitochondrial CoQ biosynthetic complex in yeast.** Coq2p is an integral membrane protein associated to the inner mitochondrial membrane (IMM). Coq3p-Coq9p are peripherally associated to the matrix side of the IMM. Adapted from *Tran and Clarke, 2007.*

However, it is still not completely clear how Coq8p regulates Coenzyme Q biosynthesis. Sequence analysis suggests that Coq8p might act as a kinase (Leonard et al., 1998). Tauche and colleagues showed that phosphorylation of Coq3p is impaired in Coq8p-deficient yeast strains, suggesting that Coq3p is a potential substrate of Coq8p (Tauche et al., 2008). Moreover, Coq5p and Coq7p were also proposed to be substrates of Coq8p (Xie et al., 2011). However, none of these experiments show direct phosphorylation of the potential substrates by Coq8p, leaving the question open.

### *2.2.1. The mevalonate pathway*

The isoprenoid chain present on the Coenzyme Q molecule is generated by the mevalonate pathway. This is an important metabolic pathway, which, through a series of reactions, converts acetyl-CoA to farnesyl-PP, the precursor of cholesterol, CoQ, dolichol and isoprenylated proteins (Figure 9) (Bentinger et al., 2010).

In the initial steps of the mevalonate pathway, Acetyl-CoA units are first converted to 3-hydroxy-3-methylglutaryl-CoA (HMG-CoA) and then to mevalonate. 3-hydroxy-3-methylglutaryl-CoA reductase (HMGCR), the rate-limiting enzyme of the mevalonate pathway, catalyzes the conversion of HMG-CoA to mevalonate. The mevalonate goes then through different steps of phosphorylation and decarboxylation to yield isopentenyl pyrophosphate (IPP). IPP is subsequently converted in farnesyl pyrophosphate (FPP), which is used as a precursor of both Coenzyme Q and cholesterol. Squalene synthase (also called

farnesyl-diphosphate farnesyltransferase 1, Fdft1) catalyzes the first committed step of cholesterol biosynthesis, by dimerizing two molecules of FPP to form squalene (Buhaescu and Izzedine, 2007). On the other branch of the pathway, Coq1, a trans-prenyl transferase, generates the polyprenyl pyrophosphate, which is the precursor of the future lateral chain of Coenzyme Q.

Since the initial reactions leading to all end-products of the mevalonate pathway are identical, it might be expected that synthesis of these various lipids is co-regulated.

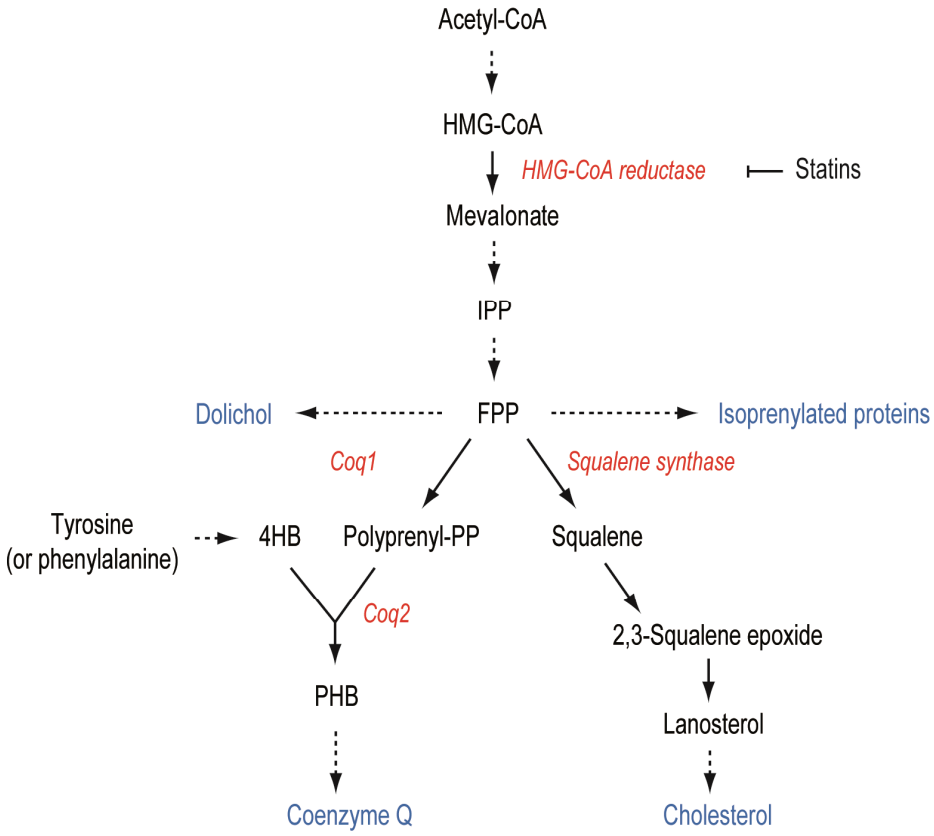


**Figure 9. The mevalonate pathway.** Several isoprenoid products (in blue) are generated by the mevalonate pathway. In red are the key enzymes of the pathway. Coq1 is a trans-prenyl transferase, Coq2 is a polyprenyl-4-hydroxy-benzoic acid transferase. Adapted from *Bentinger et al., 2010*.

### *2.2.2. Coenzyme Q biosynthesis in mammals*

Several recent studies have allowed a better understanding of Coenzyme Q biosynthesis in mammals. The mammalian homologues of yeast *coq* genes have been identified by sequence homology and functional complementation. In humans, as well as in mouse, the isoprenyl diphosphate synthase (Coq1p in yeast) is a heterotetramer composed of two subunits designated PDSS1 and PDSS2 (Saiki et al., 2005). Moreover, ADCK3 was proposed to correspond to yeast Coq8p, although a family of 5 ADCKs (ADCK1-5) is present in humans and mouse, suggesting that this function can be redundant. I will discuss the current knowledge about the ADCK family in later sections (paragraph 3.3). Finally, the remaining genes involved in the Coenzyme Q pathway are designated as in yeast (*COQ2*, *COQ3*, *COQ4*, *COQ5*, *COQ6*, *COQ7* and *COQ9*).

### *2.2.3. Localization of Coenzyme Q biosynthesis*

The classical view places the biosynthesis of Coenzyme Q in mitochondria where all enzymes involved in this pathway are localized. Coq1p and Coq3p-Coq9p were shown to be peripherally associated to the matrix side of the IMM, whereas Coq2p is an integral membrane protein associated to the IMM (Tran and Clarke, 2007, Tauche et al., 2008) (Figure 8). Once synthetized in mitochondria, Coenzyme Q moves to its final destinations to be distributed in almost all membranes of the cell. In particular, using the radiolabeled precursor [$^{14}$C]-pHB in a human cell line, it was shown that endogenous $CoQ_{10}$ is first detected in mitochondria where it is produced, and only later incorporated into the endoplasmic reticulum (ER) with the plasma membrane being the last location of newly synthetized $CoQ_{10}$ (Fernandez-Ayala et al., 2005). How mitochondrially synthetized Coenzyme Q travels into the cell is still obscure. Direct connections occur between the outer mitochondrial membrane and the endoplasmic reticulum, but with insufficient frequency to represent a major route of delivery of CoQ to the plasma membrane (Rowland and Voeltz, 2012).

Several lines of evidence suggest that Coenzyme Q biosynthesis can also occur in other cellular compartments such as the Golgi apparatus and ER, at least in vertebrates. In fact, initially only the trans-prenyltransferase activity (corresponding to Coq1p) and the prenyl-4-hydroxybenzoate transferase activity (corresponding to Coq2p) were found to locate in the

endoplasmic reticulum-Golgi apparatus complex in rat liver (Teclebrhan et al., 1995). However, more recently, enzymes involved in the last steps of Coenzyme Q biosynthesis such as COQ6 and COQ7, were also shown to localize in Golgi in murine podocytes (Heeringa et al., 2011). Interestingly, a new gene, *ubiadA*, has recently been described to be involved in $CoQ_{10}$ synthesis in zebrafish. Ubiad1 has a prenyltransferase activity similar to COQ2, but it was found to localize in Golgi (Mugoni et al., 2013). Therefore, these new findings raise the question of whether different pools of Coenzyme Q exist in mammalian cells to efficiently supply Coenzyme Q in the diverse sites where it is required. Furthermore, the existence of different biosynthetic sites could also generate multiple pools of Coenzyme Q, which will carry out different CoQ functions.

### *2.3. Coenzyme $Q_{10}$ deficiencies*

Human Coenzyme $Q_{10}$ deficiencies are clinically and genetically heterogeneous diseases all characterized by a deficit in $CoQ_{10}$. In most cases, family history and recurrence of the disease suggest an autosomal recessive mode of inheritance. Five major phenotypes have been associated to these syndromes: 1) encephalomyopathy, 2) severe infantile multisystemic disease, 3) cerebellar ataxia, 4) isolated myopathy and 5) nephrotic syndrome (Quinzii and Hirano, 2011).

The extreme clinical heterogeneity of $CoQ_{10}$ deficiencies reflects the diversity of genetic causes associated to this syndrome. So far, pathogenic mutations have been identified in genes involved in the biosynthesis of $CoQ_{10}$ (primary $CoQ_{10}$ deficiency) or in genes not directly related to $CoQ_{10}$ biosynthesis (secondary $CoQ_{10}$ deficiency).

However a big number of patients with $CoQ_{10}$ deficiency still lack a genetic diagnosis (Rahman et al., 2012). This suggests that either there are still genes involved in Coenzyme Q biosynthesis to be discovered or that $CoQ_{10}$ deficiency in those patients is a secondary phenomenon.

Coenzyme $Q_{10}$ deficiencies show a wide spectrum of symptoms. I have therefore summarized all genes responsible for this syndrome as well as the main organs affected in each form in Table 5.

### 2.3.1. Primary $CoQ_{10}$ deficiencies

Primary $CoQ_{10}$ deficiencies are rare diseases that are usually associated to severe clinical manifestations. To date, mutations in seven genes involved in $CoQ_{10}$ pathway have been reported to be associated to $CoQ_{10}$ deficiency in humans (Table 5). *PDSS2* mutations have been reported in a child with fatal Leigh syndrome and nephropathy who died at the age of 8 months because of a severe epileptic encephalopathy (Lopez et al., 2006). A homozygous mutation in *PDSS1* has been found in two siblings showing a multisystemic disease with encephaloneuropathy, deafness, mental retardation, obesity and valvulopathy (Mollet et al., 2007). Mutations in *COQ2* have been described in eight patients from six different families. Different manifestations have been described, from fatal neonatal multisystem disorders (Quinzii et al., 2006, Mollet et al., 2007) to isolated nephrotic syndrome (Diomedi-Camassei et al., 2007). Interestingly, nephrotic syndrome was present in all reported *COQ2* patients.

Curiously, although PDSS1 and PDSS2 are two subunits of the same enzyme (the transprenyltransferase, equivalent to yeast Coq1p), mutations in these genes lead to different phenotypes. In fact, the renal disease was observed in patients with mutations in PDSS2 but not PDSS1. On the other hands, *PDSS2* and *COQ2* mutations give rise to similar phenotypes.

A homozygous mutation in *COQ9* was reported in a boy with a severe infantile multisystemic disease, which includes seizures, cerebral and cerebellar atrophy, renal tubular dysfunction, mild cardiopathy and muscle defect (Duncan et al., 2009).

Mutations in *COQ6* have been reported in twelve patients, all with nephrotic syndrome and sensorineural hearing loss. Moreover, in some patients ataxia or seizures were also present (Heeringa et al., 2011).

Haploinsufficiency of *COQ4* has recently been found in a boy with mental retardation, encephalomyopathy, hypotonia, and dysmorphic features (Salviati et al., 2012).

Finally, *ADCK3* mutations have been reported in patients with slowly progressive cerebellar ataxia and atrophy (Lagier-Tourenne et al., 2008, Mollet et al., 2008, Gerards et al., 2010, Horvath et al., 2012, Terracciano et al., 2012). The clinical manifestations of these patients will be extensively discussed in paragraph 3.1.

Although primary $CoQ_{10}$ deficiencies are caused by mutations occurring in genes involved in the same pathway, a marked phenotypic diversity is evident. The explanation of this strong

clinical heterogeneity is still unclear, but it might reflect a tissue-specific regulation of $CoQ_{10}$ biosynthesis or a variable physiological sensitivity of different organs to $CoQ_{10}$ levels.

### *2.3.2. Secondary $CoQ_{10}$ deficiencies*

Secondary $CoQ_{10}$ deficiencies have been reported in different disorders caused by mutations in genes not directly involved in $CoQ_{10}$ biosynthesis. Therefore, $CoQ_{10}$ deficit appears as a secondary event in the pathology of these diseases. Moreover, $CoQ_{10}$ deficit is not a constant feature in all secondary $CoQ_{10}$ deficiencies, but is only present in a subset of patients. The mechanisms of $CoQ_{10}$ deficiency in these patients remain unknown (Hirano et al., 2012), but it could be a secondary effect due to a mitochondrial or a metabolic defect.

Mutations in *ETFDH* and *APTX*, the genes encoding the electron transfer flavoprotein dehydrogenase and aprataxin, respectively, have been associated with secondary $CoQ_{10}$ deficiency (Rahman et al., 2012). Patients with mutations in *ETFDH* have isolated myopathy, exercise intolerance and lipid accumulation in skeletal muscle (Gempel et al., 2007). Episodic encephalopathy, hepatopathy and periodic vomiting may also be present (Liang et al., 2009). Biochemical investigations with tandem mass spectrometry revealed that patients with *ETFDH* mutations are affected by multiple acyl-CoA dehydrogenase deficiency (MADD), a disorder of fatty acid and amino acid metabolism.

Mutations in *APTX* cause ataxia oculomotor apraxia 1 (AOA1) (Table 2), characterized by early onset ataxia, muscle weakness and oculomotor apraxia (defect of controlled and voluntary eye movements) (Date et al., 2001, Moreira et al., 2001). Aprataxin is a protein involved in single- and double- strand DNA break repair and localizes to nuclei and mitochondria (Sykora et al., 2011).

Secondary $CoQ_{10}$ deficiency has also been reported in patients with mitochondrial DNA (mtDNA) mutations. This is the case of 25 patients with mitochondrial encephalopathies (Matsuoka et al., 1991) and 28 patients with heterogeneous mitochondrial diseases (Sacconi et al., 2010).

| $CoQ_{10}$ deficiency's form | Gene | $CoQ_{10}$ deficiency | Main organs and tissues involved |
|---|---|---|---|
| Encephalomyopathy | *COQ2* | I | CNS, muscle and kidney |
| | *COQ4* | I | CNS, muscle |
| | *ETFDH* | II | CNS, muscle |
| Severe multisystemic disease | *COQ2* | I | CNS, liver and kidney |
| | *PDSS1* | I | CNS, eyes, heart and muscle |
| | *PDSS2* | I | CNS, kidney |
| | *COQ9* | I | Cerebrum, cerebellum, kidney, heart and muscle |
| Cerebellar ataxia | *ADCK3* | I | Cerebellum, muscle |
| | *APTX* | II | Cerebellum |
| Nephrotic syndrome | *COQ6* | I | Kidneys and ears |

**Table 5. Primary and secondary coenzyme $Q_{10}$ deficiencies.** Genes mutated in primary (I) and secondary (II) forms of $CoQ_{10}$ deficiencies and the main systems affected are reported. CNS, central nervous system.

### *2.4. Models of CoQ deficiency*

The wide range of phenotypes associated with $CoQ_{10}$ deficiency, and the involvement of $CoQ_{10}$ in many different cellular processes make it challenging to understand the pathogenesis of $CoQ_{10}$ deficiencies. Therefore, many different *in vitro* and *in vivo* models have been generated and studied to elucidate the functional and molecular consequences of Coenzyme Q deficit.

#### *2.4.1. Cellular models of CoQ deficiency*

The consequences of $CoQ_{10}$ deficiency on mitochondrial bioenergetics, oxidative stress and cell death have been studied in skin fibroblasts from patients.

Initial investigations on fibroblasts from two patients with infantile-onset of $CoQ_{10}$ deficiency showed mild energetic defects of the respiratory chain and no signs of increased ROS or apoptosis (Geromel et al., 2001).

In fibroblasts carrying mutations in *COQ2,* a defect in energy production as well as in *de novo* pyrimidine biosynthesis was found in a first study (Lopez-Martin et al., 2007). Later, *COQ2* mutations were shown to lead to increased production of ROS and increased levels of lysosomal and autophagic markers. Autophagy was suggested to have a protective role through the degradation of dysfunctional mitochondria (Rodriguez-Hernandez et al., 2009).

Interesting results were also obtained by the comparative study of fibroblasts with different degrees of $CoQ_{10}$ deficiency. It emerged from these experiments that the amount of residual $CoQ_{10}$ in the cells determines the pathogenic mechanisms. In fact, patient cell lines with 10–15% or > 60% residual $CoQ_{10}$ (carrying mutations in *PDSS2*, *COQ9*, or *ADCK3*), showed markedly reduced ATP synthesis without significant oxidative stress, whereas intermediate $CoQ_{10}$ deficiency with 30-40% of normal $CoQ_{10}$ amount (mutations in *COQ2*) caused partial bioenergetics defect but a marked increase in ROS production and oxidative damage, which correlates with increased cell death (Quinzii et al., 2008, Quinzii et al., 2010).

Thus, different mechanisms have been found to be involved in the pathogenesis of $CoQ_{10}$ deficiency *in vitro*, ranging from bioenergetics defect to increased oxidative stress and cell death. However, fibroblasts are not affected in patients with $CoQ_{10}$ deficiencies, suggesting that more relevant models are needed.

### *2.4.2. Invertebrate models of CoQ deficiency*

A number of animal mutants have been described in which different proteins involved in Coenzyme Q biosynthesis are mutated or inactivated. The advantage of studying animal models for CoQ deficiency is to gain insight into the functional consequences of CoQ deficit in different tissues and organs.

Different *C. elegans coq* mutants have been generated, and most of them are not viable. In particular, homozygous *coq-2* and *coq-3* mutants die during larval development, whereas *coq-1* mutants were slow growing but able to develop to at least the L3 stage with a few adult escapers. Mutant worms for *coq-4 and coq-6* are embryonic lethal as well as *coq-8* mutants although a few escapers die at the first larval stage. Thus, these data suggest that a complete block of CoQ biosynthesis in *C. elegans* is lethal and that CoQ is required for development in worms (Wang and Hekimi, 2013).

Unlike the *coq* mutants described above that are lethal even on a $CoQ_8$ rich diet, *clk-1/coq-7* worms are viable, fertile and long-lived if fed a diet containing $CoQ_8$. However, in the absence of $CoQ_8$, the animals no longer exhibit the pleiotropic long-lived phenotype, showing early developmental arrest and sterility, further indicating an essential requirement for CoQ during development and reproduction (Hihi et al., 2002).

The studies on worm mutants also allow to define which tissues are more susceptible to CoQ depletion. In fact, homozygous *coq-1* mutants exhibited progressive paralysis associated with the malfunction of pharyngeal muscles suggesting that Coenzyme Q has an important role in muscle (Wang and Hekimi, 2013).

Moreover *coq-1* mutant as well as *coq-1* RNAi-treated worms developed progressive loss of motor coordination and selective death of GABA neurons, suggesting that this subtype of neurons are specifically sensitive to CoQ deficit (Earls et al., 2010).

### *2.4.3. Murine models of CoQ deficiency*

In order to study the pathophysiology of Coenzyme $Q_{10}$ deficiencies and understand the role of Coenzyme Q in mammals, several murine models have been generated. A number of knockout (KO) mouse models have been generated in order to have models to study human Coenzyme Q deficiencies. Complete KO mice for *Pdss2* (Peng et al., 2008, Lu et al., 2012), *Coq7* (Levavasseur et al., 2001, Nakai et al., 2001), *Coq3* (Lapointe et al., 2012) and *Coq4* (http://www.knockoutmouse.org/about/eucomm) are embryonic lethal, demonstrating the crucial role of Coenzyme Q during mammalian development.

Whether a CoQ biosynthetic complex exists also in mammals is not known yet. However it has been shown that *Coq7* KO embryos accumulate demethoxyubiquinone 9 ($DMQ_9$), the substrate of COQ7 (Nakai et al., 2001), and not the early precursor HHB (the Coq2p product) as it occurs in yeast (Poon et al., 1997), indicating that the CoQ biosynthetic pathway before the COQ7 step is still functional and active in mouse also in absence of *Coq7*. This finding would suggest that either the complex does not exist in mammals or it is more stable and not destabilized by removing only one component.

A detailed description of these models is in manuscript 1, “Mouse models recapitulating Coenzyme $Q_{10}$ deficiency syndrome”.

Manuscript 2, “The molecular genetics of Coenzyme Q biosynthesis in health and disease”, provides a detailed overview of human coenzyme Q deficiencies and discusses the existing mouse models for coenzyme Q deficiency.

## Manuscript 1 (*submitted*)

Mouse models recapitulating Coenzyme $Q_{10}$ deficiency syndrome

Floriana Licitra and Hélène Puccio

Molecular Syndromology

### *2.4.4. Manuscript 1 (submitted)*

**Mouse models recapitulating Coenzyme $Q_{10}$ deficiency syndrome**

**Floriana Licitra[1-5] and Hélène Puccio[#1-5]**

[1] Translational Medicine and Neurogenetics, IGBMC (Institut de Génétique et de Biologie Moléculaire et Cellulaire), Illkirch, France;

[2] Inserm, U596, Illkirch, France;

[3] CNRS, UMR7104, Illkirch, France;

[4] Université de Strasbourg, Strasbourg, France;

[5] Collège de France, Chaire de génétique humaine, Illkirch, France;

[#] Correspondence to:

Hélène Puccio

E-mail: hpuccio@igbmc.fr

Tel: 33-3-88-65-32-64

Fax: 33-3-88-65-32-46

**Abstract**

Coenzyme Q, also known as ubiquinone, is an essential lipophilic molecule present in all cellular membranes and involved in a variety of cellular functions, in particular as an electron carrier in the mitochondrial respiratory chain and as a potent antioxidant. Coenzyme Q is synthesized endogenously through a complex metabolic pathway, involving over 10 different components. Primary coenzyme $Q_{10}$ deficiency in humans, due to mutations in genes involved in Coenzyme Q biosynthesis, is a heterogeneous group of rare disorders presenting severe and complex clinical symptoms. The generation of mouse models deficient in Coenzyme Q is important to further clarify the cellular function of Coenzyme Q and to unravel the complexity in the pathophysiological consequences of CoQ deficiency. This review summarizes the current knowledge on mouse models of primary Coenzyme Q deficiency.

## Introduction

Coenzyme Q (CoQ, ubiquinone) is a lipophilic molecule present in all cells and is involved in many different cellular functions. The most pivotal function of CoQ is to shuttle electrons from complexes I and II to complex III in the mitochondrial respiratory chain, thereby leading to maintenance of the mitochondrial membrane potential and the production of cellular ATP by oxidative phosphorylation. Besides, it is also a cofactor of uncoupling proteins, a potent anti-oxidant agent and a modulator of the mitochondrial permeability transition pore (Turunen et al., 2004). Coenzyme Q is distributed in all membranes throughout the cell (Crane, 2001) with the highest amounts found in mitochondrial membranes, in particular the inner membrane, lysosomes and Golgi vesicles (Turunen et al., 2004).

Coenzyme Q is synthesized endogenously through a complex and only partially elucidated metabolic pathway (Figure 1). Most available information derives from yeast studies, where initially nine genes (*coq1-9*) have been characterized as essential for CoQ biosynthesis (Tran and Clarke, 2007). Moreover, recently mitochondrial ferredoxin Yah1 and ferredoxin reductase Arh1 have been found also to be required for CoQ biosynthesis (Pierrel et al., 2010). CoQ is composed of a benzoquinone ring, derived from tyrosine, and an isoprenoid side chain (which contains 6–10 isoprene units in different species) generated from acetyl-CoA via the melavonate pathway (Bentinger et al., 2010). Briefly, the polyisoprenoid tail is assembled by polyprenyl diphosphate synthase and then covalently bound to the benzoquinone head group producing the 4-hydroxy-3-polyprenyl benzoic acid (4-HB). This is followed by several modifications of the aromatic ring, such as C-hydroxylations, decarboxylation, O-methylations and C-methylation leading to CoQ (Tran and Clarke, 2007).

Mutations in genes involved in Coenzyme Q biosynthesis lead to primary coenzyme $Q_{10}$ deficiency in humans. To date, mutations or deletion in seven genes involved in CoQ pathway have been reported: PDSS1 (Mollet et al., 2007), PDSS2 (Lopez et al., 2006), COQ2 (Quinzii et al., 2006) (Mollet et al., 2007) (Diomedi-Camassei et al., 2007), ADCK3 (Lagier-Tourenne et al., 2008, Mollet et al., 2008), COQ 4 (Salviati et al., 2012), COQ6 (Heeringa et al., 2011) and COQ9 (Duncan et al., 2009), leading to heterogeneous clinical manifestations. The complexity of symptoms associated to Coenzyme Q deficiencies has been synthetized in four main clinical phenotypes (Quinzii and Hirano, 2011): I) Encephalopathy and encophalomyopathy; II) Severe infantile multisystemic disease; III) Cerebellar ataxia; IV) Nephrotic syndrome. Moreover, a mitochondrial myopathy is reported in patients with $CoQ_{10}$ deficiency still without a genetic diagnosis (Ogasahara et al., 1989).

The explanation of this marked clinical heterogeneity is still unclear, but it might reflect a tissue specific regulation of $CoQ_{10}$ biosynthesis, a variable physiological sensitivity of different organs to $CoQ_{10}$ levels or the presence of modifier genes.

**Animal models of Coenzyme Q deficiency**

Although studies in yeast and in bacteria have been extremely useful to dissect the biosynthetic pathway of Coenzyme Q and to better unravel the multifacet function of Coenzyme Q, the generation of multicellular model organisms deficient in Coenzyme Q is important to clarify the cellular function of Coenzyme Q and to unravel the complexity in the pathophysiological consequences of CoQ deficiency. Invertebrate models have the great advantage to be easily generated and characterized compared to mouse models. Thus, worms and flies lacking CoQ have been produced and they highlighted important functions of Coenzyme Q. For instance, *coq-1* knock-down in *C. elegans* causes a specific degeneration of GABAergic neurons, suggesting that this type of neurons are more sensitive than others to CoQ ablation (Earls et al., 2010). Moreover the study of *D. melanogaster* carrying mutations in *qless*, homolog of PDSS1, suggested that CoQ promotes the growth of neuroblast lineages, protecting neural cells against mitochondrial stress and apoptosis (Grant et al., 2010).

However, invertebrate systems are not sufficient to reproduce the complexity of mammalian systems. Thus, mouse models deficient in CoQ are extremely valuable and complementary to address the cellular functions of CoQ, the biosynthesis and its regulation and the tissue-specificity that may exist in mammals. Furthermore, mouse models are helpful to study the physiopathology of CoQ deficiencies and to understand the heterogeneity of these syndromes. Finally, the use of mouse model is crucial to test new therapeutic approaches in a first phase of pre-clinical research.

In this review, we describe the available mouse models for primary Coenzyme Q deficiency, i.e. targeting the gene involved in CoQ biosynthesis, that have been characterize, and comment on the most important findings that emerged through the study of these models. Table 1 summarizes the mouse described in this review with the corresponding references.

**Constitutive knockout (KO) and knockin mice with primary Coenzyme Q deficiency**

To date, constitutive KO mice of only five genes implicated in Coenzyme Q biosynthesis have been generated (Table 1).

Polyisoprenyl diphosphate synthases is the enzyme that catalyze the formation of the isoprenoid tail of ubiquinone (Tran and Clarke, 2007). In mice, as well as in humans, this enzyme is composed of two subunits, *Pdss1* and *Pdss2,* and it is responsible for the length of the side chain of CoQ (Saiki et al., 2005). The complete KO of *Pdss2* is embryonically lethal with no homozygous embryos surviving beyond E9.5 days of gestation, demonstrating the crucial role of CoQ for early development in animals (Peng et al., 2008) (Lu et al., 2012).

Coq7 is a demethoxyubiquione (DMQ) mono-hydroxylase that functions in the penultimate modification of the benzoquinone ring of Coenzyme Q, the C6 hydroxylation. (Tran and Clarke, 2007). Two complete knockouts of Coq7 (also called *mclk1*) have been generated and both showed embryonic lethality (Nakai et al., 2001) (Levavasseur et al., 2001). In the first model, $Coq7^{-/-}$ embryos failed to survive beyond E10.5, with completly resorbed embryos by E11.5 (Nakai et al., 2001), whereas in the second model, $Mclk^{-/-}$ embryos showed a slight developmental delay by E8.5 with condensed and fragmented nuclei suggesting apoptotic cell death, and were completely resorbed by E13.5 (Levavasseur et al., 2001). In both knockout mice, $CoQ_9$ was not produced in mutant embryos and its precursor, $DMQ_9$, was found to accumulate, underlying the crucial role of Coq7 in the biosynthesis of Coenzyme Q. Moreover, $Coq7^{-/-}$ embryos showed an immature neural tube and a disorganization of the neuroepithelium, demonstrating the importance of *Coq7* for neurogenesis. Moreover in the cerebral wall of $Coq7^{-/-}$ embryos, mitochondria appeared abnormally enlarged with vesicular cristae (Nakai et al., 2001).

Interestingly, the heterozygous $Mclk1^{+/-}$ mice are not only completely viable with normal levels of ubiquinone in newborns (Levavasseur et al., 2001), but they display an increased lifespan up to 30% and lower levels of DNA damage in liver (Liu et al., 2005). Moreover, in very old (25 months) $Mclk1^{+/-}$ mice, loss of heterozygosity was observed in liver samples, where large group of cells appeared *Mclk1* negative. At this age, $CoQ_9$ content was reduced in liver but not in kidney, however, without accumulation of $DMQ_9$, suggesting that the CoQ pathway is turned off in adult hepatocytes in the absence of MCLK1 (Liu et al., 2005). A more recent study (Lapointe et al., 2012) has found that although the total amount of CoQ was the same in the mitochondria of $Mclk1^{+/-}$ mice, the distribution was altered, with a lower than normal level of $CoQ_9$ in the inner membrane associated with a decrease in the electron transport, and a higher level in the outer membrane. Supplementation with dietary $CoQ_{10}$

restored the levels of CoQ in the inner membrane as well as the respiratory chain dysfunction.

Coq3 is an O-methyltransferase responsible for the two O-methylation steps in ubiquinone biosynthesis, the second and last steps (Hsu et al., 1996). Recently a constitutive KO mouse for *Coq3* has been generated and similarly to *Pdss2* and *Coq7* knockouts resulted in embryonic lethality, although no information as to the age of embryonic lethality was reported (Lapointe et al., 2012). Furthermore, the heterozygous mouse, in contrast to the *Coq7* heterozygous mouse exhibited normal life span, normal content of ubiquinone in the mitochondria, suggesting that COQ3 is not limiting for CoQ biosynthesis

The EUCOMM (http://www.knockoutmouse.org/about/eucomm) program is currently generating knockout alleles for other genes involved in Coenzyme Q biosynthesis, and to date both *Coq4* and *Coq9* knockout lines have been produced.

First evidence shows that *Coq4* knockout mice are embryonic lethal. This finding, together with the results of *Pdss2*, *Coq7* and *Coq3* complete KO, demonstrate the crucial role of Coenzyme Q during early development, although it is not clear yet which function of CoQ is required for embryonic development.

To try to better understand the role of CoQ in development, ES cell lines from wild-type and *Coq7* KO embryos were generated and characterized. Interestingly, mitochondrial respiratory activity was found to be only mildly affected. In particular, the activity of succinate cytochrome *c* reductase, which involves respiratory Complexes II and III, was severely reduced, whereas NADH-cytochrome *c* reductase, which involves respiratory Complexes I and III was not strongly affected. Finally, the level of oxygen consumption in mutant ES cells was mildly reduced (65% of wild type). These results, although obtained in cell lines and not *in vivo*, suggest that $DMQ_9$ may be able to partially replace $CoQ_9$ in the respiratory chain. However the embryonic lethality of *Mclk1*$^{-/-}$ mice suggested that $DMQ_9$ is unable to completely replace $CoQ_9$, for one or more of its functions (Levavasseur et al., 2001).

In contrast to the embryonic lethality described in *Pdss2*, *Coq7*, *Coq3* and *Coq4* consitutive knockout, *Coq9* KO mice generated by the EUCOMM program are available. An exhaustive phenotyping protocol of the *Coq9* KO mice has started, although very little phenotype has been reported to date. Female *Coq9* KO mice appeared to be hyperactive when monitored for 10 minutes in an open field arena. The absence of a severe phenotype is surprising, and does not correlate with the human phenotype. Indeed, a homozygous nonsense mutation (R244X) in COQ9 has been associated with neonatal-onset lactic

acidosis and severe multisystem disease (Duncan et al., 2009). Although coq9 was identified in the yeast as being required for CoQ biosynthesis, the function of the *Coq9* protein in the CoQ biosynthesis pathway is unclear, although it has been shown to interact with other Coq polypeptides (Hsieh et al., 2007). However, recently a *Coq9* knockin mouse expressing a truncated COQ9 protein has been generated which presents a phenotype resembling human mitochondrial encephalomyopathy associated with CoQ deficiency (Garcia-Corzo et al., 2013). In particular, *Coq9* mutant mice (*Coq9*$^{X/X}$) presented neuronal death in the brain, demyelinization in the pons and the medulla oblongata and astrogliosis. Moreover *Coq9*$^{X/X}$ mice show significant decrease in $CoQ_9$ and $CoQ_{10}$ in all tissues tested (cerebrum, cerebellum, heart, kidney, liver and skeletal muscle) combined with an accumulation of $DMQ_9$, the CoQ precursor substrate of Coq7 activity. The energy deficit caused by CoQ misregulation lead to increased nucleic acid oxidation and caspase-independent apoptosis in the pons and in the encephalon. Moreover the heart of mutant mice showed sign of fibrosis, the kidney did not show any abnormality.

**Spontaneous mutant mice with primary Coenzyme Q deficiency**

The first reported mutation in *Pdss2,* appeared spontaneously in a CBA/CaH colony in the lab of Dr. Mary Lyon and it was designated 'kidney disease' (*kd*) (Lyon and Hulse, 1971). Homozygotes kd/kd mice are apparently healthy for the first 8 weeks of life, but starting at 12 weeks of age, histological analysis of kidneys reveals a mononuclear cell infiltrate and tubular dilatation with proteinaceous casts in cortical areas. This damage extends over time to the entire kidney leading to renal failure. Although an autoimmune mechanism was proposed in earlier work as the pathophysiological mechanism of the disease (Neilson et al., 1984) (Kelly et al., 1986), the work of Hancock and collaborators showed that the genetic defect of *kd/kd* mice is intrinsic to the kidney and that the immune response involving either effector T cells or NK cells is a secondary consequence (Hancock et al., 2003). By positional cloning strategy, the *kd* missense mutation (V117M) was found to fall within exon 2 of the *Pdss2* gene, suggesting for the first time that impairment of Coenzyme Q could lead to the renal failure (Peng et al., 2004). *Pdss2*$^{kd/kd}$ mice indeed develop a typical nephrotic syndrome in adult age with albuminuria and lipid abnormalities, such as high levels of serum triglycerides and cholesterol (Madaio et al., 2005).

**Conditional knockout (KO) mice with primary Coenzyme Q deficiency**

Conditional KO are a powerful genetic tool to study the progression of disease and to dissect the different steps of a pathological process, including the primary site of disease development, by allowing to inactivate genes in a tissue- and/or time-specific manner, overcoming the embryonic lethality issue.

To elucidate the origin of the nephrotic syndrome of *Pdss2*$^{kd/kd}$ mice at the cellular level, tissue-specific conditional *Pdss2* KO mice were obtained, by crossing mice carrying the conditional allele (exon 2 flanked by loxP sites) to transgenic mice expressing the Cre-recombinase under different promoters. The deletion of *Pdss2* was targeted to renal glomeruli in *Podocin-cre;Pdss2*$^{loxP/loxP}$ mice and to renal tubular epithelium and hepatocyes in *PEPCK-cre;Pdss2*$^{loxP/loxP}$ (Peng et al., 2008). *Podocin-cre;Pdss2*$^{loxP/loxP}$ mice had a phenotype that resembled that of *Pdss2*$^{kd/kd}$ mice, with serum albuminuria and histological renal defect characterized by dilated tubules and extensive interstitial infiltration. Moreover *Podocin-cre;Pdss2*$^{loxP/loxP}$ mice had a more severe phenotype than that observed in *Pdss2*$^{kd/kd}$ mice, suggesting that the missense allele in the *Pdss2*$^{kd/kd}$ mice has some residual activity. In contrast, *PEPCK-cre;Pdss2*$^{loxP/loxP}$ did not show any feature of renal abnormalities, suggesting that the primary defect in *Pdss2*$^{kd/kd}$ mice is due to a primary podocytes failure. In particular, *Podocin-cre;Pdss2*$^{loxP/loxP}$ mice showed a diffuse effacement of podocyte foot processes (Peng et al., 2008) as was already observed in Pdss2$^{kd/kd}$ mice (Madaio et al., 2005).

The cerebellum is one of the most often affected organs in ubiquinone deficiency, being involved in four out of five subtypes. Therefore, in order to dissect the pathological mechanism underlying the cerebellar defects due to ubiquinone deficiency, as well as to test potential novel dietary ubiquinone therapies, cerebellar conditional KOs were generated. Similarly to the work reported by Peng and colleagues, a conditional allele with loxP site flanking exon 2 was constructed, however, as it is a different conditional allele, the original nomenclature reported is *Pdss2*$^{f/f}$ (Lu et al., 2012). A first model was generated using the *Pax-cre* transgenic mice, with the recombinase expressed in the hindbrain region at E9.5 affecting many cell types in the cerebellum at birth, but also strongly expressed in kidney.*Pax2-cre;Pdss2*$^{f/-}$ suffer from neonatal death, with the presence of cerebellar hypoplasia, disorganization of cerebellum and absence of primordial Purkinje neurons at birth. This neonatal growth retardation was caused by a defect in radial cell migration at E12.5 and by ectopic apoptosis starting at E14.5 and increasing until E18.5 (Lu et al., 2012). Although the severe cerebellum hypoplasia found in the *Pax2-cre;Pdss2*$^{f/-}$ might model the

cerebellar atrophy commonly observed in $CoQ_{10}$ infants, the neonatal death precluded studies in adult stages. Therefore, to further analyze *Pdss2* function in adult cerebellum, *Pdss2* was conditionally depleted expressing the cre-recombinase under *Pcp2* promoter, which is active in cerebellar Purkinje neurons and retinal bipolar neurons from P7 (Lu et al., 2012). Although Pdss2 is depleted in Purkinje neurons at 1 month of age, the *Pcp2-cre;Pdss2*$^{f/-}$ mice do not present an impairment of coordination and there are no morphological abnormalities observed. However, by 6 months of age, the *Pcp2-cre;Pdss2*$^{f/-}$ mice exhibited a significant loss in Purkinje cell, and developed a progressive impairment of coordination starting at 9.5 months. Interestingly, dispersed apoptosis was observed in the cerebellum already at 6 months of age, which increased with age, suggesting that Purkinje cell degeneration lead to subsequent diffusive neuron death by apoptosis. This model may serve as a better model to understand the progressive forms of ataxia linked to human $CoQ_{10}$ deficiency in adults.

In agreement with the essential role of ubiquinone in the respiratory chain, *Pdss2* depletion leads to a strong decrease in $CoQ_9$ and causes mitochondrial dysfunction, with a significant alteration of the respiratory chain associated to morphological changes of the mitochondria. For example, in cerebellum depleted for *Pdss2*, the mitochondria appeared swollen and with pale matrix (Lu et al., 2012), while in the kidney of Pdss2$^{kd/kd}$ mice, the mitochondria were smaller, with compressed cristae and pale matrix (Peng et al., 2004) . Interesting, both in liver and cerebellum depleted in *Pdss2*, engulfment of mitochondria by ER was observed with the presence of autophagic like vacuoles, suggesting that mitophagy might be involved to remove abnormal mitochondria (Lu et al., 2012) (Peng et al., 2004).

In addition to the renal and cerebellar phenotype, *Pdss2* deletion has also been associated to muscle impairment. In embryonic *Pax2-cre*;*Pdss2*$^{f/-}$ conditional KO mice, lipid accumulation was observed in the forelimb skeletal muscle at P0 (Lu et al., 2012). Abnormal lipid accumulation in skeletal muscle is a common symptom of Coenzyme Q deficiency in humans (Ogasahara et al., 1989) (Horvath et al., 2012) and it may result from a defect in fatty acid metabolism. Interestingly, in liver of *Alb-cre;Pdss2*$^{loxP/loxP}$ conditional KO mice, despite the absence of over phenotype, fatty acid metabolism was found to be altered together with oxidative phosphorylation, tricarboxylic acid cycle, autophagy and DNA metabolism (Peng et al., 2008). Some of these pathways were found to be reversed after treatment with Probucol, an oral lipophilic antioxidant (Falk et al., 2011).

**Conclusions**

Several mouse models with deficiency in gene involved in CoQ biosynthesis are available for the study and modeling of primary Coenzyme Q deficiencies. These models show a large spectrum of phenotypes, in agreement with the clinical heterogeneity observed in human patients presenting primary $CoQ_{10}$ deficiency. However, as in humans, several organs appear to be more sensitive to Coenzyme Q depletion, in particular kidney, cerebellum and muscle. The specific reasons of this tissue sensitivity are not clearly elucidated, but might be linked either to an increase need of CoQ in these tissues and/or to a different tissue-specific expression level of certain genes involved in the biosynthesis of CoQ. Furthermore, the variety of functions associated with Coenzyme Q can also play a role in the tissue specific pathology. These models are important tools for pre-clinical studies of therapeutic approaches. For instance, probucol and Coenzyme $Q_{10}$ have been administered to *Pdss2* mice leading to an improvement in the renal phenotype (Falk et al., 2011). Surprisingly, an unexpected gender effect was reported in the treatment, with male mice tending to respond better to probucol therapy, whereas females tend to respond better to $CoQ_{10}$. However, whether this can be translated in humans need further studies.

To date, only five genes involved in CoQ biosynthesis have been targeted and reported, despite the involvement of at least 10 proteins in this process. In order to further dissect the Coenzyme Q biosynthetic pathway and in particular its regulation in mammals, it would be useful to inactivate other genes involved in the pathway, in particular ones coding for COQ polypeptides whose function has not be elucidated yet. One can speculate that less severe phenotypes might be associated with the inactivation of genes involved in the regulation of the pathway, rather than enzymes involved in specific modifications. To date, *Coq9* depletion is the only gene that is not associated with embryonic lethality, despite the severe clinical presentation in humans. The embryonic lethality associated with most gene deletion so far underlines the crucial role of Coenzyme Q during development. To circumvent the embryonic lethality, several conditional knockout models have recently been generated, and suggest that several functions of CoQ are crucial in vivo in adult tissues, such as its role in energy production through the respiratory chain as well as its anti-oxidant effect. Finally, although muscle impairment is often associated with Coenzyme Q deficit, a muscle specific conditional knockout has not yet been generated.

In conclusion mouse models recapitulating Coenzyme Q deficiency syndrome are powerful tools to study the pathology of this complex syndrome and to elucidate the biosynthesis of CoQ in mammals. The development of more models in the future, in

particular through the large-scale efforts of international mouse consortia should provide all the tools necessary to dissect the biosynthesis and regulation of this important and essential molecule.

**Acknowledgements:**

This work was supported by UK ataxia and the European Community under the European Research Council [206634/ISCATAXIA] (to HP). The authors have no conflicts of interest to declare.

**References:**

Bentinger M, Tekle M, Dallner G (2010) Coenzyme Q--biosynthesis and functions. Biochem Biophys Res Commun 396:74-79.

Crane FL (2001) Biochemical functions of coenzyme Q10. J Am Coll Nutr 20:591-598.

Diomedi-Camassei F, Di Giandomenico S, Santorelli FM, Caridi G, Piemonte F, Montini G, Ghiggeri GM, Murer L, Barisoni L, Pastore A, Muda AO, Valente ML, Bertini E, Emma F (2007) COQ2 nephropathy: a newly described inherited mitochondriopathy with primary renal involvement. J Am Soc Nephrol 18:2773-2780.

Duncan AJ, Bitner-Glindzicz M, Meunier B, Costello H, Hargreaves IP, Lopez LC, Hirano M, Quinzii CM, Sadowski MI, Hardy J, Singleton A, Clayton PT, Rahman S (2009) A nonsense mutation in COQ9 causes autosomal-recessive neonatal-onset primary coenzyme Q10 deficiency: a potentially treatable form of mitochondrial disease. Am J Hum Genet 84:558-566.

Earls LR, Hacker ML, Watson JD, Miller DM, 3rd (2010) Coenzyme Q protects Caenorhabditis elegans GABA neurons from calcium-dependent degeneration. Proc Natl Acad Sci U S A 107:14460-14465.

Garcia-Corzo L, Luna-Sanchez M, Doerrier C, Garcia JA, Guaras A, Acin-Perez R, Bullejos-Peregrin J, Lopez A, Escames G, Enriquez JA, Acuna-Castroviejo D, Lopez LC (2013) Dysfunctional Coq9 protein causes predominant encephalomyopathy associated with CoQ deficiency. Hum Mol Genet.

Grant J, Saldanha JW, Gould AP (2010) A Drosophila model for primary coenzyme Q deficiency and dietary rescue in the developing nervous system. Dis Model Mech 3:799-806.

Hancock WW, Tsai TL, Madaio MP, Gasser DL (2003) Cutting Edge: Multiple autoimmune pathways in kd/kd mice. J Immunol 171:2778-2781.

Heeringa SF, Chernin G, Chaki M, Zhou W, Sloan AJ, Ji Z, Xie LX, Salviati L, Hurd TW, Vega-Warner V, Killen PD, Raphael Y, Ashraf S, Ovunc B, Schoeb DS, McLaughlin HM, Airik R, Vlangos CN, Gbadegesin R, Hinkes B, Saisawat P, Trevisson E, Doimo M, Casarin A, Pertegato V, Giorgi G, Prokisch H, Rotig A, Nurnberg G, Becker C, Wang S, Ozaltin F, Topaloglu R, Bakkaloglu A, Bakkaloglu SA, Muller D, Beissert A, Mir S, Berdeli A, Varpizen S, Zenker M, Matejas V, Santos-Ocana C, Navas P, Kusakabe T, Kispert A, Akman S, Soliman NA, Krick S, Mundel P, Reiser J, Nurnberg P, Clarke CF, Wiggins RC, Faul C, Hildebrandt F (2011) COQ6 mutations in human patients produce nephrotic syndrome with sensorineural deafness. J Clin Invest 121:2013-2024.

Horvath R, Czermin B, Gulati S, Demuth S, Houge G, Pyle A, Dineiger C, Blakely EL, Hassani A, Foley C, Brodhun M, Storm K, Kirschner J, Gorman GS, Lochmuller H, Holinski-Feder E, Taylor RW,

Chinnery PF (2012) Adult-onset cerebellar ataxia due to mutations in CABC1/ADCK3. J Neurol Neurosurg Psychiatry 83:174-178.

Hsieh EJ, Gin P, Gulmezian M, Tran UC, Saiki R, Marbois BN, Clarke CF (2007) Saccharomyces cerevisiae Coq9 polypeptide is a subunit of the mitochondrial coenzyme Q biosynthetic complex. Arch Biochem Biophys 463:19-26.

Hsu AY, Poon WW, Shepherd JA, Myles DC, Clarke CF (1996) Complementation of coq3 mutant yeast by mitochondrial targeting of the Escherichia coli UbiG polypeptide: evidence that UbiG catalyzes both O-methylation steps in ubiquinone biosynthesis. Biochemistry 35:9797-9806.

Kelly CJ, Korngold R, Mann R, Clayman M, Haverty T, Neilson EG (1986) Spontaneous interstitial nephritis in kdkd mice. II. Characterization of a tubular antigen-specific, H-2K-restricted Lyt-2+ effector T cell that mediates destructive tubulointerstitial injury. J Immunol 136:526-531.

Lagier-Tourenne C, Tazir M, Lopez LC, Quinzii CM, Assoum M, Drouot N, Busso C, Makri S, Ali-Pacha L, Benhassine T, Anheim M, Lynch DR, Thibault C, Plewniak F, Bianchetti L, Tranchant C, Poch O, DiMauro S, Mandel JL, Barros MH, Hirano M, Koenig M (2008) ADCK3, an ancestral kinase, is mutated in a form of recessive ataxia associated with coenzyme Q10 deficiency. Am J Hum Genet 82:661-672.

Lapointe J, Wang Y, Bigras E, Hekimi S (2012) The submitochondrial distribution of ubiquinone affects respiration in long-lived Mclk1+/- mice. J Cell Biol 199:215-224.

Levavasseur F, Miyadera H, Sirois J, Tremblay ML, Kita K, Shoubridge E, Hekimi S (2001) Ubiquinone is necessary for mouse embryonic development but is not essential for mitochondrial respiration. J Biol Chem 276:46160-46164.

Liu X, Jiang N, Hughes B, Bigras E, Shoubridge E, Hekimi S (2005) Evolutionary conservation of the clk-1-dependent mechanism of longevity: loss of mclk1 increases cellular fitness and lifespan in mice. Genes Dev 19:2424-2434.

Lopez LC, Schuelke M, Quinzii CM, Kanki T, Rodenburg RJ, Naini A, Dimauro S, Hirano M (2006) Leigh syndrome with nephropathy and CoQ10 deficiency due to decaprenyl diphosphate synthase subunit 2 (PDSS2) mutations. Am J Hum Genet 79:1125-1129.

Lu S, Lu LY, Liu MF, Yuan QJ, Sham MH, Guan XY, Huang JD (2012) Cerebellar defects in Pdss2 conditional knockout mice during embryonic development and in adulthood. Neurobiol Dis 45:219-233.

Lyon MF, Hulse EV (1971) An inherited kidney disease of mice resembling human nephronophthisis. J Med Genet 8:41-48.

Madaio MP, Ahima RS, Meade R, Rader DJ, Mendoza A, Peng M, Tomaszewski JE, Hancock WW, Gasser DL (2005) Glomerular and tubular epithelial defects in kd/kd mice lead to progressive renal failure. Am J Nephrol 25:604-610.

Mollet J, Delahodde A, Serre V, Chretien D, Schlemmer D, Lombes A, Boddaert N, Desguerre I, de Lonlay P, de Baulny HO, Munnich A, Rotig A (2008) CABC1 gene mutations cause ubiquinone deficiency with cerebellar ataxia and seizures. Am J Hum Genet 82:623-630.

Mollet J, Giurgea I, Schlemmer D, Dallner G, Chretien D, Delahodde A, Bacq D, de Lonlay P, Munnich A, Rotig A (2007) Prenyldiphosphate synthase, subunit 1 (PDSS1) and OH-benzoate polyprenyltransferase (COQ2) mutations in ubiquinone deficiency and oxidative phosphorylation disorders. J Clin Invest 117:765-772.

Nakai D, Yuasa S, Takahashi M, Shimizu T, Asaumi S, Isono K, Takao T, Suzuki Y, Kuroyanagi H, Hirokawa K, Koseki H, Shirsawa T (2001) Mouse homologue of coq7/clk-1, longevity gene in Caenorhabditis elegans, is essential for coenzyme Q synthesis, maintenance of mitochondrial integrity, and neurogenesis. Biochem Biophys Res Commun 289:463-471.

Neilson EG, McCafferty E, Feldman A, Clayman MD, Zakheim B, Korngold R (1984) Spontaneous interstitial nephritis in kdkd mice. I. An experimental model of autoimmune renal disease. J Immunol 133:2560-2565.

Ogasahara S, Engel AG, Frens D, Mack D (1989) Muscle coenzyme Q deficiency in familial mitochondrial encephalomyopathy. Proc Natl Acad Sci U S A 86:2379-2382.

Peng M, Falk MJ, Haase VH, King R, Polyak E, Selak M, Yudkoff M, Hancock WW, Meade R, Saiki R, Lunceford AL, Clarke CF, Gasser DL (2008) Primary coenzyme Q deficiency in Pdss2 mutant mice causes isolated renal disease. PLoS Genet 4:e1000061.

Peng M, Jarett L, Meade R, Madaio MP, Hancock WW, George AL, Jr., Neilson EG, Gasser DL (2004) Mutant prenyltransferase-like mitochondrial protein (PLMP) and mitochondrial abnormalities in kd/kd mice. Kidney Int 66:20-28.

Pierrel F, Hamelin O, Douki T, Kieffer-Jaquinod S, Muhlenhoff U, Ozeir M, Lill R, Fontecave M (2010) Involvement of mitochondrial ferredoxin and para-aminobenzoic acid in yeast coenzyme Q biosynthesis. Chem Biol 17:449-459.

Quinzii C, Naini A, Salviati L, Trevisson E, Navas P, Dimauro S, Hirano M (2006) A mutation in para-hydroxybenzoate-polyprenyl transferase (COQ2) causes primary coenzyme Q10 deficiency. Am J Hum Genet 78:345-349.

Quinzii CM, Hirano M (2011) Primary and secondary CoQ(10) deficiencies in humans. Biofactors 37:361-365.

Saiki R, Nagata A, Kainou T, Matsuda H, Kawamukai M (2005) Characterization of solanesyl and decaprenyl diphosphate synthases in mice and humans. FEBS J 272:5606-5622.

Salviati L, Trevisson E, Rodriguez Hernandez MA, Casarin A, Pertegato V, Doimo M, Cassina M, Agosto C, Desbats MA, Sartori G, Sacconi S, Memo L, Zuffardi O, Artuch R, Quinzii C, Dimauro S, Hirano M, Santos-Ocana C, Navas P (2012) Haploinsufficiency of COQ4 causes coenzyme Q10 deficiency. J Med Genet 49:187-191.

Tran UC, Clarke CF (2007) Endogenous synthesis of coenzyme Q in eukaryotes. Mitochondrion 7 Suppl:S62-71.

Turunen M, Olsson J, Dallner G (2004) Metabolism and function of coenzyme Q. Biochim Biophys Acta 1660:171-199.

**Table1.** Available mouse models with primary Coenzyme Q deficiency.

| Mouse model | Reference |
|---|---|
| **Spontaneous mutation** | |
| Pdss2$^{kd/kd}$ | Lyon and Hulse, 1971; Peng et al , 2004; Madaio et al. ,2005 |
| **Constitutive KO and KI** | |
| *Pdss2* | Peng et al ., 2008 and Lu et al., 2011 |
| *Coq7* | Nakai and al., 2001 and Lavavasseur et al., 2001 |
| *Coq3* | Lapointe et al ., 2012 |
| *Coq 4* | EUCOMM (http://www.knockoutmouse.org/) |
| *Coq9* | EUCOMM (http://www.knockoutmouse.org/) |
| *Coq9* KI | Garcia-Conzo et al, 2013 |
| **Conditional KO** | |
| *Pdss2* renal KO | Peng et al., 2008 |
| *Pdss2* cerebellar KO | Lu et al., 2012 |

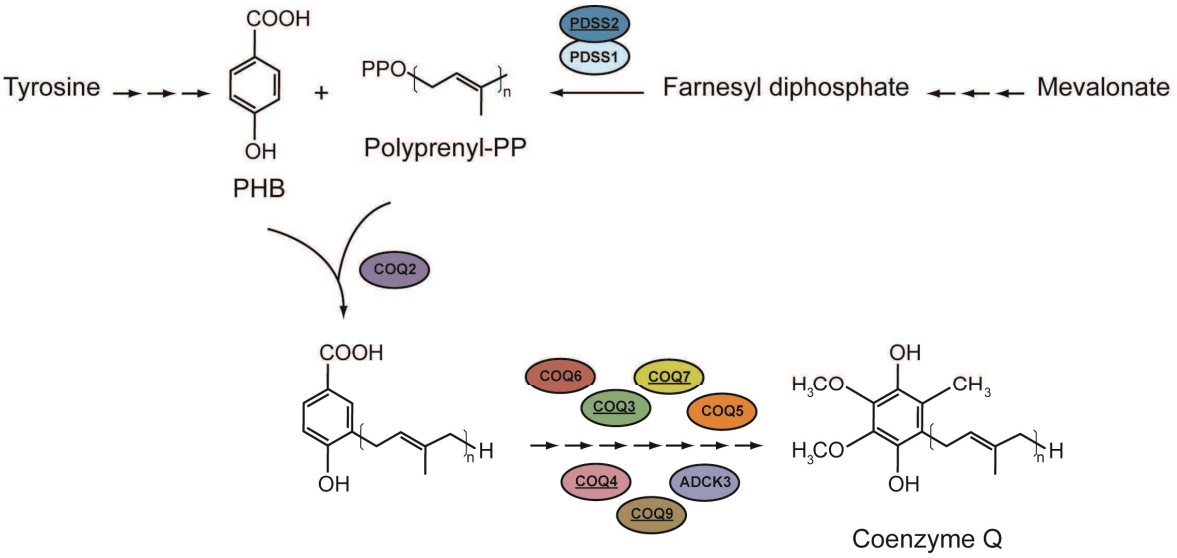


**Figure 1.** Coenzyme Q biosynthesis in eukaryotic cells. The length of the poly-isoprenoid chain (n) varies in different species (n=9 in mouse and n=10 in humans). PDSS1 and PDSS2 form the trans-polyprenyl diphosphate synthase that catalyzes the formation of polyprenyl diphosphate. COQ2 catalyzes the condensation of PHB with polyprenyl-PP. The sequence of modifications of Coenzyme Q aromatic ring is only partially elucidated and it involves several proteins with different enzymatic or regulatory role. Underlined are the proteins that have been targeted to produce mouse models. PHB: 4-hydroxybenzoate

## Manuscript 2 (*submitted*)

The molecular genetics of Coenzyme Q biosynthesis in health and disease

Leila N. Laredj, Floriana Licitra and Hélène Puccio

Biochimie

### *2.4.5. Manuscript 2 (submitted)*

**The molecular genetics of Coenzyme Q biosynthesis in health and disease**

**Leila N. Laredj[1-5], Floriana Licitra[1-5] and Hélène M. Puccio [1-5‡]**

[1] Translational Medicine and Neurogenetics, IGBMC (Institut de Génétique et de Biologie Moléculaire et Cellulaire), Illkirch, France;
[2] Inserm, U596, Illkirch, France;
[3] CNRS, UMR7104, Illkirch, France;
[4] Université de Strasbourg, Strasbourg, France;
[5] Collège de France, Chaire de génétique humaine, Illkirch, France

[‡] Correspondence to:
Hélène Puccio
Institut de Genetique et de Biologie Moleculaire et Cellulaire (IGBMC)
UMR 7104 CNRS/UdS, Inserm U964
1, rue Laurent Fries, BP 10142
67404 Illkirch Cedex, France

E-mail: hpuccio@igbmc.fr
Tel: +33-388653264
Fax: +33-388653246

**Abstract**

Coenzyme Q, or ubiquinone, is an endogenously synthesized lipid-soluble antioxidant that plays a major role in the mitochondrial respiratory chain. Although extensively studied for decades, recent data on coenzyme Q have painted an exciting albeit incomplete picture of the multiple facets of this molecule's function. In humans, mutations in the genes involved in the biosynthesis of coenzyme Q lead to a heterogeneous group of rare disorders, with most often severe and debilitating symptoms. In this review, we describe the current understanding of coenzyme Q biosynthesis, provide a detailed overview of human coenzyme Q deficiencies and discuss the existing mouse models for coenzyme Q deficiency. Furthermore, we briefly examine the current state of affairs in non-mitochondrial coenzyme Q functions and the latter's link to statin.

**Keywords:** Coenzyme Q; mitochondria; mouse models; ataxia; lipid metabolism

## Introduction

Since its discovery in 1957, Coenzyme Q (CoQ) or ubiquinone has been the focus of great interest among researchers, who have studied it extensively for its key role in mitochondrial bioenergetics. Indeed, it constitutes an essential element of the mitochondrial electron-transport chain shuttling electrons from complexes I and II to complex III at the inner mitochondrial membrane [1, 2]. This small molecule is also the only lipid soluble antioxidant that is synthesized *de novo* by animal cells, and is distributed in all membranes throughout the cell [3]. Furthermore, CoQ has been shown to regulate the mitochondrial permeability transition pore [4], to be an essential cofactor for the proton transport function of uncoupling proteins [5], and to be involved in pyrimidine nucleotide biosynthesis [6].

This lipophilic molecule comprises a benzoquinone moiety and a polyisoprenoid tail (or side-chain) of variable length amongst species: six isoprene units in *Saccharomyces cerevisiae* ($CoQ_6$), eight in *Escherichia coli* ($CoQ_8$), nine in mice ($CoQ_9$), and ten in humans ($CoQ_{10}$) [7, 8]. While the aromatic ring of $CoQ_{10}$ is the active part of the molecule, the tail bears no biological function other than anchoring CoQ into the membrane.

### Overview of the proposed Coenzyme Q biosynthesis pathway

The biochemical pathway of CoQ synthesis is complex and current knowledge derives mainly from the characterization of CoQ intermediates in bacterial and yeast studies with CoQ-deficient mutants [9, 10]. Indeed, based on studies in yeast, the products of at least nine genes, designated *Coq1* to *Coq9,* have been involved in this pathway [11, 12], which can be divided into two sets of reactions. The aromatic benzoquinone ring of CoQ derives from tyrosine or phenylalanine, whereas the isoprenoid side chain is produced from farnesylpyrophosphate (FPP), a precursor common to cholesterol and produced from acetyl-CoA by the melavonate pathway [13, 14]. While most of the early steps take place in the cytosol, the steps specific to CoQ biosynthesis, starting with the generation of the side chain from FPP, occur in the mitochondria. Recently, two additional genes, *YAH1* and *ARH1*, encoding yeast mitochondrial ferredoxin and ferredoxin reductase, were found to also be involved in CoQ biosynthesis [15].

The first committed step in this process is carried out by the Coq1 polypeptide in

yeast and by the homologous complex Pdss1/Pdss2 in animal cells [16, 17]. This trans-prenyl diphosphate synthase acts as a heterotetramer that condenses isoprene monomers derived from acetyl Co-A, and hence defines the length of the isoprene tail of CoQ [18]. Subsequent to this, a polyprenyltransferase, Coq2, mediates the conjugation of the polyisoprene tail to the head moiety, generating the first CoQ intermediate [19] **(Figure 1)**. The next series of reactions mediates the benzoquinone ring modification, such as C-hydroxylations, decarboxylation, O-methylations and C-methylation, leading to CoQ [10]. The first modification is catalyzed by Coq6, a monooxygenenase that hydroxylates the C5 position of the ring moiety [20]. Coq3 ensures the first and last O-methylation reactions [21]. Finally, Coq5 and Coq7 catalyze the C-methyltransferase and the last monooxygenase step in CoQ biosynthesis [22-24]. Furthermore, the functions of Coq4, Coq8 and Coq9 remain elusive, although data suggest that Coq4 is a structural component required for the formation of CoQ biosynthesis complex [25]. Coq8, on the other hand, is postulated to harbor a kinase activity that stabilizes the complex through phosphorylation [26], but no direct evidence seems to corroborate this hypothesis.

Both genetic and biochemical studies support the notion that Coq polypeptides exist in a multi-subunit complex in yeast, associated with the inner mitochondrial membrane. Indeed, all Coq polypeptides bear a potential mitochondrial targeting sequence, and fractionation studies revealed that they are, with the exception of Coq2, peripheral proteins associated with the matrix side of the inner mitochondrial membrane [21, 24, 27-32]. Amino acid sequence analysis of Coq2 uncovered the presence of six putative membrane-spanning motifs [19], pointing to the fact that Coq2 is an integral membrane protein. The first hint of the existence of a multi-subunit complex comes from the absence of $CoQ_6$ and accumulation of CoQ intermediates in *Coq3*-*Coq9* mutants, which suggests that the absence of one *Coq* gene product prevents the function of the others [10]. This view was further substantiated by the observation that steady-state levels of Coq3-7 and Coq9 depend on the expression of each of the other *Coq* genes [12, 24, 27, 28, 32-34]. Remarkably, this phenomenon is not observed in *E. coli*, which display a different sequence of ring-modification reactions (prenylation, decarboxylation, hydroxylation and methylation) [35]. Moreover, *Ubi* mutants were shown to accumulate all CoQ intermediates, indicating that complex formation is not a prerequisite for the biosynthetic process in prokaryotes [35, 36]. It remains to be determined whether a multi-enzymatic complex is required for CoQ biosynthesis in mammals. In fact,

although our increasing understanding of the process in yeast might lead us to expect that a similar mechanism should take place in mammals, different lines of evidence indicate otherwise. Indeed, it has been shown that murine *Coq7*$^{-/-}$ embryos and embryonic stem (ES) cells, unlike their yeast homologue, accumulate the intermediate demethoxyubiquinone ($DMQ_9$), suggesting that the previous steps in the biosynthetic pathway were maintained despite loss of Coq7 [37]. This observation raises two hypotheses: 1) that either a multisubunit complex is dispensable in mammals or 2) that, on the contrary, the latter remains stable when one of the constituents is missing.

**Human deficiencies in Coenzyme Q**

Given the essential functions of CoQ, a deficit in this molecule leads to a number of mitochondrial disorders with an unexplained heterogeneous clinical spectrum that encompasses at least five major phenotypes: 1) an encephalomyopathy, characterized by recurrent myoglobinuria; 2) a severe infantile multisystem disorder with encephalopathy; 3) an ataxic syndrome with cerebellar atrophy; 4) an isolated myopathy, and 5) a steroid-resistant nephrotic syndrome (SRNS) [38, 39]. Primary $CoQ_{10}$ disorders are rare conditions with an autosomal recessive mode of inheritance. The ataxic phenotype is the most common amongst theses symptoms, probably because it is less severe [40]. These disorders are caused by disruption of genes involved in the biosynthetic pathway. Mutations in *PDSS1*, *PDSS2*, *COQ2*, *COQ4*, *COQ6*, *COQ9* and *ADCK3* have been identified to date (detailed in **Table 1**). Secondary CoQ deficiency can also occur in diseases linked to genes not directly involved in CoQ biosynthesis (such as aprataxin (*APTX*), electron transferring-flavoprotein dehydrogenase gene (*ETFDH*), and *BRAF[41]*), or due to dietary insufficiency or use of pharmacotherapeutic agents such as statins [42].

**Table 1.** Primary $CoQ_{10}$ deficiencies

| Gene | Mutations | Number of patients | Age of onset | Clinical features | $CoQ_{10}$ levels compared to control | Mitochondrial function | Response to therapy | Ref. |
|---|---|---|---|---|---|---|---|---|
| *PDSS1* | D308E | 2 sib | 1-2 y | Deafness, encephaloneuropathy, obesity, *livedo reticularis*, and valvulopathy | 4% (Fibroblasts) | Reduced activity of CI+CIII (Fibroblasts) | - | [43] |
| *PDSS2* | Q332X-S382L | 1 | ≈ 3 mo | Leigh syndrome and nephropathy | 13% (Fibroblasts); 14% (Muscle) | Reduced activity of CII+CIII (fibroblasts and muscle), and ATP synthesis deficit (Fibroblasts) | No, died at 8 mo of *status epilepticus* | [44, 45] |
| *COQ2* | Y297C | 2 sib | ≈1 y | P1: Encephalomyopathy, nephropathy, proteinuria, hypotonia, mild psychomotor delay, optic atrophy, tremor, epilepsy, cerebellar atrophy, stroke-like lesions, and myoclonus | 37% (Muscle); 18% (Fibroblasts) | Reduced activities of CI+CII and CII+CIII (muscle), and CII+CIII (Fibroblasts), decreased ATP synthesis, increased ROS, and impaired pyrimidine metabolism | Yes, but only the neurological syndrome | [45, 46] [47, 48] |
| | | | | P2: Nephropathy | 17% (Fibroblasts) | Reduced activities of CII+CIII (Fibroblasts) | - | |
| | R197H-N228S | 1 | 18 mo | SRNS | 4.5% (Kidney); 38% (Muscle); 36% (Fibroblasts) | Dysmorphic mitochondria. Decreased COX and SDH activities (Kidney). Reduced activity of CII+CIII (Kidney + Muscle) | Yes | [48, 49] |
| | S146N | 1 | Birth | End stage renal disease, *status epilepticus*, encephalopathy, hypotonia, stroke-like lesions, and cerebral atrophy | 3.7% (Kidney); 2.5% (Muscle) | Same | Died at 6 mo | [48] |
| | N401fsX415 | 1 | Birth | Infantile multiorgan disease | 24% | Reduced activities of | Died at age 12 d | [43] |

| Gene | Mutations | Number of patients | Age of onset | Clinical features | $CoQ_{10}$ levels compared to control | Mitochondrial function | Response to therapy | Ref. |
|---|---|---|---|---|---|---|---|---|
| | | | | | (Fibroblasts) | CI+CIII and CII+CIII (Liver) | | |
| | S109N | 1 | 3 w | Myoclonic seizures, hypertrophic cardiomyopathy and nephrotic syndrome | 24% (Fibroblasts); | Reduced activity of CII+CIII (Kidney). | Died at age 5 mo | [50] |
| | A302V | 2 sib | Birth | Feeding problems, generalized edema, seizures, apneas, hypotonia, and dystonia | P1: 29%<br>P2: 3.5% (Muscle) | Severe decrease in CI activity in P1 (Muscle), normal activity of other complexes (Muscle + Fibroblasts) | Died at 5 and 6 mo | [51] |
| *COQ4* | Monoallelic deletion | 1 | Birth | Hypotonia, intellectual disability, dysmorphic features, and encephalomyopathy | 44% (Fibroblasts) | Decreased activity of CII+CIII (Fibroblasts) | Yes, improved neuromuscular symptoms | [52] |
| *COQ6* | A353D | 3 | 2.5- 6 y | SRNS, sensorineural deafness, and 1 patient with seizures and white matter abnormalities | - | - | Yes, 1 patient responded to treatment (1 untreated patient died of sepsis) | [53] |
| | G255R | 6 | 0.2 – 6.4 y | SRNS, congenital sensorineural deafness, ataxia, facial dysmorphism, seizures, and one case of bilateral nephrolithiasis and growth retardation | - | - | Yes, 1 treated patient showed improvement, (3 untreated patients died) | [54] |
| | W447–Q461fsX478 | 1 | 3 y | SRNS, and sensorineural deafness | - | - | - | [54] |
| | R162X-? | 1 | - | Cyclosporine A-dependent nephrotic syndrome | | | - | [54] |
| | W188X-? | 1 | - | Diffuse misangial sclerosis | - | - | - | [54] |
| | ? | 1 | <1 y | SRNS, and congenital sensorineural deafness | | | Died at age 5 y | [54] |
| *ADCK3* | G272D+1812-1813insG | 1 | 3 y | Exercise intolerance, cerebellar atrophy, myoclonus and one epileptic episode | Normal (Fibroblasts); <3% (Muscle) | Decreased activities of CI+CII and CII+CIII, and elevated activities | Yes | [55, 56] |

| Gene | Mutations | Number of patients | Age of onset | Clinical features | $CoQ_{10}$ levels compared to control | Mitochondrial function | Response to therapy | Ref. |
|---|---|---|---|---|---|---|---|---|
| | | | | | | of CI-IV and citrate synthase (Muscle) | | |
| | E551K | 1 | 18 mo | Cerebellar ataxia and atrophy, strabismus, tonic seizures, hypotonia, stroke-like lesions mild intellectual disability, and subsequent advent of *epilepsia partialis continua* | Normal (Fibroblasts), 8% (Muscle) | Mitochondrial accumulation and lipid droplets in 10-20% fibers, low activity of CII+CIII (Muscle) | No | [56] |
| | R213W-G272V | 2 sib | 18 mo | Cerebellar ataxia and atrophy, vermis hypoplasia, stroke-like lesions, ptosis, *talus valgus*, developmental delay, seizures, and *epilepsia partialis continua* | 29% (Muscle) | A slight increase in the individual activities of (CI, CII, CIII, and CIV) | No | [56] |
| | D420WfsX40, I467AfsX22 | 4 sib | 4-11 y | Cerebellar ataxia and atrophy. Three patients show exercise intolerance | 119% (Muscle) | Normal ATP synthesis, no increase in ROS, and a slightly decreased activity of CI+CIII (Fibroblasts) | - | [49, 57] |
| | Y514C-T584del | 1 | 5 y | Cerebellar ataxia and atrophy | 46% (Muscle), 51% (Fibroblasts) | Normal ATP synthesis, no increase in ROS, and reduced activity of CI+CIII (Fibroblasts) | Yes | [49, 57, 58] |
| | Q167LfsX36 | 1 | 4 y | Cerebellar ataxia and atrophy, mild intellectual disability, and mild axonal neuropathy | Normal (Lymphoblasts) 63% (Fibroblasts) | Reduced activity of CI+CIII, normal ATP levels and no increase in ROS production | - | [49, 57] |
| | R348X | 3 sib | 3-9 y | P1: Cerebellar ataxia, depression, myoclonus, swallowing difficulties, exercise intolerance, saccadic eye movement, tremor, dystonia, and epileptic discharges on EEG | - | - | - | [59] |
| | | | | P2: Progressive speech and | - | - | - | |

| Gene | Mutations | Number of patients | Age of onset | Clinical features | $CoQ_{10}$ levels compared to control | Mitochondrial function | Response to therapy | Ref. |
|---|---|---|---|---|---|---|---|---|
| | | | | coordination difficulties, mild cognitive impairment, saccadic eye movement, and cerebellar atrophy | | | | |
| | | | | P3: Disturbed motor development, epilepsy, and cerebellar ataxia | - | - | - | |
| | R348X-L379X | 2 sib | 1-2 y | P1: Cerebellar ataxia and atrophy, dysarthric speech, tremor, pyramidal syndrome, exercise intolerance, spasticity, and dystonia | - | - | - | [59] |
| | | | | P2: Cerebellar ataxia and atrophy, dysarthria, exercise intolerance, and bradyphrenia | - | Low oxygen consumption via CI, decreased CI+CIII activity (23%) (Muscle) | - | |
| | R271C-A304T | 2 sib | 15-18 y | Cerebellar ataxia and atrophy, myoclonus, tremor, dystonia, mild swallowing difficulties and muscle fatigability, and mild bradyphrenia | Normal (Muscle) | - | No | [60] |
| | A304V | 1 | 27 y | Cerebellar ataxia and atrophy, occipital seizures with myoclonus, mild cerebellar dysarthria, and dysmetria | Decreased in muscle | Decreased individual activities of CI, CIV, and citrate synthase (Muscle) | No | [60] |
| | R299W | 1 | 1 y | Cerebellar ataxia and atrophy, seizures, loss of speech and ability to walk by 14, severe feeding difficulties, severe intellectual disability, and thinning of *corpus callosum* | - | - | No | [60] |
| | Y429C-? | 2 sib | 1.5-2 y | Cerebellar ataxia and atrophy, muscle weakness, cognitive | Decreased in muscle | Decreased activity of CII+CIII, and reduced | No | [60] |

| Gene | Mutations | Number of patients | Age of onset | Clinical features | $CoQ_{10}$ levels compared to control | Mitochondrial function | Response to therapy | Ref. |
|---|---|---|---|---|---|---|---|---|
| | | | | impairment, horizontal nystagmus, slurred speech, and later tetraparesis, bilateral dysmetria, tremor, and depression | | individual activities of CI and CIV, elevated activity of citrate synthase (Muscle) | | |
| | R348X | 1 | 6 y | Cerebellar ataxia and atrophy, seizures, tremor, dysmetria, dysarthria, and a mild cognitive delay | Decreased in muscle | Decreased activities of CI+CII and CII+CIII (Muscle) | Yes | [61] |
| *COQ9* | R244X | 1 | Birth | Severe developmental delay with cerebral and cerebellar atrophy, seizures, left ventricular hypertrophy, and renal tubular dysfunction | 15% (Muscle) 41% (Fibroblasts) | Decreased activity of CII+CIII (Muscle), low ATP levels, and no ROS overproduction (Fibroblasts) | Died at 2 y | [49, 62, 63] |

Mutations in *ADCK3* (or *CABC1*), the human homologue of *Coq8*, cause a slowly progressive mitochondrial neurodegenerative disorder associated with $CoQ_{10}$ deficiency, termed Autosomal Recessive Cerebellar Ataxia type 2 (ARCA2) [57]. Unlike other *COQ* genes, mutations in *ADCK3* result in a mild phenotype that may be attributed to a number of factors. First, ADCK3 is postulated to have a regulatory rather than an enzymatic function in the respiratory chain [19, 22, 32]. Second, ADCK3 belongs to a highly conserved family of atypical kinases that comprises five paralogs (ADCK1-ADCK5) with possible redundant functions [57].

**Mouse models of Coenzyme Q deficiency**

Analysis of the CoQ biosynthetic pathway in yeast and bacteria contributed greatly to the understanding of human genetic diseases related to CoQ deficiency [10, 35]. However, in order to unravel the pathophysiological consequences of CoQ deficiency, it is necessary to use multicellular organisms. To date, five knockout (KO) mice have been generated for the genes implicated in CoQ biosynthesis [37, 64]. In the early 1970s, Lyon and colleagues reported the first spontaneous missense mutant mouse, designated kidney disease *(kd),* with an autosomal recessive kidney disorder [65]. At 12 weeks, homozygous mice displayed tubular dilatation and mononuclear cell infiltration, and proteinuria, leading ultimately to renal failure between five and seven months of age [66]. The susceptibility gene for the *kd/kd* phenotype was later mapped and found to encode a prenyl transferase, which was later identified as PDSS2 [67]. It was first postulated that the pathogenesis of *kd* mice was immune mediated. However the generation of conditional *Pdss2* KO mice (*Pdss2* $^{f/-}$) targeting the different cell types (renal glomerular podocytes, renal tubular epithelium and hepatocytes, monocytes or hepatocytes) [67] and the extensive characterization of *Pdss2*$^{kd/kd}$ mice revealed that glomerular podocytes were selectively affected and displayed a significant decrease in $CoQ_9$ and $CoQ_{10}$ content [67]. Interestingly, supplementation with $CoQ_{10}$ was shown to partially alleviate renal symptoms [68], indicating that CoQ deficiency impedes the respiratory chain function in the kidney leading to podocyte death. This is a puzzling observation, given the moderate energetic need of this cell type. It is therefore reasonable to consider that the antioxidant role of CoQ might also be severely impaired in these cells. It is also possible that other effects of CoQ deficiency might have developed with time, had the renal phenotype been less severe. Considering that the total *Pdss2* KO mice are embryonically lethal, arresting development at mid-gestation (around E9.5) [67], attempts were made to derive further conditional knockouts of *Pdss2* specifically

targeting the cerebellum, one of the most affected organs in CoQ deficiency, with cerebellar atrophy being a common feature in the human disease [44]. Hence, Lu *et al.* later showed that *Pdss2* $^{f/-}$; *Pax2-cre* embryos, with the Cre-recombinase expression being confined to the midbrain-hindbrain region during embryonic development, display cerebellar hypoplasia and present neonatal death due to cleft palate and micrognathia [69]. Although no apparent abnormality between the *Pdss2* $^{f/-}$; *Pax2-cre* and control mice was observed before E11.5, the E12.5–E14.5 period, which marks a critical phase for cerebellar development, displayed a number of anomalies, including a delay in radial glial cell development leading to an impaired neuroblast radial migration and intermediate zone expansion. Starting from E14.5, a drop in cell proliferation and apoptosis resulted in loss of the tissue organization and subsequent hypoplasia. The ensuing generation of *Pdss2* $^{f/-}$*; Pcp2-cre* mice with confined Cre-recombinase expression to Purkinje cells enabled the study of *Pdss2* depletion in adulthood [69]. This study revealed that most Purkinje cells were lost within six months, with signs of cerebellar ataxia appearing three months later. Although apoptosis accounted for the massive cell loss in the cerebellum, Purkinje cell degeneration could not be attributed to this phenomenon [69].

Similar to *Pdss2*, disruption of *Coq7* (also called *Mclk1*) in mice is lethal [37, 64]. Two *Coq7* null mouse models were simultaneously generated, and both studies point to an important role of CoQ in development and survival. In the first model, embryos exhibited a severe developmental delay at E9.5 and were resorbed by E13.5 [37]. Quantification of CoQ content in these embryos revealed a total absence of $CoQ_9$ and $CoQ_{10}$ but a significant rise in $DMQ_9$. Derivation of *Coq7*$^{-/-}$ ES cells showed rather unexpectedly that mitochondrial respiration is only mildly impaired, with 65% of wildtype oxygen consumption, raising the possibility that the role of CoQ in embryogenesis might be respiration-independent, and linked instead to an overall disorganized membrane structure. Alternatively, one could also argue that *in vitro* conditions do not realistically reproduce the complexity of the respiratory chain *in vivo*. Further analyses are needed to address this question.

In the second model of *Coq7* deficiency, embryos failed to survive beyond E10.5 and were considerably smaller (20 times) than wildtype littermates [64]. In addition, the mice displayed a delayed neural development, with the presence of enlarged mitochondria and lysosomes and an overall membrane disorganization in the cerebral wall, therefore implicating Coq7 in mitochondrial integrity and neurogenesis

[64]. Like the first model, embryos exhibited an abnormal accumulation of $DMQ_9$, while *Coq7* null ES cells derived from this model presented a severe growth defect when cultured in a serum-free medium, highlighting the pivotal role of CoQ in electron transfer and suggesting that $DMQ_9$ has only a minor physiological function in electron shuttling. Further characterization of *Coq7*-deficient ES cells gave new insight into the role of CoQ in respiration and revealed the presence of low levels of both basal and induced reactive oxygen species (ROS), as well as resistance to apoptosis [70]. This clear growth advantage opens the way for the novel theory that CoQ may contribute to oxidative stress. The elucidation of such a phenomenon likely hinges on the fact that CoQ can act both as an anti-oxidant and as a pro-oxidant depending on its oxidation state, ubisemiquinone versus ubiquinone.

Heterozygous *Coq7*$^{+/-}$ animals are viable and display a surprising increase in lifespan (up to 30% depending on the genetic background) [70, 71]. Moreover, *Coq7*$^{+/-}$ embryos and pups show a quinone profile comparable to wildtype controls, even though they possess less than 50% of Coq7 [37, 64, 72]. Older mice, however, have low levels of DNA damage and exhibit loss-of-heterozygozity in liver, concomitant with a drop in CoQ and a total absence of DMQ, thus challenging previous findings in *Coq7*$^{-/-}$ ES cells [37]. Subsequent work by Lapointe and colleagues reported that although the total amount of mitochondrial CoQ is similar between *Coq7*$^{+/-}$ and *Coq7*$^{+/+}$ animals, its distribution changed, with a reversed outer membrane to inner membrane ratio (OM/IM) compared to wildtype [72]. This observation is fully consistent with the argument that Coq7 has an essential role in maintaining the CoQ content of the IM to ensure a physiologically normal electron transport. The rise of CoQ in the OM is still quite perplexing, although the authors suggest that the antioxidant activity of ubiquinone may come into play [72]. Indeed, the low levels of CoQ in the IM of *Coq7*$^{+/-}$ animals are thought to increase ROS due to inhibition of the electron transport chain, and the observed accumulation of CoQ in the OM would be part of a protective response to prevent ROS leakage into the cytoplasm. Dietary supplemented CoQ was later shown to restore both the levels of CoQ in the IM and mitochondrial function.

As for other models, *Coq3* KO mice are not viable, although no further information about the stage of embryonic death or the levels of CoQ has been provided [72]. *Coq3*$^{+/-}$ mice, in contrast to *Coq7*$^{+/-}$ mice, show a normal level of CoQ in liver mitochondria but exhibit a normal lifespan [72]. The phenotype of these mice

suggests, *prima facie*, that absence of Coq3 does not limit CoQ biosynthesis, but this issue must be addressed more fully in the future.

The European Conditional Mouse Mutagenesis Program (EUCOMM) [73] is currently generating knockout alleles for other genes involved in CoQ biosynthesis including *Coq4* and *Coq9*. Preliminary data show that *Coq4* deficiency is embryonic lethal, further corroborating the initial observation that CoQ is fundamental to normal embryonic development in mice. Unexpectedly however, *Coq9*-deficient mice not only are viable animals, they also do not appear to show any overt disability, in striking contrast to the human disease [63]. The only phenotype found consisted in signs of hyperactivity (in females). The two mouse models are currently undergoing exhaustive characterization, which will help to shed light on the heterogeneity of the clinical phenotypes of CoQ deficiencies.

Very recently, a knockin mouse model for *Coq9* (R239X), termed *Coq9*$^{x/x}$ was generated [74]. This mutation is homologous to the human R244X *COQ9* mutation [63] and produces a stable truncated Coq9 protein. As expected, this model reproduced the main features of CoQ deficiency, i.e. reduced levels of $CoQ_9$ and $CoQ_{10}$ in all tested tissues (kidney, heart, cerebrum, skeletal muscle and liver) combined with an accumulation of $DMQ_9$. More importantly, *Coq9*$^{x/x}$ mice presented the clinical signs of the encephalomyopathic form of CoQ deficiency and died between 3-6 months of age. In particular, the mice developed spongiform degeneration, astrogliosis, and a caspase-independent neuronal death, as well as severe demyelinization in the pons and the white matter of the brain, and in the nerve fibers of the hind legs skeletal muscle. The presence of a dysfunctional Coq9 also resulted in energy depletion in the brain due to loss of Complex I and an increase in free Complex III, suggesting that oxidative damage contributes to the pathology of CoQ deficiency *in vivo*. Nevertheless, the precise pathogenic process leading to disease is yet to be fully understood.

**Coenzyme Q: not only in mitochondria**

Although extensively studied in mitochondria, CoQ is also localized in other cellular membranes such as lysosomes, Golgi, endoplasmic reticulum (ER), and plasma membranes, where it is present at even higher concentrations than in mitochondria [14, 75]. A recent study by Mugoni and colleagues reported that UBIAD1, a

prenyltransferase enzyme involved in the biosynthetic pathway of vitamin K2 [76], is the Golgi counterpart of COQ2 that mediates biosynthesis of CoQ and regulates eNOS activity in this organelle [77]. Interestingly, mutations in human UBIAD1 cause Schnyder's Corneal Dystrophy (SCD), in which patients suffer from elevated corneal cholesterol and phospholipids deposition [78-80]. Vitamin K2, best known for its role as a cofactor in blood coagulation, was also recently described as a mitochondrial electron carrier that maintains normal ATP synthesis in Drosophila [81], and was shown to be involved in the transcriptional regulation of lipid metabolism and cholesterol efflux [82]. Moreover, UBIAD1 was found to interact with inhibiting 3-hydroxy-3-methyl-glutaryl-CoA reductase (HMGCR), sterol O-acyltransferase (SOAT1), and Apoliporotein E (ApoE), key players in cholesterol synthesis, storage, and transport, respectively [78, 83]. These findings are intriguing and suggest that complex molecular links exist between CoQ, vitamin K2, and cholesterol. A detailed mechanism is yet to be elucidated. A number of dark zones subsist, however: UBIAD1 displays different localization, function and interactors depending on the cell type where it is investigated. Further studies are required to define the role of UBIAD1 in lipid metabolism and its link to $CoQ_{10}$.

**Coenzyme $Q_{10}$ and statins**

$CoQ_{10}$ derives its isoprenyl tail from the mevalonate pathway **(Figure 2)**. The latter is the primary pathway by which cholesterol is synthesized *de novo* in mammalian cells [84]. Besides $CoQ_{10}$, this pathway also derives a number of isoprenoid groups, such as dolichol, a lipid carrier for the glycan precursor in N-linked protein glycosylation, as well as short-chain isoprenoids FPP and geranylgeranylpyrophosphate (GGPP) that covalently attach to small GTPases and target them to membranes [84, 85]. Statins are widely prescribed to correct hypercholesterolemia [86]. This drug reduces low density lipoprotein (LDL) cholesterol by inhibiting HMGCR, the enzyme that mediates the rate-limiting step of the entire pathway by converting HMG-CoA to mevalonate. Inevitably, this block also decreases dolichol and $CoQ_{10}$ levels and leads to adverse muscle-related complications [87, 88]. These side effects are suggested to be a direct consequence of $CoQ_{10}$ and short-chain lipids depletion rather than cholesterol reduction [42]. This view was further confirmed by the observation that unlike HMGCR, inhibition of squalene synthase, the enzyme that catalyzes the first committed step in the sterol branch of the cholesterol biosynthesis pathway **(Figure 2)**, does not result in myotoxicity *in vitro* [89, 90], making squalene synthase inhibitors potential cholesterol lowering drugs. Supplementation of statin

patients with $CoQ_{10}$ shows conflicting results [91, 92] and does not seem to provide a clear answer as to the beneficial effect of CoQ on muscle symptoms. Remarkably, however, statin treatment was shown to uncover neuromuscular disorders in their presymptomatic stage [93], which could be a valuable tool for the study of CoQ deficiency in animal models.

Overall, a more thorough investigation is required to help to shed light on one of the least studied aspects of CoQ function, namely lipid metabolism. This will no doubt advance our understanding of the pathophysiology of CoQ deficiencies and perhaps pave the way for a role for CoQ that extends beyond the current electron shuttling and antioxidant properties.

**Acknowledgements:**
This work was supported by the UK ataxia association, the Fondation pour la Recherche Médicale (FRM Programme « Physiopathologie Mitochondriale» DPM20121125555) and the European Community, under the European Research Council [206634/ISCATAXIA].

**References:**

[1] C.A. Yu, L. Zhang, K.P. Deng, H. Tian, D. Xia, H. Kim, J. Deisenhofer, L. Yu, Structure and reaction mechanisms of multifunctional mitochondrial cytochrome bc1 complex, BioFactors 9 (1999) 103-109.

[2] U. Brandt, Proton translocation in the respiratory chain involving ubiquinone--a hypothetical semiquinone switch mechanism for complex I, BioFactors 9 (1999) 95-101.

[3] M. Turunen, J. Olsson, G. Dallner, Metabolism and function of coenzyme Q, Biochim. Biophys. Acta 1660 (2004) 171-199.

[4] L. Walter, H. Miyoshi, X. Leverve, P. Bernard, E. Fontaine, Regulation of the mitochondrial permeability transition pore by ubiquinone analogs. A progress report, Free Radic. Res. 36 (2002) 405-412.

[5] K.S. Echtay, E. Winkler, M. Klingenberg, Coenzyme Q is an obligatory cofactor for uncoupling protein function, Nature 408 (2000) 609-613.

[6] D.R. Evans, H.I. Guy, Mammalian pyrimidine biosynthesis: fresh insights into an ancient pathway, J. Biol. Chem. 279 (2004) 33035-33038.

[7] L. Ernster, G. Dallner, Biochemical, physiological and medical aspects of ubiquinone function, Biochim. Biophys. Acta 1271 (1995) 195-204.

[8] F.L. Crane, Biochemical functions of coenzyme Q10, J. Am. Coll. Nutr. 20 (2001) 591-598.

[9] F. Gibson, G.B. Cox, The use of mutants of Escherichia coli K12 in studying electron transport and oxidative phosphorylation, Essays Biochem. 9 (1973) 1-29.

[10] U.C. Tran, C.F. Clarke, Endogenous synthesis of coenzyme Q in eukaryotes, Mitochondrion 7 Suppl (2007) S62-71.

[11] A. Tzagoloff, C.L. Dieckmann, PET genes of Saccharomyces cerevisiae, Microbiol. Rev. 54 (1990) 211-225.

[12] A. Johnson, P. Gin, B.N. Marbois, E.J. Hsieh, M. Wu, M.H. Barros, C.F. Clarke, A. Tzagoloff, COQ9, a new gene required for the biosynthesis of coenzyme Q in Saccharomyces cerevisiae, J. Biol. Chem. 280 (2005) 31397-31404.

[13] M. Bentinger, M. Tekle, G. Dallner, Coenzyme Q--biosynthesis and functions, Biochem. Biophys. Res. Commun. 396 (2010) 74-79.

[14] M. Bentinger, M. Tekle, K. Brismar, T. Chojnacki, E. Swiezewska, G. Dallner, Stimulation of coenzyme Q synthesis, BioFactors 32 (2008) 99-111.

[15] F. Pierrel, O. Hamelin, T. Douki, S. Kieffer-Jaquinod, U. Muhlenhoff, M. Ozeir, R. Lill, M. Fontecave, Involvement of mitochondrial ferredoxin and para-aminobenzoic acid in yeast coenzyme Q biosynthesis, Chem. Biol. 17 (2010) 449-459.

[16] R. Saiki, A. Nagata, N. Uchida, T. Kainou, H. Matsuda, M. Kawamukai, Fission yeast decaprenyl diphosphate synthase consists of Dps1 and the newly characterized Dlp1 protein in a novel heterotetrameric structure, Eur. J. Biochem. 270 (2003) 4113-4121.

[17] R. Saiki, A. Nagata, T. Kainou, H. Matsuda, M. Kawamukai, Characterization of solanesyl and decaprenyl diphosphate synthases in mice and humans, FEBS J 272 (2005) 5606-5622.

[18] K. Okada, K. Suzuki, Y. Kamiya, X. Zhu, S. Fujisaki, Y. Nishimura, T. Nishino, T. Nakagawa, M. Kawamukai, H. Matsuda, Polyprenyl diphosphate synthase essentially defines the length of the side chain of ubiquinone, Biochim. Biophys. Acta 1302 (1996) 217-223.

[19] M.N. Ashby, S.Y. Kutsunai, S. Ackerman, A. Tzagoloff, P.A. Edwards, COQ2 is a candidate for the structural gene encoding para-hydroxybenzoate:polyprenyltransferase, J. Biol. Chem. 267 (1992) 4128-4136.

[20] M. Ozeir, U. Muhlenhoff, H. Webert, R. Lill, M. Fontecave, F. Pierrel, Coenzyme Q biosynthesis: Coq6 is required for the C5-hydroxylation reaction and substrate analogs rescue Coq6 deficiency, Chem. Biol. 18 (2011) 1134-1142.

[21] W.W. Poon, R.J. Barkovich, A.Y. Hsu, A. Frankel, P.T. Lee, J.N. Shepherd, D.C. Myles, C.F. Clarke, Yeast and rat Coq3 and Escherichia coli UbiG polypeptides catalyze both O-methyltransferase steps in coenzyme Q biosynthesis, J. Biol. Chem. 274 (1999) 21665-21672.

[22] B.N. Marbois, C.F. Clarke, The COQ7 gene encodes a protein in saccharomyces cerevisiae necessary for ubiquinone biosynthesis, J. Biol. Chem. 271 (1996) 2995-3004.

[23] R.J. Barkovich, A. Shtanko, J.A. Shepherd, P.T. Lee, D.C. Myles, A. Tzagoloff, C.F. Clarke, Characterization of the COQ5 gene from Saccharomyces cerevisiae. Evidence for a C-methyltransferase in ubiquinone biosynthesis, J. Biol. Chem. 272 (1997) 9182-9188.

[24] S.W. Baba, G.I. Belogrudov, J.C. Lee, P.T. Lee, J. Strahan, J.N. Shepherd, C.F. Clarke, Yeast Coq5 C-methyltransferase is required for stability of other polypeptides involved in coenzyme Q biosynthesis, J. Biol. Chem. 279 (2004) 10052-10059.

[25] B. Marbois, P. Gin, K.F. Faull, W.W. Poon, P.T. Lee, J. Strahan, J.N. Shepherd, C.F. Clarke, Coq3 and Coq4 define a polypeptide complex in yeast mitochondria for the biosynthesis of coenzyme Q, J. Biol. Chem. 280 (2005) 20231-20238.

[26] L.X. Xie, E.J. Hsieh, S. Watanabe, C.M. Allan, J.Y. Chen, U.C. Tran, C.F. Clarke, Expression of the human atypical kinase ADCK3 rescues coenzyme Q biosynthesis and phosphorylation of Coq polypeptides in yeast coq8 mutants, Biochim. Biophys. Acta 1811 (2011) 348-360.

[27] P. Gin, C.F. Clarke, Genetic evidence for a multi-subunit complex in coenzyme Q biosynthesis in yeast and the role of the Coq1 hexaprenyl diphosphate synthase, J. Biol. Chem. 280 (2005) 2676-2681.

[28] G.I. Belogrudov, P.T. Lee, T. Jonassen, A.Y. Hsu, P. Gin, C.F. Clarke, Yeast COQ4 encodes a mitochondrial protein required for coenzyme Q synthesis, Arch. Biochem. Biophys. 392 (2001) 48-58.

[29] P. Gin, A.Y. Hsu, S.C. Rothman, T. Jonassen, P.T. Lee, A. Tzagoloff, C.F. Clarke, The Saccharomyces cerevisiae COQ6 gene encodes a mitochondrial flavin-

dependent monooxygenase required for coenzyme Q biosynthesis, J. Biol. Chem. 278 (2003) 25308-25316.

[30] T. Jonassen, M. Proft, F. Randez-Gil, J.R. Schultz, B.N. Marbois, K.D. Entian, C.F. Clarke, Yeast Clk-1 homologue (Coq7/Cat5) is a mitochondrial protein in coenzyme Q synthesis, J. Biol. Chem. 273 (1998) 3351-3357.

[31] A. Tauche, U. Krause-Buchholz, G. Rodel, Ubiquinone biosynthesis in Saccharomyces cerevisiae: the molecular organization of O-methylase Coq3p depends on Abc1p/Coq8p, FEMS Yeast Res 8 (2008) 1263-1275.

[32] E.J. Hsieh, P. Gin, M. Gulmezian, U.C. Tran, R. Saiki, B.N. Marbois, C.F. Clarke, Saccharomyces cerevisiae Coq9 polypeptide is a subunit of the mitochondrial coenzyme Q biosynthetic complex, Arch. Biochem. Biophys. 463 (2007) 19-26.

[33] A.Y. Hsu, T.Q. Do, P.T. Lee, C.F. Clarke, Genetic evidence for a multi-subunit complex in the O-methyltransferase steps of coenzyme Q biosynthesis, Biochim. Biophys. Acta 1484 (2000) 287-297.

[34] U.C. Tran, B. Marbois, P. Gin, M. Gulmezian, T. Jonassen, C.F. Clarke, Complementation of Saccharomyces cerevisiae coq7 mutants by mitochondrial targeting of the Escherichia coli UbiF polypeptide: two functions of yeast Coq7 polypeptide in coenzyme Q biosynthesis, J. Biol. Chem. 281 (2006) 16401-16409.

[35] R. Meganathan, Ubiquinone biosynthesis in microorganisms, FEMS Microbiol. Lett. 203 (2001) 131-139.

[36] F. Gibson, I.G. Young, Isolation and characterization of intermediates in ubiquinone biosynthesis, Methods Enzymol. 53 (1978) 600-609.

[37] F. Levavasseur, H. Miyadera, J. Sirois, M.L. Tremblay, K. Kita, E. Shoubridge, S. Hekimi, Ubiquinone is necessary for mouse embryonic development but is not essential for mitochondrial respiration, J. Biol. Chem. 276 (2001) 46160-46164.

[38] C.M. Quinzii, S. DiMauro, M. Hirano, Human coenzyme Q10 deficiency, Neurochem. Res. 32 (2007) 723-727.

[39] V. Emmanuele, L.C. Lopez, A. Berardo, A. Naini, S. Tadesse, B. Wen, E. D'Agostino, M. Solomon, S. DiMauro, C. Quinzii, M. Hirano, Heterogeneity of coenzyme Q10 deficiency: patient study and literature review, Arch. Neurol. 69 (2012) 978-983.

[40] R. Montero, M. Pineda, A. Aracil, M.A. Vilaseca, P. Briones, J.A. Sanchez-Alcazar, P. Navas, R. Artuch, Clinical, biochemical and molecular aspects of cerebellar ataxia and Coenzyme Q10 deficiency, Cerebellum 6 (2007) 118-122.

[41] C.M. Quinzii, M. Hirano, Primary and secondary CoQ(10) deficiencies in humans, BioFactors 37 (2011) 361-365.

[42] G.P. Littarru, P. Langsjoen, Coenzyme Q10 and statins: biochemical and clinical implications, Mitochondrion 7 Suppl (2007) S168-174.

[43] J. Mollet, I. Giurgea, D. Schlemmer, G. Dallner, D. Chretien, A. Delahodde, D. Bacq, P. de Lonlay, A. Munnich, A. Rotig, Prenyldiphosphate synthase, subunit 1 (PDSS1) and OH-benzoate polyprenyltransferase (COQ2) mutations in ubiquinone deficiency and oxidative phosphorylation disorders, J. Clin. Invest. 117 (2007) 765-772.

[44] L.C. Lopez, M. Schuelke, C.M. Quinzii, T. Kanki, R.J. Rodenburg, A. Naini, S. Dimauro, M. Hirano, Leigh syndrome with nephropathy and CoQ10 deficiency due to decaprenyl diphosphate synthase subunit 2 (PDSS2) mutations, Am J Hum Genet 79 (2006) 1125-1129.

[45] C.M. Quinzii, L.C. Lopez, J. Von-Moltke, A. Naini, S. Krishna, M. Schuelke, L. Salviati, P. Navas, S. DiMauro, M. Hirano, Respiratory chain dysfunction and oxidative stress correlate with severity of primary CoQ10 deficiency, FASEB J. 22 (2008) 1874-1885.

[46] C. Quinzii, A. Naini, L. Salviati, E. Trevisson, P. Navas, S. Dimauro, M. Hirano, A mutation in para-hydroxybenzoate-polyprenyl transferase (COQ2) causes primary coenzyme Q10 deficiency, Am J Hum Genet 78 (2006) 345-349.

[47] L. Salviati, S. Sacconi, L. Murer, G. Zacchello, L. Franceschini, A.M. Laverda, G. Basso, C. Quinzii, C. Angelini, M. Hirano, A.B. Naini, P. Navas, S. DiMauro, G. Montini, Infantile encephalomyopathy and nephropathy with CoQ10 deficiency: a CoQ10-responsive condition, Neurology 65 (2005) 606-608.

[48] F. Diomedi-Camassei, S. Di Giandomenico, F.M. Santorelli, G. Caridi, F. Piemonte, G. Montini, G.M. Ghiggeri, L. Murer, L. Barisoni, A. Pastore, A.O. Muda, M.L. Valente, E. Bertini, F. Emma, COQ2 nephropathy: a newly described inherited mitochondriopathy with primary renal involvement, J. Am. Soc. Nephrol. 18 (2007) 2773-2780.

[49] C.M. Quinzii, L.C. Lopez, R.W. Gilkerson, B. Dorado, J. Coku, A.B. Naini, C. Lagier-Tourenne, M. Schuelke, L. Salviati, R. Carrozzo, F. Santorelli, S. Rahman, M. Tazir, M. Koenig, S. DiMauro, M. Hirano, Reactive oxygen species, oxidative stress, and cell death correlate with level of CoQ10 deficiency, FASEB J. 24 (2010) 3733-3743.

[50] E. Scalais, R. Chafai, R. Van Coster, L. Bindl, C. Nuttin, C. Panagiotaraki, S. Seneca, W. Lissens, A. Ribes, C. Geers, J. Smet, L. De Meirleir, Early myoclonic epilepsy, hypertrophic cardiomyopathy and subsequently a nephrotic syndrome in a patient with CoQ10 deficiency caused by mutations in para-hydroxybenzoate-polyprenyl transferase (COQ2), European journal of paediatric neurology : EJPN : official journal of the European Paediatric Neurology Society (2013).

[51] B.S. Jakobs, L.P. van den Heuvel, R.J. Smeets, M.C. de Vries, S. Hien, T. Schaible, J.A. Smeitink, R.A. Wevers, S.B. Wortmann, R.J. Rodenburg, A novel mutation in COQ2 leading to fatal infantile multisystem disease, J. Neurol. Sci. 326 (2013) 24-28.

[52] L. Salviati, E. Trevisson, M.A. Rodriguez Hernandez, A. Casarin, V. Pertegato, M. Doimo, M. Cassina, C. Agosto, M.A. Desbats, G. Sartori, S. Sacconi, L. Memo, O. Zuffardi, R. Artuch, C. Quinzii, S. Dimauro, M. Hirano, C. Santos-Ocana, P. Navas, Haploinsufficiency of COQ4 causes coenzyme Q10 deficiency, J. Med. Genet. 49 (2012) 187-191.

[53] S.F. Heeringa, G. Chernin, M. Chaki, W. Zhou, A.J. Sloan, Z. Ji, L.X. Xie, L. Salviati, T.W. Hurd, V. Vega-Warner, P.D. Killen, Y. Raphael, S. Ashraf, B. Ovunc, D.S. Schoeb, H.M. McLaughlin, R. Airik, C.N. Vlangos, R. Gbadegesin, B. Hinkes, P. Saisawat, E. Trevisson, M. Doimo, A. Casarin, V. Pertegato, G. Giorgi, H. Prokisch, A. Rotig, G. Nurnberg, C. Becker, S. Wang, F. Ozaltin, R. Topaloglu, A. Bakkaloglu, S.A. Bakkaloglu, D. Muller, A. Beissert, S. Mir, A. Berdeli, S. Varpizen, M. Zenker, V. Matejas, C. Santos-Ocana, P. Navas, T. Kusakabe, A. Kispert, S. Akman, N.A. Soliman, S. Krick, P. Mundel, J. Reiser, P. Nurnberg, C.F. Clarke, R.C. Wiggins, C. Faul, F. Hildebrandt, COQ6 mutations in human patients produce nephrotic syndrome with sensorineural deafness, The Journal of clinical investigation 121 (2011) 2013-2024.

[54] S.F. Heeringa, G. Chernin, M. Chaki, W. Zhou, A.J. Sloan, Z. Ji, L.X. Xie, L. Salviati, T.W. Hurd, V. Vega-Warner, P.D. Killen, Y. Raphael, S. Ashraf, B. Ovunc, D.S. Schoeb, H.M. McLaughlin, R. Airik, C.N. Vlangos, R. Gbadegesin, B. Hinkes, P. Saisawat, E. Trevisson, M. Doimo, A. Casarin, V. Pertegato, G. Giorgi, H. Prokisch, A. Rotig, G. Nurnberg, C. Becker, S. Wang, F. Ozaltin, R. Topaloglu, A. Bakkaloglu, S.A. Bakkaloglu, D. Muller, A. Beissert, S. Mir, A. Berdeli, S. Varpizen, M. Zenker, V. Matejas, C. Santos-Ocana, P. Navas, T. Kusakabe, A. Kispert, S. Akman, N.A. Soliman, S. Krick, P. Mundel, J. Reiser, P. Nurnberg, C.F. Clarke, R.C. Wiggins, C. Faul, F. Hildebrandt, COQ6 mutations in human patients produce nephrotic syndrome with sensorineural deafness, J. Clin. Invest. 121 (2011) 2013-2024.

[55] K. Aure, J.F. Benoist, H. Ogier de Baulny, N.B. Romero, O. Rigal, A. Lombes, Progression despite replacement of a myopathic form of coenzyme Q10 defect, Neurology 63 (2004) 727-729.

[56] J. Mollet, A. Delahodde, V. Serre, D. Chretien, D. Schlemmer, A. Lombes, N. Boddaert, I. Desguerre, P. de Lonlay, H.O. de Baulny, A. Munnich, A. Rotig, CABC1 gene mutations cause ubiquinone deficiency with cerebellar ataxia and seizures, Am J Hum Genet 82 (2008) 623-630.

[57] C. Lagier-Tourenne, M. Tazir, L.C. Lopez, C.M. Quinzii, M. Assoum, N. Drouot, C. Busso, S. Makri, L. Ali-Pacha, T. Benhassine, M. Anheim, D.R. Lynch, C. Thibault, F. Plewniak, L. Bianchetti, C. Tranchant, O. Poch, S. DiMauro, J.L. Mandel, M.H. Barros, M. Hirano, M. Koenig, ADCK3, an ancestral kinase, is mutated in a form of recessive ataxia associated with coenzyme Q10 deficiency, Am J Hum Genet 82 (2008) 661-672.

[58] C. Lamperti, A. Naini, M. Hirano, D.C. De Vivo, E. Bertini, S. Servidei, M. Valeriani, D. Lynch, B. Banwell, M. Berg, T. Dubrovsky, C. Chiriboga, C. Angelini, E. Pegoraro, S. DiMauro, Cerebellar ataxia and coenzyme Q10 deficiency, Neurology 60 (2003) 1206-1208.

[59] M. Gerards, B. van den Bosch, C. Calis, K. Schoonderwoerd, K. van Engelen, M. Tijssen, R. de Coo, A. van der Kooi, H. Smeets, Nonsense mutations in CABC1/ADCK3 cause progressive cerebellar ataxia and atrophy, Mitochondrion 10 (2010) 510-515.

[60] R. Horvath, B. Czermin, S. Gulati, S. Demuth, G. Houge, A. Pyle, C. Dineiger, E.L. Blakely, A. Hassani, C. Foley, M. Brodhun, K. Storm, J. Kirschner, G.S. Gorman, H. Lochmuller, E. Holinski-Feder, R.W. Taylor, P.F. Chinnery, Adult-onset cerebellar ataxia due to mutations in CABC1/ADCK3, J. Neurol. Neurosurg. Psychiatry 83 (2012) 174-178.

[61] A. Terracciano, F. Renaldo, G. Zanni, A. D'Amico, A. Pastore, S. Barresi, E.M. Valente, F. Piemonte, G. Tozzi, R. Carrozzo, M. Valeriani, R. Boldrini, E. Mercuri, F.M. Santorelli, E. Bertini, The use of muscle biopsy in the diagnosis of undefined ataxia with cerebellar atrophy in children, European journal of paediatric neurology : EJPN : official journal of the European Paediatric Neurology Society 16 (2012) 248-256.

[62] S. Rahman, I. Hargreaves, P. Clayton, S. Heales, Neonatal presentation of coenzyme Q10 deficiency, J. Pediatr. 139 (2001) 456-458.

[63] A.J. Duncan, M. Bitner-Glindzicz, B. Meunier, H. Costello, I.P. Hargreaves, L.C. Lopez, M. Hirano, C.M. Quinzii, M.I. Sadowski, J. Hardy, A. Singleton, P.T. Clayton, S. Rahman, A nonsense mutation in COQ9 causes autosomal-recessive neonatal-onset primary coenzyme Q10 deficiency: a potentially treatable form of mitochondrial disease, Am J Hum Genet 84 (2009) 558-566.

[64] D. Nakai, S. Yuasa, M. Takahashi, T. Shimizu, S. Asaumi, K. Isono, T. Takao, Y. Suzuki, H. Kuroyanagi, K. Hirokawa, H. Koseki, T. Shirsawa, Mouse homologue of coq7/clk-1, longevity gene in Caenorhabditis elegans, is essential for coenzyme Q synthesis, maintenance of mitochondrial integrity, and neurogenesis, Biochem. Biophys. Res. Commun. 289 (2001) 463-471.

[65] M.F. Lyon, E.V. Hulse, An inherited kidney disease of mice resembling human nephronophthisis, J. Med. Genet. 8 (1971) 41-48.
[66] V. Sibalic, X. Fan, R.P. Wuthrich, Characterisation of cellular infiltration and adhesion molecule expression in CBA/CaH-kdkd mice with tubulointerstitial renal disease, Histochem. Cell Biol. 108 (1997) 235-242.
[67] M. Peng, M.J. Falk, V.H. Haase, R. King, E. Polyak, M. Selak, M. Yudkoff, W.W. Hancock, R. Meade, R. Saiki, A.L. Lunceford, C.F. Clarke, D.L. Gasser, Primary coenzyme Q deficiency in Pdss2 mutant mice causes isolated renal disease, PLoS Genet 4 (2008) e1000061.
[68] R. Saiki, A.L. Lunceford, Y. Shi, B. Marbois, R. King, J. Pachuski, M. Kawamukai, D.L. Gasser, C.F. Clarke, Coenzyme Q10 supplementation rescues renal disease in Pdss2kd/kd mice with mutations in prenyl diphosphate synthase subunit 2, Am J Physiol Renal Physiol 295 (2008) F1535-1544.
[69] S. Lu, L.Y. Lu, M.F. Liu, Q.J. Yuan, M.H. Sham, X.Y. Guan, J.D. Huang, Cerebellar defects in Pdss2 conditional knockout mice during embryonic development and in adulthood, Neurobiol. Dis. 45 (2012) 219-233.
[70] X. Liu, N. Jiang, B. Hughes, E. Bigras, E. Shoubridge, S. Hekimi, Evolutionary conservation of the clk-1-dependent mechanism of longevity: loss of mclk1 increases cellular fitness and lifespan in mice, Genes Dev. 19 (2005) 2424-2434.
[71] J. Lapointe, Z. Stepanyan, E. Bigras, S. Hekimi, Reversal of the mitochondrial phenotype and slow development of oxidative biomarkers of aging in long-lived Mclk1+/- mice, J. Biol. Chem. 284 (2009) 20364-20374.
[72] J. Lapointe, Y. Wang, E. Bigras, S. Hekimi, The submitochondrial distribution of ubiquinone affects respiration in long-lived Mclk1+/- mice, J. Cell Biol. 199 (2012) 215-224.
[73] R.H. Friedel, C. Seisenberger, C. Kaloff, W. Wurst, EUCOMM--the European conditional mouse mutagenesis program, Brief Funct Genomic Proteomic 6 (2007) 180-185.
[74] L. Garcia-Corzo, M. Luna-Sanchez, C. Doerrier, J.A. Garcia, A. Guaras, R. Acin-Perez, J. Bullejos-Peregrin, A. Lopez, G. Escames, J.A. Enriquez, D. Acuna-Castroviejo, L.C. Lopez, Dysfunctional Coq9 protein causes predominant encephalomyopathy associated with CoQ deficiency, Hum. Mol. Genet. 22 (2013) 1233-1248.
[75] F.L. Crane, Discovery of ubiquinone (coenzyme Q) and an overview of function, Mitochondrion 7 Suppl (2007) S2-7.
[76] K. Nakagawa, Y. Hirota, N. Sawada, N. Yuge, M. Watanabe, Y. Uchino, N. Okuda, Y. Shimomura, Y. Suhara, T. Okano, Identification of UBIAD1 as a novel human menaquinone-4 biosynthetic enzyme, Nature 468 (2010) 117-121.

[77] V. Mugoni, R. Postel, V. Catanzaro, E. De Luca, E. Turco, G. Digilio, L. Silengo, M.P. Murphy, C. Medana, D.Y. Stainier, J. Bakkers, M.M. Santoro, Ubiad1 is an antioxidant enzyme that regulates eNOS activity by CoQ10 synthesis, Cell 152 (2013) 504-518.

[78] M.L. Nickerson, B.N. Kostiha, W. Brandt, W. Fredericks, K.P. Xu, F.S. Yu, B. Gold, J. Chodosh, M. Goldberg, W. Lu da, M. Yamada, T.M. Tervo, R. Grutzmacher, C. Croasdale, M. Hoeltzenbein, J. Sutphin, S.B. Malkowicz, L. Wessjohann, H.S. Kruth, M. Dean, J.S. Weiss, UBIAD1 mutation alters a mitochondrial prenyltransferase to cause Schnyder corneal dystrophy, PLoS One 5 (2010) e10760.

[79] J.S. Weiss, H.S. Kruth, H. Kuivaniemi, G. Tromp, P.S. White, R.S. Winters, W. Lisch, W. Henn, E. Denninger, M. Krause, P. Wasson, N. Ebenezer, S. Mahurkar, M.L. Nickerson, Mutations in the UBIAD1 gene on chromosome short arm 1, region 36, cause Schnyder crystalline corneal dystrophy, Invest. Ophthalmol. Vis. Sci. 48 (2007) 5007-5012.

[80] A. Orr, M.P. Dube, J. Marcadier, H. Jiang, A. Federico, S. George, C. Seamone, D. Andrews, P. Dubord, S. Holland, S. Provost, V. Mongrain, S. Evans, B. Higgins, S. Bowman, D. Guernsey, M. Samuels, Mutations in the UBIAD1 gene, encoding a potential prenyltransferase, are causal for Schnyder crystalline corneal dystrophy, PLoS One 2 (2007) e685.

[81] M. Vos, G. Esposito, J.N. Edirisinghe, S. Vilain, D.M. Haddad, J.R. Slabbaert, S. Van Meensel, O. Schaap, B. De Strooper, R. Meganathan, V.A. Morais, P. Verstreken, Vitamin K2 is a mitochondrial electron carrier that rescues pink1 deficiency, Science 336 (2012) 1306-1310.

[82] W.J. Fredericks, H. Yin, P. Lal, R. Puthiyaveettil, S.B. Malkowicz, N.J. Fredericks, J. Tomaszewski, F.J. Rauscher, 3rd, Ectopic expression of the TERE1 (UBIAD1) protein inhibits growth of renal clear cell carcinoma cells: Altered metabolic phenotype associated with reactive oxygen species, nitric oxide and SXR target genes involved in cholesterol and lipid metabolism, Int. J. Oncol. 43 (2013) 638-652.

[83] T.W. McGarvey, T.B. Nguyen, S.B. Malkowicz, An interaction between apolipoprotein E and TERE1 with a possible association with bladder tumor formation, J. Cell. Biochem. 95 (2005) 419-428.

[84] J.L. Goldstein, M.S. Brown, Regulation of the mevalonate pathway, Nature 343 (1990) 425-430.

[85] G.P. Hooff, W.G. Wood, W.E. Muller, G.P. Eckert, Isoprenoids, small GTPases and Alzheimer's disease, Biochim. Biophys. Acta 1801 (2010) 896-905.

[86] J.J. Krukemyer, R.L. Talbert, Lovastatin: a new cholesterol-lowering agent, Pharmacotherapy 7 (1987) 198-210.

[87] P.D. Thompson, P. Clarkson, R.H. Karas, Statin-associated myopathy, JAMA : the journal of the American Medical Association 289 (2003) 1681-1690.

[88] D. Gaist, L.A. Rodriguez, C. Huerta, J. Hallas, S.H. Sindrup, Lipid-lowering drugs and risk of myopathy: a population-based follow-up study, Epidemiology 12 (2001) 565-569.

[89] O.P. Flint, B.A. Masters, R.E. Gregg, S.K. Durham, HMG CoA reductase inhibitor-induced myotoxicity: pravastatin and lovastatin inhibit the geranylgeranylation of low-molecular-weight proteins in neonatal rat muscle cell culture, Toxicol. Appl. Pharmacol. 145 (1997) 99-110.

[90] O.P. Flint, B.A. Masters, R.E. Gregg, S.K. Durham, Inhibition of cholesterol synthesis by squalene synthase inhibitors does not induce myotoxicity in vitro, Toxicol. Appl. Pharmacol. 145 (1997) 91-98.

[91] G. Caso, P. Kelly, M.A. McNurlan, W.E. Lawson, Effect of coenzyme q10 on myopathic symptoms in patients treated with statins, The American journal of cardiology 99 (2007) 1409-1412.

[92] J.M. Young, C.M. Florkowski, S.L. Molyneux, R.G. McEwan, C.M. Frampton, P.M. George, R.S. Scott, Effect of coenzyme Q(10) supplementation on simvastatin-induced myalgia, The American journal of cardiology 100 (2007) 1400-1403.

[93] G. Tsivgoulis, K. Spengos, N. Karandreas, M. Panas, A. Kladi, P. Manta, Presymptomatic neuromuscular disorders disclosed following statin treatment, Arch. Intern. Med. 166 (2006) 1519-1524.

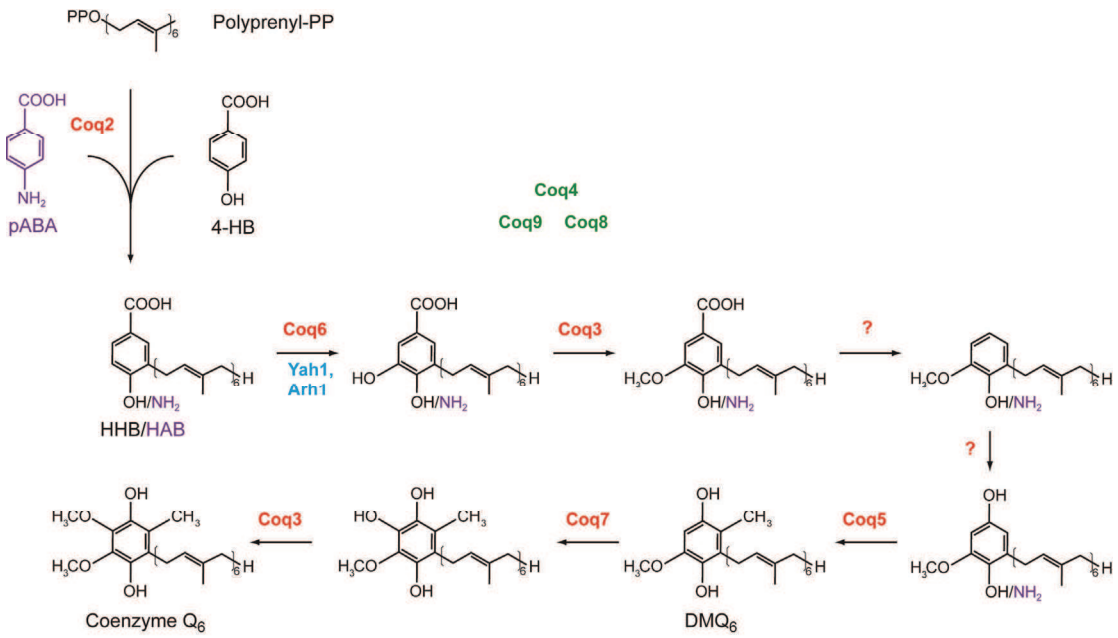


**Figure 1.** Coenzyme Q biosynthesis pathway in *Saccharomyces cerevisiae*. The pathway starts with the assembly of the isoprenoid tail (polyprenyl-PP) catalyzed by Coq1p (not shown). $NH_2$ and the intermediate HAB derived from pABA are shown in purple. Enzymes required for modifications of benzoquinone ring are shown in red. Question mark (?) indicates that the enzyme involved the reaction has not been identified yet. Coq proteins involved in the regulation of the pathway or with undefined function are shown in green. Abbreviations: pABA, para-aminobenzoic acid; HHB, 3-hexaprenyl-4-hydroxybenzoic acid; HAB, 3-hexaprenyl-4-aminobenzoic acid; DMQ, demethoxyubiquinone.

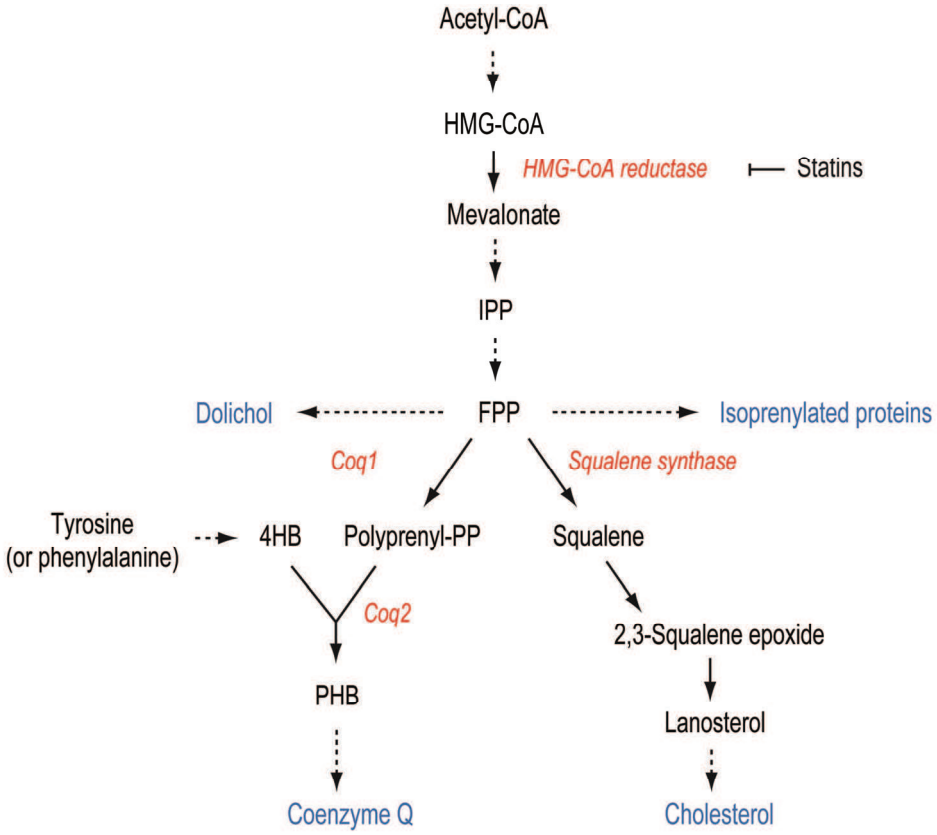


**Figure 2.** The mevalonate pathway. The mevalonate pathway produces isoprenoid precursor units. These metabolites are required for the biosynthesis of a variety of important molecules, including $CoQ_{10}$ and cholesterol.Adapted from [13].

## 3. ARCA2: a new form of recessive ataxia with Coenzyme $Q_{10}$ deficit

### *3.1. ARCA2: clinical description*

ARCA2 (autosomal recessive cerebellar ataxia type 2), also called SCAR9 (spinocerebellar ataxia recessive 9), is a rare form of recessive ataxia. The genetic cause of ARCA2 was identified by two independent groups in 2008 (Lagier-Tourenne et al., 2008, Mollet et al., 2008). The disease has initially been described as a slowly progressive cerebellar ataxia with childhood onset. In subsequent studies, other patients have been described, some of them with an adult onset of symptoms (Horvath et al., 2012) (Terracciano et al., 2012).

All ARCA2 patients present cerebellar ataxia and atrophy. The clinical peculiarity of ARCA2 is to be associated with Coenzyme $Q_{10}$ ($CoQ_{10}$ or ubiquinone) deficiency. While $CoQ_{10}$ measurement in fibroblasts is not always indicative of ubiquinone deficit, $CoQ_{10}$ content was decreased in ARCA2 patients when assessed in skeletal muscle. For this reason, Coenzyme $Q_{10}$ deficit is considered as a hallmark of the disease. Although ARCA2 is a rare disease, it is the most frequent form of Coenzyme $Q_{10}$ deficiency. Indeed, ARCA2 patients represent 50% of all patients with primary Coenzyme $Q_{10}$ deficiencies.

Apart from gait ataxia and cerebellar atrophy, other symptoms are present in ARCA2 patients to different degrees resulting in highly heterogeneous phenotypes. Some of these symptoms are rare, such as spasticity, migraine and depression. Others are more frequent, such as epilepsy, intellectual disability, exercise intolerance and movement disorders, mainly dystonia and myoclonus. Table 6 summarizes the frequency of the most common symptoms of all ARCA2 patients published so far (Lagier-Tourenne et al., 2008) (Mollet et al., 2008) (Horvath et al., 2012) (Terracciano et al., 2012) (Gerards et al., 2010). Among these, epilepsy and/or seizures are reported in almost 70% of patients, whereas intellectual disability is frequent in early childhood cases, but absent in adult cases (Horvath et al., 2012).

Interestingly, although the neurological signs are usually slowly progressive, in some patients an acute worsening of the phenotype was observed after an epileptic crisis (Horvath et al., 2012). In a few patients, stroke-like episodes are reported with a fatal outcome for one of them (personal communication from Dr. Mathieu Anheim).

| Patient ID | Sex | Onset (years) | Cerebellar ataxia | Cerebellar atrophy | Epilepsy | Exercise intolerance | Intellectual disability | $CoQ_{10}$ | Predicted aa change | Patient ID in the original paper | Reference |
|---|---|---|---|---|---|---|---|---|---|---|---|
| 1 | M | 11 | + | + | nd | - | - | nd | p.D420Wfs*40, p.I467Afs*22 | 1 (1) | Lagier-Tourenne et al., 2008 |
| 2 | M | 4 | + | + | nd | + | mild | nd | p.D420Wfs*40, p.I467Afs*22 | 2 (1) | |
| 3 | M | 7 | + | + | nd | + | - | Fibro normal | p.D420Wfs*40, p.I467Afs*22 | 3 (1) | |
| 4 | F | 8 | + | + | nd | + | - | nd | p.D420Wfs*40, p.I467Afs*22 | 4 (1) | |
| 5 | M | 4 | + | + | nd | - | mild | Fibro ↓ | p.Q167Lfr*36 | 5 (2) | |
| 6 | M | 5 | + | + | nd | nd | - | Fibro ↓ | p.Y514C, p.T584del | 6 (3) | |
| 7 | F | 3 | + | nd | nd | nd | moderate | Lympho ↓ | p.K314_Q360del, p.G549S | 7 (4) | |
| 8 | M | 1.5-2 | + | + | + | - | + | Muscle ↓ Fibro normal | p.E551K | 1 (1) | Mollet et al,2008 |
| 9 | F | 1,5 | + | + | + | - | - | Muscle ↓ | p.R213W, p.G272V | 2 (2) | |
| 10 | F | 1,5 | + | + | + | - | - | nd | p.R213W, p.G272V | 3 (2) | |
| 11 | F | 3 | + | + | + | + | - | Muscle ↓ Fibro normal | p.G272D, p.E605Gfs*125 | 4 (3) | |
| 12 | M | 3 | + | + | + | + | mild | nd | p.R348* | IV:1 (A) | Gerards et al., 2010 |
| 13 | M | 9 | + | + | - | + | mild | nd | p.R348* | IV:2 (A) | |
| 14 | M | 3 | + | + | + | + | - | nd | p.R348* | IV:4 (A) | |
| 15 | F | 2 | + | + | - | + | - | nd | p.R348*, p.L379* | II:1 (B) | |
| 16 | M | 2 | + | + | - | + | bradyphrenia | nd | p.R348*, p.L379* | II:4 (B) | |
| 17 + sib | F | 15-18 | + | + | + | nd | - | Muscle normal | p.R271C, pA304T | 1 (1) | Horvath et al., 2012 |
| 18 | F | 27 | + | + | + | nd | - | Muscle ↓ | p.A304V | 2 (2) | |
| 19 | F | 1 | + | + | + | nd | + | nd | p.R299W | 3 (3) | |
| 20 + sib | F | 1.5-2 | + | + | - | nd | + | Muscle ↓ | p.Y429C, ? | 4 (4) | |
| 21 | F | 6 | + | + | + | - | mild | Muscle ↓ | p.R348* | CHA987 | Terracciano et al., 2012 |
| 22 | M | 15 | + | + | nd | nd | nd | nd | p.L453Rfs*, p.R299W | | Personal communication from Prof. Michel Koenig (confidential) |
| 23 | M | 6 | + | + | - | nd | + | nd | p.F508S | | |
| 24 | F | 7 | + | + | + | nd | + | nd | p.G615D | | |
| 25 | M | child | + | + | + | nd | + | nd | p.G615D | | |
| 26 | F | child | + | + | + | nd | + | nd | p.L197Vfs*20 | | |
| 27 | F | 2 | + | + | - | nd | + | nd | p.G360_Y361ins* | | |
| 28 | F | 4 | + | + | + | nd | + | nd | p.R299W, p.R410* | | |
| 29 | F | 4 | + | + | + | nd | + | nd | p.R299W, p.R410* | | |
| 30 | F | 1.5 | + | + | + | nd | + | nd | p.R271C | | |

**Table 6. Clinical and genetic description of ARCA2 patients.** The main symptoms of ARCA2 patients as well as the causing mutations are reported. When one mutation is reported it is homozygous. In brackets is the nomenclature of the family in the original papers. (Sib), sibling with similar phenotype. (?), only one heterozygous mutation was detected in this patient. (Nd), not determined. (*), stop codon. (Fs), frameshift.

Skeletal muscle is often affected in ARCA2 patients, although muscle pathology is poorly investigated due to lack of muscle biopsies. In the few patients tested, muscle histology reveals mitochondrial proliferation, COX-deficient fibers and increased lipid accumulation (Aure et al., 2004, Mollet et al., 2008, Horvath et al., 2012).

Interestingly, although other Coenzyme $Q_{10}$ deficiencies are associated to renal dysfunction, no kidney defect has been described so far.

### *3.2. Genetic causes of ARCA2*

ARCA2 is due to loss-of-function mutations in the gene encoding ADCK3/CABC1, a putative mitochondrial kinase. Figure 10 shows all mutations described so far and where they map on the ADCK3 protein. Different kinds of mutations have been reported, such as missense mutations, stop codons, splice mutations and short deletions (Table 6). Consistent with the recessive inheritance of the disease, all ARCA2 patients are either homozygous or compound heterozygous for the mutations.

Mutations responsible for ARCA2 are considered to lead to a loss of function of ADCK3. In fact, two missense mutations leading to premature stop codon, p.R348* and p.L379*, are reported to trigger non sense mediated decay (NMD) (Gerards et al., 2010). NMD is a control mechanism that degrades mRNA containing errors to prevent the synthesis of C-terminally truncated polypeptides, protecting the cell from its deleterious dominant-negative or gain-of-function (Silva and Romao, 2009). Although it has never been directly proved, it is likely that the single amino acid change mutations lead to loss of function of the mutated protein as well.

Although ARCA2 patients can present different symptoms, a clear correlation between mutations and severity of the phenotype has not been observed. In fact, patients carrying big deletions, such as patient 5 (Table 6), do not necessarily show severe phenotypes. On the other hand, patients carrying single amino acid substitution can display a severe phenotype, suggesting that a toxic effect could be associated to single changes in the protein. This is the case for patient 8 (Table 6) carrying a homozygous mutation (p.E551K) and showing intellectual regression, severe movement disorder (at 13 years she was unable to walk or speak), recurrent epilepsy and muscle abnormalities (Mollet et al., 2008). Moreover patients with the same mutation can present different symptoms. This is the case for patients 12, 13

and 14 (Table 6) carrying the homozygous mutation p. R348* where epilepsy and intellectual disability are present in two out of three brothers.

The lack of a genotype-phenotype correlation is still unclear, also because little is known about the function of ADCK3. A better understanding of its activity and interactors could clarify the effect of the different mutations. In fact, it is possible that modifier genes or compensatory effects due to the presence of paralogs of ADCK3, play a role in the determination of the phenotype.

### *3.3. ADCK3: the gene responsible for ARCA2*

ADCK3, also called CABC1, is a putative mitochondrial kinase homologous to the bacterial UbiB and yeast Coq8, two proteins involved in Coenzyme Q biosynthesis (Lagier-Tourenne et al., 2008). The exact function of ADCK3 has not been elucidated in mammals. However, since ARCA2 patients present $CoQ_{10}$ deficit and based on the homology with UbiB and Coq8, it has been suggested that the mammalian protein ADCK3 is also involved in Coenzyme Q biosynthesis. The involvement of yeast Coq8p in CoQ biosynthesis has already been discussed in previous sections (see paragraph 2.2).

ADCK3 belongs to the ADCK family, which comprises five members in human and mouse. ADCK3 and ADCK4 are highly similar and appear to result from gene duplication in vertebrates while ADCK1, ADCK2 and ADCK5 split from ADCK3 and ADCK4 very early during evolution. Moreover, ADCK3 and ADCK4 appear to be closer to the yeast ABC1/Coq8 than to the bacterial UbiB (Lagier-Tourenne et al., 2008).

Based on sequence analysis, the group of Prof Koenig suggested that the ADCK proteins belong to the protein kinase-like superfamily described by Scheeff and Bourne (Scheeff and Bourne, 2005, Lagier-Tourenne et al., 2008). This superfamily contains typical protein kinases (TPKs) and atypical kinases (AKs). All TPKs share a common catalytic core composed of a small N-terminal subdomain and a larger C-terminal subdomain. AKs clearly share homology with the TPKs, but they do not conserve all the usual kinase motifs. Atypical kinases diverged early in evolution and acquired the capacity to recognize and specifically phosphorylate different types of substrates. Examples of AKs are choline kinases, which are involved in the pathway of phosphatidylcholine, and phosphoinositide 3-kinases, which phosphorylate various forms of phosphatidylinositol at the 3-hydroxyl position (Scheeff and Bourne, 2005).

The ADCK family is an AK family that contains only 5 out of 12 protein kinases motifs (I, II, III, VIB and VII). These include the “universal core” of a kinase corresponding to the regions required for ATP binding and for phosphotransfer reaction (Figure 9, in red) (Lagier-Tourenne et al., 2008).

Figure 10 is a schematic representation of the domains present in ADCK proteins. Apart from the five kinase motifs (in red), ADCKs contain an N-terminal domain containing the KxGQ motif (in green) and a C-terminal domain (in yellow) specific to each ADCK subgroups (subgroup 1: ADCK1, ADCK2 and ADCK5; subgroup II: ADCK3 and ADCK4) (Lagier-Tourenne et al., 2008).

None of the substrates of the ADCK proteins is known. However, based on the fact that they are AKs, it cannot be excluded that they act on non protein substrates. It is also not known whether ADCKs show functional redundancy. However, based on sequence analysis, it is reasonable to suppose that ADCK3 and ADCK4 can replace each other’s function since they share 45 % amino acid identity.

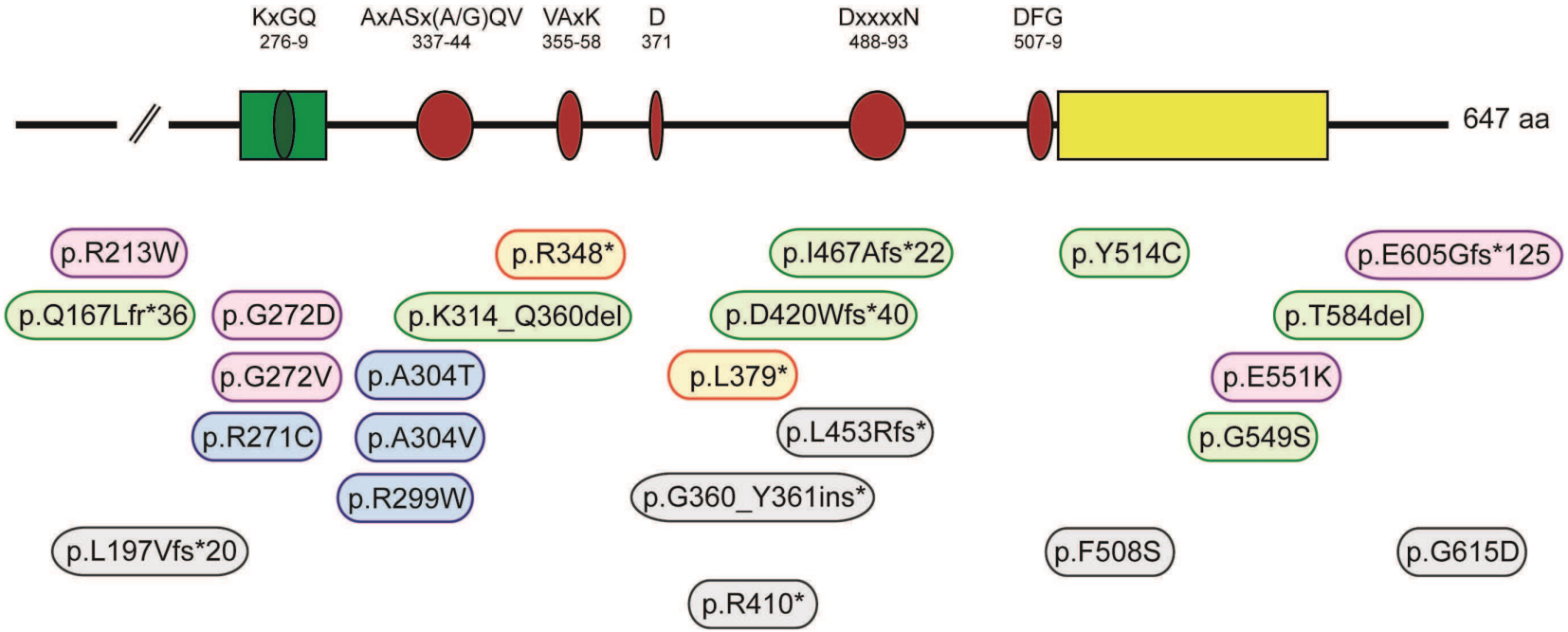


**Figure 10. ARCA2 mutations found in ADCK3.** In the upper part, schematic view of the human protein ADCK3 with: a domain conserved among all members of the ADCK family and containing the KxGQ motif (green), five kinase motifs (red) and a domain specific to each ADCK subgroup (yellow). In the lower part, ARCA2 mutations. The different colors of the mutations refer to different references that reported them for the first time (green: *Lagier-Tourenne et al., 2008*; purple: *Mollet et al., 2008*; orange: *Gerards et al., 2010*; blue: *Horvath et al., 2012*; grey: Prof. Koenig communication). Adapted from *Lagier-Tourenne et al., 2008*.

# RESULTS

# RESULTS

## 1. Aims of my PhD project

At my arrival in the laboratory of Dr. Puccio in 2009, the *ADCK3* had recently been identified as the causing gene in several patients with cerebellar ataxia and $CoQ_{10}$ deficiency. This syndrome was called ARCA2 since the ataxic gait was the predominant symptom, and it was discovered after ARCA1. In order to homogenize the nomenclature of all recessive ataxias, ARCA2 is officially referred to as SCAR9 (OMIM: #612016).

Since the discovery of the genetic cause of ARCA2 in 2008 (Lagier-Tourenne et al., 2008, Mollet et al., 2008), this disease appeared to be very interesting because, contrary to the other forms of $CoQ_{10}$ deficiencies, the phenotype of patients was mild, slowly progressive and mainly associated to ataxia. However, apart from the clinical signs observed in ARCA2 patients, nothing was known at that time about the pathophysiology of the disease.

Moreover, there was little information about the function of ADCK3. In fact, using bioinformatics analysis, ADCK3 was postulated to be a putative atypical kinase, but its substrates were unknown (Lagier-Tourenne et al., 2008). However, by homology with the yeast Coq8, ADCK3 was suggested to be involved in the biosynthesis of Coenzyme Q.

The goal of my PhD project was to elucidate the pathophysiology of ARCA2. In order to achieve this aim, a mouse model for ARCA2 was generated in the lab by a constitutive knockout of *Adck3* (*Adck3*$^{-/-}$ mice). Therefore, most of my thesis aimed to characterize *Adck3*$^{-/-}$ mice and to evaluate whether they represent a good model to investigate the human disease, i.e. ARCA2. In parallel, the second aim of my thesis was to investigate the function of ADCK4, the closest paralog of ADCK3. However, since the characterization of *Adck3*$^{-/-}$ mice required massive effort, I obtained preliminary data about ADCK4 localization and expression and further investigations will be needed to fully achieve this aim.

### *1.1. Biological questions*

In order to achieve the goals of my project and understand the pathophysiology of ARCA2, I used *Adck3*$^{-/-}$ mice to answer a number of biological questions. These include:

1. What are the organs and tissues that are mainly affected in ARCA2?
2. What are the molecular mechanisms underlying ARCA2?

Moreover, I wondered why ARCA2 patients presented a mild phenotype compared to patients with other forms of $CoQ_{10}$ deficiency. Therefore:

3. Is there any redundant effect of other ADCKs that could mitigate the phenotype observed in patients?

## 2. The generation of ADCK3 KO mice

The *Adck3* KO (*Adck3*$^{-/-}$) allele was generated by homologous recombination. Our targeting strategy placed two LoxP sites in introns 9 and 15 in order to generate a LoxP-flanked (conditional) allele. The advantage of the conditional allele is that it can be used to delete *Adck3* in a tissue and/or time specific manner in case the constitutive knockout was embryonic lethal. We chose to target large introns to increase recombination efficiency. Conditional mice were then crossed with a mouse strain expressing the *Cre* recombinase under the CMV promoter in order to generate a constitutive KO for *Adck3.* The deletion of exon 9 to 14 (*Adck3_Δex9-14*) in the mRNA of the *Adck3*$^{-/-}$ allele would give rise, if translated, to an in-frame protein lacking 193 aa (from 358 to 550), including a large part of the kinase domain and the ADCK specific domain (Figure 11).

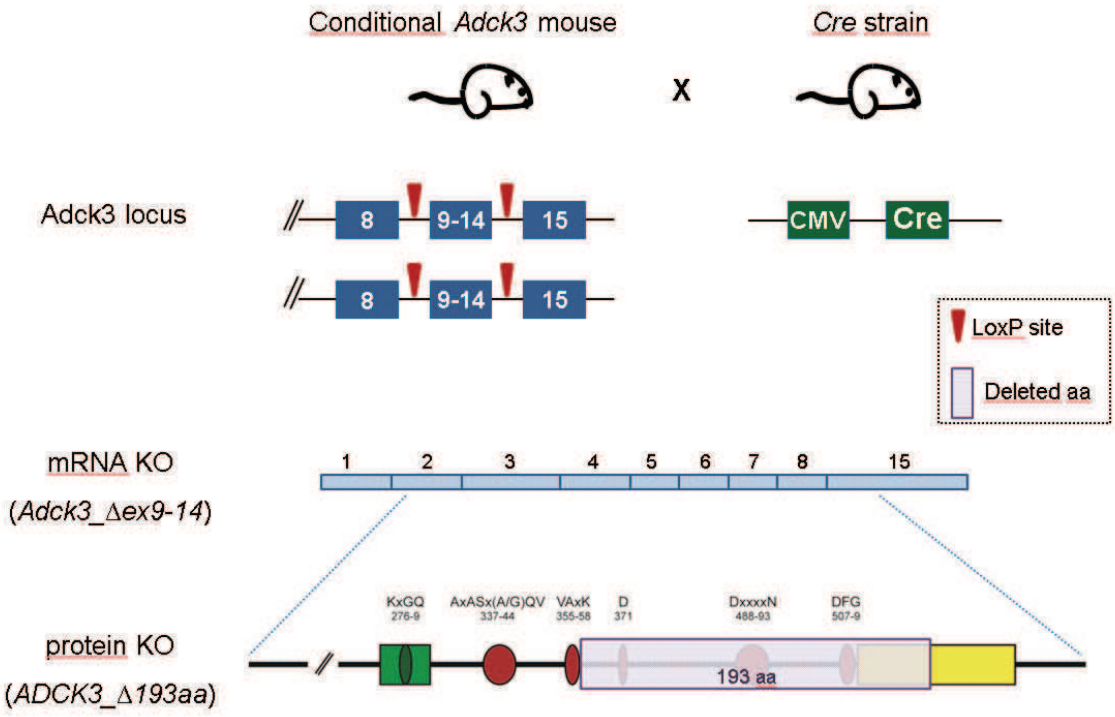


**Figure 11. Generation of the constitutive KO for *Adck3*.** Targeting of *Adck3* locus with LoxP sites gives rise to a knockout allele lacking exons 9 to 14. The ADCK3 KO protein, if expressed, lacks 193 aa (purple box).

Most of the data describing the initial characterization of *Adck3*$^{-/-}$ mice are reported in the following manuscript, which is still in the form of a draft since a few investigations are needed to strengthen the impact of our results. Additional data will be presented in the 'Results' section. *Adck3*$^{-/-}$ are also named knockout or mutant mice in this manuscript.

## Manuscript 3 (*in preparation*)

Loss of *Adck3* leads to Purkinje cells dysfunction, skeletal muscle defect and Coenzyme $Q_9$ deficiency, recapitulating the pathophysiology of human ARCA2

Floriana Licitra, Anais Grangeray, Anna Isabel Schlagowski, Laurence Reutenauer, Fabien Pierrel, Joffrey Zoll, Philippe Isope and Hélène Puccio

## 3. Manuscript 3 *in preparation*

**Loss of *Adck3* leads to Purkinje cells dysfunction, skeletal muscle defect and Coenzyme $Q_9$ deficiency, recapitulating the pathophysiology of human ARCA2**

**Floriana Licitra[1-5], Anais Grangeray[6], Anna Isabel Schlagowski[7-8], Laurence Reutenauer[1-5], Fabien Pierrel[9-10], Joffrey Zoll[7-8], Philippe Isope[6] and Hélène Puccio[#1-5]**

[1] Translational Medicine and Neurogenetics, IGBMC (Institut de Génétique et de Biologie Moléculaire et Cellulaire), Illkirch, France;

[2] Inserm, U596, Illkirch, France;

[3] CNRS, UMR7104, Illkirch, France;

[4] Université de Strasbourg, Strasbourg, France;

[5] Collège de France, Chaire de génétique humaine, Illkirch, France;

[6]Institut des Neurosciences Cellulaires et Intégratives, Centre National de la Recherche Scientifique, Unité Propre de Recherche 3212, Strasbourg, F-67084 France;

[7]Université de Strasbourg, EA3072, Faculté de Médicine et Faculté des Sciences du Sport, Strabourg, France;

[8]Service de Physiologie et d'explorations fonctionnelles, Pole de Pathologie thoracique, Hopitaux universitaires, CHRU de Strasbourg, France;

[9]Commissariat à l'Energie Atomique (CEA), Institut de Recherches en Technologies et Sciences pour le Vivant, Laboratoire Chimie et Biologie des Métaux, F-38054 Grenoble, France;

[10]CNRS, UMR5249, F-38054 Grenoble, France.

[#] Correspondence to:

Hélène Puccio

E-mail: hpuccio@igbmc.fr

## Introduction

ARCA2 (autosomal recessive cerebellar ataxia type 2), also known as SCAR9 (spinocerebellar ataxia recessive 9), is a rare form of cerebellar ataxia, characterized by cerebellar atrophy and a slow progression of gait imbalance (Lagier-Tourenne et al., 2008, Mollet et al., 2008). Most ARCA2 patients show a childhood onset of the neurological symptoms, although adult onset has been reported in a few patients (Horvath et al., 2012). In addition to the gait ataxia and cerebellar atrophy, variable neurological signs have been reported in ARCA2 patients, making it a very heterogeneous disease. While spasticity, migraine and depression are rare symptoms, epilepsy, intellectual disability, dystonia and myoclonus are relatively frequent. In addition, most ARCA2 patients have a history of exercise intolerance in childhood and elevated serum lactate at rest or after moderate exercise, suggesting skeletal muscle pathology. Indeed, in the rare muscle biopsies tested, histological analysis reveals mitochondrial proliferation, COX-deficient fibers and increased lipid accumulation (Horvath et al., 2012) (Mollet et al., 2008) (Aure et al., 2004). Moreover, ARCA2 is associated with a mild to moderate deficiency in Coenzyme $Q_{10}$ ($CoQ_{10}$), a lipophilic molecule involved in the mitochondrial respiratory chain (Lagier-Tourenne et al., 2008, Horvath et al., 2012) (Mollet et al., 2008). As a consequence of $CoQ_{10}$ deficiency, the bioenergetics metabolism is often variably altered in skeletal muscle biopsies from ARCA2 patients, with reduced combined activities of the respiratory chain complexes CI+CIII and CII+CIII (Lagier-Tourenne et al., 2008, Mollet et al., 2008, Horvath et al., 2012).

ARCA2 is due to loss-of-function mutations in the gene encoding ADCK3/CABC1, a putative mitochondrial kinase homologous to the bacterial UbiB and yeast Coq8, two proteins involved in CoQ biosynthesis (Lagier-Tourenne et al., 2008, Mollet et al., 2008). Although the exact function of ADCK3 has not been elucidated in mammals, it has been suggested that the mammalian protein ADCK3 is also involved in CoQ biosynthesis (Lagier-Tourenne et al., 2008). The relatively mild clinical presentation of ARCA2 compared to patients with a primary block in $CoQ_{10}$ synthesis suggests an indirect, more regulatory role for ADCK3 in CoQ biosynthesis.

Coenzyme Q is a lipophilic molecule composed of a substituted benzoquinone and a polyprenyl chain containing six units in *S. cerevisiae* ($Q_6$), nine in mouse ($Q_9$) and ten in humans ($Q_{10}$). CoQ plays an essential role in oxidative phosphorylation (OXPHOS), carrying electrons from complexes I and II to complex III. It is also an important antioxidant in its reduced form (ubiquinol) (Turunen et al., 2004). Although the terminal steps of the Coenzyme Q biosynthesis occur in mitochondria, the intracellular distribution of Coenzyme Q

is not restricted to these organelles. In fact, Coenzyme Q is present in almost all cellular membranes and is particularly abundant in Golgi, lysosomes and mitochondria membranes (Crane, 2001).

In order to elucidate the pathophysiology of ARCA2, we generated a constitutive knockout (KO) mouse for *Adck3*. Here we show that *Adck3*$^{-/-}$ mice present a slowly progressive gait ataxia with an increase in seizure susceptibility and mild exercise intolerance. In addition, deficiency in Coenzyme Q was observed. Furthermore, specific functional and morphological defects in the cerebellar Purkinje neurons were found, while the skeletal muscle presented a mild mitochondrial phenotype.

## Results

### Generation of *Adck3* knockout (*Adck3*$^{-/-}$) mice

*Adck3* KO (*Adck3*$^{-/-}$) mice were produced using the Cre-LoxP system to delete exons 9-14 as outlined in Fig. 1A. Although this is an in-frame deletion, if translated, the protein would be laking a large proportion of its putative kinase domain (Δ193 aa). Crosses between the heterozygous *Adck3*$^{+/-}$ produced all 3 genotypes (wild-type (WT), heterozygotes and homozygote knockouts (Fig. 1B) and a Mendelian inheritance pattern was observed (23% WT mice, 54% *Adck3*$^{+/-}$, 23% *Adck3*$^{-/-}$; n=104), indicating no substantial embryonic lethality. Inactivation of the *Adck3* gene was confirmed by RT-PCR, and the presence of the deleted mRNA in the knockout and heterozygous mouse was observed in mRNA samples from skeletal muscle (Fig. 1C). Furthermore, by RNA deep sequencing, we quantified the levels of the expressed exons (exons 1 to 8 and exon 15) in the deleted form as well as in the WT (Fig. 1D). In KO skeletal muscle, we observed a trend to a decreased expression (25%) of the deleted alleles, whereas in cerebellum no alteration was found. Unfortunately, due to lack of antibody capable of detecting the endogenous ADCK3 protein, the expression of the deleted protein could not be assessed.

### *Adck3*$^{-/-}$ mice develop a slowly progressive loss of coordination and gait ataxia and are seizure prone.

*Adck3*$^{-/-}$ mice exhibit normal growth and life expectancy, and are indistinguishable from WT littermates in standard home-cage environment. To assess the neurological consequences and to determine stages in the disease progression, KO animals were analyzed by several

motor skill and behavioral tests. Although no over clinical phenotype was observed at 10 weeks, both female and male *Adck3*$^{-/-}$ mice showed a significant decrease in performance on the accelerating rotarod after 4 days of trial ($p<0.05$) (Fig. 2A), demonstrating a loss of coordination in comparison to the control littermates. To further assess the symptoms, gait parameters of KO and control mice were evaluated by footprint analysis at 10 weeks (Fig. 2B). The footprint patterns were assessed quantitatively by five parameters: step length and width, alternation coefficient, linearity, and variation of step length (see Materials and Methods). The linear coefficient, an assessment of ataxia that describes the regularity of direction, was significantly increased in *Adck3*$^{-/-}$ animals, indicating a nonlinear movement of mutant animals (Fig. 2B). All other parameters did not show any significant difference between the two genotypes. Together, these results demonstrate that *Adck3*$^{-/-}$ mice develop a mild ataxia. To further assess the progression of the symptoms, the *Adck3*$^{-/-}$ mice were subjected to the beam walk test, a test not subjected to learning effects, at 5, 10 and 20 weeks. At 10 weeks, *Adck3*$^{-/-}$ mice showed a significant increased in the number of hindfoot gait mistakes compared to WT littermates, which worsen by 20 weeks, showing that the loss of coordination was slowly progressive (Fig. 2C). At an early age (5 weeks), *Adck3*$^{-/-}$ mice already showed increased number of mistakes, although not significant in females (Fig. 2C). All together these results demonstrate that *Adck3*$^{-/-}$ mice develop locomotor troubles starting after birth, between 5-10 weeks of age, with gait defect and slowly progressive loss of coordination typical of ataxic phenotype.

Epilepsy and seizures are common symptoms found in ARCA2 patients (Lagier-Tourenne et al., 2008, Mollet et al., 2008, Horvath et al., 2012). Interestingly, a few spontaneous seizure-like crises in *Adck3*$^{-/-}$ mice during daily manipulation were observed, leading us to investigate whether mutant mice presented an epileptic phenotype. Susceptibility to seizures was assessed in 6 months old mutant and WT mice, by testing the sensitivity of the animals to pentylene-tetrazol (PTZ), a drug with convulsant property. When the PTZ was administered IP at the dose of 30 mg/kg, *Adck3*$^{-/-}$ mice displayed increased seizure susceptibility as compared to WT littermates (Fig. 2D). The number of mice showing clonic or tonic seizures was significantly higher ($p<0.05$) and the latency of clonic-tonic seizures tented to be lower ($p=0.06$) in mutants than in WTs (Fig. 2D).

In addition to epilepsy, many ARCA2 patients present mild to moderate intellectual disability. To investigate the neurobehavioral phenotype of the *Adck3*$^{-/-}$ mice, Y maze spontaneous alternation (working memory), object recognition (recognition memory), water maze (spatial learning memory) and elevated plus maze (anxiety) tests were carried out (Fig. S1). No

difference in any of the test was detected between *Adck3*$^{-/-}$ and WT mice, with the exception of the Morris water maze. Indeed, while the distance and the latency to locate the submerged platform decreased significantly over the course of the experiment in both WT and *Adck3*$^{-/-}$ mice, the mutant mice showed significantly higher latency and distance than WT, particularly on the third testing day, suggesting delayed spatial learning in mutants (Fig. S1).

Finally, another common symptom in ARCA2 patients is the presence of exercise intolerance. To evaluate exercise tolerance in *Adck3*$^{-/-}$ mice, accelerating treadmill tests were performed in 10 months old mice. Blood lactate measurement immediately after running was performed to verify that mice reached exhaustion. The maximum speed reached by the mice ($V_{max}$) was significantly decreased in *Adck3*$^{-/-}$ mice compared to WT (Fig. 2E). The endurance of the mice was further tested by running until exhaustion at, 80% of their respective $V_{max}$. Although not significant, a trend towards decreased duration of the run was observed in *Adck3*$^{-/-}$ mice (Fig. 2E). No difference in muscle strength was observed by grip analysis (data not shown). Together, these data suggest that *Adck3*$^{-/-}$ mice show a mild defective muscle performance.

### *Adck3* depletion leads to decrease in CoQ levels and ROS production

To determine whether *Adck3* depletion leads to CoQ deficiency in mice, levels of ubiquinone and the main intermediates of the biosynthesis pathway were measured by HPLC in several tissues of *Adck3*$^{-/-}$ and WT littermates. While no difference in CoQ content was observed at early stage of disease development (5 weeks, Fig. S2), coenzyme $Q_9$ ($CoQ_9$), the most abundant form of ubiquinone in mouse, was found to be significantly reduced in kidney, liver and skeletal muscle (quadriceps and soleus) of *Adck3*$^{-/-}$ mice at an advanced stage (7 months, Fig. 3A). A significant reduction of $CoQ_{10}$ was also observed in the soleus and liver in advanced stage *Adck3*$^{-/-}$ mice (Fig. S3). Interestingly, no precursor of CoQ was found to accumulate in any tissues (data not shown), suggesting that *Adck3* depletion does not lead to an enzymatic block of the CoQ biosynthesis in mammals.

As CoQ is a potent antioxidant, to determine whether reactive oxygen species (ROS) might contribute to the pathophysiology, total ROS content was measured by electron paramagnetic resonance in skeletal muscle (quadriceps and soleus) and blood of *Adck3*$^{-/-}$ and WT mice at 10 months of age. While no difference was observed in blood samples, a significant reduction of total ROS levels was found in *Adck3* depleted quadriceps muscle (Fig. 3B). Although not significant, a trend in reduction of ROS levels was also observed in

the soleus in *Adck3*$^{-/-}$ mice. Furthermore, the production of $H_2O_2$, in permeabilized quadriceps fiber, was found significantly reduced in *Adck3* depleted quadriceps (Fig. 3C). Together, these results suggest that, contrary to expected, ROS production is decreased in skeletal muscle, maybe as a consequence of decrease mitochondrial function. However, the combined activity of the respiratory complexes I, II and III in quadriceps showed no difference between *Adck3*$^{-/-}$ and WT mice (data not shown), suggesting that the decrease in endogeneous pools of CoQ is not sufficient to affect the mitochondrial respiratory chain.

Finally, measurements of various blood metabolites, ions and enzymes and the serum lipid concentrations were performed in *Adck3*$^{-/-}$ mice at an advanced stage (6 months) to determine the major metabolic functions. Interestingly, total plasma cholesterol, HDL, LDL and free fatty concentrations were significantly increased in *Adck3*$^{-/-}$ male mice (Fig. 3D). Total plasma cholesterol and HDL concentrations were also found to be significantly increased in *Adck3*$^{-/-}$ female mice (Fig. 3D). A trend toward increased triglycerides was also observed in male and female *Adck3*$^{-/-}$ animals. No other blood parameter was significantly affected (data not shown). Together, these results suggest the presence of a mild dyslipidemia in *Adck3*$^{-/-}$ mice that may contribute to the pathophysiology.

**Depletion of *Adck3* specifically affects the cerebellar Purkinje cells without cerebellar atrophy**

To examine whether the manifestation of gait ataxia in *Adck3*$^{-/-}$ mice might be associated with any pathological changes, a comprehensive histological analysis was performed. No severe cerebellar atrophy, contrary to what is observed in ARCA2 patients, and no gross defects in the brain and spinal cord of *Adck3*$^{-/-}$ animals were observed (data not shown). However, a specific defect in the cerebellar Purkinje cells layer was observed in *Adck3*$^{-/-}$ mice, with the presence of dark shrunken neurons and patches of gaps in calbinding staining (Fig. 4A), suggestive of neuronal degeneration. Ultrastructure examination by transmission electron microscopy revealed additional Purkinje cell changes in the cerebellum of 30 weeks old *Adck3*$^{-/-}$ mice. A significant portion (around 10-20%) of *Adck3*$^{-/-}$ Purkinje cells was dark and shrunken, with irregular shaped nuclei and abnormal membranes structure (Fig. 4B). Interestingly, most *Adck3*$^{-/-}$ Purkinje cells, whether dark or not, showed dilated Golgi apparatus, with some presenting numerous vesicles, suggesting signs of Golgi fragmentation, and dilated cisternae of ribosomes-rich endoplasmic reticulum (Fig. 4B and S4). Surprisingly, no gross defect was observed in Purkinje cell soma and dendrites mitochondria (data not shown). Furthermore, although most cerebellar granule cells were

unaffected ultrastructurally, a few cerebellar granule neurons with degenerating mitochondria were observed (data not shown). Quantitative analyses of calbindin-positive cells on cerebellar sections (Fig. 4C) and of the expression levels the Purkinje cell specific markers Pcp2 and calbindin in total cerebellar mRNA extract (Fig. 4D), did not identify any difference between *Adck3*$^{-/-}$ and WT mice. In agreement with these results, no increase in TUNEL positive cells was detected in *Adck3*$^{-/-}$ mice (data not shown). Therefore, although Purkinje cells were clearly morphologically affected, no massive loss of Purkinje neurons was observed in *Adck3*$^{-/-}$ mice.

To assess the possible physiological deficits, we performed electrophysiological recording of Purkinje cells. Normal Purkinje cells exhibit spontaneous and regular firing of pacemaking action potentials (Hausser and Clark 1997). Using whole-cell recordings, we measured the spontaneous firing of Purkinje cells in acute cerebellar slices of *Adck3*$^{-/-}$ and WT mice, at 3 months of age (Fig. 4E-G). Compared to WT cells, *Adck3*$^{-/-}$ Purkinje cells exhibited a significant increase in the interspike interval (ISI), while the coefficient of variation between two adjacent spikes (CV2) was unchanged (Fig. 4F). Furthermore, the distribution analysis of the ISI values demonstrate that there is a significant proportion of *Adck3*$^{-/-}$ Purkinje cells that displayed high ISI values (>40) (Fig. 4G). These data suggest that *Adck3* deficient Purkinje cells showed an altered peacemaker activity characterized by regular but less frequent spikes.

**Mitochondrial defect in skeletal muscle of *Adck3*$^{-/-}$ mice**

To determine if pathological changes in skeletal muscle are associated with the decrease in exercise tolerance and the mild $CoQ_9$ deficiency, histological and ultratructural analyses were performed on 7 months old *Adck3*$^{-/-}$ mice. Interestingly, while no defect was observed histologically (data not shown), ultrastructural analysis of quadriceps muscle revealed specific mitochondrial impairment, with the presence of broken mitochondria or mitochondria presenting collapsed cristae (Fig. 5A and 5B). In occasional fibers, the mitochondrial defect lead to a mild fiber degeneration (Fig. 5A). Although in a few fibers, accumulation of mitochondria at the periphery was observed, by quantification of mitochondrial DNA, no evidence of massive mitochondrial proliferation in *Adck3*$^{-/-}$ mice was found (Fig 5C).

In order to evaluate the functional consequences of the mitochondrial defect observed in skeletal muscle, mitochondrial respiration was assessed in quadriceps and soleus fibers of 10 months old *Adck3*$^{-/-}$ and WT mice. Maximal rate of oxygen consumption ($V_{max}$) was

determined in saponin-skinned fibers after exogenous ADP addition. No difference in $V_{max}$ of $O_2$ consumption was observed between *Adck3*$^{-/-}$ and WT mice (Fig. 5D). Moreover, the oxidative phosphorylation efficiency, which indicates the efficiency of coupling between oxygen consumption and ADP phosphorylation, was evaluated. The acceptor control ratio (ACR), defined by the ratio between $V_{max}$ and Vo, was unchanged (Fig. 5D). Thus, despite reduced $CoQ_9$ and the presence of ultrastructurally abnormal mitochondria, the mitochondrial respiration and uncoupling of oxidative phosphorylation was unaffected in *Adck3*$^{-/-}$ mice.

### Molecular pathways altered in *Adck3*$^{-/-}$ mice

To identify molecular pathways that are misregulated in the affected tissues, the expression profile in adult cerebella and quadriceps from *Adck3*$^{-/-}$ mice was determined by RNA deep sequencing. Interestingly, gene expression variations between WT and mutant samples were very small. In cerebella, significant changes (adjusted p-value<0.05) in the expression of 74 genes were found, with equal distribution between genes that showed increased or decreased expression. In skeletal muscle, 118 genes were found to be significantly misregulated (adjusted p-value<0.05), with 60% being upregulated and 40% downregulated. The expression patterns of 10 genes were validated by qRT-PCR. The subset of overall differentially expressed genes was classified according to GO biological process, cellular component and molecular function, using the DAVID resources. Interesting, the secretory pathway annotation showed a significant over-representation in both cerebellum and skeletal muscle datasets (Table 1 and 2). In addition, other pathways identified included amino acid transport, immune response and phosphorus metabolic process (Table 1 and 2). No significant over-representation in the mitochondrial cellular component was detected. In conclusion, the gene ontology categorization suggests that secretory pathway might be altered in the cerebellum as well as in the skeletal muscle of *Adck3*$^{-/-}$ mice.

## Discussion

In the present manuscript, we report the generation of a mouse model for ARCA2 that developed the most prominent features of the human disease: progressive cerebellar ataxia, susceptibility to epileptic seizure, mild exercise intolerance and $CoQ_9$ deficiency in several tissues. In contrast to other mouse models of CoQ deficiencies which are embryonic lethal at the homozygous state (Peng et al., 2008, Lu et al., 2012) (Levavasseur et al., 2001, Nakai et al., 2001) (Lapointe et al., 2012), *Adck3*$^{-/-}$ mice develop a mild phenotype. This is in

agreement with ARCA2 patients presenting a less severe disease than other diseases linked to $CoQ_{10}$ deficiency, with a complete block in $CoQ_{10}$ biosynthesis. The yeast homolog coq8 has been suggested to play a regulatory role in the CoQ biosynthesis. The mild $CoQ_9$ deficiency and the absence of accumulation of intermediates of the biosynthesis of CoQ further support a regulatory role of ADCK3 in the CoQ biosynthesis process.

While the cerebellar structure is largely preserved in the *Adck3*$^{-/-}$ mice, the gait ataxia probably results from a direct consequence of the specific electrophysiological and morphological defects observed in cerebellar Purkinje cells. Our data demonstrated that Purkinje cells present an altered pacemaking activity with a reduced spontaneous firing. Spontenous pacemaking activity of Purkinje cells is dependent on ion current mediated by specific ion channels, such as the voltage-gated sodium channel $\alpha$ subunit $Na_v1.6$ (Levin et al., 2006). Although the function of ADCK3 is unknown, it is unlikely that it plays a direct role in maintaining the pacemaking activity of Purkinje cells. This reduced spontaneous firing is most likely a direct consequence of the ultrastructural defects observed in Purkinje cells.

Indeed, although there is no overt loss of Purkinje cells, dark degenerating Purkinje cells were observed. While the presence of dark degenerating Purkinje cells is a common feature observed in cerebellar ataxic mouse models, the cellular mechanisms involved are diverse, from mitochondrial impairment to misregulation of solute or macromolecule transporters. From the ultrastructural analysis, one of the early events in Purkinje cell in *Adck3*$^{-/-}$ mice is the presence of swollen and mildly fragmented Golgi apparatus. The Golgi apparatus consists of closely arranged stacks of flat cisternae that sort and process nascent membrane proteins, secreted proteins and lipids (van Vliet et al., 2003). In neurons, the Golgi apparatus is involved in the axoplasmic flow of numerous proteins and macromolecules transported by orthograde, retrograde, and trans-synaptic routes. Interestingly, Golgi apparatus defects have been reported in many neurodegenerative diseases, such as amyotrophic lateral sclerosis (ALS) (Gonatas et al., 1998), Parkinson's disease (Cooper et al., 2006), Alzheimer's disease (Muhammad et al., 2008), Niemann-Pick type C disease (Reddy et al., 2006), SCA2 (Huynh et al., 2003) and SCA5 (Perkins et al., 2010, Stankewich et al., 2010). Alteration of the Golgi apparatus could impair the highly regulated process of protein sorting in neuronal compartments likely to be associated with significant impairment of axons and presynaptic terminals. In agreement with this hypothesis, secretory pathway is one of the significant GO cellular processes identified in the transcriptomic analysis. In particular, two genes implicated in vesicle trafficking were found to be misregulated in the cerebella of *Adck3*$^{-/-}$ mice, COPA and Complexin 1. Therefore, a defect in intracellular trafficking could be

the underlying cellular mechanism responsible for the reduced pacemaking activity of the *Adck3*$^{-/-}$ Purkinje cells, due to impairment in maturation and transport of the voltage-gated sodium channels.

The morphology of the Golgi apparatus is dynamic and influenced by many factors, such as acidification, impaired processing and glycosylation of proteins and lipids, and altered cargo sorting (Ohtsubo and Marth, 2006) (Nilsson et al., 2009). How ADCK3 deficit affects the Golgi apparatus is uncertain. Although CoQ is present in almost all membranes of the cell, it is present in the Golgi apparatus at an even higher concentration than in the mitochondria or plasma membrane. Therefore, it is possible that loss of ADCK3 specifically affects the Golgi pool of CoQ, thereby reducing the antioxidant capacity and damaging the membrane. Although unlikely, we cannot completely exclude that the Golgi damage was induced by the truncated ADCK3 protein. However, our data demonstrate that overexpression of the truncated protein did not localized to the Golgi.

Interestingly, the *Adck3*$^{-/-}$ mice presented with a high susceptibility to PTZ-induced epilepsy. The cellular mechanisms underlying epilepsy are varied, from mitochondrial ATP deficiency to defects in neurotransmitters transport or synaptic plasticity. It remains to be determined whether the seizure found in the *Adck3*$^{-/-}$ mice are due to cortical or hippocampal dysfunction. However, it is tempting to speculate that a Golgi apparatus defect could also be involved.

Unexpectedly, despite the mitochondrial localization of ADCK3, the mitochondria in the *Adck3*$^{-/-}$ mice do not appear to be affected. In the soma of Purkinje cells, the mitochondria were ultrastructurally completely normal. In muscle, despite the presence of ultrastructurally abnormal mitochondria and the deficiency in $CoQ_9$, mitochondrial function was unaffected, as seen by the measurement of mitochondrial respiration rate. In agreement, the mitochondria were not part of the GO cellular processes in the transcriptomic analysis. Further work is necessary to understand the mechanism underlying the mild exercise intolerance observed in *Adck3*$^{-/-}$ mice.

Finally, other tissues, such as kidney and liver, showed a decreased level of Coenzyme Q without presenting gross pathological signs. However, the mild dyslipidemia observed in the mice suggested that liver function is not completely normal.

Although no upregulation of other *Adck* genes was observed in any Adck3 KO tissues tested (data not shown), it is likely that other ADCKs can functionally replace and compensate ADCK3.

In conclusion, we have generated a faithful mouse model for ARCA2 that has a mild and slowly progressive phenotype.

**Materials and Methods**

**Mouse Genotyping.** Mice were maintained in a temperature and humidity controlled animal facility, with a 12 hours light/dark cycle and free access to water and a standard rodent chow (D03, SAFE, Villemoisson-sur-Orge, France). All animal procedures and experiments were approved by the local ethical committee for Animal Care and Use. For genotyping of mice, DNA was extracted from the tail and PCR with the following primers was performed: WT allele: 5'-CTTTCAGTTTTTAGTACTGGCTGCG-3', 5'-GCTCATTAGTGTCCCAGCCATATCC-3'; KO allele: 5'-CTTTCAGTTTTTAGTACTGGCTGCG-3', 5'-AGAGCACTGGAGGGACAAGGGGC-3'

**Behavior tests.** *Beam-walking test.* Mice were trained to walk along a beam (2 cm wide × 90 cm long) suspended 30 cm above bedding. Three trials were performed for each mouse, and the number of hindfoot missteps was counted while the mouse walked along the length of the beam. The time required to cross the beam from start to end (latency) was also evaluated. Mice were trained to walk the length of the beam for 1 d before testing (Carter et al., 1999). *Accelerating rodarod test.* Coordination, equilibrium, and motor skill acquisition were tested using an accelerating rotating rod (Panlab, Barcelona, Spain) test as described previously (Clark et al., 1997). Briefly, mice were placed on the rod in four trials every day for a period of 4 d (ten controls and ten mutants at each age). The rod accelerated from 4 to 40 rpm in 5 min and remained at maximum speed for the next 5 min. Animals were scored for their latency to fall (in seconds) for each trial and rested a minimum of 10 min between trials to avoid fatigue and exhaustion. Results were analyzed by a repeated-measure ANOVA test considering three factors: days (fixed); genotype (fixed); animals (variable), nested in genotype and crossed with days. *Footprint.* The test was performed as previously described (Simon et al., 2004). Briefly, after coating of the hindfeet with nontoxic ink, mice were allowed to walk through a tunnel (50 cm long, 9 cm wide, 6 cm high) with paper lining the floor. Five parameters were quantified: Step length, the average distance of forward movement between alternate steps; sigma, describing the regularity of step length; gait width, the average lateral distance between opposite left and right steps; alternation coefficient, describing the uniformity of step alternation; linearity, average change in angle between consecutive right-right steps. A high linearity score is indicative of nonlinear movement. *Y-maze spontaneous alternation.* The apparatus used is a Y-maze made of Plexiglas and

having three identical arms (40x9x16 cm) placed at 120° from each other. Arms are easily distinguishable by specific motifs on their walls. Each mouse was placed at the end of one of the three arms, and allowed to freely explore the apparatus for 5min, with the experimenter away from the animal's sight. Alternations are operationally defined as successive entries into each of the three arms as on overlapping triplet sets (i.e., ABC, BCA ...). The percentage of spontaneous alternations was calculated as an index of working memory performance. Total arm entries and the latency to exit the starting arm were also scored as indexes of ambulatory activity and emotionality in the Y-maze, respectively. *Morris water maze*. The water maze consisted of a white circular tank (1.50 m diameter) filled with opaque water. Pool temperature was adjusted to 21+1°C. For the hidden platform task, the escape platform (10 cm diameter) was positioned 1cm below water level in the center of one of the pool quadrants. For the cued task, platform position was signaled by the addition of a small flag. The walls surrounding the water maze were hung with posters and flags, which served as visual cues and are visible during all stages of training and testing. Movement of the mice within the pool was tracked and analyzed with a computerized tracking system (ViewPoint, France). Animals were first trained in the hidden platform protocol (spatial learning). Mice were required to locate a submerged hidden platform by using only extra-maze cues. Each mouse received 5 blocks of training trials over five consecutive days in which they were placed in the pool at one of four randomized start positions, and allowed to locate the hidden platform. Trials lasted for a maximum of 120s and were separated by 15-20 min intervals. If a mouse failed to find the platform within this period, it is guided to its position by the experimenter. Spatial learning performance was assessed during a probe trial 1h after training, and for which the target platform was removed from the pool. Mice were then tested for cued training (visible platform), in which they were placed in the pool facing the edge at one of four start positions (NE, SE, SW, NW), and required to locate a flagged platform whose position varies across trials. Each mouse received 4 trials per day for 2 consecutive days. Trials lasted for a maximum of 120s and were separated by 15-20 min intervals. If a mouse failed to find the platform within this period, it was guided to its position by the experimenter. The latency, distance and the average speed were used to evaluate performance during training trials. For the probe trial, the percentage of time in each quadrant and the number of platform crosses were used as an index of spatial learning performance. *Elevated plus maze*. The apparatus used was completely automated and made of PVC (Imetronic, Pessac, France). It consisted of two open arms (30 X 5 cm) opposite one to the other and crossed by two enclosed arms (30 X 5 X 15 cm). The apparatus was equipped with infrared captors allowing the detection of the mouse in the enclosed arms and

different areas of the open arms. The number of entries into and the time spent in the open arms were used as an index of anxiety. Closed arm entries were used as measures of general motor activity. Ethological parameters such as stretching, attempts and head dips were also automatically scored.

**PTZ-induced seizures:** PTZ was dissolved in saline (0.9 % NaCl) and injected IP at the dose of 30 mg/kg. Immediately after injection, the mouse was placed into a new cage and observed for at least 20 min. The seizure profile (myoclonic, clonic, tonic) and the latency to clonico-tonic seizure were recorded.

**Immunohistochemistry**. For histology, animals were intracardially perfused with 4% paraformaldehyde (PFA) in 0.1 m phosphate buffer (PBS), pH 7.3, and the various tissues were dissected, fixed for several days, and embedded in paraffin. The sequential slides (7 µm) of the paraffin blocks were stained with hematoxylin and eosin (H&E), or calbindin (1:1000; rabbit anti-calbindin d-28K; Swant, Bellinzona, Switzerland) to label the cytoplasmic region of Purkinje cells. For calbindin staining, sections were visualized using the Vectastain ABC Kit (Vector Laboratories, Burlingame, CA) as described in the manufacturer's protocol. Quantification of Purkinje cells was performed in a blinded manner. Pictures of the Purkinje cell layers were taken with an objective 20X. 3 mice per genotype and 10 pictures per mouse were included in the analysis.

**Electron microscopy.** Animals were intracardially perfused with 2.5% glutaraldehyde in PBS. After overnight fixation, the tissues was dissected from the column and fixed for 1 additional day. Tissues were rinsed in PBS, postfixed in 1% osmium tetroxide-PBS for 2 hr at 4°C, dehydrated, and embedded in Epon. Regions of interest were localized on 2 µm sections and stained with toluidine blue. Ultrathin sections from selected areas were stained with uranyl acetate and lead citrate and examined with a Philips 208 electron microscope, operating at 80 kV.

**Electrophysiology.** *Slice preparation*. Adck3 KO mice and WT littermates (8-36 weeks old) were decapitated under isoflurane anesthesia. The cerebellum was dissected out and transferred into ice-cold ACSF-medium containing (in mM): 120 NaCl, 3 KCl, 26 $NaHCO_3$, 1.25 $NaH_2PO_4$, 2 $CaCl_2$, 1 $MgCl_2$, 10 glucose, 0.00005 minocyclin bubbled with 95% $O_2$ and 5% $CO_2$. Parasagittal slices (300-µm-thick) of the cerebellar vermis were prepared (HM 650V, Microm, Germany) in potassium-based medium containing the following (in mM): 130 K-gluconate, 14.6 KCl, 2 EGTA, 20 HEPES, 25 glucose, 0.00005 minocyclin, and 1 kynurenic acid. After cutting, slices were soaked for a few seconds in a sucrose-based medium at 34°C containing the following (in mM): 230 sucrose, 2.5 KCl, 26 $NaHCO_3$, 1.25

$NaH_2PO_4$, 25 glucose, 0.8 $CaCl_2$, 8 $MgCl_2$, 0.00005 minocyclin, and 0.05 d-APV. Slices were maintained in bubbled ACSF for >1 hr at 34°C before being transferred to the recording chamber. The recording chamber was continuously perfused with bubbled ACSF at 34°C $^{+}/_{-}$ 1°C containing 100µM picrotoxin to block inhibitory transmission. All chemicals were purchased from Sigma Aldrich (USA) and Abcam (UK). *Recordings.* Single-cell extracellular recordings of Purkinje cell action-potential activity were performed using 15-30 MΩ pipettes pulled from borosilicate glass capillaries (GC150TF-10, Harvard Apparatus) filled with 0.5 M NaCl and using an Axopatch 200A (Axon Instruments). Purkinje cells were visualized with an upright Olympus microscope (40X objective, Olympus BX51WI, USA). Data acquisition was performed using WinWCP 4.5.4 freeware (John Dempster, University of Strathclyde, UK). Recordings were filtered at 2 kHz and sampled at 50 kHz. Whole-cell patch-clamp recordings in voltage-clamp mode were obtained using 3–4 MΩ pipettes and optimal series resistance ($R_s$) compensation (70% of 6–18 MΩ, typically) was applied. $R_s$ was monitored in all experiments, and cells were held at −60 mV. The pipette internal solution contained the following (in mM): 135 $CsMeSO_4$, 6 NaCl, 10 HEPES, 4 MgATP, and 0.4 $Na_2GTP$, 1 $MgCl_2$, $6H_2O$ with pH adjusted to 7.3 with CsOH (osmolarity to 290 mOsm). Excitatory Post Synaptic Currents (EPSCs) were evoked by extracellular stimulation (100µs, 0.2-0.4 mA) of the parallel fibers using a glass pipette (G150T-4, Warner Instruments) filled with HEPES-buffered saline. This stimulation electrode was placed at the surface of the molecular layer at a distance of 100–200 µm from the recorded Purkinje cell. Analyses. Spike detection was performed using OpenElectrophy (http://neuralensemble.org/trac/OpenElectrophy; Garcia and Fourcaud-Trocmé, 2009) and custom based routines written in Python (SynaptiQs developed by Antoine Valera). The instantaneous regularity of firing was calculated using the coefficient of variation (CV) of interspike-intervals (ISIs) and the CV2 of ISIs: ($CV2 = 2|ISI_{n+1} - ISI_n|/(ISI_{n+1} + ISI_n)$) (Holt et al., 1996). For statistical analysis, we used the Student's t test and the Mann–Whitney U test where appropriate.

**Quantitative real-time PCR.** Total RNA was extracted from frozen tissues with the Precellys24 homogeniser (Bertin Technologies) and using TRI Reagent (MRC) according to the manufacturer's protocol. cDNA was generated by reverse transcription using the Transcriptor First strand cDNA synthesis kit (Roche biosciences). Quantitative RT-PCR was performed using the SYBR Green I Master (Roche biosciences) and light Cycler 480 (Roche biosciences) with the primers described below. *Gapdh* or *Hprt* were used as internal standard for the quantification.

*Pcp2*: ACAGTTAATTCCCTGCCTGG and CTCAAGGAGCTTGTGTCTGG

*Calb1:* GATTGGAGCTATCACCGGAA and TTCCTCGCAGGACTTCAGTT

*Gapdh*: TTGTGATGGGTGTGAACCAC and TTCAGCTCTGGGATGACCTT

*Hprt*: GTAATGATCAGTCAACGGGGGAC and CCAGCA AGCTTGCAACCTTAACCA

**mRNA sequencing.** Total cerebellar or muscle (quadriceps) RNA was isolated using the TRIreagent (Ambion) solution according to the manufacturer's instructions. 3 mice per genotype (WT and *Adck3*-KO) were used for the experiment. The concentration and integrity of isolated RNA were checked spectrophotometrically (Nanodrop ND 1000, Thermo Scientific) and using Agilent's RNA 6000 Nano Kit on Agilent Bioanalyzer 2100 (Agilent Technologies). RNA samples with RNA integrity numbers (RINs) above eight were chosen. Libraries of template molecules suitable for high throughput DNA sequencing were created using "TruSeq™ RNA Sample Preparation v2 Kit" (Illumina). Briefly, mRNA was purified from 2 µg total RNA using poly-T oligo-attached magnetic beads and fragmented using divalent cations at 94°C for 8 minutes. The cleaved mRNA fragments were reverse transcribed to cDNA using random primers then the second strand of the cDNA was synthesized using DNA Polymerase I and RNase H. The double stranded cDNA fragments were blunted using T4 DNA polymerase, Klenow DNA polymerase and T4 PNK. A single 'A' nucleotide was added to the 3' ends of the blunt DNA fragments using a Klenow fragment (3' to 5'exo minus) enzyme. The cDNA fragments were ligated to double stranded adapters using T4 DNA Ligase. The ligated products were enriched by PCR amplification (30 sec at 98°C; [10 sec at 98°C, 30 sec at 60°C, 30 sec at 72°C] x 12 cycles; 5 min at 72°C). Then surplus PCR primers were removed by purification using AMPure XP beads (Agencourt Biosciences Corporation). DNA libraries were checked for quality and quantified using 2100 Bioanalyzer (Agilent). The libraries were loaded in the flow cell at 8pM concentration and clusters were generated in the Cbot and sequenced in the Illumina Hiseq 2500 as single-end 50 base reads. FASTQ files were generated with CASAVA v1.8.2. Reads were mapped onto the mm9 assembly of the mouse genome by using Tophat v1.4.1(Trapnell et al., 2009) and the bowtie v0.12.7 aligner (Langmead et al., 2009). Only uniquely aligned reads have been retained. Quantification of gene expression was performed using HTSeq v0.5.3p5 (S.Anders1) using gene annotations from Ensembl release 67. Read counts have been normalized across libraries with the method proposed by Anders andHuber (2010). Comparisons of interest (KO vs WT in muscle and in cerebellum) have been performed using the statistical method proposed by Anders and Huber (2010) and implemented in the DESeq v1.10.1 Bioconductor library. Resulting p-values were adjusted for multiple testing by using the Benjamini and Hochberg (1995) method.

**Coenzyme Q measurement.** Lipid were extracted and HPLC-MS/MS was carried out as previously described (Xie et al., 2012). $CoQ_9$ and $CoQ_{10}$ were quantified in 6 mice per genotype at 5 and 32 weeks of age.

**Mitochondria respiration analysis.** Mice were anesthetized with 300 µL of intraperitoneal injection (10 % pentobarbital solution in 10 mM NaCl). Muscles were collected and placed in S solution (see below). Fibers were separated under a binocular microscope in solution S at 4°C and permeabilized for 30 min in solution S supplemented with 50 µg/mL of saponin. Isolated fibers were subsequently placed for 10 min in solution R (see below) to wash out adenine nucleotides and creatine phosphate. They were then transferred to a 3 mL water-jacketed oxygraphic cell (Strathkelvin Instruments, Glasgow, UK) equipped with a Clark electrode, as previously described (Jeukendrup et al., 1997). Solutions R and S contained 2.77 mM CaK2EGTA, 7.23 mM K2EGTA, 6.56 mM MgCl2, 20 mM taurine, 0.5 mM DTT, 50 mM potassium-methane sulfonate (160 mM ionic strength) and 20 mM imidazole (pH 7.1). Solution S also contained 5.7 mM Na2ATP, 15 mM creatine-phosphate, while solution R also contained 5 mM glutamate, 2 mM malate, 3 mM phosphate, and 2 mg/mL fatty acid free bovine serum. $V_{INIT}$ was measured in the absence of fibers and substrates at 22°C under continuous stirring. $V_0$ corresponds to the rate of $O_2$ consumption after addition of muscle fibers and glutamate-malate as substrate, to which $V_{INIT}$ is subtracted. $V_{MAX}$ (maximal respiration) corresponds to the rate of $O_2$ consumption after addition of 2 mM of ADP as a phosphate acceptor, to which $V_{INIT}$ is subtracted. The acceptor control ratio, ACR, is defined as the ratio between $V_{MAX}$ and $V_0$. After measurement, fibers were dried, and respiration rates were expressed as micromoles of $O_2$ per minute per gram of dry weight.

**$H_2O_2$ production in permeabilized fibers.** The permeabilized bundles were placed in ice-cold buffer Z containing 110 mM K-methane sulfonate, 35 mM KCl, 1 mM EGTA, 5 mM $K_2HPO_4$, 3 mM $MgCl_2$, 6 mM $H_2O$, 0.05 mM glutamate, and 0.02 mM malate supplemented with 0.5 mg/ml BSA (pH 7.1, 295 mosmol/kg $H_2O$). Permeabilized fibers remained in buffer Z on a rotator at 4°C until analysis without any deterioration in mitochondrial function. $H_2O_2$ production was measured with Amplex Red (Invitrogen), which reacts with $H_2O_2$ in a 1:1 stoichiometry (catalyzed by horseradish peroxidase; HRP; Invitrogen) to yield the fluorescent compound resorufin and a molar equivalent of $O_2$. Resorufin has an excitation and emission wavelength of 563 nm and 587 nm, respectively, and is extremely stable once formed. Fluorescence was measured continuously with a Fluoromax 3 (Jobin Yvon) spectrofluorometer with temperature control and magnetic stirring. After a baseline (reactants only) was established, the reaction was initiated by adding a permeabilized fiber bundle to

600 µl of buffer Z. Buffer Z contained 5 mM Amplex Red, 0.5 U/ml HRP, 5 mM glutamate, and 2 mM malate as substrates at 37°C. At the end of each experiment, fibers were harvested and dried for 15 min at 150°C. The results were reported in pmol/min/mg of dry weight and as a percentage compared to the control group.

**Electron paramagnetic resonance in blood and tissue (EPR).** Blood samples were removed from the tail immediately before sacrifice to measure blood ROS. The experimental protocol for ROS detection in blood was adapted from (Mrakic-Sposta et al., 2012). 25ul of blood were collected on the tip of the tail and stored on ice at 4°C. After 30min, 20ul of blood were mixed with 20ul of spin probe CMH (1-hydroxy-3-methoxycarbonyl-2, 2, 5, 5-tetramethylpyrrolidine HCl)/Heparin (400uM/100U per mL) solution and introduced in a capillary. The stock solution of CMH (5mM, 2.3 mg in 2ml buffer) was in Krebs-HEPES buffer containing 25uM deferoxamine methane-sulfonate salt (DF) chelating agent and 5mM sodium diethyldithio-carbamatetrihydrate (DETC) at pH 7.4. Immediately after, 40ul of the obtained solution was put in a glass EPR capillary tube (Noxygen Science Transfer & Diagnostics, Germany), that was placed inside the cavity of the e-scan spectrometer (Bruker, Germany) for data acquisition. Sample temperature was first stabilized and then kept at 37°C by the Temperature & Gas Controller “Bio III” unit that was interfaced to the spectrometer. Detection of ROS production was conducted using BenchTop EPR spectrometer E-SCAN under the following EPR settings: center field g = 2.011; field sweep 60G; microwave power 20mW; modulation amplitude 2G; conversion time 10.24ms; time constant 40.96 ms, number of scans: 10 .The EPR signal is proportional to the unpaired electron numbers and could, in turn, be transformed in absolute produced micromoles (umol/min). For tissues, small portions (15-20 mg) of muscle from each animal were minced and placed into a 24-well plate with Krebs Hepes Buffer containing 25 µmol/L deferoxamin and 5 µmol/L DETC. Tissues were then washed twice with the same buffer and incubated at 37°C with the spin probe CMH (1-hydroxy-3-methoxycarbonyl-2, 2, 5, 5-tetramethylpyrrolidine HCl) for 30 minutes under 20 mmHg of oxygen partial pressure using Gas-Controller (Noxygen Sciences Transfer, Elzach, Germany). The incubation of tissues was stopped by placing the plate on ice. All tissue EPR experiments measuring the concentration of oxidized CM were conducted at 15°C in disposable capillary tubes. Detection of ROS was conducted under the following EPR settings: center field g=2.002; field sweep 60G; microwave power 21.85mW; modulation amplitude 2.48G; conversion time 10.24ms; time constant 40.96 ms.

**Blood analysis.** Blood was collected by retro orbital puncture under isoflurane anesthesia after 4 hr fasting at the age of 25 weeks. Blood chemistry was performed on an OLYMPUS AU-400 automated laboratory work station (Olympus France SA, Rungis, France) using commercial reagents (Olympus Diagnostica GmbH, Lismeehan, Ireland). All the data are expressed as mean +/- SEM. Comparison between mutant and control mice was performed using the ANOVA test followed by a Student t test. A statistically significant difference was considered for $p<0.05$.

**Statistical Analysis.** All data are presented as mean ± standard deviation of the mean (SD) or standard error of mean (SEM). Statistical analysis was carried out using the Statview software (SAS Institute Inc). For statistical comparison of three experimental groups, one-way ANOVA test was used. A value of $P < 0.05$ was considered significant. For the statistical comparison of two experimental groups, the bilateral Student's *t*-test was used. $P <0.05$ was considered significant.

## Bibliography

Aure K, Benoist JF, Ogier de Baulny H, Romero NB, Rigal O, Lombes A (2004) Progression despite replacement of a myopathic form of coenzyme Q10 defect. Neurology 63:727-729.

Clark HB, Burright EN, Yunis WS, Larson S, Wilcox C, Hartman B, Matilla A, Zoghbi HY, Orr HT (1997) Purkinje cell expression of a mutant allele of SCA1 in transgenic mice leads to disparate effects on motor behaviors, followed by a progressive cerebellar dysfunction and histological alterations. J Neurosci 17:7385-7395.

Cooper AA, Gitler AD, Cashikar A, Haynes CM, Hill KJ, Bhullar B, Liu K, Xu K, Strathearn KE, Liu F, Cao S, Caldwell KA, Caldwell GA, Marsischky G, Kolodner RD, Labaer J, Rochet JC, Bonini NM, Lindquist S (2006) Alpha-synuclein blocks ER-Golgi traffic and Rab1 rescues neuron loss in Parkinson's models. Science 313:324-328.

Crane FL (2001) Biochemical functions of coenzyme Q10. J Am Coll Nutr 20:591-598.

Gonatas NK, Gonatas JO, Stieber A (1998) The involvement of the Golgi apparatus in the pathogenesis of amyotrophic lateral sclerosis, Alzheimer's disease, and ricin intoxication. Histochem Cell Biol 109:591-600.

Horvath R, Czermin B, Gulati S, Demuth S, Houge G, Pyle A, Dineiger C, Blakely EL, Hassani A, Foley C, Brodhun M, Storm K, Kirschner J, Gorman GS, Lochmuller H, Holinski-Feder E, Taylor RW, Chinnery PF (2012) Adult-onset cerebellar ataxia due to mutations in CABC1/ADCK3. J Neurol Neurosurg Psychiatry 83:174-178.

Huynh DP, Yang HT, Vakharia H, Nguyen D, Pulst SM (2003) Expansion of the polyQ repeat in ataxin-2 alters its Golgi localization, disrupts the Golgi complex and causes cell death. Hum Mol Genet 12:1485-1496.

Lagier-Tourenne C, Tazir M, Lopez LC, Quinzii CM, Assoum M, Drouot N, Busso C, Makri S, Ali-Pacha L, Benhassine T, Anheim M, Lynch DR, Thibault C, Plewniak F, Bianchetti L, Tranchant C, Poch O, DiMauro S, Mandel JL, Barros MH, Hirano M, Koenig M (2008) ADCK3, an ancestral kinase, is mutated in a form of recessive ataxia associated with coenzyme Q10 deficiency. Am J Hum Genet 82:661-672.

Lapointe J, Wang Y, Bigras E, Hekimi S (2012) The submitochondrial distribution of ubiquinone affects respiration in long-lived Mclk1+/- mice. J Cell Biol 199:215-224.

Levavasseur F, Miyadera H, Sirois J, Tremblay ML, Kita K, Shoubridge E, Hekimi S (2001) Ubiquinone is necessary for mouse embryonic development but is not essential for mitochondrial respiration. J Biol Chem 276:46160-46164.

Levin SI, Khaliq ZM, Aman TK, Grieco TM, Kearney JA, Raman IM, Meisler MH (2006) Impaired motor function in mice with cell-specific knockout of sodium channel Scn8a (NaV1.6) in cerebellar purkinje neurons and granule cells. J Neurophysiol 96:785-793.

Lu S, Lu LY, Liu MF, Yuan QJ, Sham MH, Guan XY, Huang JD (2012) Cerebellar defects in Pdss2 conditional knockout mice during embryonic development and in adulthood. Neurobiol Dis 45:219-233.

Mollet J, Delahodde A, Serre V, Chretien D, Schlemmer D, Lombes A, Boddaert N, Desguerre I, de Lonlay P, de Baulny HO, Munnich A, Rotig A (2008) CABC1 gene mutations cause ubiquinone deficiency with cerebellar ataxia and seizures. Am J Hum Genet 82:623-630.

Muhammad A, Flores I, Zhang H, Yu R, Staniszewski A, Planel E, Herman M, Ho L, Kreber R, Honig LS, Ganetzky B, Duff K, Arancio O, Small SA (2008) Retromer deficiency observed in Alzheimer's disease causes hippocampal dysfunction, neurodegeneration, and Abeta accumulation. Proc Natl Acad Sci U S A 105:7327-7332.

Nakai D, Yuasa S, Takahashi M, Shimizu T, Asaumi S, Isono K, Takao T, Suzuki Y, Kuroyanagi H, Hirokawa K, Koseki H, Shirsawa T (2001) Mouse homologue of coq7/clk-1, longevity gene in Caenorhabditis elegans, is essential for coenzyme Q synthesis, maintenance of mitochondrial integrity, and neurogenesis. Biochem Biophys Res Commun 289:463-471.

Nilsson T, Au CE, Bergeron JJ (2009) Sorting out glycosylation enzymes in the Golgi apparatus. FEBS Lett 583:3764-3769.

Ohtsubo K, Marth JD (2006) Glycosylation in cellular mechanisms of health and disease. Cell 126:855-867.

Peng M, Falk MJ, Haase VH, King R, Polyak E, Selak M, Yudkoff M, Hancock WW, Meade R, Saiki R, Lunceford AL, Clarke CF, Gasser DL (2008) Primary coenzyme Q deficiency in Pdss2 mutant mice causes isolated renal disease. PLoS Genet 4:e1000061.

Perkins EM, Clarkson YL, Sabatier N, Longhurst DM, Millward CP, Jack J, Toraiwa J, Watanabe M, Rothstein JD, Lyndon AR, Wyllie DJ, Dutia MB, Jackson M (2010) Loss of beta-III spectrin leads to Purkinje cell dysfunction recapitulating the behavior and neuropathology of spinocerebellar ataxia type 5 in humans. J Neurosci 30:4857-4867.

Reddy JV, Ganley IG, Pfeffer SR (2006) Clues to neuro-degeneration in Niemann-Pick type C disease from global gene expression profiling. PLoS One 1:e19.

Simon D, Seznec H, Gansmuller A, Carelle N, Weber P, Metzger D, Rustin P, Koenig M, Puccio H (2004) Friedreich ataxia mouse models with progressive cerebellar and sensory ataxia reveal autophagic neurodegeneration in dorsal root ganglia. J Neurosci 24:1987-1995.

Stankewich MC, Gwynn B, Ardito T, Ji L, Kim J, Robledo RF, Lux SE, Peters LL, Morrow JS (2010) Targeted deletion of betaIII spectrin impairs synaptogenesis and generates ataxic and seizure phenotypes. Proc Natl Acad Sci U S A 107:6022-6027.

Turunen M, Olsson J, Dallner G (2004) Metabolism and function of coenzyme Q. Biochim Biophys Acta 1660:171-199.

van Vliet C, Thomas EC, Merino-Trigo A, Teasdale RD, Gleeson PA (2003) Intracellular sorting and transport of proteins. Prog Biophys Mol Biol 83:1-45.

Xie LX, Hsieh EJ, Watanabe S, Allan CM, Chen JY, Tran UC, Clarke CF (2011) Expression of the human atypical kinase ADCK3 rescues coenzyme Q biosynthesis and phosphorylation of Coq polypeptides in yeast coq8 mutants. Biochim Biophys Acta 1811:348-360.

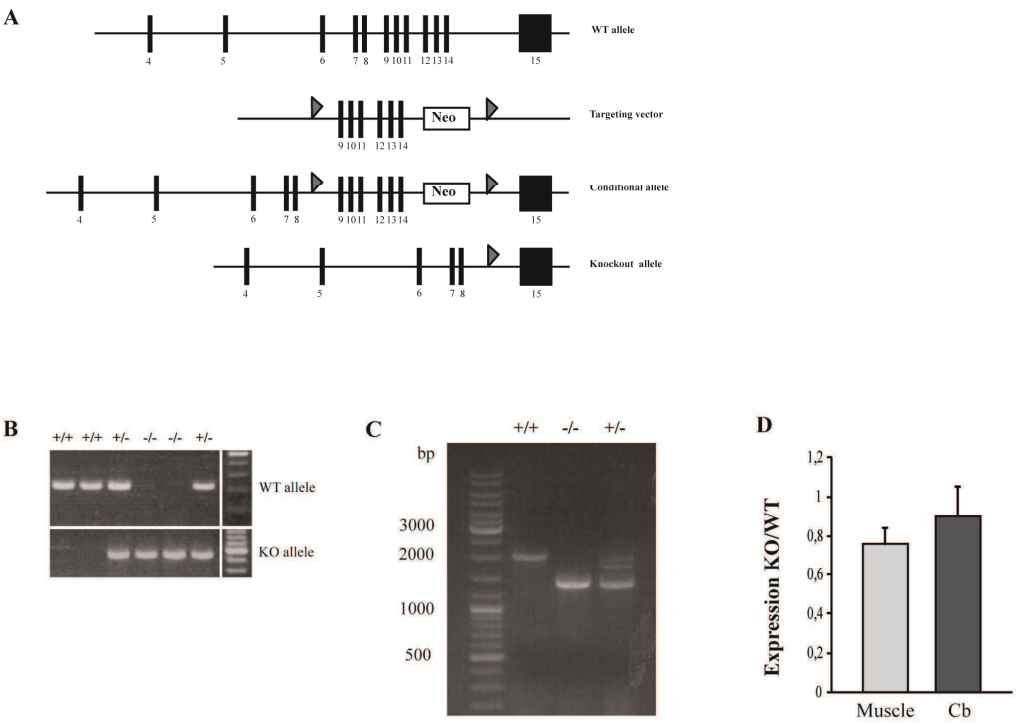


**Figure 1. Targeted disruption of the murine *Adck3* gene**. **A**. Schematic representation of the wild-type (WT) *Adck3* locus, the targeting vector, the conditional allele after homologous recombination and the constitutive knockout after the *Cre*-mediated excision. **B**. The presence of WT and/or KO allele was verified by PCR in WT, *Adck3*$^{+/-}$ and *Adck3*$^{-/-}$ mice. **C** and **D.** Analysis of the deleted allele expression by RT-PCR (**C**) in skeletal muscle and by RNA sequencing (**D**) in skeletal muscle and cerebellum (Cb).

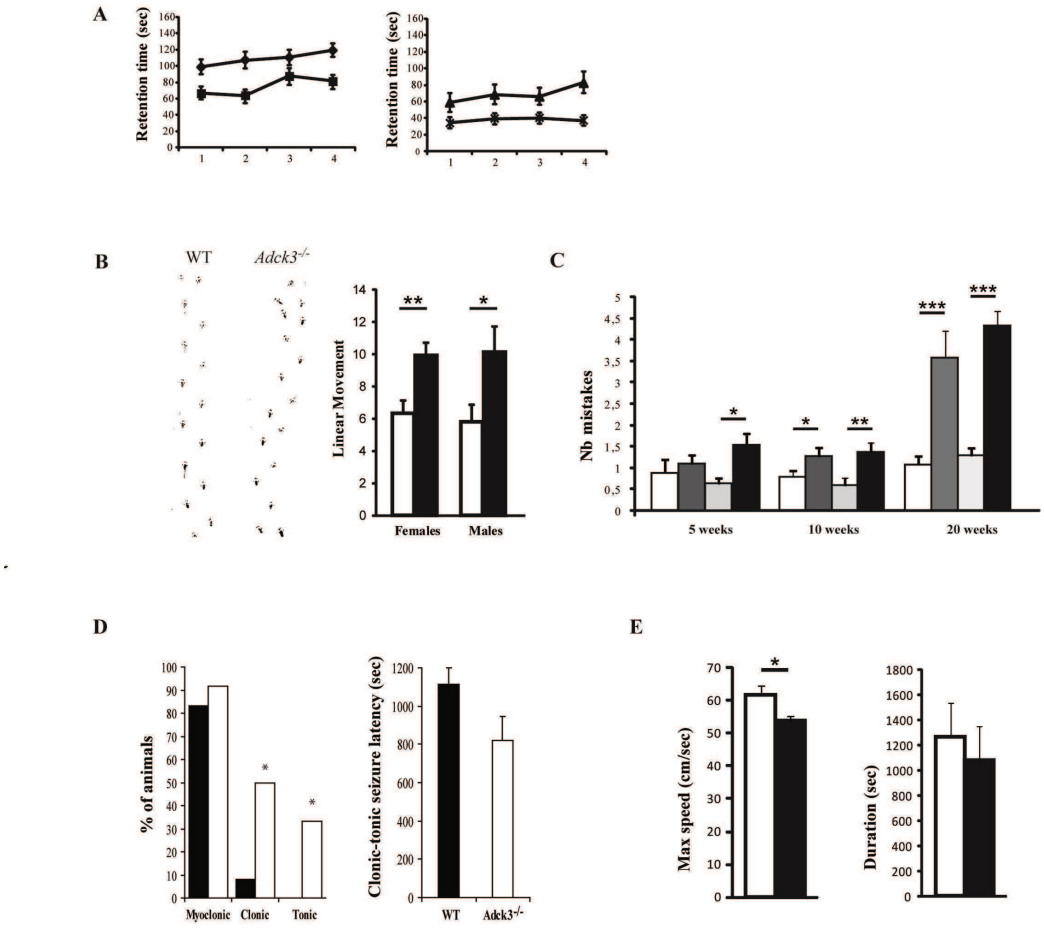


**Figure 2. Motor impairment and susceptibility to epilepsy in *Adck3*$^{-/-}$ mice. A.** Retention time on accelerating rotarod of females (left) and males (right) mice at 10 weeks of age. WT curves are as rhombus and triangle, *Adck3*$^{-/-}$ curves as rectangle and cross. p<0.05 for both genders (repeated-measure ANOVA test). **B.** Representative footprints of 10 weeks old WT and *Adck3*$^{-/-}$ mice. Right, linear movement coefficient significantly increased in mutant mice. **C.** Number of mistakes performed by WT and *Adck3*$^{-/-}$ mice in beam walk test. In white, WT females, in light grey WT males; in dark grey KO females; in black KO males. n=8-12.* p<0.05, ** p<0.01, *** p<0.01. **D.** Susceptibility to epilepsy tested by PTZ injection in 6 months old WT (black) and *Adck3*$^{-/-}$ (white) mice. Left, percentage of mice which displayed myoclonic, clonic or tonic crisis. Right, latency to clonic-tonic seizure. n=12.* p<0.05. **E.** Treadmill performance of WT (white) and *Adck3*$^{-/-}$ (black) mice. Error bars=SEM; n=8

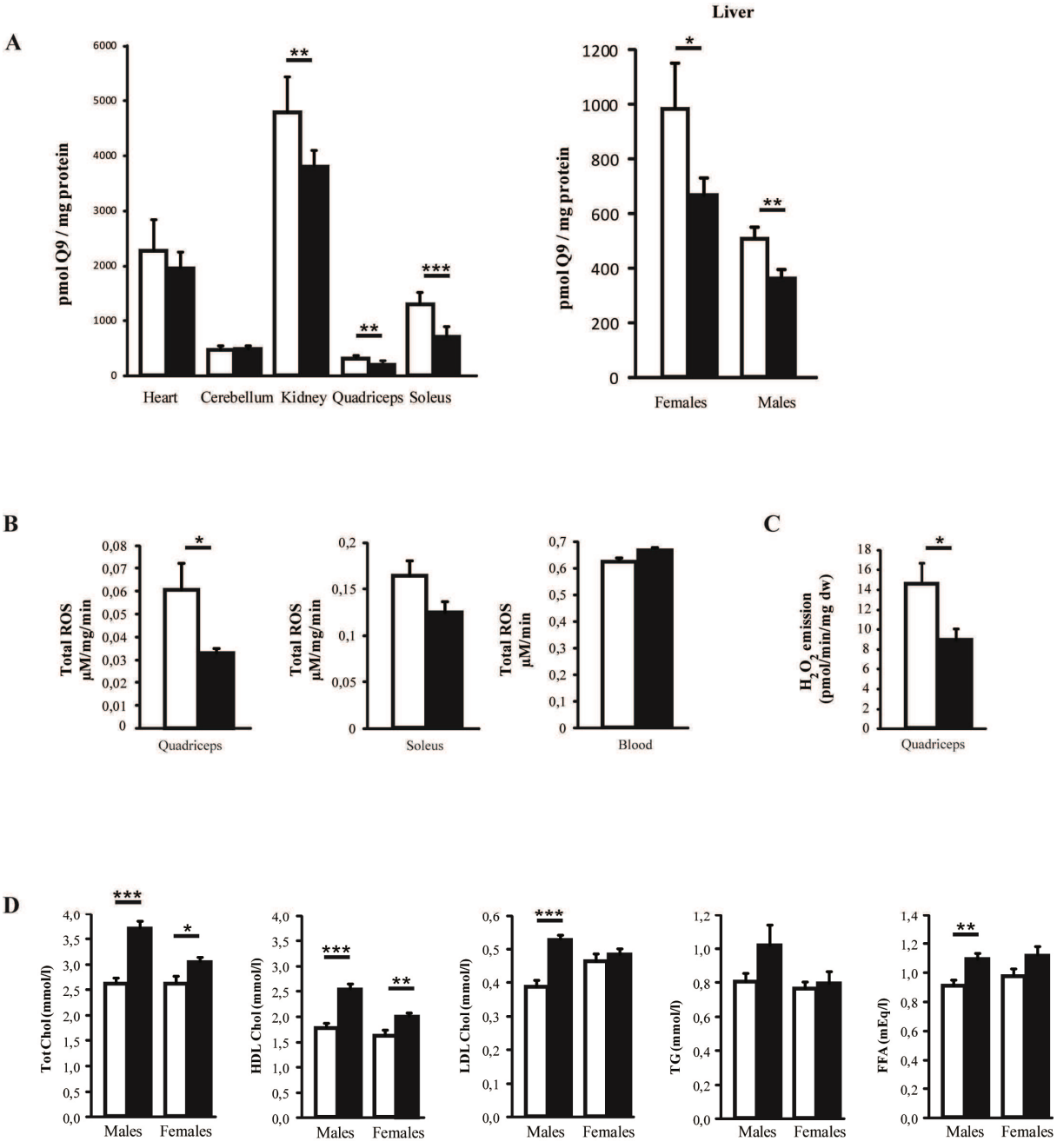


**Figure 3. *Adck3*$^{-/-}$ mice show decreased levels of $CoQ_9$ and ROS and an increase in blood lipids. A.** Coenzyme $CoQ_9$ ($Q_9$) content in 7 months old WT (white) and *Adck3*$^{-/-}$ (black) mice. n=6. Error bar, standard deviation.* p<0.05, ** p<0.01, *** p<0.001. **B.** Total ROS production measured by electron paramagnetic resonance in quadriceps, soleus and bood of WT (white) and *Adck3*$^{-/-}$ (black) mice. **C.** $H_2O_2$ production in permeabilized fibers. Error bar, SEM. p<0.05. **D.** Measurement of blood lipids in *Adck3*$^{-/-}$ (black) and WT (white) mice at 25 weeks. n=9. Error bar, SEM.* p<0.05, ** p<0.01, *** p<0.001.

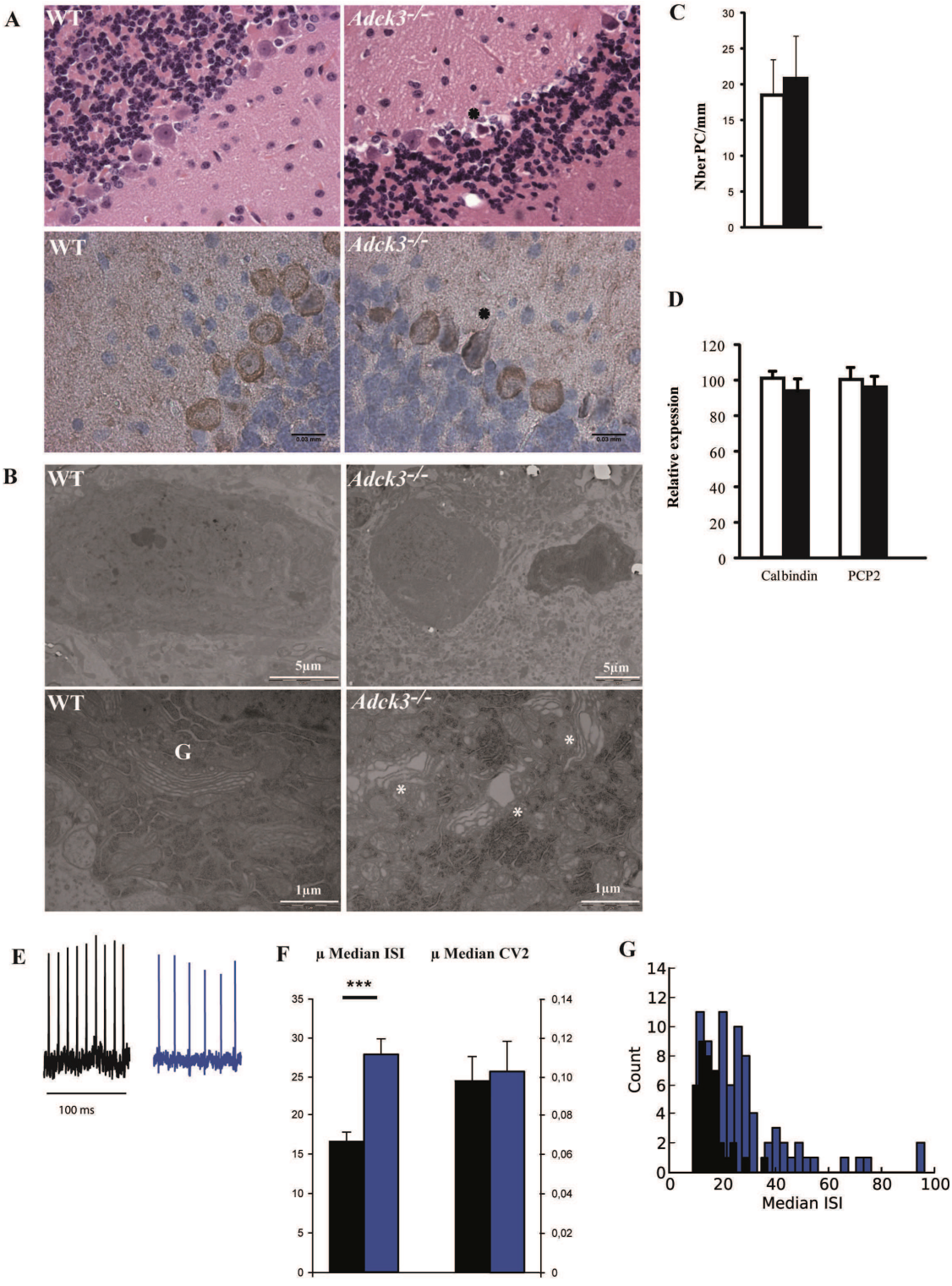


**Figure 4. *Adck3*$^{-/-}$ mice show a specific defect of Purkinje cells. A.** H&E (upper) and Calbindin (lower) stainings of cerebellar sections. Asterisks label shrunken Purkinje neurons. **B.** Electron microscopy images of cerebella (30 weeks old).G; Golgi apparatus. Asterisks mark dilated Golgi apparatus. **C.** Purkinje cell count on cerebellar sections and quantification of cerebellar markers (Calbindin and Pcp2) by qRT-PCR. WT (white) and *Adck3*$^{-/-}$ (black)

mice. **E-F** Electrophysiological recording of Purkinje cells in WT (back) and *Adck3*$^{-/-}$ (blue) mice. ISI, interspike intervan. CV2, coefficient of variation. Number of cells>40. $p<0.01$ (Mann-Whitney Rank Sum Test).

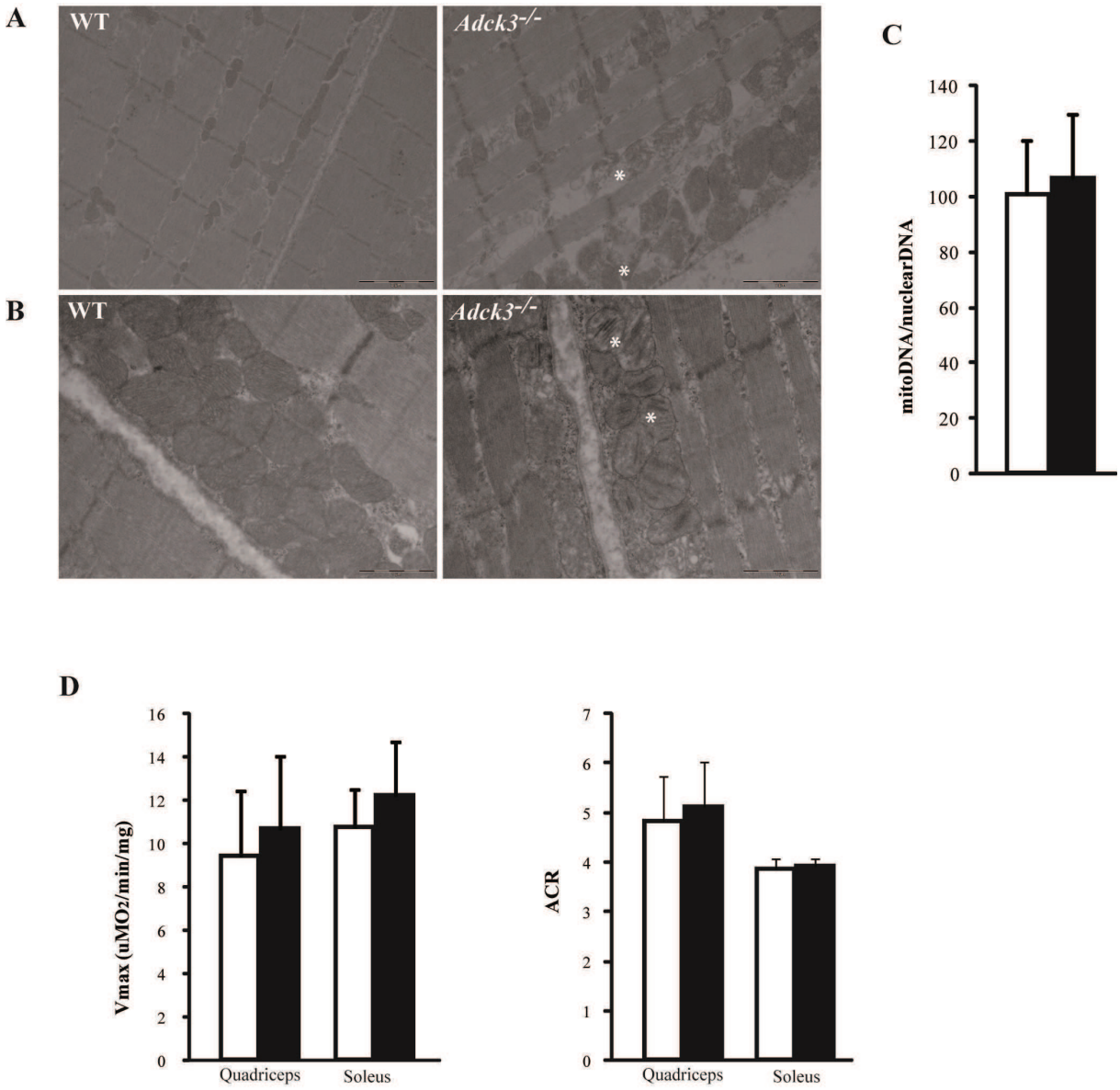


**Figure 5. Mitochondrial defect in *Adck3*$^{-/-}$ mice. A**) Electron microscopy images of quadriceps of 7 months and **B**) 15 months old mice. Asterisks indicate broken mitochondria (A) and mitochondria with collapsing cristae (B). **C**) Quantification of mitochondrial content by qRT-PCR. **D**) Oxygen consumption in quadriceps fibers in presence of ($V_{max}$) ADP and evaluation of mitochondria uncoupling by the acceptor control ratio (ACR).

| Category | Annotation term | Nber of genes | p value | Fold enrichment | Benjamini |
|---|---|---|---|---|---|
| SP_PIR_KEYWORDS | Amino-acid transport | 3 | 5.5 $e^{-3}$ | 26.6 | 5.7 $e^{-1}$ |
| GOTERM_BP_FAT | Extracellular region part | 8 | 6.8 $e^{-3}$ | 23.5 | 5.3 $e^{-1}$ |
| SP_PIR_KEYWORDS | Phosphoprotein | 32 | 6.9 $e^{-3}$ | 1.5 | 4.1 $e^{-1}$ |
| GOTERM_BP_FAT | Secreted | 12 | 7.1 $e^{-3}$ | 2.5 | 3.1 $e^{-1}$ |
| GOTERM_BP_FAT | Phosphorus metabolic process | 8 | 1.4 $e^{-2}$ | 3 | 1 $e^{-0}$ |
| GOTERM_BP_FAT | Immunoglobulin mediated immune response | 3 | 1.5 $e^{-2}$ | 15.4 | 9.1 $e^{-1}$ |
| GOTERM_BP_FAT | Amino-acid transport | 3 | 1.9 $e^{-2}$ | 13.7 | 7.8 $e^{-1}$ |

**Table 1. Cellular pathways (annotation terms) enriched in cerebella dataset.** Analysis performed using DAVID resources (http://david.abcc.ncifcrf.gov/).

| Category | Annotation term | Nber of genes | p value | Fold enrichment | Benjamini |
|---|---|---|---|---|---|
| SP_PIR_KEYWORDS | Glycoprotein | 41 | 4.5 $e^{-5}$ | 1.8 | 8.7 $e^{-3}$ |
| GOTERM_BP_FAT | Regulation of peptide secretion | 4 | 6.1 $e^{-4}$ | 23.5 | 1.8 $e^{-1}$ |
| GOTERM_BP_FAT | Regulation of secretion | 6 | 1.3 $e^{-3}$ | 7.3 | 1.6 $e^{-1}$ |
| GOTERM_BP_FAT | Lipid catabolic process | 6 | 1.8 $e^{-3}$ | 6.8 | 1.3 $e^{-1}$ |
| GOTERM_BP_FAT | Phosphorus metabolic process | 13 | 9.7 $e^{-3}$ | 2.3 | 3.3 $e^{-1}$ |
| GOTERM_BP_FAT | Secretion | 6 | 1.4 $e^{-2}$ | 2.3 | 2.6 $e^{-1}$ |

**Table 2. Cellular pathways (annotation terms) enriched in skeletal muscle dataset.** Analysis performed using DAVID resources (http://david.abcc.ncifcrf.gov/).

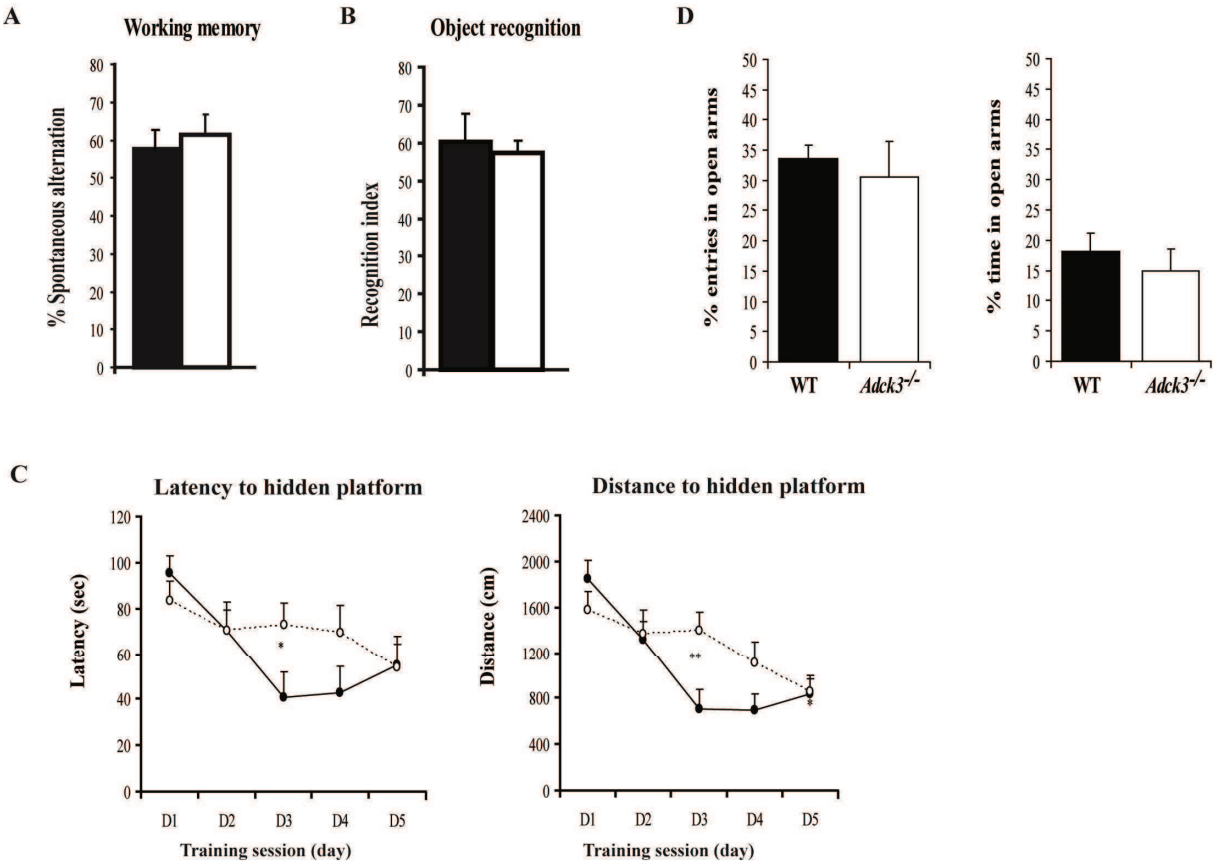


**Figure S1. Memory and anxiety test in WT (black) and *Adck3*$^{-/-}$ mice (white).** Y maze spontaneous alternation (working memory) (A), object recognition (recognition memory) (B), elevated plus maze (anxiety) (D) and Morris water maze (spatial learning memory) (C) tests were performed in WT and *Adck3*$^{-/-}$ mice at 5 months of age. Latency and distance to reach a hidden platform in the water maze are increased in *Adck3*$^{-/-}$ mice. n=12. P<0.05

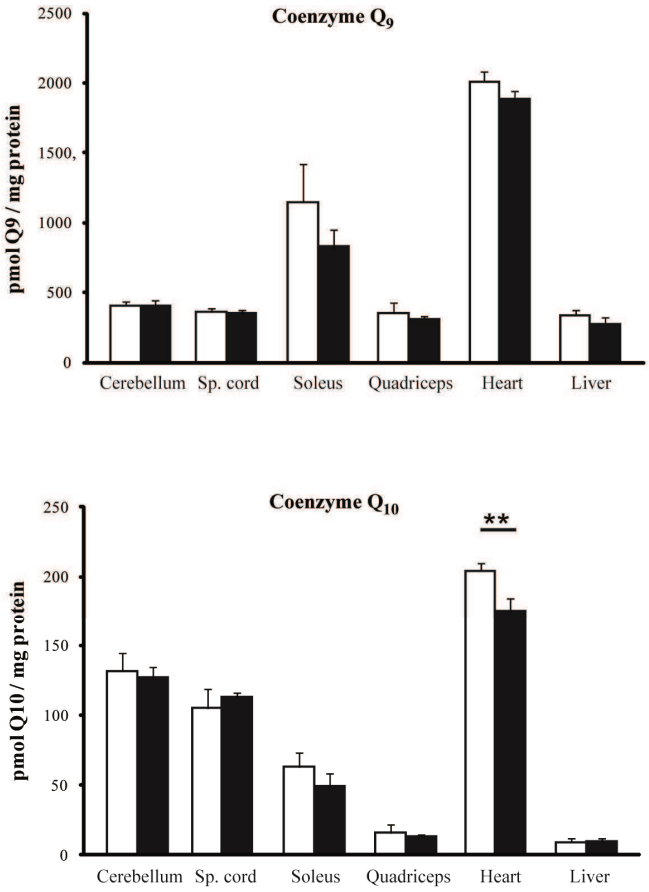


**Figure S2. Coenzyme Q levels in WT (white) and *Adck3*$^{-/-}$ (black) mice.** $CoQ_9$ and $CoQ_{10}$ levels in 5 weeks old mice. n=9. ** p<0.01.

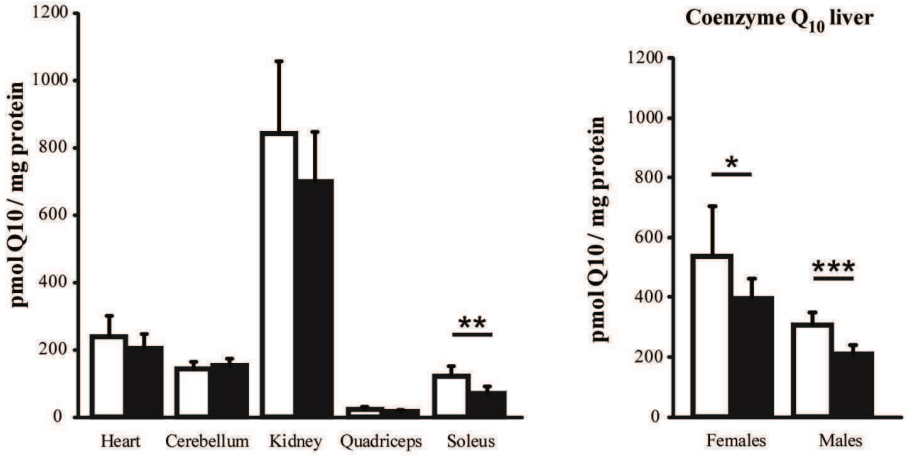


**Figure S3. Coenzyme $Q_{10}$ levels in WT (white) and *Adck3*$^{-/-}$ (black) mice.** $CoQ_{10}$ levels in 7 months old mice. n=6. *p<0.05, ** p<0.01, *** p<0.001

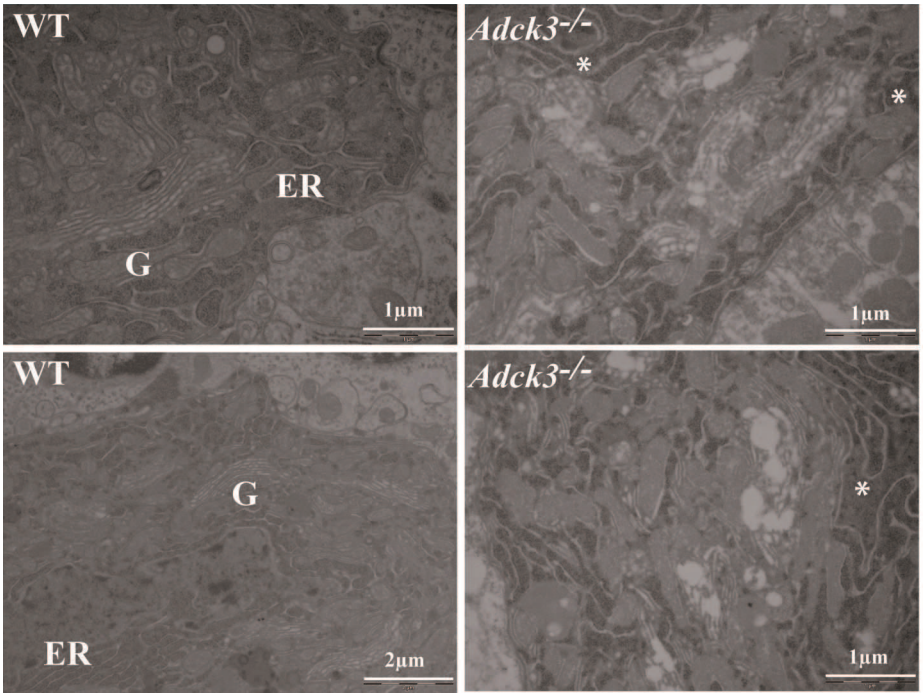


**Figure S4. *Adck3*$^{-/-}$ Purkinje cells show dilated Golgi apparatus and dilated cisternae of endoplasmic reticulum.** Electron microscopy images of cerebella (30 weeks old). G, Golgi apparatus. ER, endoplasmic reticulum. Asterisks mark dilated ER cisternae.

## 4. The metabolic characterization of *Adck3*$^{-/-}$ mice

*Adck3*$^{-/-}$ mice display a misregulation of cholesterol metabolism (manuscript 3). In order to investigate the energy balance of *Adck3* depleted mice, we performed in collaboration with the metabolic platform of the ICS (Institut clinique de la souris), a complete analysis of the energy metabolism and the glucose homeostasis. All the tests were performed under basal conditions, in two cohorts of mice, one of males and another one of females, with 9 WT and 9 *Adck3*$^{-/-}$ mice in each cohort.

No significant change was observed in body weight in male and female *Adck3*$^{-/-}$ mice. However, it should be noted that body weight tended to be higher in old KO male mice when compared to controls (Figure 12).

The body composition of the mice was assessed using Nuclear Magnetic Resonance (NMR) at 6 months of age. Body composition (lean, fat and free body fluid content), were similar between mutant and control mice in both males and females (Figure 13).

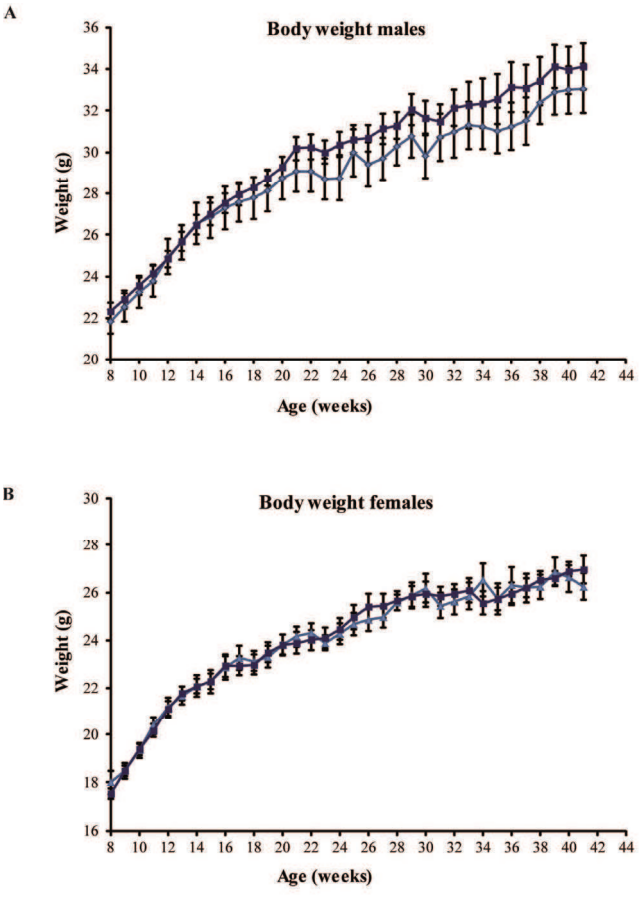


**Figure 12. Body weight curves**. Weight of males (**A**) and females (**B**) mice, WT mice, light blue triangles, and *Adck3*$^{-/-}$ mice, dark blue rectangles. Error bar = SEM. n=9.

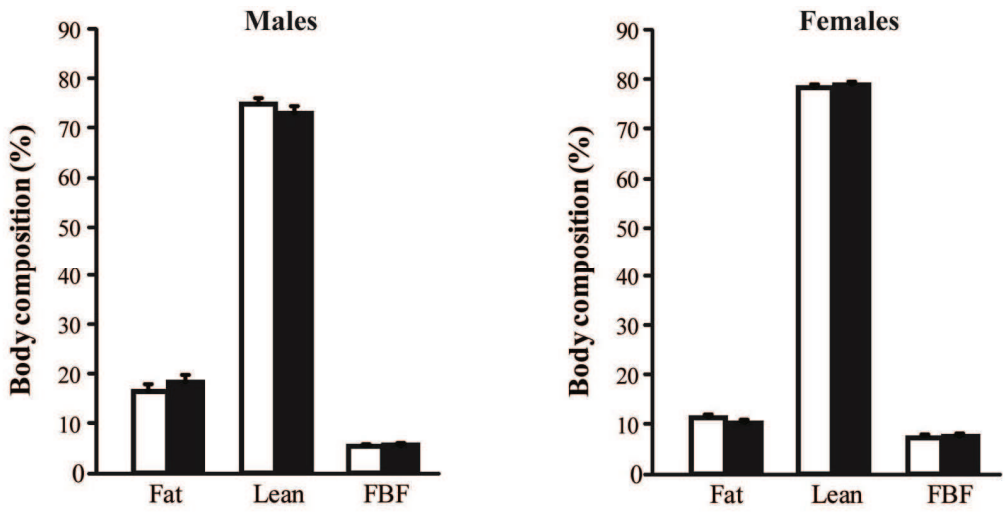


**Figure 13. Body composition analysis.** Body composition (%) of *Adck3*$^{-/-}$ (black) and WT (white) mice (6 months of age). FBF, free body fluid amount. Error bar = SEM. n=9.

In order to evaluate glucose homeostasis, oral glucose tolerance test was performed at 6 months of age. Glucose levels at time 0, 30, 60 and 120 minutes were mildly higher in mutant males than in controls. A different trend was observed in females where glucose levels were slightly lower in mutants than in control mice at time 0 and 120 minutes (Figure 14A). However, in males and females, the area under the curve (AUC) did not change significantly in *Adck3*$^{-/-}$ mice when compared to WT (Figure 14B).

In conclusion, although some interesting variations were observed in mutant mice compared to WT, with different trends in males and females, there was no overt change in glucose tolerance in *Adck3*$^{-/-}$ mice. However, cholesterol levels were altered in the plasma of mutant mice (Manuscript 3), suggesting that a mild dyslipidemia, likely linked to a liver dysfunction, is part of the phenotype of *Adck3*$^{-/-}$ mice. In the investigation reported so far, mice were fed a standard chow diet. As regulation of metabolism is closely dependent on the type of diet, it is possible that under challenging conditions the mild metabolic impairment observed in *Adck3*$^{-/-}$ mice would worsen. Therefore, a complete metabolic investigation is ongoing with mice fed a high fat diet. This approach will allow us to determine whether *Adck3* depletion affects metabolism when mice are subjected to metabolic stress.

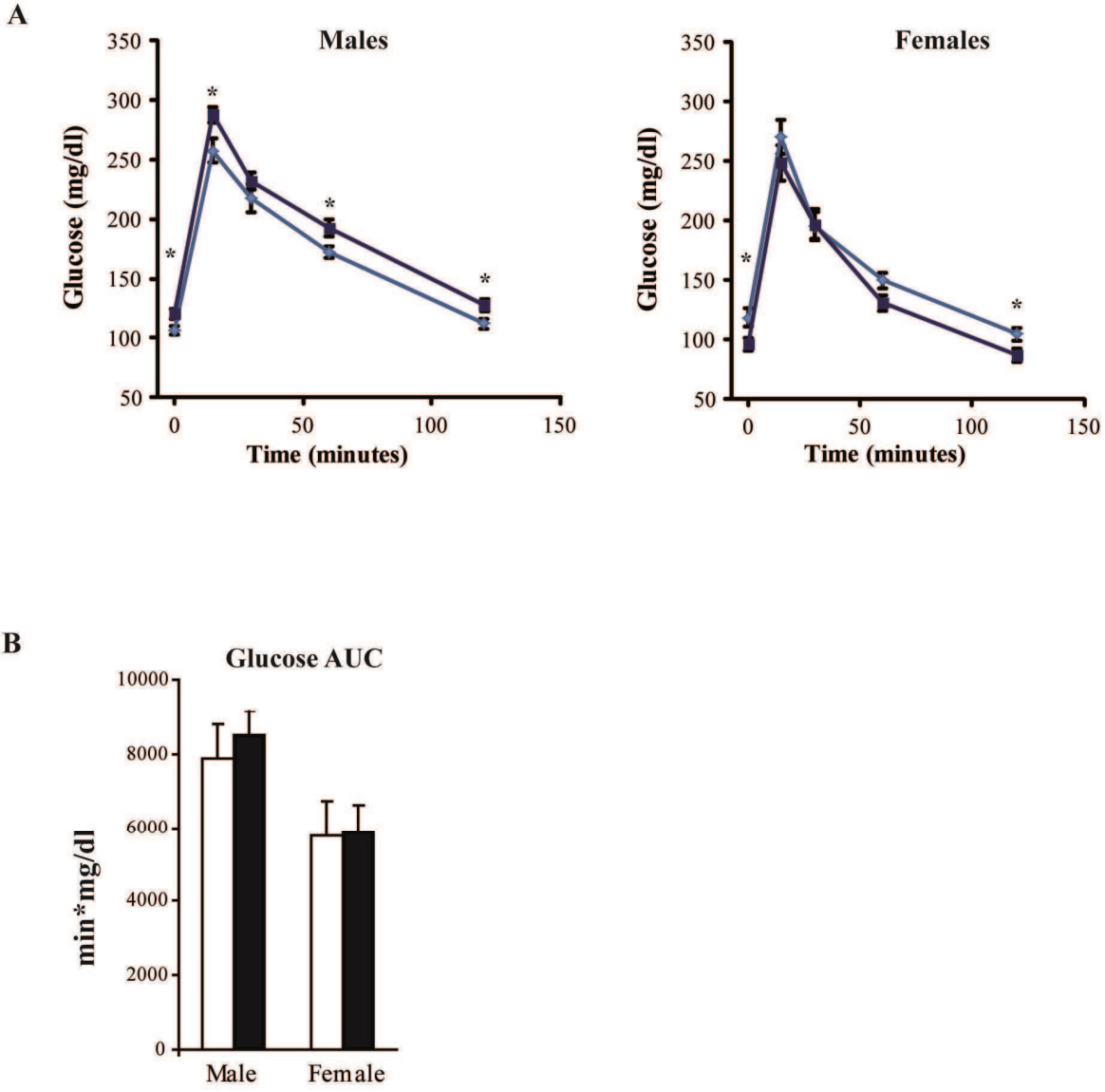


**Figure 14. Oral glucose tolerance test. A.** Glucose levels in WT (triangles, light blue) and *Adck3*$^{-/-}$ (rectangle, dark blue) mice in males (left) and female (right) mice. **B.** Area under the curve (AUC). Error bar = SEM. n=9.

## 5. Study of cholesterol metabolism

$CoQ_{10}$ shares the initial steps of the biosynthetic pathway with cholesterol. In particular, the mevalonate pathway produces farnesyl-PP (FPP), the precursor of cholesterol and CoQ (Figure 9).

Defects in cholesterol metabolism have been reported in several neurodegenerative diseases, such as Niemann–Pick type C, a lysosome storage disorder due to impairment of intracellular cholesterol trafficking (Peake and Vance, 2010). This severe condition is characterized by ataxia and accumulation of cholesterol in Purkinje neurons.

Since I have observed a defect in the ultrastructure of almost all membranes of the PCs in *Adck3*$^{-/-}$ mice, I decided to determine whether misregulation of cholesterol metabolism could be implicated in the cerebellar degeneration observed in *Adck3*$^{-/-}$ mice. To do so, I undertook three different strategies: 1) study of the expression of genes encoding key enzymes involved in the mevalonate and cholesterol pathway, 2) quantification of cholesterol in cerebellar extracts, 3) quantification of cholesterol on cerebellar sections.

All these investigations were carried out in old mice (more than 17 months of age) in case cholesterol misregulation is a secondary and/or late event in the pathology of *Adck3*$^{-/-}$ mice.

Using qRT-PCR, the expression levels of two genes involved in cholesterol biosynthesis: 3-hydroxy-3-methylglutaryl-CoA reductase (*Hmgcr*), the rate-limiting enzyme of the mevalonate pathway, and farnesyl-diphosphate farnesyltransferase 1 (*Fdft1*), also called squalene synthase, which catalyzes the first committed step of the cholesterol biosynthesis (Figure 9) was verified (Buhaescu and Izzedine, 2007).

The expression levels of *Hmgcr* and *Fdft1* in *Adck3*$^{-/-}$ cerebella were comparable with WT at 22 months of age (Figure 15A).

In collaboration with the Clinical Chemistry platform of the ICS, total cholesterol, free cholesterol and cholesterol ester were quantified in the cerebella of 2 years old mice. This was achieved by an enzymatic reaction carried out on a total extract of cerebellar lipids. Total cholesterol was slightly decreased in *Adck3*$^{-/-}$ mice compared to WT, whereas free cholesterol and ester cholesterol remained unchanged (Figure 15B).

In parallel, in order to quantify cholesterol on cerebellar sections, I performed filipin staining on 17 months old mice. Filipin is a fluorescent probe, which detects unesterified cholesterol bound to membranes. A double staining with an antibody against Calbindin was performed to

label Purkinje neurons. The intensity of fluorescence between the molecular layer, the Purkinje layer and the granular layer was comparable. Therefore, I quantified the intensity of fluorescence in at least four big areas (40*70 µm) of each cerebellar section considered. Strikingly, *Adck3*$^{-/-}$ mice displayed an increase of about 30% in filipin fluorescence compared to WTs (Figure 15C).

The three approaches that I have undertaken gave opposite results, hence not allowing a definitive conclusion to our initial question. In fact, although the expression levels of two key enzymes of the mevalonate pathway are not altered in mutant mice, the quantification of cholesterol in cerebellar extracts and on sections through filipin staining give opposite results. However, the intensity of filipin fluorescence is not strong and photobleaches rapidly. On the other hand, filipin staining is widely used to detect accumulation on cholesterol in tissue sections (Ko et al., 2005) and it may not be sensitive enough to quantify cholesterol levels. In *Adck3*$^{-/-}$ mice, a misregulation of cholesterol metabolism was found in plasma, suggesting that indeed cholesterol dysfunction can play a role in the pathophysiology of *Adck3*$^{-/-}$ mice. Therefore, a more sensitive method to quantify cholesterol, such as a lipidomic study, would be more suitable.

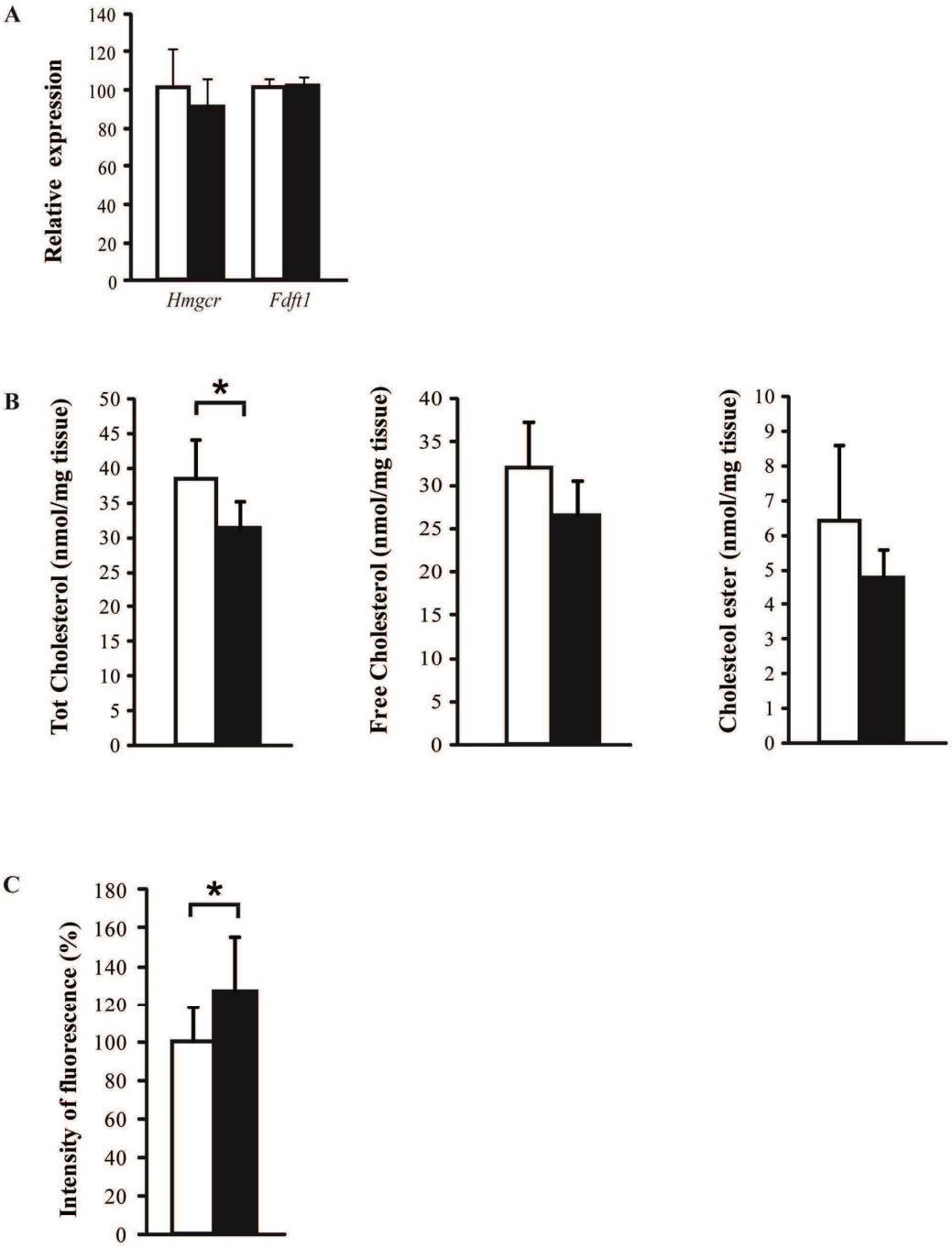


**Figure 15. Cerebellar cholesterol metabolism.** Evaluation of cholesterol metabolism of WT (white) and *Adck3*$^{-/-}$ (black) mice. **A.** Quantification of the cholesterol genes *Hmgcr* and *Fdft1* by qRT-PCR. Error bar=standard deviation. n=5. **B.** Quantification of cholesterol in cerebellar extracts expressed as nmol cholesterol/mg tissue. Error bar=standard deviation. n=5. **C.** Quantification of filipin fluorescence on cerebellar sections. Error bar = SEM. n=3

## 6. Study of Purkinje cell synapses

*Adck3*$^{-/-}$ Purkinje cells showed an altered capacity to spontaneously induce action potentials (peacemaker activity) (manuscript 3). This functional defect was found to occur at an early stage of the disease. In order to gain further insight into the function of degenerating Purkinje neurons, I decided to quantify the presence of excitatory synapses, to study the capacity of *Adck3*$^{-/-}$ Purkinje cells to respond to stimuli. PCs establish synapses with the axon terminals of cerebellar granule cells (parallel fibers) and with those of the inferior olivary neurons (climbing fibers) (Figure 3).

In order to quantify the number and the morphology of these synapses, immunofluorescence was performed on slices of adult mice (10 months of age). PCs were marked with Calbindin and two markers were used to distinguish the different synapses: vGlut1 to stain synapses with granule cells, and vGlut2 to stain synapses with climbing fibers (Liguz-Lecznar and Skangiel-Kramska, 2007, Lorenzetto et al., 2009). Using confocal analysis, I then evaluated the morphometric parameters (number and position) of PC synapses.

VGlut1 staining appeared dense and diffuse in the molecular layer without any gross differences between WT and KO animals (Figure 16A). Because of the high synapse density, it was not possible to achieve a precise quantification of vGlut1 positive synapses. VGlut2 synapses appeared less dense than vGlut1 positive synapses and localized along the dendrites of PCs (Figure 16B). In order to quantify vGlut2 positive synapses, I counted the number of synapses along a specific dendrite, normalizing the value to the length of the dendrite. Using this approach, I found that the density of vGlut2 positive synapses was slightly higher in *Adck3*$^{-/-}$ compared to WT mice (Figure 16C).

This data give important insight into the dysfunction of *Adck3*$^{-/-}$ Purkinje cells, suggesting that, not only the spontaneous firing activity is altered, but also the capacity to respond to stimuli can be affected in *Adck3*$^{-/-}$ Purkinje cells. Therefore, it would be relevant to explore this aspect using an electrophysiology study, in order to evaluate whether the inputs arriving to Purkinje cells are increased in *Adck3*$^{-/-}$ mice and whether the excitability of *Adck3*$^{-/-}$ Purkinje cells is altered.

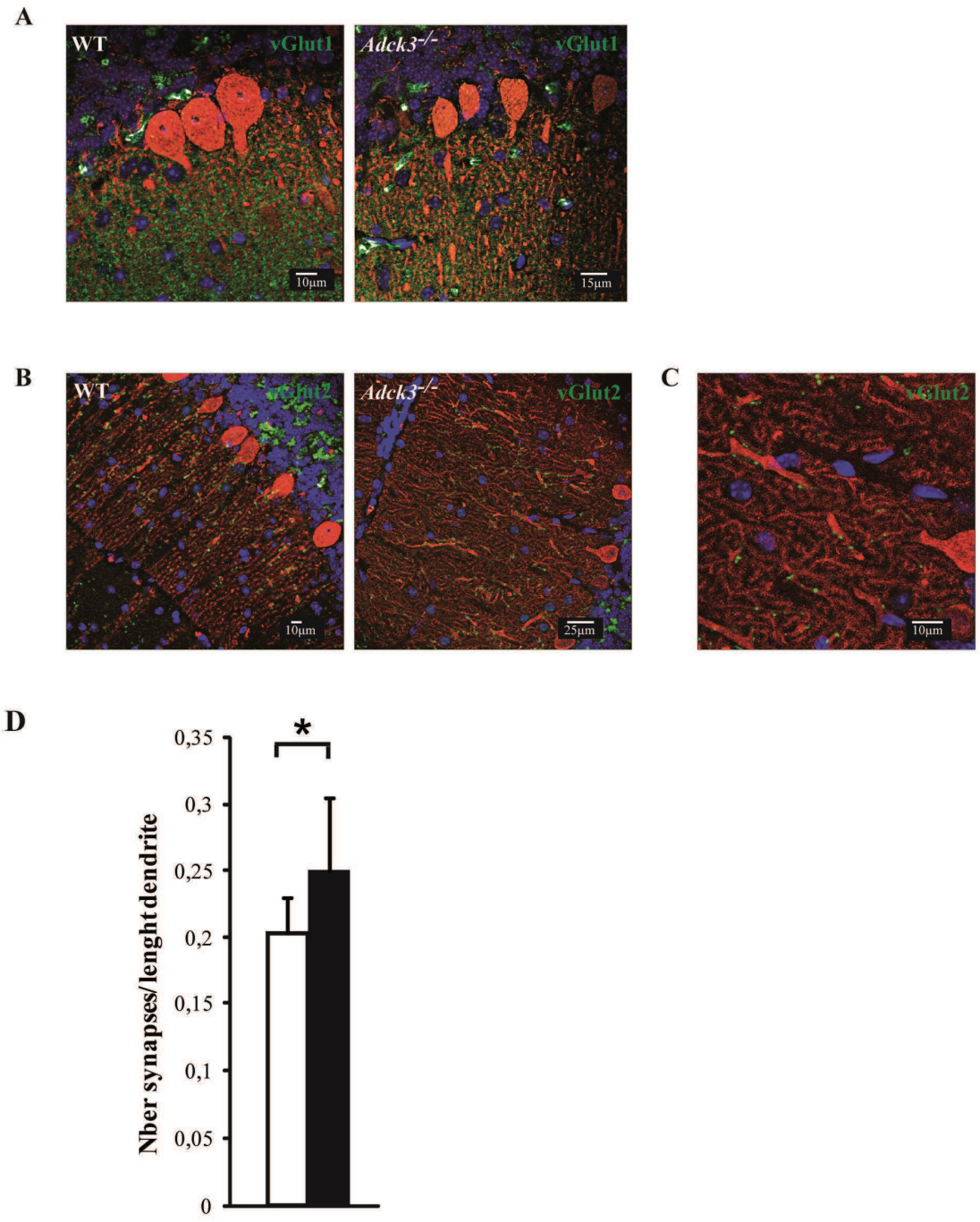


**Figure 16. Quantification of synapses in *Adck3*$^{-/-}$ and WT mice.** (**A-C**) Confocal images of vGlut1-labeled (green, A) parallel fibers synapses and vGlut2-labeled climbing fibers terminations (green, B-C) on PCs stained with Calbindin (red) in WT and Adck3-KO mice. Small portions of the molecular layer were acquired at higher magnification (C) to calculate the number of vGlut2 positive synapses per µm of dendrite length (**D**). An increase of vGlut2 positive synapses was found in KO mice ($p<0.05$ by t test; number of measured dendrites >42).

## 7. Oxidative stress in *Adck3*$^{-/-}$ mice

Coenzyme Q is an antioxidant and a deficit in CoQ can be linked to an increase in ROS production (Quinzii et al., 2010). In order to evaluate whether high oxidative stress could play a role in the pathophysiology of the muscle defect observed in *Adck3*$^{-/-}$ mice, I undertook different strategies: 1) staining of muscle sections with reduced dyes; 2) quantification of expression of enzymes involved in the oxidative stress response; 3) quantification of lipid peroxidation.

In order to quantify reactive oxygen species in skeletal muscle, I used two dyes that fluoresce upon oxidation: Dihydroethidium (DHE) and MitoTracker Orange CM-$H_2$TMRos. Dihydroethidium is a non-fluorescent compound, which once internalized in cells can be oxidized by superoxide to the fluorescent ethidium, which then intercalates into DNA (Budd et al., 1997). MitoTracker Orange CM-$H_2$TMRos is a reduced dye derivative of dihydrotetramethylrosamine. In its reduced form, MitoTracker Orange CM-$H_2$TMRos does not fluoresce. When it enters cells, it is oxidized by superoxide and $H_2O_2$ (Kweon et al., 2001) to the corresponding fluorescent probe and is sequestered in the mitochondria. Thus, the fluorescence measured with both dyes is an indirect indication of ROS levels in the sample. Dihydroethidium staining results in a red labeling of the nuclei, whereas MitoTracker Orange labels mitochondria (Figure 17A and 17C).

Stainings were performed on quadriceps sections of old mice (22 month of age) to take into account the possibility that increased oxidative stress is a late event in the pathology of *Adck3*$^{-/-}$ muscle. The intensity of fluorescence of DHE, as well as MitoTracker Orange, was similar in WT and mutant mice (Figure 17B and 17D).

The expression of *Sod1*, *Sod2* and Catalase was quantified by qRT-PCR in the quadriceps of 17 months old mice. Moreover, the expression of Catalase and SOD2 was determined by western blot. Unfortunately, the antibody against SOD1 was not available at that time.

The expression levels of the genes and proteins tested appeared similar between WT and *Adck3*$^{-/-}$ mice

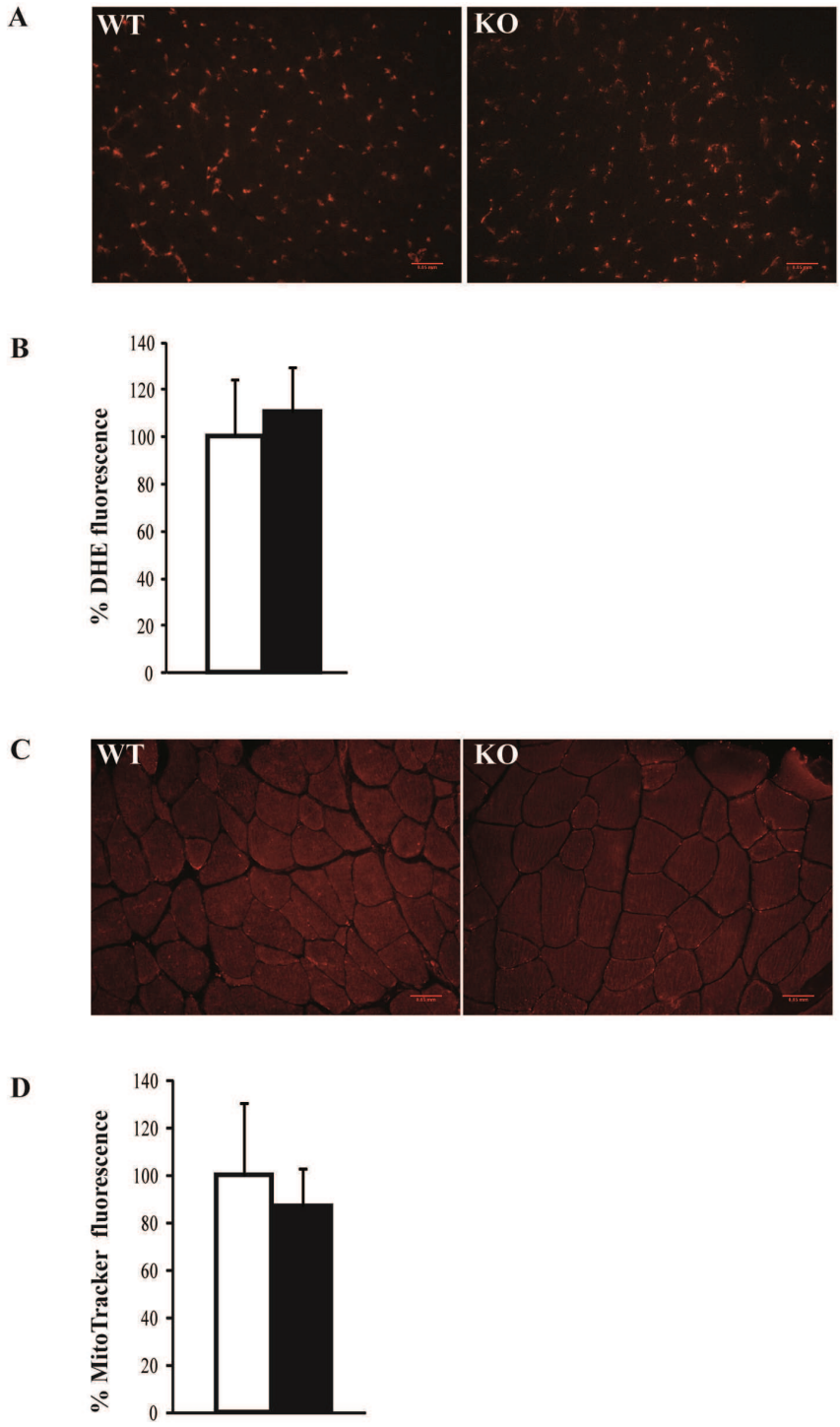


**Figure 17. Staining of quadriceps sections with DHE (A) and MitoTracker Orange (C)** in 22 months old mice (scale bar, 0.05mm). Quantification of the fluorescence intensity for DHE (**B**) and Mitotracker Orange (**D**) in WT (white) and *Adck3*$^{-/-}$ (black) mice. Error bar, standard deviation.

. **A)** **B)**

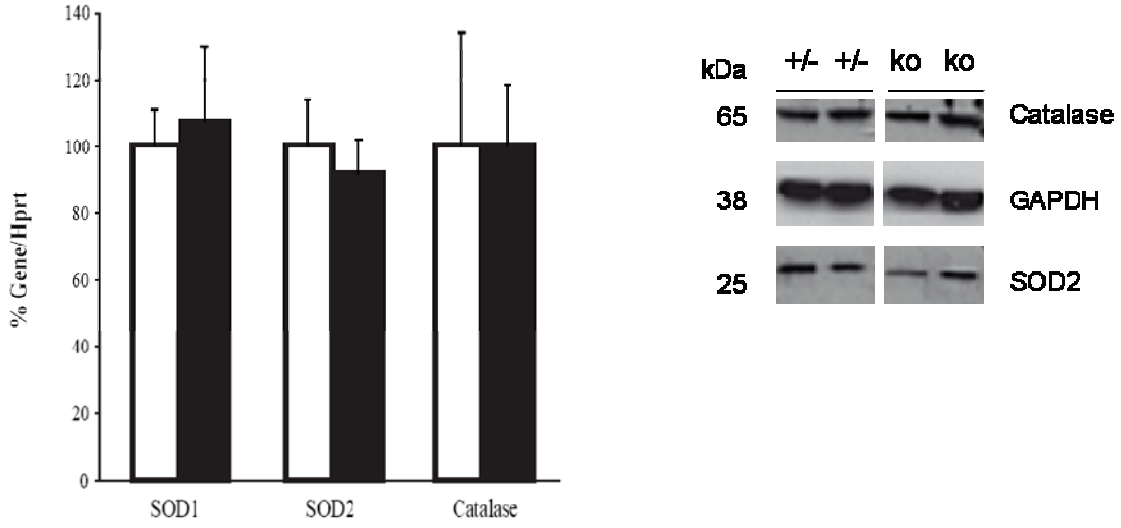


**Figure 18. Quantification of the oxidative stress response.** A) SOD1, SOD2 and Catalase levels assessed by RT-qPCR in WT (white) and *Adck3*$^{-/-}$ (black) mice (**A**) and western blot (**B**).

Thiobarbituric acid reactive substances (TBARS) are low-molecular-weight aldehydes that are end products of the lipid peroxidation process. The main aldehyde produced by lipid peroxidation is MDA (malonaldehyde or malonyldialdehyde). In the TBARS assay, MDA is quantified through a reaction with TBA (thiobarbituric acid), which generates a pink colored product that absorbs at 535 nm and can be measured by UV/visible spectrophotometry (Devasagayam et al., 2003).

The TBARS assay was performed on skeletal muscle (quadriceps) homogenates from *Adck3*$^{-/-}$ and WT mice at 7 and 22 months of age. Although no differences were observed at 7 months, a significant increase in MDA concentration was found in the quadriceps of *Adck3*$^{-/-}$ mice at 22 months (Figure 19B).

In order to verify whether lipid peroxidation could play a role in the pathology not only of muscle but also of *Adck3*$^{-/-}$ cerebella in a late stage of the disease, I performed the TBARS assay on cerebellar extracts of 22 months old mice. However, *Adck3*$^{-/-}$ and WT mice showed similar levels of MDA concentration (Figure 19A).

These results suggest that oxidative stress does not globally increase in *Adck3*$^{-/-}$ mice, which show a decrease in ROS levels in skeletal muscle fibers (manuscript 3). The DHE and MitoTracker Orange stainings of muscle sections were probably not sensitive enough to evaluate this change in ROS content. The expression levels of genes involved in the oxidative stress response were unaltered. However, an increase in lipid peroxidation was observed in skeletal muscle, but not in cerebella, at a very late stage (22 months) of the disease. As this data is the only indication of a possible increase in oxidative stress, it would be relevant to determine whether an increase in lipid content is occurring in *Adck3*$^{-/-}$ muscle to exclude that the increased lipid peroxidation is due to a misregulation of lipid metabolism.

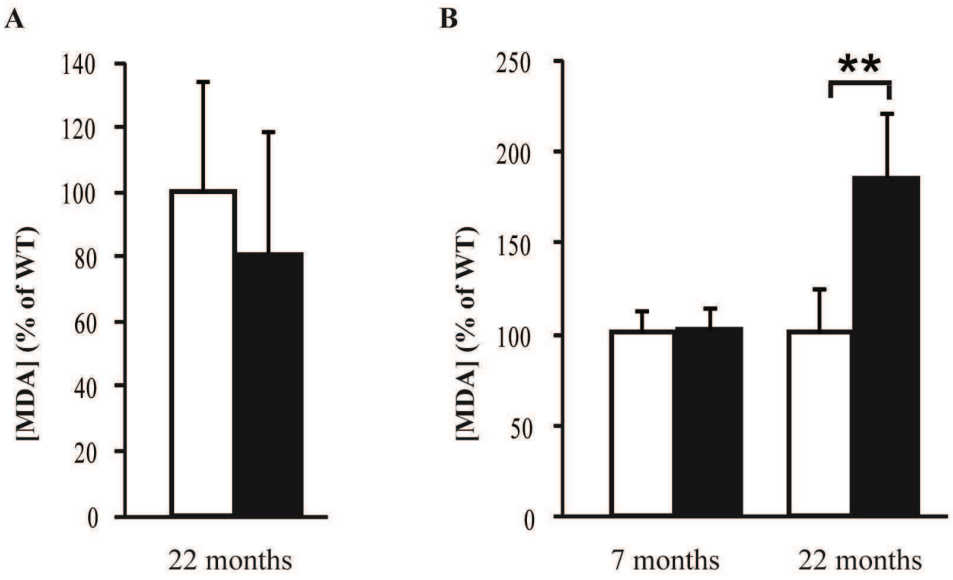


**Figure 19. TBARS assay.** MDA concentration (% of WT) in cerebellar extracts (**A**) and skeletal muscle extracts (**B**) in WT (white) and *Adck3*$^{-/-}$ (black) mice: Error bar is standard deviation. $p<0.01$.

## 8. ADCK4 characterization: study of the expression pattern and the maturation of ADCK4 protein.

The second part of my PhD project aimed to characterize the function of ADCK4. To this end, I studied the expression pattern and the localization of the murine ADCK4. In parallel, I have started to investigate the maturation process of ADCK4 protein. However, since I was fully involved in the characterization of *Adck3*$^{-/-}$ mice, the data obtained so far on ADCK4 are preliminary and need further investigation.

In mouse, as well as in humans, ADCK4 is the closest paralog of ADCK3. The murine form of these two proteins share 45% of identities (Figure 20).


**Figure 20. Alignment of murine ADCK3 and ADCK4.** Alignment performed with the Uniprot_Align software. The different domains (see Introduction paragraph 3.3 and Figure 10) of the two proteins are shown: the KxGQ motif (green), the five kinase motifs (red) and the domain specific to the ADCK3-ADCK4 subgroup (yellow).

To date, nothing is known about the function of ADCK4. However, in some ARCA2 patients, a transcriptional downregulation of *ADCK4* that parallels $CoQ_{10}$ levels in patient fibroblasts has been reported (Lagier-Tourenne et al., 2008). This finding suggests that ADCK4 might also be involved in the regulation of $CoQ_{10}$ synthesis.

For this reason, the expression of the murine *Adck4* was determined by qRT-PCR. In adult mice (10 months of age), *Adck4* shows a ubiquitous expression pattern, although higher levels are present in lung, kidney and liver. Interestingly, no difference in *Adck4* expression was detected in WT and *Adck3*$^{-/-}$ tissues, suggesting that no compensatory effect is present in mutant mice due to overexpression of *Adck4*.

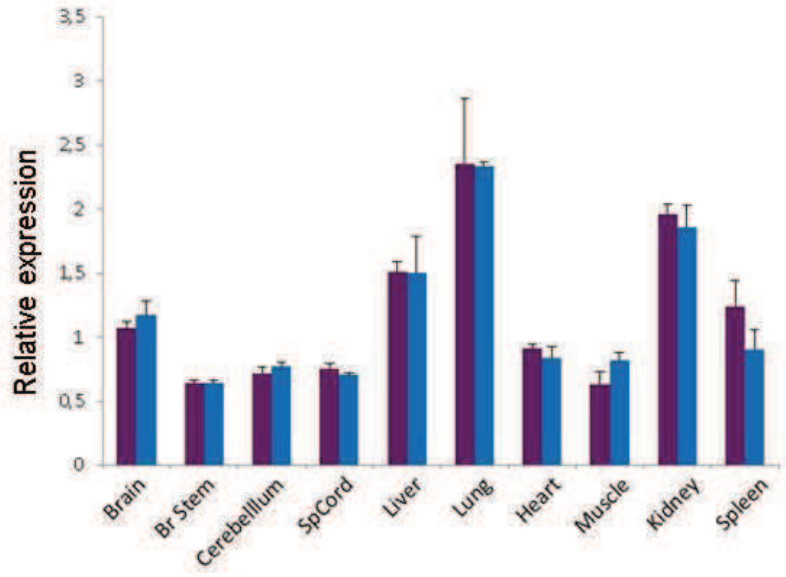


**Figure 21. Expression of murine *Adck4*.** Levels of *Adck4* in WT (purple) and *Adck3*$^{-/-}$ (blue) tissues at 10 months of age.

Furthermore, *Adck3* is more expressed than *Adck4* in adult mice (Figure 22). Moreover, the two paralogs seem to have a different expression profile. In fact, *Adck3* is highly expressed in muscle and heart. This different expression profile leaves open the possibility that the two paralogs have the same function with different tissue specificity.

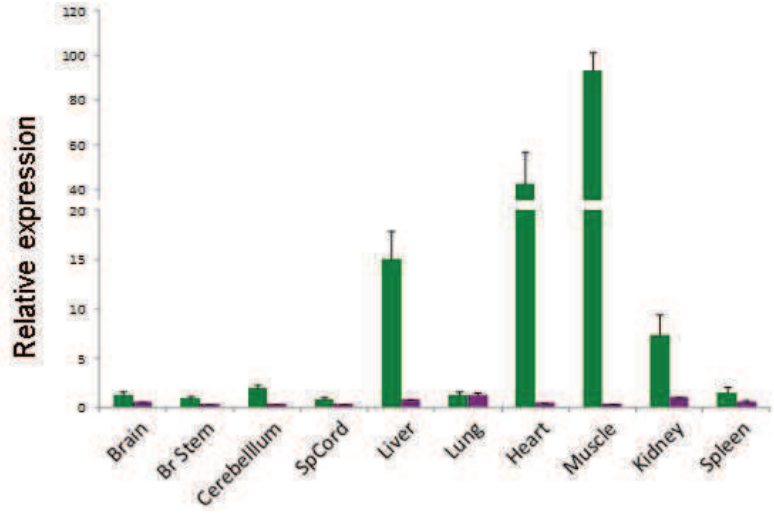


**Figure 22. Expression of murine *Adck3* and *Adck4*.** Levels of *Adck3* (green) and *Adck4* (purple) in WT tissues at 10 months of age.

In order to investigate the subcellular localization of ADCK4, the murine form of *Adck4* was cloned with a C-terminal myc tag in a mammalian expression vector (pcDNA3.1/Zeo). ADCK4_myc was overexpressed in COS cells and was found to localize in mitochondria (Figure 23A), as shown by colocalization with Mitotracker. Moreover, mitochondrial enrichment of protein extracts from COS cells overexpressing ADCK4_myc was performed. Two bands were detected in total protein extract (Figure 23B), likely corresponding to the mature form (around 55kDa) and the precursor (around 60 kDa). Only the mature form was present in the mitochondria enriched extract, whereas the precursor was found in the cytosolic fraction. These data show that overexpressed ADCK4 has a mitochondrial localization and it is presumably maturated prior to import into mitochondria.

In order to investigate the maturation of ADCK4, flag-tagged ADCK4 was overexpressed in Hela cells, then immunoprecipitated with an anti-FLAG antibody. After SDS-PAGE migration, the bands corresponding to the precursor and the mature (Figure 24A) forms of ADCK4 were digested with trypsin and analyzed by mass spectrometry (MALDI-TOF).

The trypsin peptides detected by MALDI-TOF analysis are shown in Figure 24B. Since peptide 22-31 (LPCGGALGPR) is detected in the precursor but not in the mature form of ADCK4, the cleavage site would probably be located downstream of position 31. Moreover, since peptide 54-62 (GLSEDDIRR) is detected in the precursor and the mature form, the cleavage site is likely upstream of amino acid 54. This finding suggests that the cleavage site

of ADCK4 is located between aa 32 and 53, giving rise to a protein of 53-55 kDa, corresponding to the size of the mature form that was detected (Figure 24A).

These results indicate that, similar to ADCK3, ADCK4 is a mitochondrial protein and that it is likely maturated to be imported into mitochondria. Whether a redundant effect is present between ADCK3 and ADCK4 is not clear yet, since *Adck4* expression is unaltered in *Adck3*$^{-/-}$ tissues. Interestingly, although both paralogs are ubiquitously expressed, *Adck4* is less expressed than *Adck3* (Figure 22), indicating that mammalian cells require a different amount of the two proteins. The redundancy between the two paralogs will be further discussed in the 'Discussion and perspectives' section.

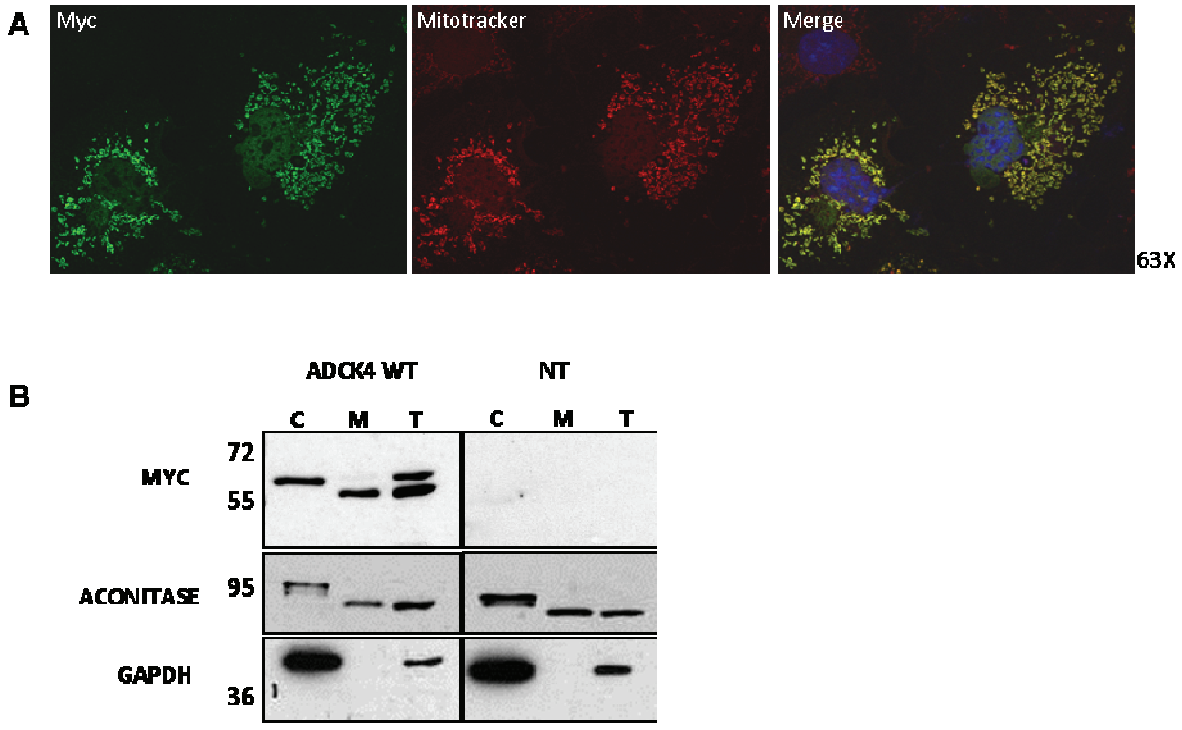


**Figure 23. Mitochondrial localization of ADCK4. A)** Confocal analysis of COS cells overexpressing Myc-tagged ADCK4 (green). Mitochondria are stained in red with Mitotracker and nuclei in blue. **B)** Mitochondrial enrichment of protein extracts from COS cells overexpressing myc-tagged ADCK4. The mature form of ADCK4 is present in total (T) and mitochondrial fractions (M) and absent in cytoplasmic (C) fraction. NT, not transfected. Aconitase and GAPDH are control of mitochondrial and cytosolic fractions, respectively.

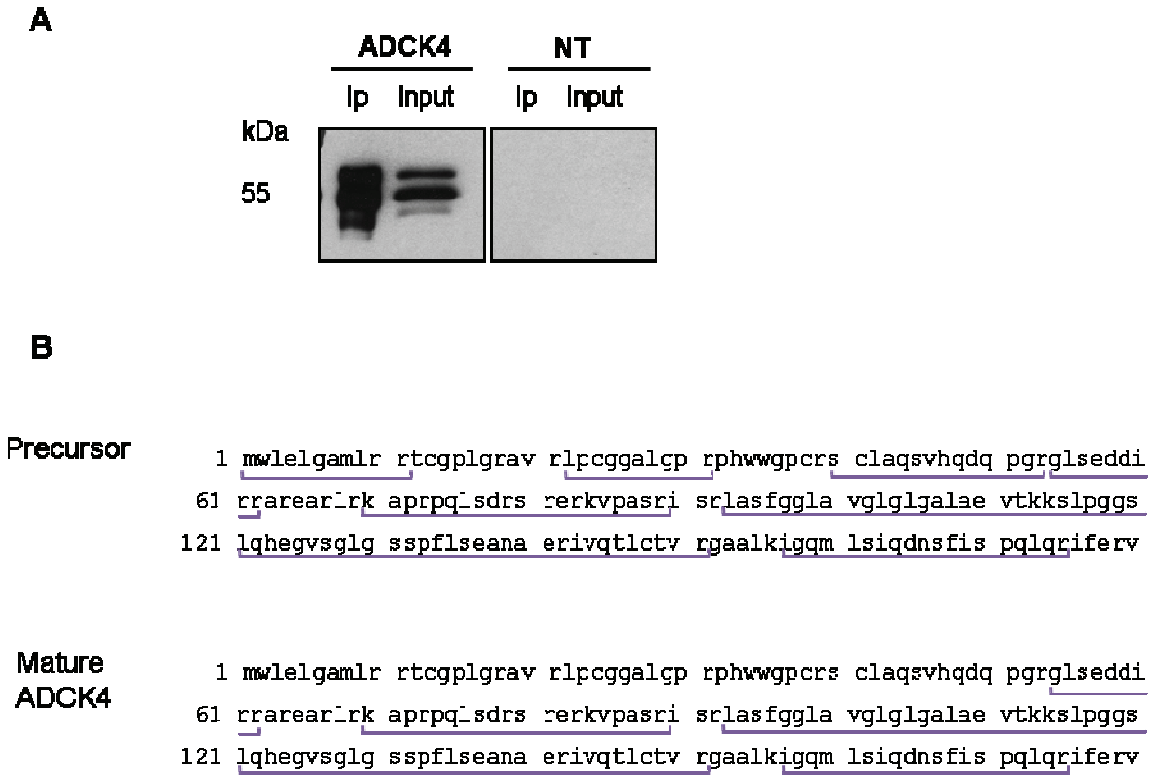


**Figure 24. Maturation of ADCK4. A)** Immunoprecipitation (Ip) of flag-tagged ADCK4. The upper band (around 60 kDa) is the precursor, the middle band (around 55 kDa) is the mature form. **B)** A schematic view of the trypsin-peptides detected by MALDI-TOF analysis (underlined in purple).

# DISCUSSION AND PERSPECTIVES

# DISCUSSION AND PERSPECTIVES

## 1. *Adck3*$^{-/-}$ mice as a model to study ARCA2

### *1.1. ARCA2: the emergence of new interesting features*

ARCA2 is a form of recessive ataxia characterized by a slow progression of the ataxic phenotype and a mild deficit in Coenzyme $Q_{10}$. The genetic causes of ARCA2, identified in 2008, are mutations in the gene *ADCK3* (Lagier-Tourenne et al., 2008) (Mollet et al., 2008). In these two original studies, a large heterogeneity in the phenotype of ARCA2 patients was reported, with many secondary clinical signs. Since then, new patients have been described (Table 6) (Gerards et al., 2010) (Horvath et al., 2012) (Terracciano et al., 2012) and it is now becoming clear that symptoms initially thought to be secondary, are instead quite frequent in ARCA2 patients. This is the case for intellectual disability, epilepsy and exercise intolerance. Thus, it is possible that *ADCK3* mutations result in more pleiotropic phenotypes that associate mainly with one of these secondary symptoms, without necessarily causing ataxia. Therefore it would be interesting to sequence different cohorts of patients, such as patients with intellectual disability, without a genetic diagnosis and determine whether *ADCK3* is mutated.

The definitions of epileptic seizure and epilepsy have been defined by the International League Against Epilepsy (ILAE) and the International Bureau for Epilepsy (IBE). An epileptic seizure is a 'transient occurrence of signs and/or symptoms due to abnormal excessive or synchronous neuronal activity in the brain'. Epilepsy is a 'disorder of the brain characterized by an enduring predisposition to generate epileptic seizures and by the neurobiologic, cognitive, psychological, and social consequences of this condition' (Fisher et al., 2005). Epilepsy is a common feature of ARCA2 patients. Indeed, ARCA2 patients are often reported to show seizures, *epilepsia partialis continua* and myoclonic epilepsy (Mollet et al., 2008) (Horvath et al., 2012) (Terracciano et al., 2012) (Gerards et al., 2010). Interestingly, epilepsy and seizures are often associated to mitochondrial diseases, a group of disorders that affect the mitochondrial respiratory chain, either by mutations in mtDNA or by mutations in nuclear genes essential for the mitochondrial respiratory chain function. While epilepsy has been reported in 14% of patients with mitochondrial diseases (Finsterer and Mahjoub, 2013), seizures occur in 35 to 60% of individuals with biochemically confirmed mitochondrial

diseases (Debray et al., 2007, Khurana et al., 2008). Moreover, apart from *ARCA2*, seizures have been reported in other forms of primary Coenzyme $Q_{10}$ deficiencies due to mutations in *COQ2* (Mollet et al., 2007), *PDSS2* (Lopez et al., 2006), *COQ6* (Heeringa et al., 2011) and *COQ9* (Duncan et al., 2009).

The mechanisms underlying seizures in mitochondrial disorders are not clear. However, it has been suggested that energy failure due to mitochondrial defect can trigger epilepsy, disrupting the neuronal membrane potential (Rahman, 2012). On the other hand, seizures themselves can cause mitochondrial dysfunction, implicating a vicious spiral in the pathogenesis of mitochondrial epilepsy (Figure 25).

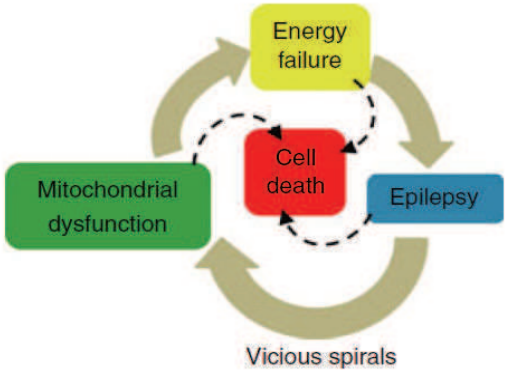


**Figure 25. Pathogenesis of mitochondrial epilepsy.** Adapted from *Rahman, 2012.*

However, not all mitochondrial diseases show epilepsy, suggesting that, apart from energy failure, other pathogenic mechanisms can be associated to mitochondrial defect, such as ROS production and fatty acid metabolism. Moreover, it is likely that the distribution of the mitochondrial defect within the CNS is a determining factor in the association of a certain mutations with epilepsy (Kunz, 2002).

Moreover, a few ARCA2 patients present stroke-like episodes (Mollet et al., 2008) (personal communication from Dr. Mathieu Anheim). These episodes are frequently reported in patients carrying mutations in *POLG* that causes many different conditions including progressive external ophthalmoplegia (PEO), Alpers syndrome and mitochondrial recessive ataxia syndrome (MIRAS) (Table 2) (Horvath et al., 2006). These stroke-like episodes have been extensively studied in mitochondrial myopathy, encephalopathy, lactic acidosis and stroke-like episodes (MELAS) syndrome but their primary cause is not clear yet. One of the hypotheses that were put forward suggested that they are caused by an oxidative phosphorylation defect in neurons, glia, or both (Koga et al., 2010).

### *1.2. Critical analysis of the models generated to understand $CoQ_{10}$ deficiencies*

Considering the models that have been generated so far to study Coenzyme $Q_{10}$ deficiencies, it becomes clear that the information they provide is limited. A large amount of data were obtained from studies on patient fibroblasts (Lopez-Martin et al., 2007) (Quinzii et al., 2008, Rodriguez-Hernandez et al., 2009, Quinzii et al., 2010). However, these data are often heterogeneous and contradictory, probably because fibroblasts are not affected in patients. Moreover, most of the complete knockout mice for genes involved in primary Coenzyme $Q_{10}$ deficiencies are embryonic lethal (Manuscript 1), underlying the severity of the human diseases and the crucial role of Coenzyme Q in development. Therefore, in order to study primary $CoQ_{10}$ deficiencies, it is necessary to generate new models showing less severe phenotypes and no embryonic lethality. Several conditional knockouts for genes involved in Coenzyme $Q_{10}$ deficiencies have been generated to study specific defects associated to these diseases, such as the renal and the neurological phenotype (Manuscript 1) (Peng et al., 2008) (Lu et al., 2012). Moreover, since ARCA2 displays a heterogeneous and mild spectrum of symptoms, it constitutes a good candidate for the generation of a mouse model, hence allowing the study of the pathophysiology of human Coenzyme $Q_{10}$ deficiencies.

### *1.3. The constitutive knockout for Adck3 mimics ARCA2*

In order to study the pathophysiology of ARCA2, we generated a mouse model by constitutive knockout of *Adck3*. Characterization of this model reveals that *Adck3*$^{-/-}$ mice recapitulate well many different features of the human phenotype. Table 7 shows a comparison between the ARCA2 symptoms and the phenotype displayed by *Adck3*$^{-/-}$ mice.

*Adck3*$^{-/-}$ mice develop early ataxia and motor impairment (Manuscript 3). As in humans, the ataxic phenotype was slowly progressive and not severe. Indeed, most ARCA2 patients manage to walk with supports until adult age and only a few are bedridden (Mollet et al., 2008) (Horvath et al., 2012). While a mild to severe cerebellar atrophy is reported in all ARCA2 patients, no gross atrophy of the cerebellum was observed in *Adck3*$^{-/-}$ mice. One possible explanation for this difference is that the life span of mice is not long enough to develop cerebellar atrophy.

| Symptoms | ARCA2 patients | *Adck3*$^{-/-}$ mice |
|---|---|---|
| **Gait ataxia** | yes | yes |
| **Slow progression** | yes | yes |
| **Cerebellar atrophy** | yes | no |
| **Intellectual disability** | yes | no |
| **Epilepsy** | yes | yes |
| **CoQ deficit in muscle** | yes | yes |
| **Elevated plasma cholesterol** | no | yes |

**Table 7. Comparison between the human and the mouse phenotype.** Main symptoms observed in ARCA2 patients and *Adck3*$^{-/-}$ mice.

Moreover, most ARCA2 patients present intellectual disability (Table 6). In order to assess memory and the learning capacity of *Adck3*$^{-/-}$ mice, several behavior tests (object recognition, Morris water maze and Y maze) were performed and a delay in spatial memory was observed using the water maze test. Epilepsy and seizures are frequent symptoms in ARCA2 patients (Table 6) and, interestingly, mutant mice also show increased susceptibility to PTZ-induced epilepsy. The delay in spatial memory and the increased susceptibility to epilepsy could both be due to an alteration in the hippocampus, suggesting that further investigation of hippocampal function is needed.

Furthermore, *Adck3*$^{-/-}$ mice show a mild Coenzyme Q deficit in several tissues. Interestingly, the deficiency is present in skeletal muscle, which also appears to be informative of CoQ deficiency in humans. Moreover, exercise capacity was also reduced in *Adck3*$^{-/-}$ mice. Although many different disorders can cause exercise intolerance, from myopathy to heart failure (Conraads et al., 2013), one possibility is that exercise intolerance is a consequence of the muscle mitochondrial defect in *Adck3*$^{-/-}$ mice.

Interestingly, other *Adck3*$^{-/-}$ tissues, such as kidney and liver, showed a decreased level of Coenzyme Q without presenting evident and gross pathological signs. However, the mild dyslipidemia found in *Adck3*$^{-/-}$ mice (Manuscript 3) is probably caused by alterations in liver function. Because of the elevated cholesterol levels observed in *Adck3*$^{-/-}$ mice, we suggested to investigate the lipid content in blood of ARCA2 patients. A few ARCA2 patients were tested so far and no alteration in plasma cholesterol was found (personal communication Dr Mathieu Anheim, confidential).

Altogether, these data, suggest that the mouse model that we developed is indeed a good model that mimics the human disease. This finding allowed us to use the ARCA2 mouse

model to elucidate the pathophysiology of ARCA2 and of Coenzyme $Q_{10}$ deficiencies in general (see section 2 of the discussion). In parallel, although the characterization of the pathogenic mechanisms needs further investigation, *Adck3*$^{-/-}$ mice can be used in the future to test new therapeutic strategies.

### *1.4. Developing new therapeutic approaches*

Supplementation with $CoQ_{10}$ has been tested in several patients with primary Coenzyme $Q_{10}$ deficiencies. While the treatment was effective in patients with *COQ2* mutations for the neurological and renal symptoms, poor responses have been reported in patients with *PDSS2* and *COQ9* mutations (Hirano et al., 2012). Treatment with oral $CoQ_{10}$ has also been tried on several ARCA2 patients (patient 8, 9, 17, 18, 19 and 20. Table 6), but no clinical benefit has been observed. Moreover, supplementation with idebenone, a short-chain quinone, was shown to worsen the phenotype in patient 8 (Table 6) (Mollet et al., 2008) (Horvath et al., 2012).

Because of its hydrophobicity and large molecular weight, absorption of dietary $CoQ_{10}$ is slow and limited. In rats, administration of radioactive Coenzyme $Q_{10}$ resulted in an efficient uptake into the circulation, with high concentrations found in spleen, liver, and white blood cells, but practically no uptake was observed in kidney, muscle, and brain (Bentinger et al., 2003). Moreover, in liver homogenates, mitochondria had a very low concentration of Coenzyme $Q_{10}$, which was mainly present in lysosomes.

The limited absorption of Coenzyme $Q_{10}$ especially by the brain, suggests that new therapeutic strategies are required to treat patients with Coenzyme $Q_{10}$ deficiency. To improve drug efficacy in the treatment of brain diseases, solid lipid nanoparticles (SLN) as colloidal carriers for drug delivery to the brain have been developed. Due to their lipophilicity and their small particle size, SLN could reach the central nervous system, overcoming the blood−brain barrier. A recent study evaluated the efficacy of SLN loaded with idebenone to cross an *in vitro* system similar to the blood brain barrier (Montenegro et al., 2012). Although promising, similar therapeutic approaches need to be tested *in vivo*. Because of their availability, *Adck3*$^{-/-}$ mice could indeed be used as good model to test drugs to treat Coenzyme Q deficiency. Although no Coenzyme Q deficit was observed in total cerebellar extract of *Adck3*$^{-/-}$ mice, it cannot be excluded that a CoQ deficit is restricted to a specific population of neurons and be responsible for the ataxic phenotype. Interestingly, in case of a

positive outcome, these approaches would also clarify whether the neurological phenotype observed in *Adck3*$^{-/-}$ mice is linked to Coenzyme Q deficiency.

Furthermore, Coenzyme Q supplementation is also used to treat muscle defect in patients with myopathy. A few ARCA2 patients treated with oral Coenzyme $Q_{10}$ reported an improvement of the muscle tone and tremors (personal communication from Dr. Mathieu Anheim, confidential). In *Adck3*$^{-/-}$ mice, a mild deficit in Coenzyme Q as well as a morphological defect of mitochondria were observed in skeletal muscle. However, the respiration rate was not altered (Manuscript 3). Therefore, *Adck3*$^{-/-}$ mice are currently not a good model to test potential treatments of the muscle defect present in ARCA2 patients. However, to achieve this goal, it would be interesting to worsen the muscle phenotype of *Adck3*$^{-/-}$ mice. This could be carried out, for instance, by treating the mice with statins, which are reported to cause myopathy as a side effect, probably through decreasing Coenzyme Q content in muscle (Folkers et al., 1990, Willis et al., 1990).

## 2. *Adck3*$^{-/-}$ mice as a model to study the pathophysiology of ARCA2

### *2.1. The degeneration of Purkinje cells*

The neurological phenotype observed in *Adck3*$^{-/-}$ mice is specific to Purkinje cells. This is likely due to the fact that *Adck3* is highly expressed in PCs (from Allen brain atlas). (Figure 26)

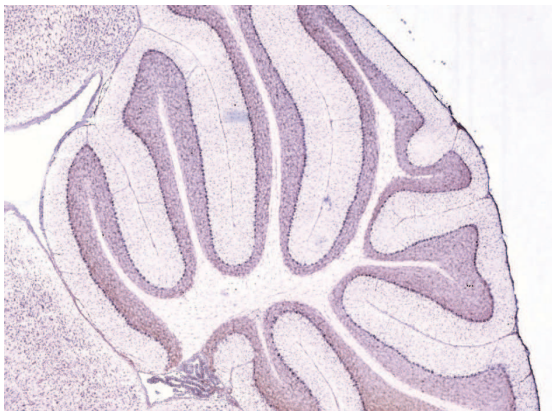

**Figure 26. Expression of murine *Adck3* in PCs.** *From Allen Brain Atlas.*

Although there was not a massive loss of Purkinje cells, some of them appeared dark. The presence of dark neurons has been reported in other neurodegenerative diseases, including Huntington disease (Turmaine et al., 2000). Contracted and intensely stained neurons, observed with H&E staining, represent the most common artifact encountered in the central nervous system tissues. These artifacts can be generated by post-mortem manipulation or trauma in brain tissues (Jortner, 2006). However, when observed by electron microscopy, dark neurons are generally accepted as sign of degeneration.

Interestingly, dark Purkinje cells as well as granule cells were reported in other mouse models that developed ataxia. Tao and colleagues disrupted the microRNA maturation deleting Dicer in postnatal astroglia and they observed a non-cell-autonomous neuronal degeneration in the cerebellum (Tao et al., 2011). The mice develop ataxia probably as a consequence of granule cells that appeared condensed and darkened. Moreover, dark degeneration of Purkinje cells was also observed in mice carrying mutations in genes

associated to human forms of ataxia, such as SCA5, SCA7 and SCA28. In heterozygous *Afg3l2*$^{+/-}$ mice, the gene mutated in SCA28 patients, dark Purkinje cells were observed with aberrant mitochondria. Although Purkinje cell loss was reported, no signs of apoptosis were detected (Maltecca et al., 2009). Dark degeneration of Purkinje cells has also been reported in knockout mice for *β-III Spectrin*, the gene mutated in SCA5 patients, (Perkins et al., 2010). Interestingly, similar to *Adck3*$^{-/-}$ mice, *β-III Spectrin*$^{-/-}$ PCs displayed dilation of the ER and the Golgi apparatus. Moreover, mutant mice expressing polyglutamine-expanded *ataxin-7* in Bergmann glia showed dark degeneration of Purkinje cells due to impaired glutamate transport (Custer et al., 2006).

Overall, the presence of dark degenerating Purkinje cells can be caused by different kinds of defects, from mitochondrial impairment to misregulation of membrane transporters. This would suggest that the dark phenotype is a general sign of neuron impairment, more than a feature of specific cellular defect. Therefore, in *Adck3*$^{-/-}$ mice, the Golgi defect together with the membrane abnormalities should be considered as the most relevant pathological sign.

Interestingly, as previously mentioned, dilatation of the Golgi apparatus has also been reported in the Purkinje neurons of *β-III Spectrin*$^{-/-}$ mice (Stankewich et al., 2010) (Perkins et al., 2010) where a decrease in the glutamate transporter EAAT4 was observed. Five distinct glutamate transporters have been found in the mammalian central nervous system (EAAT1 to 5). They are considered to play an important role in the maintenance of low extracllular concentrations of glutamate and in the clearance of synapses, preventing the neurotoxic effect of glutamate (Takayasu et al., 2009). Interestingly, downregulation of EAAT1 (also known as GLAST) was found in the cereballa of mutant mice expressing polyglutamine-expanded *ataxin-7* in Bergmann glia (Custer et al., 2006). Moreover, a heterozygous mutation in EAAT1 with a dominant negative effect was reported in a patient with episodic ataxia and seizure (Jen et al., 2005). Altogether this evidence strongly suggests that impairment of glutamate homeostasis can lead to Purkinje cell degeneration. However, no change in glutamate transporters was observed by qRT-PCR in the cerebella of *Adck3*$^{-/-}$ mice (data not shown). Therefore, it would be interesting to determine whether levels of glutamate transporters change at the protein level, in order to determine if this can be a pathological mechanism in *Adck3*$^{-/-}$ mice.

In addition to its role in post-translational modification and quality control of newly synthesized polypeptides, the Golgi-ER system is crucial to ensure a functional vesicular trafficking of proteins and lipids in the cell. Because of their high polarized structure, intracellular trafficking is particularly important in neurons, to ensure efficient delivery of

molecules to axons and dendrites (Sann et al., 2009). Therefore, a possible hypothesis is that the defect observed in Golgi and ER morphology in *Adck3*$^{-/-}$ mice could cause a defect in the intracellular trafficking of Purkinje neurons. Interestingly, two genes implicated in secretory pathway and vesicle trafficking were found to be misregulated in the cerebella of *Adck3*$^{-/-}$ mice by RNA deep sequencing: *COPA* (fold change=0.68, $p<10^{-12}$) and Complexin 1 (fold change=1.2, $p<10^{-5}$). Both genes are highly expressed in Purkinje cells (Allen brain atlas). COPA (Coatomer protein complex, subunit alpha) is a subunit of the coatomer complex, which is required for retrograde transport from Golgi to ER (Szul and Sztul, 2011). Interestingly, disruption of the δ-subunit of the coatomer complex leads to Purkinje cell degeneration in mice (Xu et al., 2010). Complexin 1 is a SNARE-associated protein involved in vesicle exocytosis. SNARE proteins are responsible for calcium-dependent vesicle fusion and their activity is regulated by proteins of the complexin family (Melia, 2007). This finding suggests that intracellular vesicle trafficking can play a crucial role in the pathogenic mechanisms underlying the Purkinje cells degeneration observed in *Adck3*$^{-/-}$ mice.

Vesicular transport plays a crucial role also in the intracellular trafficking of lipids. Most of lipids are synthetized in ER and they reach their final localization through different routes, including vesicular transport (van Meer et al., 2008). Based on phylogenetic studies, ADCK3 was suggested to be a lipid kinase (Lagier-Tourenne et al., 2008). Therefore, an interesting hypothesis is that ADCK3 is directly involved in the modulation of lipid metabolism and disruption of its function could lead to a defect in lipid transport.

Alteration of intracellular trafficking could also explain the reduced firing activity of *Adck3*$^{-/-}$ Purkinje neurons. Regular firing of Purkinje cells is mediated by the action of ion channels, including sodium channels that promote rapid recovery from an inactivated to an open channel state (Raman and Bean, 1997). Voltage gated sodium channels ($Na_v$) consist of an α-subunit of approximately 260 kDa, which forms the ion pore, and accessory β-subunits of about 33-36 kDa (Marban et al., 1998). A variety of α-subunits exist and several of them have been associated to defects in the firing activity of Purkinje cells. A defect in the maturation of the voltage-gated sodium channel α-subunits Nav1.6 (*Scn8a*) results in a regular but reduced firing activity in PCs, similar to what we observed in *Adck3*$^{-/-}$ mice (Gehman et al., 2012). Furthermore, a conditional Purkinje cell knockout for *Scn8a* results in a 10-fold decrease in the firing rates of PCs, leading to ataxia and tremors (Levin et al., 2006). Sodium channels are large proteins that need to be correctly folded and transported to the plasma membrane, and an impairment of intracellular trafficking could lead to a mislocalization of $Na_v$. Therefore it would be relevant to verify whether voltage-gated sodium

channel proteins, especially Nav1.6, are correctly processed and whether they reach their final destination in the plasma membrane.

### *2.2. Oxidative stress*

Coenzyme Q is known to be an antioxidant and a widely accepted hypothesis in the field is that an increase in ROS levels plays a role in the pathological mechanisms of Coenzyme Q deficiencies. For instance, fibroblasts from *COQ2* patients with 30-40% of control $CoQ_{10}$ levels showed an increase in ROS production and oxidative damage (Quinzii et al., 2008, Quinzii et al., 2010). Therefore we have checked whether increased oxidative stress could be involved in the pathological mechanisms of *Adck3*$^{-/-}$ mice. Surprisingly, a reduced amount of ROS was found in the skeletal muscle of *Adck3*$^{-/-}$ mice. Since the respiration rate of muscle fibers was comparable between mutant and control mice, a drop in the activity of OXPHOS cannot be an explanation for these data. A possible justification would be that, although there is a general decrease in Coenzyme Q content in the skeletal muscle of *Adck3*$^{-/-}$ mice, the proportion of the oxidized form of Coenzyme Q (ubiquinol) is decreased compared to the reduced form (ubiquinone) in mutant mice. Moreover, the partially oxidized form of Coenzyme Q, ubisemiquinone, could also play a role in the generation of ROS. In fact, complexes I, II and III of the respiratory chain can generate ubisemiquinone. In case of accumulation of ubisemiquinone it can be auto-oxidized and produce superoxide (McLennan and Degli Esposti, 2000). Therefore it would be relevant to measure the different redox states of Coenzyme Q in skeletal muscle to determine whether a change in the ratio ubiquinol/ubiquinone could explain the decrease in ROS production in mutant mice.

The only piece of evidence pointing to an increased oxidative stress in *Adck3*$^{-/-}$ mice was the increased lipid peroxidation observed in skeletal muscle of old mutant mice (Figure 19). This result could also be explained by a possible increase in the total concentration of lipids. Therefore, a quantification of lipid content in skeletal muscle would clarify whether the increased lipid peroxidation is due to increased oxidative stress or to misregulation of lipid metabolism. However, it cannot be excluded that the increase of lipid peroxidation is due to the deficit of Coenzyme Q, which is known to inhibit lipid peroxidation, even without an increase in ROS content.

### *2.3. Epilepsy*

*Adck3*$^{-/-}$ mice show increased susceptibility to PTZ-induced epilepsy. The presence of epilepsy within the spectrum of ARCA2 symptoms is intriguing because the increased neuronal excitability can be due to different causes. First, it can originate from a mitochondrial defect and a decreased intracellular ATP level in the central nervous system. This hypothesis is puzzling because it would raise the possibility of a mitochondrial involvement in the neurological phenotype of *Adck3*$^{-/-}$ mice. In fact, it is surprising that despite the fact that ADCK3 is a mitochondrial protein, no mitochondrial defect was found in the neurological defect of *Adck3*$^{-/-}$ mice. The second possibility is that epilepsy is due to alteration in calcium homeostasis (Delorenzo et al., 2005, Carter et al., 2006), which can be due to defects in different organelles, such as mitochondria or ER.

Interestingly, the activity of sodium channels can, not only modulate the activity of Purkinje neurons, but also of other neurons and be therefore implicated in epilepsy. In fact, complete loss of function of Nav1.1 channel, encoded by the *SCN1A* gene, is associated with severe myoclonic epilepsy in infancy (SMEI), an infantile-onset epilepsy with ataxia and cognitive dysfunction. In a mouse model for SMEI, a reduction in the frequency of action potentials in hippocampal and cortical interneurons neurons was reported (Yu et al., 2006). Moreover, mutations in voltage-gated $K^+$ channels ($K_v$) have been implicated in different forms of seizures. Functional $K_v$ are formed by four α-subunits that assemble into a channel, and four cytoplasmic auxiliary $K_v$ β-subunits. Therefore, sodium and potassium channels are good candidate to explore in order to determine the molecular mechanisms underlying epilepsy in *Adck3*$^{-/-}$ mice.

Interestingly, an upregulation (fold change= 1.7; $p<10^{-12}$) of the gene *Kcnab3* was observed in the cerebella of *Adck3*$^{-/-}$ mice by RNA deep sequencing. *Kcnab3* encodes a β-subunit of the potassium channel, voltage-gated (shaker-related subfamily). Therefore, *Kcnab3* is a good candidate and it would be relevant to check if misregulation of *Kcnab3* is present also in other regions of the brain, such as hippocampus, in order to determine if a dysfunction of $K_v$ can be implicated in epilepsy in our mutant mice.

## 3. *Adck3*$^{-/-}$ mice as a model to study the function of *Adck3* in mammals

### *3.1. Understanding the mild Coenzyme Q deficit in Adck3*$^{-/-}$ *mice*

The function of ADCK3 in mammals is poorly understood. The mitochondrial localization of murine ADCK3 (Figure 27) and Coenzyme Q deficit observed in ARCA2 patients, strongly suggest that ADCK3 is involved in CoQ biosynthesis. However, the phenotype displayed by *Adck3*$^{-/-}$ mice is mild compared to other CoQ deficient mice (see manuscript 1) and although CoQ is required for development (Manuscript 1), constitutive KO mice for *Adck3* are available. On the other hand, the mild phenotype observed in *Adck3*$^{-/-}$ mice correlates with the mild CoQ deficit present in the mice, as well as in ARCA2 patients.

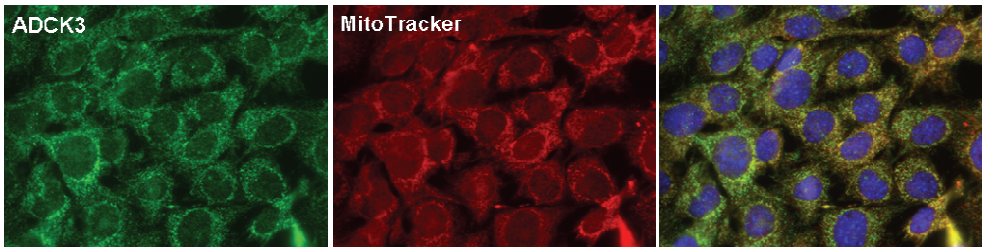


**Figure 27. Mitochondrial localization of murine ADCK3.** ADCK3 colocalizes with Mitotracker in C2C12 cells. Data from Dr. Leila Laredj (antibody produced by the IGBMC's facility).

The mild Coenzyme Q deficit observed in mammals upon depletion of *Adck3* would suggest that either a compensatory effect due to other ADCKs takes place, or ADCK3 is not directly involved in Coenzyme Q biosynthesis. As to the ADCK redundancy issue, the best candidate is ADCK4, which is the closest paralog of ADCK3. In order to investigate whether ADCK4 could take over at least partially the function of ADCK3, the expression of *Adck4* was assessed by qRT-PCR but no upregulation of its expression was observed in *Adck3*$^{-/-}$ tissues (Figure 21). Although this data suggest that ADCK4 does not replace ADCK3 function, it cannot be excluded that ADCK4 might compensate the absence of ADCK3 without a change in its expression.

The fact that all ADCKs have a mitochondrial localization (personal communication from Dr. Leila Laredj) and are ubiquitously expressed may suggest that they have a redundant

function. On the other hand, it is also possible that they are localized in different mitochondrial compartments, showing similar function in different sites. Moreover, ADCKs may also be regulated differently. For instance, ADCK3 has a long N-terminal sequence that is not present in ADCK4 (Figure 20). This sequence may be implicated in a different sub-mitochondrial localization or interaction with different proteins and/or substrates.

Another interesting hypothesis is that, although ubiquitously expressed, some of the ADCKs can play a role in stress conditions. Therefore, it would be interesting to evaluate whether there is a change in the expression of any ADCKs in mice fed a high fat diet or treated with statins.

### *3.2. Is* ADCK3 *involved in Coenzyme Q biosynthesis in mammals?*

Because of its homology to the yeast Coq8, ADCK3 was suggested to be implicated in Coenzyme Q biosynthesis. Our results on Coenzyme Q levels in murine tissues show that no accumulation of CoQ intermediates was found, suggesting that there is not a complete block of Coenzyme Q biosynthesis upon *Adck3* depletion. This would suggest that ADCK3 has a regulatory role in the pathway rather than being directly involved in the enzymatic cascade that modify the benzoquinone ring. In agreement with this, yeast Coq8 was suggested to have a regulatory role in the pathway where it has been proposed to modulate the activity of other Coq proteins through phosphorylation (Tauche et al., 2008) (Xie et al., 2011).

Interestingly, although Coenzyme Q is a key component of the mitochondrial respiratory chain, a mild mitochondrial phenotype was observed in *Adck3*$^{-/-}$ mice. In skeletal muscle, a morphological mitochondrial defect was observed (manuscript 3) with a deficit in Coenzyme Q. However, this did not dramatically affect the function of skeletal muscle. Apart from a decreased performance on treadmill, likely due to exercise intolerance, the mitochondrial function of *Adck3*$^{-/-}$ mice was overall not affected, showing a normal respiration rate. Indeed, a strong deficit in Coenzyme Q is required to affect the activity of the mitochondrial respiratory chain (personal communication from Prof. Pierre Rustin). Moreover, the cerebellar mitochondria of *Adck3*$^{-/-}$ mice appeared mostly normal. The mild mitochondrial deficit observed in *Adck3*$^{-/-}$ mice is surprising, not only because the main function of Coenzyme Q is in mitochondria, but also because ADCK3 is a mitochondrial protein. For this reason, although ADCK3 was found to localize in mitochondria in cell lines, it would be

informative to check the exact localization of ADCK3, also in murine tissues. Unfortunately, this proves impossible for the time being due to the lack of a good antibody against ADCK3. Interestingly, COQ6 and COQ7, two proteins involved in the Coenzyme Q biosynthetic pathway, have been found to localize in the Golgi apparatus in murine podocytes (Heeringa et al., 2011).

An intriguing possibility is that ADCK3 is indeed involved in Coenzyme Q biosynthesis, but it participates to the biosynthesis of a specific pool of Coenzyme Q. As mentioned in the Introduction, it is likely that different pools of Coenzyme Q exist in diverse sites of the cell and/or with different CoQ functions. This would explain the phenotype observed in the cerebella of *Adck3*$^{-/-}$ mice, where the mitochondria appeared unaffected, while a Golgi apparatus defect was evident in Purkinje neurons (Manuscript 3). As different pool of CoQ may exist in the cell, it is likely that the Golgi apparatus hosts one of them, since it contains a high amount of Coenzyme Q (Table 4). Therefore, a potential Coenzyme Q deficit could cause the Golgi defect observed in Purkinje cells. In fact, although Coenzyme Q levels were not affected in the cerebellum of *Adck3*$^{-/-}$ mice, it cannot be excluded that, as *Adck3* is highly expressed in PCs, there is a specific deficit in Coenzyme Q in PCs. This deficiency would not be detected because PCs represent a small proportion of neurons in the cerebellum.

Furthermore, a general impairment of the membrane was found in the Purkinje cells of *Adck3*$^{-/-}$ mice. The plasma membrane of affected PCs was often wavy and sometimes a swelling of the endoplasmic reticulum was also evident. Similarly to the Golgi defect, the membrane abnormality could also be due to a specific deficit in Coenzyme Q at this site in the cell. Moreover, CoQ is known to influence the fluidity of membranes (Figure 5). However, it cannot be excluded that the membrane defect could be a secondary consequence of the Purkinje cell degeneration.

### *3.3. Is* ADCK3 *involved in other cellular functions?*

The absence of a strong mitochondrial phenotype and the involvement of the Golgi apparatus in the cerebellar pathology raise the question of whether *Adck3* is involved in other cellular processes and whether additional functions can be found in different tissues. ADCK3 is an atypical kinase, close to groups of kinases that have lipids as substrates, such as choline kinases and phosphoinositide 3-kinases (Lagier-Tourenne et al., 2008). Therefore, it is likely that ADCK3 does not act on protein but on lipid substrates. For this reason, it would

be interesting to better elucidate the potential involvement of ADCK3 in lipid metabolism. Lipids are a wide class of molecules; a lipidomic study can therefore be informative to evaluate which lipid species are misregulated. To this effect, a lipidomic study performed on different *Adck3*$^{-/-}$ tissues is currently ongoing. Moreover, a better understanding of this topic would be given by a characterization of the *in vitro* function of ADCK3, and investigating whether it is able to bind lipids and if it acts as a kinase.

Interestingly, *Adck3*$^{-/-}$ mice display a mild dyslipidemia with altered levels of cholesterol in blood. Moreover, the transcriptome profile of skeletal muscle revealed that interesting genes linked to lipid function are misregulated (Manuscript 3). The fact that cholesterol and Coenzyme Q biosynthesis are linked via the mevalonate pathway, suggests that cholesterol alterations can be pathological in *Adck3*$^{-/-}$ mice. However, so far it is not clear whether a misregulation of cholesterol can be involved in the pathological mechanisms of the neurological phenotype. On the other hand, measurement of plasma cholesterol in three ARCA2 patients showed no alteration (personal communication from Dr. Mathieu Anheim, confidential). Therefore, the mild dyslipidemia observed in *Adck3*$^{-/-}$ mice can be a consequence of an altered lipid metabolism in liver. This could be due to either the direct involvement of ADCK3 in lipid metabolism or a secondary consequence of the reduced Coenzyme Q biosynthesis as well as a misregulation of cholesterol metabolism.

The possibility that ADCK3 is a lipid kinase is interesting also with regards to the function of the other ADCKs. In fact, it is intriguing that all ADCKs have a mitochondrial localization (personal communication from Dr. Leila Laredj) and are ubiquitously expressed. Therefore, in order to explain this redundancy, it would be interesting to verify whether the other ADCKs would have similar functions but would act on different lipid species.

## 4. Final and long term perspectives

I have discussed the perspectives of the different parts of my PhD project in earlier paragraphs. However, I would like to conclude this chapter with a number of long term perspectives that would allow answering new emerging questions regarding the characterization of *Adck3*$^{-/-}$ mice and the pathophysiology of ARCA2.

### *4.1. Study of the degeneration of Purkinje cells*

The specific degeneration of Purkinje cells that was observed in *Adck3*$^{-/-}$ mice (Manuscript 3) does not lead to a massive loss of these neurons. This raised a number of interesting questions. First, is this degeneration cell-autonomous? In order to answer this question, conditional knockouts for *Adck3* might be generated with a deletion of *Adck3* in specific cerebellar cells, such as Bergmann glia or granule cells. This approach would allow us to understand whether other cerebellar neurons or glial cells are responsible for the dysfunction observed in Purkinje cells.

Moreover, since Purkinje cells represent a small population of cerebellar neurons, it would be useful to isolate them in order to investigate the molecular pathways that are specifically implicated in their degeneration. To achieve this aim, a laser capture microdissection experiment can be set up in order to collect Purkinje cells from cerebellar slices. Nevertheless, this technique only allows the isolation of the cell bodies of the neurons and limits the study of dendrites and the axons. The microdissected Purkinje cells can be used to extract total RNA and perform a transcriptome analysis in order to gain insight into the molecular pathways that are specifically misregulated in these neurons.

### *4.2. Generation of cell lines to study the pathophysiology of ARCA2*

The characterization of *Adck3*$^{-/-}$ mice revealed that interesting cellular pathways may be involved in the pathological mechanisms underlying the neuronal phenotype. One of this processes is intracellular trafficking that was found by RNA deep sequencing to be misregulated in *Adck3*$^{-/-}$ cerebella. Moreover, since neurons are highly polarized cells,

alteration in intracellular trafficking can cause defects in the axonal/dendritic transport. Moreover, although no mitochondrial defect was observed in the Purkinje neurons of *Adck3*$^{-/-}$ mice, it would be interesting also to study mitochondrial dynamics. This would help to evaluate whether a mitochondrial dysfunction is present in dendrites and axons. In order to study these cellular processes, the generation of primary neuronal cultures would be useful. Cerebellar primary cultures can be relevant to study this processes in Purkinje neurons, although these cells can be difficult to culture *in vitro* because they are particularly sensitive to culture conditions. Moreover, it would be relevant to investigate these pathways in other types of neurons. For instance, cultures of hippocampal neurons would allow to study whether these neurons are affected, which may explain the epileptic phenotype of *Adck3*$^{-/-}$ mice.

### *4.3. In vivo studies of the ADCK family redundancy*

ARCA2 is the most frequent form of primary Coenzyme $Q_{10}$ deficiencies, probably because of the mild phenotype. One possible explanation of the mild phenotype is the redundant effect of the other ADCKs. In order to investigate this aspect, double knockouts for two *Adck* genes could be generated. A worsening of the neurological or muscle phenotype would suggest that indeed a compensatory effect is occurring in *Adck3*$^{-/-}$ mice. Moreover, if other organ defects are present, it would suggest that other ADCKs have an important role in other tissues. Since Coenzyme $Q_{10}$ deficiencies are often associated with renal dysfunction, it would be interesting to evaluate whether one of the ADCKs can be implicated in kidney function.

Furthermore, in order to investigate redundancy in the family of ADCKs, a combined approach of knockout and knockdown can also be undertaken. For instance, it would be possible to knockdown one or more *Adck* genes in *Adck3*$^{-/-}$ mice. This can be achieved using viral vectors expressing shRNA against *Adck* genes. This strategy may be useful to worsen some mild phenotype observed in *Adck3*$^{-/-}$ mice, such as the muscle and the metabolic phenotypes. Therefore, using this approach it would be possible to have a better model to study the involvement of muscle dysfunction in ARCA2 and Coenzyme $Q_{10}$ deficiencies.

# ANNEX I – Materials and methods

## ANNEX – Materials and methods

This section is supplemental to the section 'Material and methods' of manuscript 3. The procedures that were not included in manuscript 3 will be reported here.

**Cholesterol measurement (enzymatic assay).** Total lipid extracts from cerebella were obtained by classical Folch method (chloroform/methanol). Total cholesterol, free cholesterol and cholesterol ester were quantified by enzymatic reaction (confidential protocol ICS). Briefly, cholesteryl esters are hydrolyzed to cholesterol by cholesterol esterase. Cholesterol is then oxidized by cholesterol oxidase to yield $H_2O_2$, which reacts with HPPA (4-hydroxy phenylacetic acid) to produce a fluorescent compound ($\lambda_{ex}$=305 nm and $\lambda_{em}$=405 nm). The assay detects total cholesterol (cholesterol and cholesterol esters) in the presence of cholesterol esterase, or free cholesterol in the absence of cholesterol esterase.

**Filipin staining.** Cerebellar cryosections were blocked and permeabilized in 5% normal goat serum (NGS)/1% BSA/ 0.02% saponin/PBS and incubated in anti-Calbindin (mouse, Sigma) antibody overnight at 4°C. The next day, sections were washed 3 x 10 min in 0.01% saponin/PBS and incubated in anti-mouse IgG secondary antibody (Alexa Fluor 594 from Invitrogen) for 1 hr. After washing, sections were incubated in a quenching solution (1.5mg/ml glycine in PBS) and then probed with 0.5 mg/ml filipin (Sigma). Filipin fluorescence was acquired from whole cerebellar sections using a slide scanner. The intensity of fluorescence was quantified using the Fiji software in an area of 40*70 µm. Four different areas were quantified in at least 3 different parasagittal sections (3 mice per genotype).

**Synapses quantification.** PFA fixed cerebella were cut using the vibratome to prepare parasagittal sections of 100 micrometers. The sections were blocked and permeabilized overnight in Triton 0.2%/NGS 10%/BSA1%/PBS. They were then incubated with primary antibody (anti-Calbindin, Sigma; anti-vGlut2, Merck-Millipore; anti vGlut1, SY), washed, incubated with IgG secondary antibody (Alexa Fluor 594 or Alexa Fluor 488, from Invitrogen) and Hoechst to stain nuclei. After mounting, the sections were visualized using a confocal microscope.

**ROS detection in muscle sections.** Skeletal muscle cryosections were let thaw for 30 min at 37° in PBS. After removing PBS, the sections were incubated for 30 min at 37° with Dihydroethidium or Mitotracker Orange CM-$H_2$TMRos at a final concentration of 2.5 nM and 300nM, respectively. After two washes with PBS, the sections were mounted and visualized

under a DMRXA2 epifluorescent microscope (Leica). Dihydroethidium emission wavelength is 610 nm. Mitotracker Orange emission wavelength is 580 nm.

Images were analyzed using the Fiji software. For Mitotracker Orange staining, fluorescence was quantified in 16 pictures per genotype. 3 WT and 3 *Adck3*$^{-/-}$ mice were used. For dihydroethidium staining at least 40 pictures per genotype were taken. 4 WT and 4 *Adck3*$^{-/-}$ mice were used.

**TBARS.** Samples (cerebellum or quadriceps) were homogenized and directly mixed with a TCA/TBA/HCl solution (ratio 1:2). The reactions were boiled for 15 minutes. After cooling down, they were centrifuged 10 min at 1000 x g and the absorbance at 535 nm was determined. The concentration of MDA was calculated using an extinction coefficient of 1.56 x $10^5$ $M^{-1}$ $cm^{-1}$ and normalized to the mg of tissue. The TCA/TBA/HCL solution contains: TCA (trichloroacetic acid) 15%, TBA (thiobarbituric acid) 0.375% and HCl 0.25 N. 8 mice per genotype were used.

**Blood collection, sampling and analyses.** Following an overnight fast, blood was collected at 8 a.m. by retro-orbital puncture after a short anesthesia with isoflurane. 300 microliters of blood were collected into a heparinized tube for biochemical analysis. Several biochemical parameters were measured, including glucose, triglycerides, total cholesterol, HDL cholesterol, LDL cholesterol, and glycerol. These parameters were determined using an Olympus analyzer with kits and controls supplied by Olympus or other suppliers (see EMPReSS website).

**OGGT (Oral glucose tolerance test)**. OGGT was performed on mice that fasted overnight. After measurement of the basal glucose level using a drop of blood collected from the tail (time 0), mice were injected with a solution of 20% glucose in sterile saline (0.9% NaCl) at a dose of 1 g glucose/kg body weight. Blood was collected for glucose determination from the tail 10, 20, 30, 45, 60, 90, 120, 150, 180 min after injection of the glucose solution. The incremental area of the glucose curve was then calculated as a measure of insulin sensitivity (see EMPReSS standard operating procedures).

**Cell culture and transfections.** COS-1 cells were grown at 37°C, 5% $CO_2$ in Dulbecco's modified Eagle's medium with 1 g/l glucose supplemented with 5% fetal calf serum (FCS). COS-1 cells were transiently transfected with the different *Adck4* constructs using Fugene Reagent 6 (Roche Diagnostic) as recommended by the manufacturer. Cells were harvested 24 hr after transfection.

**Total protein extraction and subcellular fractionation.** Cells were washed twice with PBS and then scraped in Tris–HCl 100 mM, pH 7.5, 10% glycerol, and complete protease inhibitor cocktail (Roche) (Buffer A). Total extracts were obtained by re-suspending cells in the same buffer supplemented with 0.2% Triton X-100 and incubating them on ice for 30 min. Suspensions were centrifuged at 10 000 *g* for 10 min at 4°C and the protein concentration of supernatants was determined using the Bradford reagent. For subcellular fractionation, cells were washed twice with PBS and then scraped in Buffer A. The cell pellet was washed once with the same buffer before adding 0.014% digitonin for 10 min at 4°C. The suspension was centrifuged at 10 000 *g* for 10 min at 4°C. The supernatant was further centrifuged at 13 000*g* for 30 min at 4°C to get the soluble cytosolic fraction. The resulting pellet, which corresponds to the enriched mitochondrial fraction, was re-suspended in buffer A and centrifuged at 500*g* for 5 min at 4°C to eliminate membranes and nuclear fractions. The mitochondrial fraction was obtained by centrifugation at 10 000*g* for 10 min at 4°C and washed twice with buffer A. The mitochondrial pellet was re-suspended in buffer A containing 0.2% Triton X-100 and incubated for 30 min at 4°C to get, after another round of centrifugation, mitochondrial extracts. Western blot was performed according to the classical protocol separating the proteins in SDS Tris-Glycin PAGE with 8% acrylamide. Antibodies were diluted as follows: anti-myc 1/1000; anti-GAPDH 1/20000; anti-Aconitase 1/1000; anti-FLAG 1/3000. HRP-coupled secondary antibodies were diluted at 1/5000.

**Immunopurification and staining of precursor and mature ADCK4**. Immunoprecipitation was performed using beads coupled with an anti-FLAG antibody (ANTI-Flag M2, SIGMA). Total cell extracts were prepared from Hela cells transiently transfected with ADCK4_FLAG. Immunoprecipitation was carried out in Tris–HCl 100 mm, pH 7.5, containing protease inhibitors (Roche), using 3 mg of total proteins overnight at 4°C. Beads were washed four times with PBS. Elution was performed with glycine 0.1 M, pH 2.5, to elute immunoprecipitated ADCK4. Several immunoprecipitations were pooled together and concentrated in a small volume using the Vivaspin system (Vivascience). Loading buffer was added and samples were boiled for 10 min prior to analysis on an 8% SDS–Tris–Glycine–PAGE. Immunoprecipitated ADCK4 was detected by classical Coomassie staining. Slices from the blue stained gel were excised and subjected to a MALDI-TOF spectrometry analysis. In gel enzymatic digestion of excised bands was performed using Porcine Trypsin (V511A, Promega), as previously described (Schmucker et al., 2008). After digestion, the peptide extracts were used for MALDI analyses. MALDI measurements: peptide extracts were processed as previously described (Schmucker et al., 2008).

**Quantitative real-time PCR.** Total RNA was extracted from frozen tissues with the Precellys24 homogeniser (Bertin Technologies) and using TRI Reagent (MRC) according to the manufacturer's protocol. cDNA was generated by reverse transcription using the Transcriptor First strand cDNA synthesis kit (Roche biosciences). Quantitative RT-PCR was performed using the SYBR Green I Master (Roche biosciences) and light Cycler 480 (Roche biosciences) with the primers described below. *Gapdh* or *Hprt* were used as internal standards for the quantification.

*Sod1*: ACC ATC CAC TTC GAG CAG AA and AGT CAC ATT GCC CAG GTC TC

*Sod2:* CAC ACA TTA ACG CGC AGA TC and GGC TCA GGT TTG TCC AGA AA

*Catalase*: TTGGCCTCACAAGGACTACC and GCGGTAGGGACAGTTCACAG

*Hmgcr:* TGATTGGAGTTGGCACCAT and TGGCCAACACTGACATGC

*Fdft1:* ATCAGACCAGTCGCAGCTTT and CGGAGAACCAGGTAGAACACA

*Gapdh*: TTGTGATGGGTGTGAACCAC and TTCAGCTCTGGGATGACCTT

*Hprt*: GTAATGATCAGTCAACGGGGGAC and CCAGCAAGCTTGCAACCTTAACCA

# ANNEX II– Résumé en français

## ANNEX II – Résumé en français

**Caractérisation physiopathologique et moléculaire d'un modèle murin de ARCA2, une ataxie cérébelleuse récessive associée à un déficit en Coenzyme $Q_{10}$.**

### *Introduction*

Les ataxies cérébelleuses constituent un groupe hétérogène de pathologies neurologiques caractérisées par une perte de coordination et un déséquilibre. Le cervelet est habituellement principalement affecté, soit par une dégénérescence, soit par un développement anormal, bien que des lésions extra-cérébelleuses puissent être également présentes, en particulier dans le cerveau et la moelle épinière. Les ataxies cérébelleuses ont un large éventail de causes potentielles et de nombreuses ataxies cérébelleuses sont héréditaires (Manto et Marmolino, 2009).

Les ataxies génétiques sont habituellement progressives, et en fonction de leur mode de transmission, elles peuvent être classées comme autosomiques dominantes, autosomiques récessives ou liées à l'X. En outre, les études épidémiologiques révèlent que les ataxies autosomiques récessives sont les plus fréquentes (5 sur 100.000) (Sailer et Houlden, 2012). Les ataxies cérébelleuses peuvent aussi être classées en fonction des mécanismes moléculaires impliqués.

Un sous-ensemble des ataxies récessives résulte d'un défaut de protéines impliquées dans la fonction mitochondriale, la plus courante étant l'ataxie de Friedreich. Bien que n'étant pas une caractéristique commune à toutes les ataxies récessives, certaines formes d'ataxie récessives sont associées à un déficit en coenzyme $Q_{10}$ (Auré et al., 2004, Boitier et al., 1998). Ce déficit peut être primaire et induire la pathologie ou être secondaire résultant des conséquences d'une pathologie neurodégénérative.

Récemment, une nouvelle forme d'ataxie cérébelleuse pure, ARCA2 (autosomal recessive cerebellar ataxia type 2), a été identifiée (Lagier-Tourenne et al., 2008; Mollet et al., 2008). Les patients atteints d'ARCA2 présentent une forme précoce d'ataxie cérébelleuse ainsi qu'une atrophie cérébelleuse sévère. Par ailleurs, une épilepsie et un retard mental léger sont des caractéristiques communes, souvent présents chez les patients ARCA2. Au niveau biochimique, les patients ARCA2 ont un déficit en coenzyme $Q_{10}$ (Ubiquinone or CoQ), confirmé par une diminution de l'activité combinée des complexes de la chaîne respiratoire

CI + CII et CII + CIII (valeurs indicatives du pool de $CoQ_{10}$ endogène) et par un contenu d'ubiquinone diminué dans le muscle.

Cette nouvelle forme d'ataxie est due à des mutations perte-de-fonction (Figure 1) dans le gène codant pour la protéine ADCK3, une kinase mitochondriale homologue de COQ8 chez la levure et UbiB chez la bactérie. Ces deux protéines sont nécessaires à la biosynthèse du CoQ.

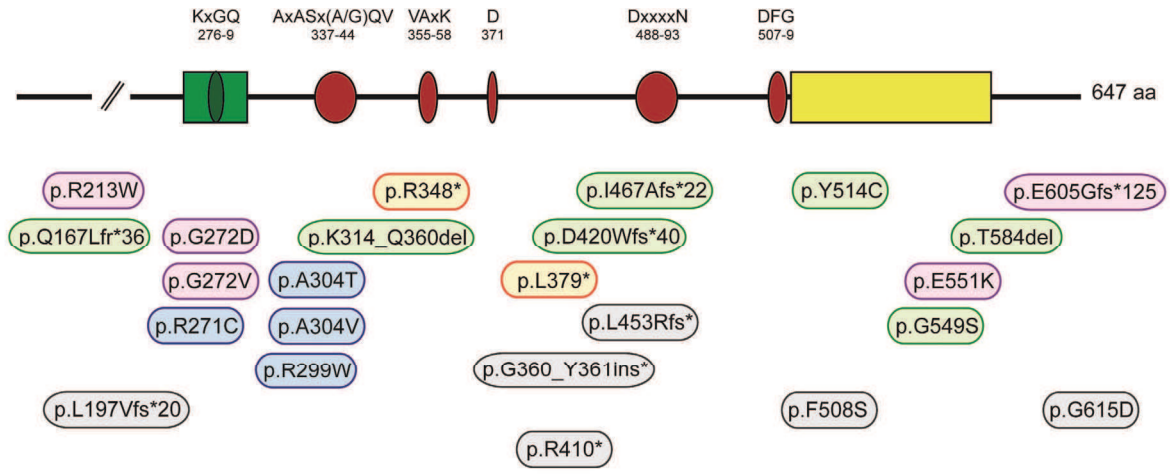


**Figure 1. Mutations d'ADCK3 trouvées chez les patients ARCA2.** En haut, vue schématique de la protéine humaine ADCK3 avec: un domaine conservé parmi tous les membres de la famille ADCK et contenant le motif KxGQ (vert), cinq motifs de kinases (rouge) et un domaine spécifique à chaque sous-groupe ADCK (jaune). En bas, mutations retrouvées chez des patients ARCA2. Les différentes couleurs des mutations se réfèrent aux différents articles qui les ont rapportés pour la première fois (en vert: Lagier-Tourenne et al, 2008; violet: Mollet et al, 2008; orange: Gerards et al, 2010; bleu: Horvath et al, 2012; gris: communication personnelle du Prof. Koenig). Adapté de Lagier-Tourenne et al., 2008.

ADCK3 appartient à la famille des kinases ADCK atypiques, qui comprend cinq membres chez l'homme et la souris. ADCK3 et ADCK4 présentent une forte homologie (55% d'identité) et semblent résulter d'une duplication génique chez les vertébrés. La divergence de ce sous-groupe avec les autres membres de la famille (ADCK1, ADCK2 et ADCK5) est beaucoup plus ancienne (Lagier-Tourenne et al., 2008). La fonction exacte d'ADCK3 ainsi que celle d'ADCK4 demeurent jusqu'ici inconnues, bien qu'un rôle régulateur de l'homologue COQ8

dans la biosynthèse du Coenzyme Q ait été proposé chez la levure. En particulier, il a été proposé que Coq3p, Coq5p et Coq7p soient des substrats potentiels de Coq8p (Tauche et al., 2008; Xie et al., 2011).

Le coenzyme Q est une molécule lipophile composée d'une benzoquinone substituée et une chaîne polyprényle contenant six unités chez S. cerevisiae ($Q_6$), neuf chez la souris ($Q_9$) et dix chez les humains ($Q_{10}$). Le coenzyme Q joue un rôle essentiel dans la phosphorylation oxydative (OXPHOS) en transportant des électrons du complexe I et II au complexe III.

La voie de biosynthèse du CoQ a surtout été étudiée dans la levure où, jusqu'à présent, onze gènes (COQ1-9, ferrédoxine et ferrédoxine réductase) ont été caractérisés comme essentiels pour la biosynthèse du CoQ (Figure 2). En bref, la boucle quinone (un noyau aromatique) du CoQ est dérivée de la tyrosine ou de la phénylalanine, tandis que la voie du mévalonate génère la chaîne polyprénylique. Après la formation d'une liaison covalente entre la benzoquinone et la chaine polyprénylique, le 3-polyprényl-4-hydroxybenzoate de méthyle résultant subit plusieurs modifications telles que l'hydroxylation, la méthylation et la décarboxylation pour générer l'ubiquinone. Des données génétiques et biochimiques ont montré que la biosynthèse du CoQ nécessite la formation d'un complexe multiprotéique chez la levure. Ce dernier est associé à la membrane mitochondriale interne du côté de la matrice (Tran et Clarke, 2007). Récemment, la découverte d'un nouveau précurseur du CoQ, l'acide para-aminobenzoïque (pABA), a été rapportée (Pierrel et al., 2010).

Plusieurs formes de déficit en coenzyme $Q_{10}$ existent chez l'homme. Ces maladies rares et sévères, à l'exception de ARCA2, sont toutes caractérisées par une encéphalomyopathie infantile, une insuffisance rénale, ou les deux, et ont été récemment liées à des mutations dans les gènes codant des protéines spécifiques de la biosynthèse du $CoQ_{10}$ (PDSS1, PDSS2, COQ2 et COQ9) (Quinzii et al., 2005; Lopez et al., 2006; Mollet et al., 2007; Duncan et al., 2009). Le phénotype modéré des patients ARCA2 par rapport à d'autres déficits en $CoQ_{10}$ nous permet ainsi de proposer un rôle régulateur plutôt qu'une fonction enzymatique d'ADCK3 dans la biosynthèse du coenzyme $Q_{10}$. Par ailleurs, la forte similitude entre ADCK3 et ADCK4 donne lieu à la possibilité d'un effet compensatoire d'ADCK4 chez les patients ARCA2.

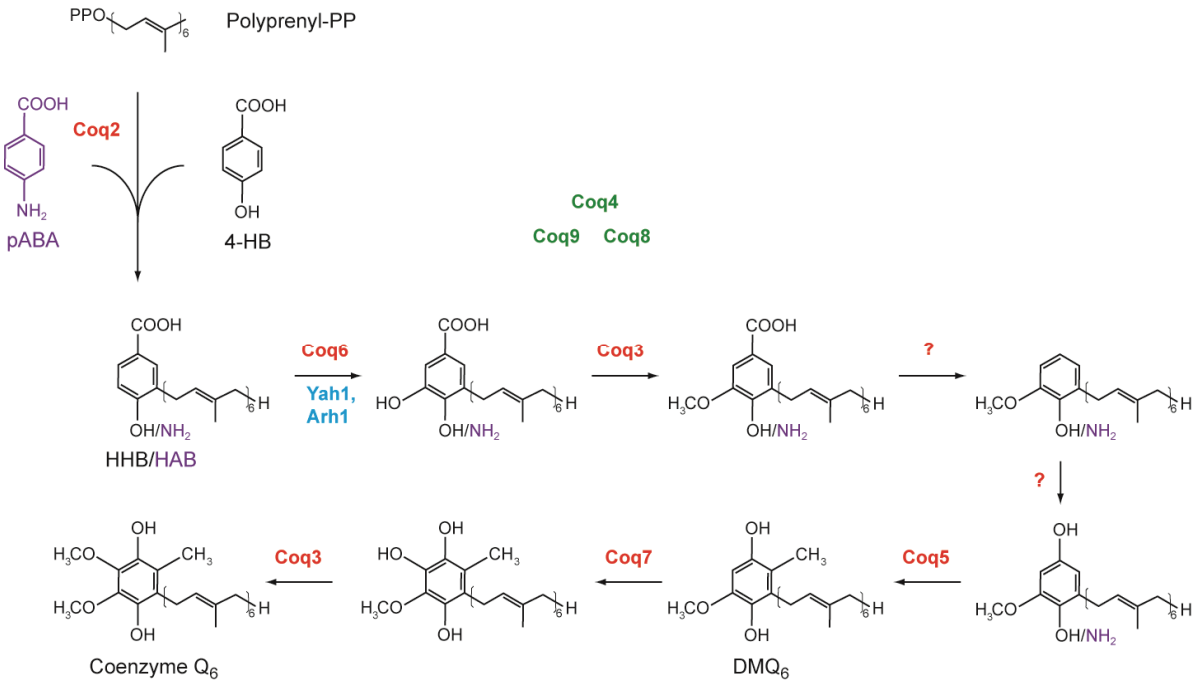


**Figure 2. La biosynthèse du Coenzyme Q chez *Saccharomyces cerevisiae*.** Les enzymes nécessaires à la modification du cycle de benzoquinone sont indiquées en rouge. Les points d'interrogation (?) indiquent que l'enzyme impliquée dans la réaction n'a pas encore été identifiée. Les protéines Coq impliquées dans la régulation de la voie et ou avec une fonction non définie sont indiquées en vert. Abréviations: PABA, acide para-aminobenzoïque; HHB, acide 3-hexaprenyl-4-hydroxybenzoïque; HAB, acide 3-hexaprenyl-4-aminobenzoïque; DMQ, déméthoxyubiquinone.

Le but de mon projet de thèse était d'élucider la physiopathologie d'ARCA2. Pour atteindre cet objectif, un modèle de souris pour ARCA2, une souris knock-out (KO) constitutive d'*Adck3* (souris *Adck3*$^{-/-}$ ou *Adck3* KO), a été générée dans le laboratoire. Par conséquent, la plupart de ma thèse a visé à caractériser les souris *Adck3*$^{-/-}$ et à déterminer si elles représentent un bon modèle pour étudier ARCA2. En parallèle, le deuxième objectif de ma thèse était d'étudier la fonction de ADCK4, le paralogue proche de ADCK3. Cependant, comme la caractérisation des souris *Adck3*$^{-/-}$ a nécessité un effort massif, j'ai obtenu des données préliminaires sur la localisation et le taux d'expression de ADCK4, mais d'autres investigations seront nécessaires pour atteindre pleinement cet objectif.

***Résultats***

*Caractérisation d'un modèle murin pour ARCA2*

Le modèle murin KO pour *Adck3* généré dans le laboratoire a été produit par recombinaison homologue. En particulier, l'allèle KO est une délétion entre l'exon 9 et 14 du gène *Adck3*, aboutissant à une protéine tronquée dépourvue d'une grande partie du domaine kinase et du domaine spécifique ADCK. Le KO constitutif pour *Adck3* ne présente pas de létalité embryonnaire, puisqu'un ratio mendélien est observé à la naissance.

J'ai effectué une analyse du comportement pour évaluer l'activité locomotrice des souris KO. En particulier, j'ai effectué plusieurs essais tel que le rotarod, le string test, les tests de barre et footprint à des âges différents. Le test rotarod montre une altération de l'activité locomotrice chez la souris KO à partir de 10 semaines (Figure 3). Par ailleurs, le test de barre indique que cette perte de coordination est légèrement progressive et l'analyse du footprint montre clairement un phénotype ataxique de souris KO *Adck3* (Figure 3).

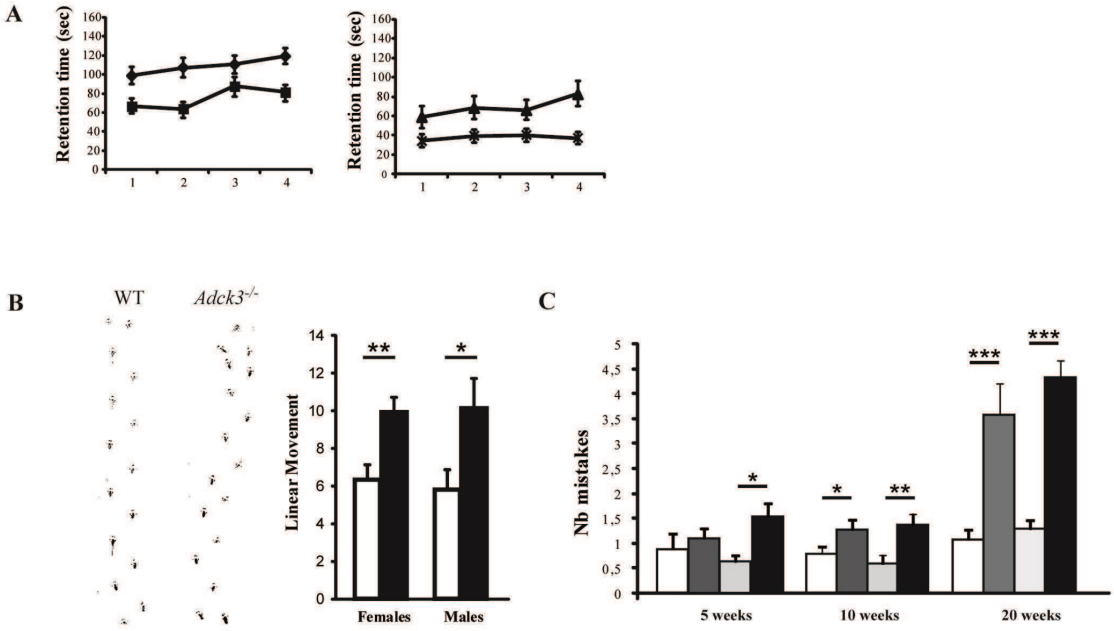


**Figure 3. Déficience motrice chez la souris *Adck3*$^{-/-}$. A.** Temps de rétention sur le rotarod des souris femelles (à gauche) et des mâles (à droite), âgés de 10 semaines. Courbes : losanges et triangles souris WT, rectangles et croix *Adck3*$^{-/-}$. p<0,05 pour les deux sexes. **B.** Empreintes représentatives de souris WT et *Adck3*$^{-/-}$ âgées de 10

semaines. Droite, le coefficient de mouvement linéaire significativement augmentée chez les souris mutantes. **C.** Nombre d'erreurs effectuées par souris WT et *Adck3*$^{-/-}$ dans le test de marche sur la barre. En blanc, les femelles WT, en gris clair les mâles WT, en gris foncé les femelles KO, en noir les mâles KO. n=8-12.* p<0.05, ** p<0.01, *** p<0.01.

ARCA2 est associée à un déficit en coenzyme Q. Par conséquent, nous avons vérifié les niveaux d'ubiquinone dans plusieurs tissus des souris *Adck3* KO par HPLC. Aucune différence dans le taux de coenzyme Q n'a été décelée à un stade précoce (5 semaines). Cependant, le coenzyme $Q_9$, la forme la plus abondante de l'ubiquinone chez la souris, a été retrouvé significativement réduit dans les reins, le foie et le muscle squelettique chez les souris de 7 mois d'âge. Fait intéressant, aucune accumulation du précurseur du CoQ n'a été observée, ce qui suggère que la délétion d'*Adck3* ne conduit pas à un blocage enzymatique de la biosynthèse du CoQ chez les mammifères.

Les données obtenues jusqu'à présent démontrent que les souris *Adck3* KO récapitulent des caractéristiques importantes des patients ARCA2, avec le développement d'une ataxie progressive et d'une carence en coenzyme Q.

En parallèle du comportement neurologique, la fonction musculaire a été caractérisée puisqu'un niveau réduit de $CoQ_{10}$ dans le muscle a été rapporté chez plusieurs patients ARCA2, ainsi qu'une intolérance à l'exercice, ce qui suggère une altération de la fonction mitochondriale dans le muscle. En outre, dans certains patients ARCA2, les études histologiques du muscle squelettique ont révélé une accumulation mitochondriale et des gouttelettes lipidiques dans 10-20% des fibres (Mollet et al, 2008). Pour cette caractérisation, des tests de force musculaire (par le grip test) ainsi que des mesures d'endurance (avec un tapis roulant) ont été effectué. Le test du grip n'a montré aucune faiblesse des muscles squelettiques chez les souris jusqu'à l'âge de 30 semaines. Par conséquent, afin d'évaluer les conséquences cliniques de l'anomalie mitochondriale observée dans le muscle squelettique de souris *Adck3* KO, nous avons effectué des tests sur tapis roulant avec des souris âgées de 40 semaines. Lorsque nous avons évalué la vitesse maximale des souris, nous avons trouvé que $V_{max}$ était significativement diminuée chez les KO par rapport aux WT. Lorsque nous avons testé l'endurance des souris, en les faisant courir à 80% de leur vitesse maximale, nous avons observé une tendance vers une diminution de la durée de la course. Ces données suggèrent qu'en effet, les souris KO montrent une performance musculaire défectueuse avec une tendance à l'intolérance à l'exercice.

Nous avons ensuite examiné les anomalies morphologiques dans les différents tissus murins par coloration classique d'hématoxyline/éosine (H&E). Étonnamment, aucun signe d'atrophie cérébelleuse sévère n'a été trouvé. Par contre, une détérioration morphologique des cellules de Purkinje (PC) dans le cervelet était évidente. En particulier, certaines PC semblaient foncées et contractées (Figure 4A). Une analyse par microscopie électronique a confirmé ces résultats, montrant d'autres anomalies dans les PC, notamment un gonflement et fractionnement de l'appareil de Golgi (Figure 4B).

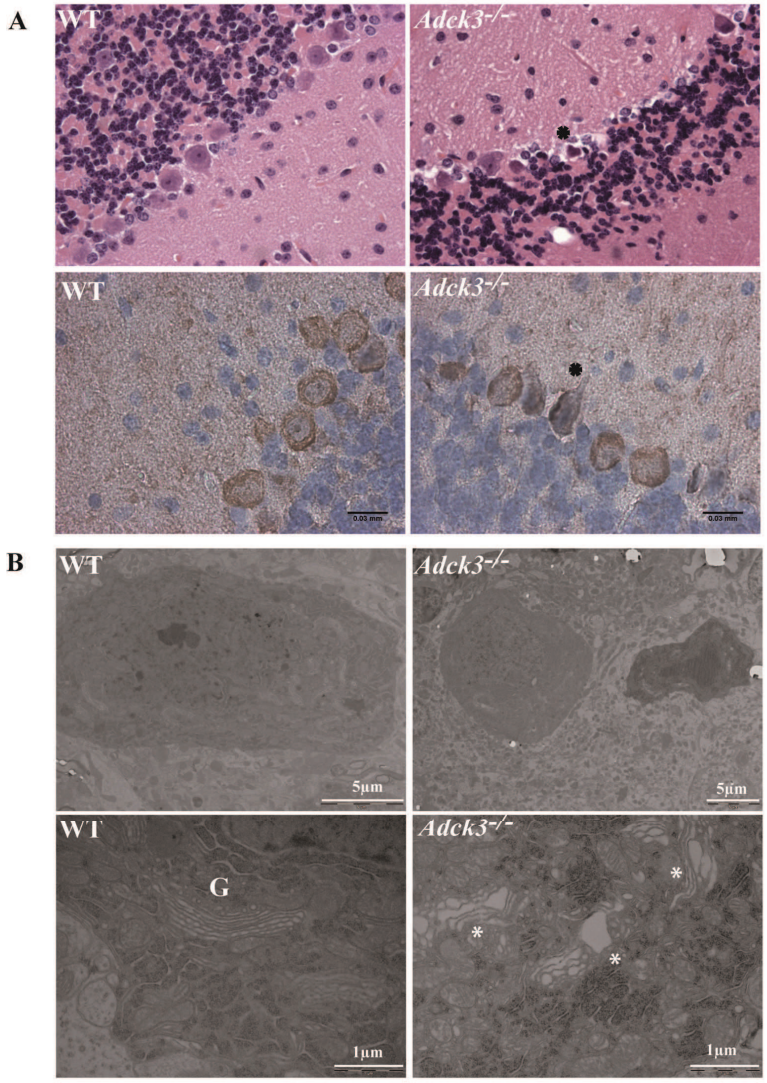


**Figure 4. Les souris *Adck3*$^{-/-}$ montrent un défaut spécifique des cellules de Purkinje. A.** Colorations H&E (en haut) et Calbindin (inférieur) des coupes cérébelleuses. Les astérisques marquent les cellules de Purkinje rétrécies. **B.** Images de microscopie électronique du cervelet (à 30 semaines). G, appareil de Golgi. Les astérisques marquent les appareils de Golgi dilatée.

La structure globale du muscle squelettique par coloration H&E parait normale chez les souris *Adck3 KO.* Cependant, l'analyse en microscopie électronique des quadriceps à 7 mois a montré une anomalie morphologique des mitochondries.

Afin d'étudier l'activité fonctionnelle de la dégénérescence des neurones de Purkinje, en collaboration avec Dr. Philippe ISOPE (INCI, Strasbourg), nous avons mesuré les propriétés électrophysiologiques de ces cellules. Nous avons constaté qu'à l'âge de 3 mois, les PC KO montrent une activité de décharge spontanée réduite, avec la fréquence des potentiels d'action significativement diminuée dans les PC déficientes en Adck3.

Afin d'évaluer si le déficit en Coenzyme Q observée chez les souris *Adck3* KO affectait le métabolisme global des souris, nous avons analysé plusieurs paramètres sanguins. De façon intéressante, nous avons constaté que le métabolisme du cholestérol était modifié chez les souris âgées de 20 semaines. Le cholestérol total et le HDL étaient significativement augmentés chez les souris KO, ainsi que le LDL et les acides gras libres chez les souris KO mâles. Une tendance vers une augmentation des triglycérides a également été observée. Tous ensemble, ces résultats suggèrent que les souris *Adck3* KO sont affectées par une dyslipidémie avec un phénotype plus sévère chez les mâles.

*La caractérisation fonctionnelle d'Adck4*

ADCK4 est le plus proche paralogue d'ADCK3 et une possible compensation fonctionnelle d'ADCK4 dans les patients ARCA2 doit être évaluée. Pour cette raison, j'ai commencé une caractérisation de l'homologue murin d'ADCK4.

Afin d'étudier la localisation subcellulaire d'ADCK4, j'ai cloné la forme murine d'*Adck4* avec différents tags (myc et flag) dans un vecteur d'expression de mammifère. Par enrichissement mitochondrial et des expériences d'immunolocalisation, j'ai confirmé la localisation mitochondriale d'ADCK4 (Figure 5). Par ailleurs, afin de déterminer la forme mature d'ADCK4, après une immunoprécipitation, une analyse par spectrométrie de masse du précurseur et la forme mature d'ADCK4 a été effectuée. Les informations préliminaires montrent qu'ADCK4 possède un site de clivage situé entre les acides aminés 39 et 53.

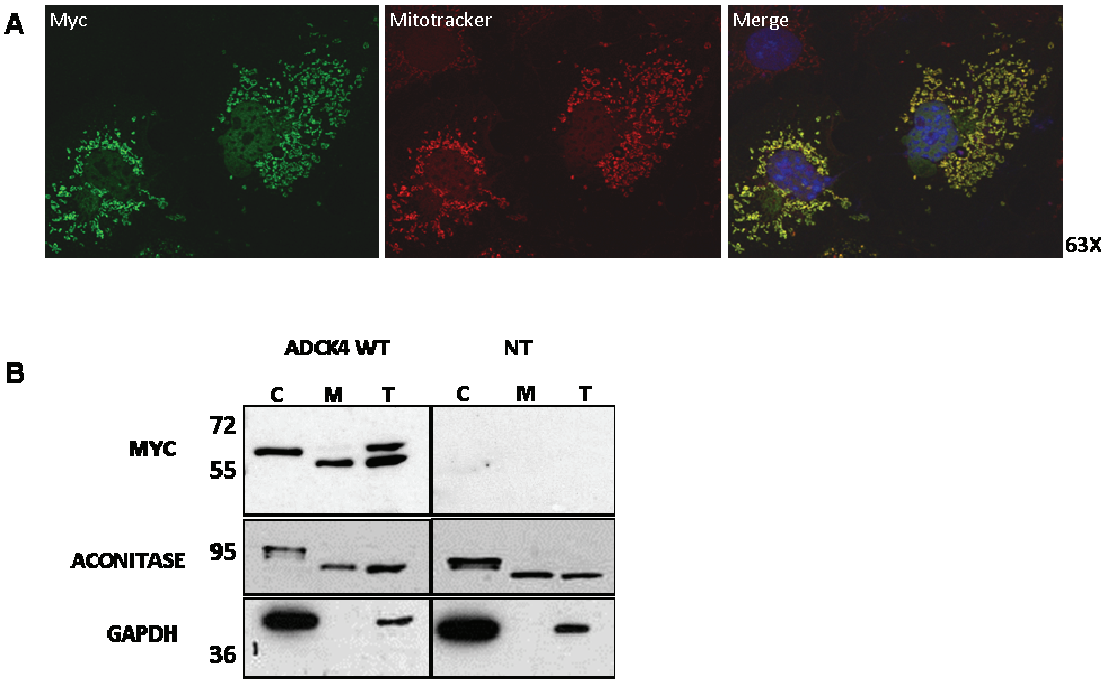


**Figure 5. Localisation mitochondriale d'ADCK4.** A) Analyse confocale de cellules COS surexprimant ADCK4 avec un tag Myc (vert). Les mitochondries sont colorées en rouge avec le Mitotracker et les noyaux en bleu. B) Enrichissement mitochondrial des extraits protéiques de cellules COS surexprimant ADCK4 avec un tag Myc. La forme mature d'ADCK4 est présente dans les fractions totales (T) et mitochondriales (M) et absente dans la fraction cytoplasmique (C). NT, non transfectées. Aconitase et GAPDH sont les contrôles des fractions mitochondriales et cytosoliques respectivement.

Par ailleurs, j'ai généré deux anticorps contre la protéine murine ADCK4. J'ai purifié ces anticorps à partir du sérum immunisé, vérifié l'efficacité de ces anticorps sur la forme surexprimée et endogène de la protéine. J'ai trouvé que les deux anticorps ne reconnaissent pas la forme recombinante d'ADCK3 et qu'au moins un des anticorps est capable de reconnaître la forme endogène d'ADCK4 dans plusieurs types cellulaires. Le signal endogène d'ADCK4 révèle deux bandes autour de 55 et 60 kDa qui nécessitent plus de caractérisation.

À ce jour, on ne sait rien sur la fonction d'ADCK4. Toutefois, dans certains fibroblastes de patients ARCA2, une forte diminution de la transcription d'ADCK4 survient en parallèle de la

diminution du taux de $CoQ_{10}$ (Lagier-Tourenne et al., 2008). Cette constatation suggère qu'ADCK4, pourrait également être impliquée dans la physiopathologie d'ARCA2.

Par des expériences de PCR en temps réel, le profil d'expression d'*Adck4* et *Adck3* dans différents tissus murins a été entrepris. Chez les souris adultes, *Adck3* est plus exprimé qu'*Adck4* et les deux paralogues semblent avoir un profil d'expression différent. En effet, *Adck4* est fortement exprimé dans le foie, le poumon et le rein alors qu'*Adck3* est fortement exprimé dans les muscles et le cœur. Ce profil d'expression différent laisse ouverte la possibilité que les deux paralogues ont la même fonction avec une spécificité tissulaire différente. Par conséquent, il serait intéressant de savoir si ADCK4 peut compenser le déficit d'ADCK3.

### *Conclusions*

En conclusion, nous avons généré une souris KO pour le gène *Adck3* qui récapitule bien les caractéristiques d'ARCA2 présentant une ataxie progressive et un déficit en Coenzyme Q. Nous avons utilisé ce modèle pour étudier la physiopathologie d'ARCA2 et nous avons constaté une dégénérescence spécifique des neurones de Purkinje dans le cervelet. Par ailleurs, un défaut mitochondrial est présent dans le muscle squelettique. Une caractérisation plus poussée, notamment au niveau moléculaire par des expériences de transcriptome, nous permettra de concevoir et de tester des approches thérapeutiques potentielles.

***Bibliographie***

Auré K, Benoist JF, Ogier de Baulny H, Romero NB, Rigal O, Lombès A. (2004) Progression despite replacement of a myopathic form of coenzyme Q10 defect. Neurology, 63(4):727-9.

Boitier E, Degoul F, Desguerre I, Charpentier C, François D, Ponsot G, Diry M, Rustin P, Marsac C (1998) A case of mitochondrial encephalomyopathy associated with a muscle coenzyme Q10 deficiency. J Neurol Sci. 156(1):41-6.

Duncan AJ, Bitner-Glindzicz M, Meunier B, Costello H, Hargreaves IP, López LC, Hirano M, Quinzii CM, Sadowski MI, Hardy J, Singleton A, Clayton PT, Rahman S (2009) A nonsense mutation in COQ9 causes autosomal-recessive neonatal-onset primary coenzyme Q10 deficiency: a potentially treatable form of mitochondrial disease. Am J Hum Genet. 84(5):558-66.

Lagier-Tourenne C, Tazir M, López LC, Quinzii CM, Assoum M, Drouot N, Busso C, Makri S, Ali-Pacha L, Benhassine T, Anheim M, Lynch DR, Thibault C, Plewniak F, Bianchetti L, Tranchant C, Poch O, DiMauro S, Mandel JL, Barros MH, Hirano M, Koenig M (2008) ADCK3, an ancestral kinase, is mutated in a form of recessive ataxia associated with coenzyme Q10 deficiency. Am J Hum Genet. 82(3):661-72.

López LC, Schuelke M, Quinzii CM, Kanki T, Rodenburg RJ, Naini A, Dimauro S, Hirano M (2006) Leigh syndrome with nephropathy and CoQ10 deficiency due to decaprenyl diphosphate synthase subunit 2 (PDSS2) mutations. Am J Hum Genet. 79(6):1125-9. Epub 2006 Oct 27.

Manto M, Marmolino D (2009) Cerebellar ataxias. Curr Opin Neurol 22:419-429.

Mollet J, Giurgea I, Schlemmer D, Dallner G, Chretien D, Delahodde A, Bacq D, de Lonlay P, Munnich A, Rötig A (2007) Prenyldiphosphate synthase, subunit 1 (PDSS1) and OH-benzoate polyprenyltransferase (COQ2) mutations in ubiquinone deficiency and oxidative phosphorylation disorders. J Clin Invest. 117(3):765-72.

Mollet J, Delahodde A, Serre V, Chretien D, Schlemmer D, Lombes A, Boddaert N, Desguerre I, de Lonlay P, de Baulny HO, Munnich A, Rötig A (2008) CABC1 gene mutations cause ubiquinone deficiency with cerebellar ataxia and seizures. Am J Hum Genet. 82(3):623-30.

Pierrel F, Hamelin O, Douki T, Kieffer-Jaquinod S, Mühlenhoff U, Ozeir M, Lill R, Fontecave M (2010) Involvement of mitochondrial ferredoxin and para-aminobenzoic acid in yeast coenzyme Q biosynthesis. Chem Biol. 28;17(5):449-59.

Quinzii C, Naini A, Salviati L, Trevisson E, Navas P, Dimauro S, Hirano M (2005) A mutation in para-hydroxybenzoate-polyprenyl transferase (COQ2) causes primary coenzyme Q10 deficiency. Am J Hum Genet. 78(2):345-9. Epub 2005 Dec 22.

Sailer A, Houlden H (2012) Recent advances in the genetics of cerebellar ataxias. Curr Neurol Neurosci Rep 12:227-236.

Tauche A, Krause-Buchholz U, Rödel G (2008) Ubiquinone biosynthesis in Saccharomyces cerevisiae: the molecular organization of O-methylase Coq3p depends on Abc1p/Coq8p. FEMS Yeast Res. 8(8):1263-75

Tran UC, Clarke CF (2007) Endogenous synthesis of coenzyme Q in eukaryotes. Mitochondrion 7 Suppl:S62-71.

Xie LX, Hsieh EJ, Watanabe S, Allan CM, Chen JY, Tran UC, Clarke CF (2011) Expression of the human atypical kinase ADCK3 rescues coenzyme Q biosynthesis and phosphorylation of Coq polypeptides in yeast coq8 mutants. Biochim Biophys Acta. [Epub ahead of print].

# BIBLIOGRAPHY

## BIBLIOGRAPHY


Aberg F, Appelkvist EL, Dallner G, Ernster L (1992) Distribution and redox state of ubiquinones in rat and human tissues. Arch Biochem Biophys 295:230-234.

Allikmets R, Raskind WH, Hutchinson A, Schueck ND, Dean M, Koeller DM (1999) Mutation of a putative mitochondrial iron transporter gene (ABC7) in X-linked sideroblastic anemia and ataxia (XLSA/A). Hum Mol Genet 8:743-749.

Apps R, Garwicz M (2005) Anatomical and physiological foundations of cerebellar information processing. Nat Rev Neurosci 6:297-311.

Assoum M, Salih MA, Drouot N, Hnia K, Martelli A, Koenig M (2013) The Salih Ataxia Mutation Impairs Rubicon Endosomal Localization. Cerebellum.

Aure K, Benoist JF, Ogier de Baulny H, Romero NB, Rigal O, Lombes A (2004) Progression despite replacement of a myopathic form of coenzyme Q10 defect. Neurology 63:727-729.

Bekri S, Kispal G, Lange H, Fitzsimons E, Tolmie J, Lill R, Bishop DF (2000) Human ABC7 transporter: gene structure and mutation causing X-linked sideroblastic anemia with ataxia with disruption of cytosolic iron-sulfur protein maturation. Blood 96:3256-3264.

Bentinger M, Brismar K, Dallner G (2007) The antioxidant role of coenzyme Q. Mitochondrion 7 Suppl:S41-50.

Bentinger M, Dallner G, Chojnacki T, Swiezewska E (2003) Distribution and breakdown of labeled coenzyme Q10 in rat. Free Radic Biol Med 34:563-575.

Bentinger M, Tekle M, Dallner G (2010) Coenzyme Q--biosynthesis and functions. Biochem Biophys Res Commun 396:74-79.

Blankman JL, Long JZ, Trauger SA, Siuzdak G, Cravatt BF (2013) ABHD12 controls brain lysophosphatidylserine pathways that are deregulated in a murine model of the neurodegenerative disease PHARC. Proc Natl Acad Sci U S A 110:1500-1505.

Bour S, Carmona MC, Galinier A, Caspar-Bauguil S, Van Gaal L, Staels B, Penicaud L, Casteilla L Coenzyme Q as an antiadipogenic factor. Antioxid Redox Signal 14:403-413.

Bour S, Carmona MC, Galinier A, Caspar-Bauguil S, Van Gaal L, Staels B, Penicaud L, Casteilla L (2011) Coenzyme Q as an antiadipogenic factor. Antioxid Redox Signal 14:403-413.

Budd SL, Castilho RF, Nicholls DG (1997) Mitochondrial membrane potential and hydroethidine-monitored superoxide generation in cultured cerebellar granule cells. FEBS Lett 415:21-24.

Buhaescu I, Izzedine H (2007) Mevalonate pathway: a review of clinical and therapeutical implications. Clin Biochem 40:575-584.

Carpenter MB (1996) Core text of neuroanatomy.

Carter DS, Haider SN, Blair RE, Deshpande LS, Sombati S, DeLorenzo RJ (2006) Altered calcium/calmodulin kinase II activity changes calcium homeostasis that underlies epileptiform activity in hippocampal neurons in culture. J Pharmacol Exp Ther 319:1021-1031.

Clark HB, Burright EN, Yunis WS, Larson S, Wilcox C, Hartman B, Matilla A, Zoghbi HY, Orr HT (1997) Purkinje cell expression of a mutant allele of SCA1 in transgenic mice leads to disparate effects on motor behaviors, followed by a progressive cerebellar dysfunction and histological alterations. J Neurosci 17:7385-7395.

Conraads VM, Van Craenenbroeck EM, De Maeyer C, Van Berendoncks AM, Beckers PJ, Vrints CJ (2013) Unraveling new mechanisms of exercise intolerance in chronic heart failure: role of exercise training. Heart Fail Rev 18:65-77.

Cooper AA, Gitler AD, Cashikar A, Haynes CM, Hill KJ, Bhullar B, Liu K, Xu K, Strathearn KE, Liu F, Cao S, Caldwell KA, Caldwell GA, Marsischky G, Kolodner RD, Labaer J, Rochet JC, Bonini NM, Lindquist S (2006) Alpha-synuclein blocks ER-Golgi traffic and Rab1 rescues neuron loss in Parkinson's models. Science 313:324-328.

Crane FL (2001) Biochemical functions of coenzyme Q10. J Am Coll Nutr 20:591-598.

Crane FL, Hatefi Y, Lester RL, Widmer C (1957) Isolation of a quinone from beef heart mitochondria. Biochim Biophys Acta 25:220-221.

Crane FL, Sun IL, Barr R, Low H (1991) Electron and proton transport across the plasma membrane. J Bioenerg Biomembr 23:773-803.

Custer SK, Garden GA, Gill N, Rueb U, Libby RT, Schultz C, Guyenet SJ, Deller T, Westrum LE, Sopher BL, La Spada AR (2006) Bergmann glia expression of polyglutamine-expanded ataxin-7 produces neurodegeneration by impairing glutamate transport. Nat Neurosci 9:1302-1311.

Date H, Onodera O, Tanaka H, Iwabuchi K, Uekawa K, Igarashi S, Koike R, Hiroi T, Yuasa T, Awaya Y, Sakai T, Takahashi T, Nagatomo H, Sekijima Y, Kawachi I, Takiyama Y, Nishizawa M, Fukuhara N, Saito K, Sugano S, Tsuji S (2001) Early-onset ataxia with ocular motor apraxia and hypoalbuminemia is caused by mutations in a new HIT superfamily gene. Nat Genet 29:184-188.

Debray FG, Lambert M, Chevalier I, Robitaille Y, Decarie JC, Shoubridge EA, Robinson BH, Mitchell GA (2007) Long-term outcome and clinical spectrum of 73 pediatric patients with mitochondrial diseases. Pediatrics 119:722-733.

Delorenzo RJ, Sun DA, Deshpande LS (2005) Cellular mechanisms underlying acquired epilepsy: the calcium hypothesis of the induction and maintainance of epilepsy. Pharmacol Ther 105:229-266.

Devasagayam TP, Boloor KK, Ramasarma T (2003) Methods for estimating lipid peroxidation: an analysis of merits and demerits. Indian J Biochem Biophys 40:300-308.

Diomedi-Camassei F, Di Giandomenico S, Santorelli FM, Caridi G, Piemonte F, Montini G, Ghiggeri GM, Murer L, Barisoni L, Pastore A, Muda AO, Valente ML, Bertini E, Emma F (2007) COQ2 nephropathy: a newly described inherited mitochondriopathy with primary renal involvement. J Am Soc Nephrol 18:2773-2780.

Duncan AJ, Bitner-Glindzicz M, Meunier B, Costello H, Hargreaves IP, Lopez LC, Hirano M, Quinzii CM, Sadowski MI, Hardy J, Singleton A, Clayton PT, Rahman S (2009) A nonsense mutation in COQ9 causes autosomal-recessive neonatal-onset primary coenzyme Q10 deficiency: a potentially treatable form of mitochondrial disease. Am J Hum Genet 84:558-566.

Durr A (2010) Autosomal dominant cerebellar ataxias: polyglutamine expansions and beyond. Lancet Neurol 9:885-894.

Earls LR, Hacker ML, Watson JD, Miller DM, 3rd (2010) Coenzyme Q protects Caenorhabditis elegans GABA neurons from calcium-dependent degeneration. Proc Natl Acad Sci U S A 107:14460-14465.

Echtay KS, Winkler E, Klingenberg M (2000) Coenzyme Q is an obligatory cofactor for uncoupling protein function. Nature 408:609-613.

Embirucu EK, Martyn ML, Schlesinger D, Kok F (2009) Autosomal recessive ataxias: 20 types, and counting. Arq Neuropsiquiatr 67:1143-1156.

Fernandez-Ayala DJ, Brea-Calvo G, Lopez-Lluch G, Navas P (2005) Coenzyme Q distribution in HL-60 human cells depends on the endomembrane system. Biochim Biophys Acta 1713:129-137.

Festenstein GN, Heaton FW, Lowe JS, Morton RA (1955) A constituent of the unsaponifiable portion of animal tissue lipids (lambda max. 272 m mu). Biochem J 59:558-566.

Finkel T, Holbrook NJ (2000) Oxidants, oxidative stress and the biology of ageing. Nature 408:239-247.

Finsterer J, Mahjoub SZ (2013) Presentation of adult mitochondrial epilepsy. Seizure 22:119-123.

Fisher RS, van Emde Boas W, Blume W, Elger C, Genton P, Lee P, Engel J, Jr. (2005) Epileptic seizures and epilepsy: definitions proposed by the International League Against Epilepsy (ILAE) and the International Bureau for Epilepsy (IBE). Epilepsia 46:470-472.

Fogel BL, Perlman S (2007) Clinical features and molecular genetics of autosomal recessive cerebellar ataxias. Lancet Neurol 6:245-257.

Folkers K, Langsjoen P, Willis R, Richardson P, Xia LJ, Ye CQ, Tamagawa H (1990) Lovastatin decreases coenzyme Q levels in humans. Proc Natl Acad Sci U S A 87:8931-8934.

Fontaine E, Ichas F, Bernardi P (1998) A ubiquinone-binding site regulates the mitochondrial permeability transition pore. J Biol Chem 273:25734-25740.

Gehman LT, Meera P, Stoilov P, Shiue L, O'Brien JE, Meisler MH, Ares M, Jr., Otis TS, Black DL (2012) The splicing regulator Rbfox2 is required for both cerebellar development and mature motor function. Genes Dev 26:445-460.

Gempel K, Topaloglu H, Talim B, Schneiderat P, Schoser BG, Hans VH, Palmafy B, Kale G, Tokatli A, Quinzii C, Hirano M, Naini A, DiMauro S, Prokisch H, Lochmuller H, Horvath R (2007) The myopathic form of coenzyme Q10 deficiency is caused by mutations in the electron-transferring-flavoprotein dehydrogenase (ETFDH) gene. Brain 130:2037-2044.

Gerards M, van den Bosch B, Calis C, Schoonderwoerd K, van Engelen K, Tijssen M, de Coo R, van der Kooi A, Smeets H (2010) Nonsense mutations in CABC1/ADCK3 cause progressive cerebellar ataxia and atrophy. Mitochondrion 10:510-515.

Geromel V, Kadhom N, Ceballos-Picot I, Chretien D, Munnich A, Rotig A, Rustin P (2001) Human cultured skin fibroblasts survive profound inherited ubiquinone depletion. Free Radic Res 35:11-21.

Gille L, Nohl H (2000) The existence of a lysosomal redox chain and the role of ubiquinone. Arch Biochem Biophys 375:347-354.

Gonatas NK, Gonatas JO, Stieber A (1998) The involvement of the Golgi apparatus in the pathogenesis of amyotrophic lateral sclerosis, Alzheimer's disease, and ricin intoxication. Histochem Cell Biol 109:591-600.

Hagerman P (2013) Fragile X-associated tremor/ataxia syndrome (FXTAS): pathology and mechanisms. Acta Neuropathol 126:1-19.

Heeringa SF, Chernin G, Chaki M, Zhou W, Sloan AJ, Ji Z, Xie LX, Salviati L, Hurd TW, Vega-Warner V, Killen PD, Raphael Y, Ashraf S, Ovunc B, Schoeb DS, McLaughlin HM, Airik R, Vlangos CN, Gbadegesin R, Hinkes B, Saisawat P, Trevisson E, Doimo M, Casarin A, Pertegato V, Giorgi G, Prokisch H, Rotig A, Nurnberg G, Becker C, Wang S, Ozaltin F, Topaloglu R, Bakkaloglu A, Bakkaloglu SA, Muller D, Beissert A, Mir S, Berdeli A, Varpizen S, Zenker M, Matejas V, Santos-Ocana C, Navas P, Kusakabe T, Kispert A, Akman S, Soliman NA, Krick S, Mundel P, Reiser J, Nurnberg P, Clarke CF, Wiggins RC, Faul C, Hildebrandt F (2011) COQ6 mutations in human patients produce nephrotic syndrome with sensorineural deafness. J Clin Invest 121:2013-2024.

Hersheson J, Haworth A, Houlden H (2012) The inherited ataxias: genetic heterogeneity, mutation databases, and future directions in research and clinical diagnostics. Hum Mutat 33:1324-1332.

Hihi AK, Gao Y, Hekimi S (2002) Ubiquinone is necessary for Caenorhabditis elegans development at mitochondrial and non-mitochondrial sites. J Biol Chem 277:2202-2206.

Hirano M, Garone C, Quinzii CM (2012) CoQ(10) deficiencies and MNGIE: two treatable mitochondrial disorders. Biochim Biophys Acta 1820:625-631.

Horvath R, Czermin B, Gulati S, Demuth S, Houge G, Pyle A, Dineiger C, Blakely EL, Hassani A, Foley C, Brodhun M, Storm K, Kirschner J, Gorman GS, Lochmuller H, Holinski-Feder E, Taylor RW, Chinnery PF (2012) Adult-onset cerebellar ataxia due to mutations in CABC1/ADCK3. J Neurol Neurosurg Psychiatry 83:174-178.

Horvath R, Hudson G, Ferrari G, Futterer N, Ahola S, Lamantea E, Prokisch H, Lochmuller H, McFarland R, Ramesh V, Klopstock T, Freisinger P, Salvi F, Mayr JA, Santer R, Tesarova M, Zeman J, Udd B, Taylor RW, Turnbull D, Hanna M, Fialho D, Suomalainen A, Zeviani M, Chinnery PF (2006) Phenotypic spectrum associated with mutations of the mitochondrial polymerase gamma gene. Brain 129:1674-1684.

Hsieh EJ, Gin P, Gulmezian M, Tran UC, Saiki R, Marbois BN, Clarke CF (2007) Saccharomyces cerevisiae Coq9 polypeptide is a subunit of the mitochondrial coenzyme Q biosynthetic complex. Arch Biochem Biophys 463:19-26.

Huynh DP, Yang HT, Vakharia H, Nguyen D, Pulst SM (2003) Expansion of the polyQ repeat in ataxin-2 alters its Golgi localization, disrupts the Golgi complex and causes cell death. Hum Mol Genet 12:1485-1496.

Jen JC, Wan J, Palos TP, Howard BD, Baloh RW (2005) Mutation in the glutamate transporter EAAT1 causes episodic ataxia, hemiplegia, and seizures. Neurology 65:529-534.

Jortner BS (2006) The return of the dark neuron. A histological artifact complicating contemporary neurotoxicologic evaluation. Neurotoxicology 27:628-634.

Kalen A, Norling B, Appelkvist EL, Dallner G (1987) Ubiquinone biosynthesis by the microsomal fraction from rat liver. Biochim Biophys Acta 926:70-78.

Kandel ER, Schwartz, J. H, Jessel, T.M, Siegelbaum S.A, Hudspeth A.J (2013) Principle Of neural science.

Khurana DS, Salganicoff L, Melvin JJ, Hobdell EF, Valencia I, Hardison HH, Marks HG, Grover WD, Legido A (2008) Epilepsy and respiratory chain defects in children with mitochondrial encephalopathies. Neuropediatrics 39:8-13.

Ko DC, Milenkovic L, Beier SM, Manuel H, Buchanan J, Scott MP (2005) Cell-autonomous death of cerebellar purkinje neurons with autophagy in Niemann-Pick type C disease. PLoS genetics 1:81-95.

Koga Y, Povalko N, Nishioka J, Katayama K, Kakimoto N, Matsuishi T (2010) MELAS and L-arginine therapy: pathophysiology of stroke-like episodes. Ann N Y Acad Sci 1201:104-110.

Kunz WS (2002) The role of mitochondria in epileptogenesis. Curr Opin Neurol 15:179-184.

Kweon SM, Kim HJ, Lee ZW, Kim SJ, Kim SI, Paik SG, Ha KS (2001) Real-time measurement of intracellular reactive oxygen species using Mito tracker orange (CMH2TMRos). Biosci Rep 21:341-352.

Lagier-Tourenne C, Tazir M, Lopez LC, Quinzii CM, Assoum M, Drouot N, Busso C, Makri S, Ali-Pacha L, Benhassine T, Anheim M, Lynch DR, Thibault C, Plewniak F, Bianchetti L, Tranchant C, Poch O, DiMauro S, Mandel JL, Barros MH, Hirano M, Koenig M (2008) ADCK3, an ancestral kinase, is mutated in a form of recessive ataxia associated with coenzyme Q10 deficiency. Am J Hum Genet 82:661-672.

Lapointe J, Wang Y, Bigras E, Hekimi S (2012) The submitochondrial distribution of ubiquinone affects respiration in long-lived Mclk1+/- mice. J Cell Biol 199:215-224.

Larm JA, Vaillant F, Linnane AW, Lawen A (1994) Up-regulation of the plasma membrane oxidoreductase as a prerequisite for the viability of human Namalwa rho 0 cells. J Biol Chem 269:30097-30100.

Le Ber I, Rivaud-Pechoux S, Brice A, Durr A (2006) [Autosomal recessive cerebellar ataxias with oculomotor apraxia]. Rev Neurol (Paris) 162:177-184.

Lenaz G, Samori B, Fato R, Battino M, Parenti Castelli G, Domini I (1992) Localization and preferred orientations of ubiquinone homologs in model bilayers. Biochem Cell Biol 70:504-514.

Leonard CJ, Aravind L, Koonin EV (1998) Novel families of putative protein kinases in bacteria and archaea: evolution of the "eukaryotic" protein kinase superfamily. Genome Res 8:1038-1047.

Levavasseur F, Miyadera H, Sirois J, Tremblay ML, Kita K, Shoubridge E, Hekimi S (2001) Ubiquinone is necessary for mouse embryonic development but is not essential for mitochondrial respiration. J Biol Chem 276:46160-46164.

Levin SI, Khaliq ZM, Aman TK, Grieco TM, Kearney JA, Raman IM, Meisler MH (2006) Impaired motor function in mice with cell-specific knockout of sodium channel Scn8a (NaV1.6) in cerebellar purkinje neurons and granule cells. J Neurophysiol 96:785-793.

Liang WC, Ohkuma A, Hayashi YK, Lopez LC, Hirano M, Nonaka I, Noguchi S, Chen LH, Jong YJ, Nishino I (2009) ETFDH mutations, CoQ10 levels, and respiratory chain activities in patients with riboflavin-responsive multiple acyl-CoA dehydrogenase deficiency. Neuromuscul Disord 19:212-216.

Liguz-Lecznar M, Skangiel-Kramska J (2007) Vesicular glutamate transporters (VGLUTs): the three musketeers of glutamatergic system. Acta Neurobiol Exp (Wars) 67:207-218.

Lopez-Martin JM, Salviati L, Trevisson E, Montini G, DiMauro S, Quinzii C, Hirano M, Rodriguez-Hernandez A, Cordero MD, Sanchez-Alcazar JA, Santos-Ocana C, Navas P (2007) Missense mutation of the COQ2 gene causes defects of bioenergetics and de novo pyrimidine synthesis. Hum Mol Genet 16:1091-1097.

Lopez LC, Schuelke M, Quinzii CM, Kanki T, Rodenburg RJ, Naini A, Dimauro S, Hirano M (2006) Leigh syndrome with nephropathy and CoQ10 deficiency due to decaprenyl diphosphate synthase subunit 2 (PDSS2) mutations. Am J Hum Genet 79:1125-1129.

Lorenzetto E, Caselli L, Feng G, Yuan W, Nerbonne JM, Sanes JR, Buffelli M (2009) Genetic perturbation of postsynaptic activity regulates synapse elimination in developing cerebellum. Proceedings of the National Academy of Sciences of the United States of America 106:16475-16480.

Lu S, Lu LY, Liu MF, Yuan QJ, Sham MH, Guan XY, Huang JD (2012) Cerebellar defects in Pdss2 conditional knockout mice during embryonic development and in adulthood. Neurobiol Dis 45:219-233.

Maltecca F, Magnoni R, Cerri F, Cox GA, Quattrini A, Casari G (2009) Haploinsufficiency of AFG3L2, the gene responsible for spinocerebellar ataxia type 28, causes mitochondria-mediated Purkinje cell dark degeneration. J Neurosci 29:9244-9254.

Manto M, Marmolino D (2009) Cerebellar ataxias. Curr Opin Neurol 22:419-429.

Marban E, Yamagishi T, Tomaselli GF (1998) Structure and function of voltage-gated sodium channels. J Physiol 508 ( Pt 3):647-657.

Marbois B, Gin P, Faull KF, Poon WW, Lee PT, Strahan J, Shepherd JN, Clarke CF (2005) Coq3 and Coq4 define a polypeptide complex in yeast mitochondria for the biosynthesis of coenzyme Q. J Biol Chem 280:20231-20238.

Martelli A, Napierala M, Puccio H (2012) Understanding the genetic and molecular pathogenesis of Friedreich's ataxia through animal and cellular models. Dis Model Mech 5:165-176.

Matsuoka T, Maeda H, Goto Y, Nonaka I (1991) Muscle coenzyme Q10 in mitochondrial encephalomyopathies. Neuromuscul Disord 1:443-447.

McLennan HR, Degli Esposti M (2000) The contribution of mitochondrial respiratory complexes to the production of reactive oxygen species. J Bioenerg Biomembr 32:153-162.

Melia TJ, Jr. (2007) Putting the clamps on membrane fusion: how complexin sets the stage for calcium-mediated exocytosis. FEBS Lett 581:2131-2139.

Mitchell P (1975) Protonmotive redox mechanism of the cytochrome b-c1 complex in the respiratory chain: protonmotive ubiquinone cycle. FEBS Lett 56:1-6.

Mollet J, Delahodde A, Serre V, Chretien D, Schlemmer D, Lombes A, Boddaert N, Desguerre I, de Lonlay P, de Baulny HO, Munnich A, Rotig A (2008) CABC1 gene mutations cause ubiquinone deficiency with cerebellar ataxia and seizures. Am J Hum Genet 82:623-630.

Mollet J, Giurgea I, Schlemmer D, Dallner G, Chretien D, Delahodde A, Bacq D, de Lonlay P, Munnich A, Rotig A (2007) Prenyldiphosphate synthase, subunit 1 (PDSS1) and OH-benzoate polyprenyltransferase (COQ2) mutations in ubiquinone deficiency and oxidative phosphorylation disorders. J Clin Invest 117:765-772.

Montenegro L, Ottimo S, Puglisi G, Castelli F, Sarpietro MG (2012) Idebenone loaded solid lipid nanoparticles interact with biomembrane models: calorimetric evidence. Mol Pharm 9:2534-2541.

Montero R, Pineda M, Aracil A, Vilaseca MA, Briones P, Sanchez-Alcazar JA, Navas P, Artuch R (2007) Clinical, biochemical and molecular aspects of cerebellar ataxia and Coenzyme Q10 deficiency. Cerebellum 6:118-122.

Moreira MC, Barbot C, Tachi N, Kozuka N, Uchida E, Gibson T, Mendonca P, Costa M, Barros J, Yanagisawa T, Watanabe M, Ikeda Y, Aoki M, Nagata T, Coutinho P, Sequeiros J, Koenig M (2001) The gene mutated in ataxia-ocular apraxia 1 encodes the new HIT/Zn-finger protein aprataxin. Nat Genet 29:189-193.

Mugoni V, Postel R, Catanzaro V, De Luca E, Turco E, Digilio G, Silengo L, Murphy MP, Medana C, Stainier DY, Bakkers J, Santoro MM (2013) Ubiad1 is an antioxidant enzyme that regulates eNOS activity by CoQ10 synthesis. Cell 152:504-518.

Muhammad A, Flores I, Zhang H, Yu R, Staniszewski A, Planel E, Herman M, Ho L, Kreber R, Honig LS, Ganetzky B, Duff K, Arancio O, Small SA (2008) Retromer deficiency observed in Alzheimer's disease causes hippocampal dysfunction, neurodegeneration, and Abeta accumulation. Proc Natl Acad Sci U S A 105:7327-7332.

Nakai D, Yuasa S, Takahashi M, Shimizu T, Asaumi S, Isono K, Takao T, Suzuki Y, Kuroyanagi H, Hirokawa K, Koseki H, Shirsawa T (2001) Mouse homologue of coq7/clk-1, longevity gene in Caenorhabditis elegans, is essential for coenzyme Q synthesis, maintenance of mitochondrial integrity, and neurogenesis. Biochem Biophys Res Commun 289:463-471.

Nilsson T, Au CE, Bergeron JJ (2009) Sorting out glycosylation enzymes in the Golgi apparatus. FEBS Lett 583:3764-3769.

Ohtsubo K, Marth JD (2006) Glycosylation in cellular mechanisms of health and disease. Cell 126:855-867.

Padilla S, Tran UC, Jimenez-Hidalgo M, Lopez-Martin JM, Martin-Montalvo A, Clarke CF, Navas P, Santos-Ocana C (2009) Hydroxylation of demethoxy-Q6 constitutes a control point in yeast coenzyme Q6 biosynthesis. Cell Mol Life Sci 66:173-186.

Palau F, Espinos C (2006) Autosomal recessive cerebellar ataxias. Orphanet J Rare Dis 1:47.

Papucci L, Schiavone N, Witort E, Donnini M, Lapucci A, Tempestini A, Formigli L, Zecchi-Orlandini S, Orlandini G, Carella G, Brancato R, Capaccioli S (2003) Coenzyme q10 prevents apoptosis by inhibiting mitochondrial depolarization independently of its free radical scavenging property. J Biol Chem 278:28220-28228.

Parrado-Fernandez C, Lopez-Lluch G, Rodriguez-Bies E, Santa-Cruz S, Navas P, Ramsey JJ, Villalba JM (2011) Calorie restriction modifies ubiquinone and COQ transcript levels in mouse tissues. Free Radic Biol Med 50:1728-1736.

Peake KB, Vance JE (2010) Defective cholesterol trafficking in Niemann-Pick C-deficient cells. FEBS Lett 584:2731-2739.

Peng M, Falk MJ, Haase VH, King R, Polyak E, Selak M, Yudkoff M, Hancock WW, Meade R, Saiki R, Lunceford AL, Clarke CF, Gasser DL (2008) Primary coenzyme Q

deficiency in Pdss2 mutant mice causes isolated renal disease. PLoS Genet 4:e1000061.
Perkins EM, Clarkson YL, Sabatier N, Longhurst DM, Millward CP, Jack J, Toraiwa J, Watanabe M, Rothstein JD, Lyndon AR, Wyllie DJ, Dutia MB, Jackson M (2010) Loss of beta-III spectrin leads to Purkinje cell dysfunction recapitulating the behavior and neuropathology of spinocerebellar ataxia type 5 in humans. J Neurosci 30:4857-4867.
Pierrel F, Hamelin O, Douki T, Kieffer-Jaquinod S, Muhlenhoff U, Ozeir M, Lill R, Fontecave M (2010) Involvement of mitochondrial ferredoxin and para-aminobenzoic acid in yeast coenzyme Q biosynthesis. Chem Biol 17:449-459.
Poon WW, Do TQ, Marbois BN, Clarke CF (1997) Sensitivity to treatment with polyunsaturated fatty acids is a general characteristic of the ubiquinone-deficient yeast coq mutants. Mol Aspects Med 18 Suppl:S121-127.
Quinzii C, Naini A, Salviati L, Trevisson E, Navas P, Dimauro S, Hirano M (2006) A mutation in para-hydroxybenzoate-polyprenyl transferase (COQ2) causes primary coenzyme Q10 deficiency. Am J Hum Genet 78:345-349.
Quinzii CM, Hirano M (2011) Primary and secondary CoQ(10) deficiencies in humans. Biofactors 37:361-365.
Quinzii CM, Lopez LC, Gilkerson RW, Dorado B, Coku J, Naini AB, Lagier-Tourenne C, Schuelke M, Salviati L, Carrozzo R, Santorelli F, Rahman S, Tazir M, Koenig M, DiMauro S, Hirano M (2010) Reactive oxygen species, oxidative stress, and cell death correlate with level of CoQ10 deficiency. FASEB J 24:3733-3743.
Quinzii CM, Lopez LC, Von-Moltke J, Naini A, Krishna S, Schuelke M, Salviati L, Navas P, DiMauro S, Hirano M (2008) Respiratory chain dysfunction and oxidative stress correlate with severity of primary CoQ10 deficiency. FASEB J 22:1874-1885.
Rahman S (2012) Mitochondrial disease and epilepsy. Dev Med Child Neurol 54:397-406.
Rahman S, Clarke CF, Hirano M (2012) 176th ENMC International Workshop: diagnosis and treatment of coenzyme Q(1)(0) deficiency. Neuromuscul Disord 22:76-86.
Raman IM, Bean BP (1997) Resurgent sodium current and action potential formation in dissociated cerebellar Purkinje neurons. J Neurosci 17:4517-4526.
Ramnani N (2006) The primate cortico-cerebellar system: anatomy and function. Nat Rev Neurosci 7:511-522.
Reddy JV, Ganley IG, Pfeffer SR (2006) Clues to neuro-degeneration in Niemann-Pick type C disease from global gene expression profiling. PLoS One 1:e19.
Rodriguez-Hernandez A, Cordero MD, Salviati L, Artuch R, Pineda M, Briones P, Gomez Izquierdo L, Cotan D, Navas P, Sanchez-Alcazar JA (2009) Coenzyme Q deficiency triggers mitochondria degradation by mitophagy. Autophagy 5:19-32.
Rowland AA, Voeltz GK (2012) Endoplasmic reticulum-mitochondria contacts: function of the junction. Nat Rev Mol Cell Biol 13:607-625.
Sacconi S, Trevisson E, Salviati L, Ayme S, Rigal O, Redondo AG, Mancuso M, Siciliano G, Tonin P, Angelini C, Aure K, Lombes A, Desnuelle C (2010) Coenzyme Q10 is frequently reduced in muscle of patients with mitochondrial myopathy. Neuromuscul Disord 20:44-48.
Saiki R, Nagata A, Kainou T, Matsuda H, Kawamukai M (2005) Characterization of solanesyl and decaprenyl diphosphate synthases in mice and humans. FEBS J 272:5606-5622.
Sailer A, Houlden H (2012) Recent advances in the genetics of cerebellar ataxias. Curr Neurol Neurosci Rep 12:227-236.
Salviati L, Trevisson E, Rodriguez Hernandez MA, Casarin A, Pertegato V, Doimo M, Cassina M, Agosto C, Desbats MA, Sartori G, Sacconi S, Memo L, Zuffardi O, Artuch R, Quinzii C, Dimauro S, Hirano M, Santos-Ocana C, Navas P (2012) Haploinsufficiency of COQ4 causes coenzyme Q10 deficiency. J Med Genet 49:187-191.

Sann S, Wang Z, Brown H, Jin Y (2009) Roles of endosomal trafficking in neurite outgrowth and guidance. Trends Cell Biol 19:317-324.
Santoro MR, Bray SM, Warren ST (2012) Molecular mechanisms of fragile X syndrome: a twenty-year perspective. Annu Rev Pathol 7:219-245.
Scandalios JG (2005) Oxidative stress: molecular perception and transduction of signals triggering antioxidant gene defenses. Braz J Med Biol Res 38:995-1014.
Scheeff ED, Bourne PE (2005) Structural evolution of the protein kinase-like superfamily. PLoS Comput Biol 1:e49.
Schmelzer C, Kitano M, Hosoe K, Doring F (2012) Ubiquinol affects the expression of genes involved in PPARalpha signalling and lipid metabolism without changes in methylation of CpG promoter islands in the liver of mice. J Clin Biochem Nutr 50:119-126.
Schmelzer C, Okun JG, Haas D, Higuchi K, Sawashita J, Mori M, Doring F (2010) The reduced form of coenzyme Q10 mediates distinct effects on cholesterol metabolism at the transcriptional and metabolite level in SAMP1 mice. IUBMB Life 62:812-818.
Schmucker S, Argentini M, Carelle-Calmels N, Martelli A, Puccio H (2008) The in vivo mitochondrial two-step maturation of human frataxin. Hum Mol Genet 17:3521-3531.
Shiloh Y (2003) ATM and related protein kinases: safeguarding genome integrity. Nat Rev Cancer 3:155-168.
Silva AL, Romao L (2009) The mammalian nonsense-mediated mRNA decay pathway: to decay or not to decay! Which players make the decision? FEBS Lett 583:499-505.
Simon D, Seznec H, Gansmuller A, Carelle N, Weber P, Metzger D, Rustin P, Koenig M, Puccio H (2004) Friedreich ataxia mouse models with progressive cerebellar and sensory ataxia reveal autophagic neurodegeneration in dorsal root ganglia. J Neurosci 24:1987-1995.
Somayajulu M, McCarthy S, Hung M, Sikorska M, Borowy-Borowski H, Pandey S (2005) Role of mitochondria in neuronal cell death induced by oxidative stress; neuroprotection by Coenzyme Q10. Neurobiol Dis 18:618-627.
Stankewich MC, Gwynn B, Ardito T, Ji L, Kim J, Robledo RF, Lux SE, Peters LL, Morrow JS (2010) Targeted deletion of betaIII spectrin impairs synaptogenesis and generates ataxic and seizure phenotypes. Proc Natl Acad Sci U S A 107:6022-6027.
Swenson RS (2006) Review of clinical and functional neuroscience.
Sykora P, Croteau DL, Bohr VA, Wilson DM, 3rd (2011) Aprataxin localizes to mitochondria and preserves mitochondrial function. Proc Natl Acad Sci U S A 108:7437-7442.
Szul T, Sztul E (2011) COPII and COPI traffic at the ER-Golgi interface. Physiology (Bethesda) 26:348-364.
Takayasu Y, Iino M, Takatsuru Y, Tanaka K, Ozawa S (2009) Functions of glutamate transporters in cerebellar Purkinje cell synapses. Acta Physiol (Oxf) 197:1-12.
Tao J, Wu H, Lin Q, Wei W, Lu XH, Cantle JP, Ao Y, Olsen RW, Yang XW, Mody I, Sofroniew MV, Sun YE (2011) Deletion of astroglial Dicer causes non-cell-autonomous neuronal dysfunction and degeneration. J Neurosci 31:8306-8319.
Tauche A, Krause-Buchholz U, Rodel G (2008) Ubiquinone biosynthesis in Saccharomyces cerevisiae: the molecular organization of O-methylase Coq3p depends on Abc1p/Coq8p. FEMS Yeast Res 8:1263-1275.
Teclebrhan H, Jakobsson-Borin A, Brunk U, Dallner G (1995) Relationship between the endoplasmic reticulum-Golgi membrane system and ubiquinone biosynthesis. Biochim Biophys Acta 1256:157-165.
Terracciano A, Renaldo F, Zanni G, D'Amico A, Pastore A, Barresi S, Valente EM, Piemonte F, Tozzi G, Carrozzo R, Valeriani M, Boldrini R, Mercuri E, Santorelli FM, Bertini E (2012) The use of muscle biopsy in the diagnosis of undefined ataxia with cerebellar atrophy in children. Eur J Paediatr Neurol 16:248-256.

Todd PK, Paulson HL (2010) RNA-mediated neurodegeneration in repeat expansion disorders. Ann Neurol 67:291-300.
Tran UC, Clarke CF (2007) Endogenous synthesis of coenzyme Q in eukaryotes. Mitochondrion 7 Suppl:S62-71.
Tran UC, Marbois B, Gin P, Gulmezian M, Jonassen T, Clarke CF (2006) Complementation of Saccharomyces cerevisiae coq7 mutants by mitochondrial targeting of the Escherichia coli UbiF polypeptide: two functions of yeast Coq7 polypeptide in coenzyme Q biosynthesis. J Biol Chem 281:16401-16409.
Tranchant C, Anheim M (2009) [Autosomal recessive cerebellar ataxias]. Presse Med 38:1852-1859.
Treuting PM, Dintzis, S. M (2012) Comparative anatomy and histology: Elsevier.
Turmaine M, Raza A, Mahal A, Mangiarini L, Bates GP, Davies SW (2000) Nonapoptotic neurodegeneration in a transgenic mouse model of Huntington's disease. Proc Natl Acad Sci U S A 97:8093-8097.
Turunen M, Olsson J, Dallner G (2004) Metabolism and function of coenzyme Q. Biochim Biophys Acta 1660:171-199.
van Meer G, Voelker DR, Feigenson GW (2008) Membrane lipids: where they are and how they behave. Nat Rev Mol Cell Biol 9:112-124.
van Vliet C, Thomas EC, Merino-Trigo A, Teasdale RD, Gleeson PA (2003) Intracellular sorting and transport of proteins. Prog Biophys Mol Biol 83:1-45.
Wang Y, Hekimi S (2013) Molecular genetics of ubiquinone biosynthesis in animals. Crit Rev Biochem Mol Biol 48:69-88.
Watson C, Paxinos, G., Puelles, L., (2012) The mouse nervous system: Elsevier.
Willis RA, Folkers K, Tucker JL, Ye CQ, Xia LJ, Tamagawa H (1990) Lovastatin decreases coenzyme Q levels in rats. Proc Natl Acad Sci U S A 87:8928-8930.
Xie LX, Hsieh EJ, Watanabe S, Allan CM, Chen JY, Tran UC, Clarke CF (2011) Expression of the human atypical kinase ADCK3 rescues coenzyme Q biosynthesis and phosphorylation of Coq polypeptides in yeast coq8 mutants. Biochim Biophys Acta 1811:348-360.
Xie LX, Ozeir M, Tang JY, Chen JY, Jaquinod SK, Fontecave M, Clarke CF, Pierrel F (2012) Overexpression of the Coq8 kinase in Saccharomyces cerevisiae coq null mutants allows for accumulation of diagnostic intermediates of the coenzyme Q6 biosynthetic pathway. J Biol Chem 287:23571-23581.
Xu X, Kedlaya R, Higuchi H, Ikeda S, Justice MJ, Setaluri V, Ikeda A (2010) Mutation in archain 1, a subunit of COPI coatomer complex, causes diluted coat color and Purkinje cell degeneration. PLoS Genet 6:e1000956.
Yu FH, Mantegazza M, Westenbroek RE, Robbins CA, Kalume F, Burton KA, Spain WJ, McKnight GS, Scheuer T, Catterall WA (2006) Reduced sodium current in GABAergic interneurons in a mouse model of severe myoclonic epilepsy in infancy. Nat Neurosci 9:1142-1149.
Zampol MA, Busso C, Gomes F, Ferreira-Junior JR, Tzagoloff A, Barros MH (2010) Over-expression of COQ10 in Saccharomyces cerevisiae inhibits mitochondrial respiration. Biochem Biophys Res Commun 402:82-87.
Zanni G, Cali T, Kalscheuer VM, Ottolini D, Barresi S, Lebrun N, Montecchi-Palazzi L, Hu H, Chelly J, Bertini E, Brini M, Carafoli E (2012) Mutation of plasma membrane Ca2+ ATPase isoform 3 in a family with X-linked congenital cerebellar ataxia impairs Ca2+ homeostasis. Proc Natl Acad Sci U S A 109:14514-14519.

**Pathophysiological and molecular characterization of a mouse model of ARCA2, a recessive cerebellar ataxia associated to Coenzyme $Q_{10}$ deficiency**

ARCA2 is a form of recessive ataxia characterized by a slow progression of the ataxic phenotype, cerebellar atrophy and mild deficit in Coenzyme $Q_{10}$. In addition, ARCA2 patients present variable symptoms, such as epilepsy, exercise intolerance and intellectual disability, resulting in a highly heterogeneous phenotype. Mutations in the *ADCK3* gene were recently identified as the genetic cause of ARCA2. *ADCK3* encodes a putative mitochondrial kinase homologous to the yeast Coq8 and the bacterial UbiB proteins, which are required for Coenzyme Q biosynthesis. The goal of my PhD project was to elucidate the pathophysiology of ARCA2. In order to achieve this aim, a constitutive knockout mouse for *Adck3* was generated. *Adck3*$^{-/-}$ mice reproduce many ARCA2 symptoms: impaired motor activity, slow progression of the ataxic phenotype, increased susceptibility to epilepsy and a mild Coenzyme Q deficit. Therefore, *Adck3*$^{-/-}$ mice are a good model to study ARCA2. Strikingly, a defect was found specifically in cerebellar *Adck3*$^{-/-}$ Purkinje cells, which presented morphological and functional impairment. Moreover, a mild mitochondrial defect was observed in the skeletal muscle of *Adck3*$^{-/-}$ mice. Interestingly, transcriptomic analyses of both tissues revealed alteration in a number of molecular pathways implicating ADCK3 in novel cellular processes.

**Caractérisation physiopathologique et moléculaire d'un modèle murin d'ARCA2, une ataxie cérébelleuse récessive associée à un déficit en coenzyme $Q_{10}$**

ARCA2 est une ataxie récessive qui se caractérise par une progression lente du phénotype ataxique, une atrophie du cervelet et un léger déficit en coenzyme $Q_{10}$. D'autres symptômes peuvent y être associés, tels qu'une épilepsie, une intolérance à l'effort ou encore un retard mental, rendant le tableau clinique hétérogène. Des mutations dans le gène *ADCK3* ont été récemment identifiées comme étant la cause d'ARCA2. *ADCK3* code pour une kinase mitochondriale atypique, homologue aux protéines Coq8 de la levure et UbiB de la bactérie, toutes deux indispensables à la biosynthèse du coenzyme $Q_{10}$. L'objectif de mon projet de thèse était d'élucider la physiopathologie d'ARCA2 en utilisant le modèle murin knockout pour *Adck3* qui venait d'être généré au laboratoire. J'ai ainsi pu montrer que les souris *Adck3*$^{-/-}$ reproduisent de nombreux symptômes associés à ARCA2 : une altération de la marche, une évolution lente du phénotype ataxique, une susceptibilité à l'épilepsie et un léger déficit en coenzyme Q. Ces données montrent que les souris *Adck3*$^{-/-}$ constituent un bon modèle pour étudier ARCA2. Les souris *Adck3*$^{-/-}$ présentent une atteinte du cervelet et du muscle squelettique. Au niveau du cervelet, les cellules de Purkinje sont spécifiquement touchées et présentent des anomalies morphologiques et fonctionnelles. Un léger défaut mitochondrial a, quant à lui, été observé dans les muscles squelettiques des souris *Adck3*$^{-/-}$. Enfin, une analyse transcriptomique de ces deux tissus a révélé des altérations de nombreuses voies, impliquant ADCK3 dans de nouveaux processus cellulaires.

Floriana LICITRA

# Pathophysiological and molecular characterization of a mouse model of ARCA2, a recessive cerebellar ataxia associated to Coenzyme $Q_{10}$ deficiency


## Résumé

ARCA2 est une ataxie récessive qui se caractérise par une atrophie du cervelet et un léger déficit en coenzyme $Q_{10}$. Des mutations dans le gène *ADCK3* ont été récemment identifiées comme étant la cause d'ARCA2. *ADCK3* code pour une kinase mitochondriale atypique, qui pourrait être impliquée dans la biosynthèse du coenzyme $Q_{10}$. L'objectif de mon projet de thèse était d'élucider la physiopathologie d'ARCA2 en utilisant le modèle murin knockout pour *Adck3*. J'ai ainsi pu montrer que les souris *Adck3*$^{-/-}$ reproduisent de nombreux symptômes associés à ARCA2 et constituent un bon modèle pour étudier ARCA2. Au niveau du cervelet, les cellules de Purkinje sont spécifiquement touchées et présentent des anomalies morphologiques et fonctionnelles. Un léger défaut mitochondrial a été observé dans les muscles squelettiques des souris *Adck3*$^{-/-}$. Enfin, une analyse transcriptomique de ces deux tissus a révélé des altérations de nombreuses voies, impliquant ADCK3 dans de nouveaux processus cellulaires.


Mots-clés : ataxie, ARCA2, Coenzyme Q, ADCK3, cellules de Purkinje.


## Résumé en anglais

ARCA2 is a form of recessive ataxia characterized by a slow progression of the ataxic phenotype, cerebellar atrophy and mild deficit in Coenzyme $Q_{10}$. ARCA2 was recently found associated with mutations in the *ADCK3* gene that encodes a putative mitochondrial kinase homologous to the yeast Coq8 and the bacterial UbiB proteins, which are required for Coenzyme Q biosynthesis. In order to elucidate the pathophysiology of ARCA2, a constitutive knockout mouse for *Adck3* was generated. *Adck3*$^{-/-}$ mice reproduce many ARCA2 symptoms such as slow progression of the ataxic phenotype and mild Coenzyme Q deficit, suggesting that *Adck3*$^{-/-}$ mice are a good model to study ARCA2. Strikingly, a morphological and functional impairment was found in cerebellar *Adck3*$^{-/-}$ Purkinje cells, whereas a mild mitochondrial defect was observed in the skeletal muscle of *Adck3*$^{-/-}$ mice. Interestingly, transcriptomic analyses revealed alteration in a number of molecular pathways implicating ADCK3 in novel cellular processes.


Keywords: ataxia, ARCA2, Coenzyme Q, ADCK3, Purkinje cells.